# Control of Distonic Radical Cations by a Chiral Borate Ion under Asymmetric Photocatalytic Conditions

KIMURA Yuto

Department of Molecular and Macromolecular Chemistry
Graduate School of Engineering
Nagoya University

**Contents**

# Chapter 1

# General Introduction and Summary

Radical reactions have long been attracting a high degree of attention as a strategy for achieving molecular transformations that are quite different from simple ionic reactions. However, due to the high reactivity of radical species, catalytic stereocontrol of radical intermediates in the bond-forming step is still a difficult task in organic synthesis. Radical ions, on the other hand, are not only highly reactive radical species but also have ionic properties. In particular, radical ion species are key intermediates in photoredox reactions which have been rapidly developed in recent years, and it is possible to produce targeted radical ion species by selecting photocatalysts that match the redox potential of the substrate.

In this thesis, focusing on the ionic nature of the radical ion species, the author demonstrate that radical ion intermediates in photoredox reactions can be precisely controlled through chiral ion-pair formation with optically active counterions, facilitating stereoselective bond formations.

## 1.1. Catalytic Asymmetric Radical Reactions under Non-Light Conditions

Research on catalytic stereocontrol of radical reactions has a short history. This is due to the fact that induction of stereoselectivity in radical reactions is difficult to achieve because of the high reactivity of the radical species themselves, and that there has been no method to promote radical reactions under mild conditions until recently. In the following sections, the author will focus on reactions in which radical species are involved in the stereo-determining step, and introduce advances in catalytic asymmetric radical reactions.[1]

### 1.1.1. Chiral Lewis Acid Coordination in Radical Reactions

Chiral Lewis acids can induce enantioselectivity in the radical bond-forming step by binding to prochiral compounds and sterically shielding a certain face of a substrate. In 1996, the first pioneering catalytic enantioselective radical reaction was reported by Sibi and Porter, which was the conjugate addition of alkyl radicals using a chiral Lewis acid catalyst (Scheme 1).[2a] However, they struggled to suppress the background reaction and required a stoichiometric chiral source to achieve high enantioselectivity. Afterward, through modification of the chiral ligand, a similar highly enantioselective reaction with a catalytic amount of a chiral Lewis acid was achieved by Sibi in 1997 (Scheme 2).[2b] These reports demonstrated that radical reactions, which have been considered to be highly reactive, can be controlled by catalytic amounts of chiral sources for the first time.

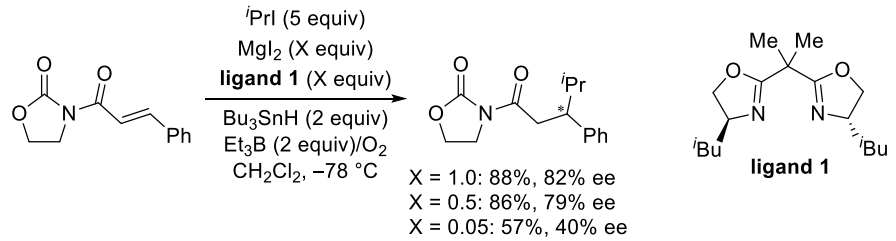


**Scheme 1.** Chiral Lewis Acid-Promoted Enantioselective Conjugate Radical Addition

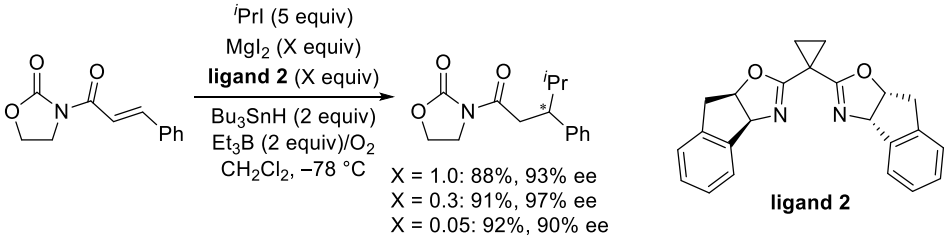


**Scheme 2.** Chiral Lewis Acid-Catalyzed Enantioselective Conjugate Radical Addition

## 1.1.2. Hydrogen Atom Transfer by Catalytic Amounts of Chiral Reagents

The employment of optically active atom transfer agents is a simple strategy to discriminate the prochiral faces of radical intermediates and obtain stereoselectivity in radical-bond formations. The first radical reaction with a catalytic amount of a chiral hydrogen-atom-transfer agent under non-light-irradiated conditions was introduced by Roberts *et al.* in 1996 (Scheme 3).[3] In this report, a moderately enantioselective, radical-chain hydrosilylation was achieved using a optically-active thiol catalyst **3** with di-*tert*-butyl hyponitrite (TBHN) as a radical initiator at 60 °C. Furthermore, in 1997, Metzger and co-workers demonstrated an enantioselective reduction of α-bromoesters via radical-hydrogen-atom transfer using 50 mol% of a chiral tin hydride **4** (Scheme 4).[4]

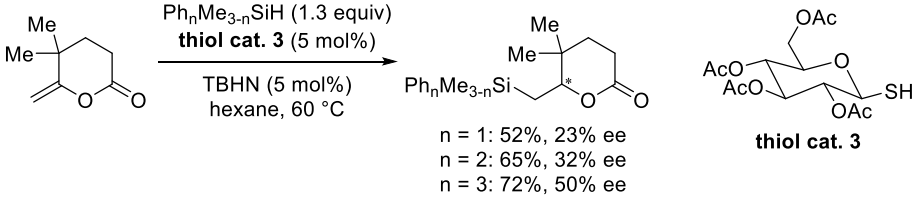


**Scheme 3.** Hydrosilylation of a Lactone by Catalytic Amount of a Chiral Thiol

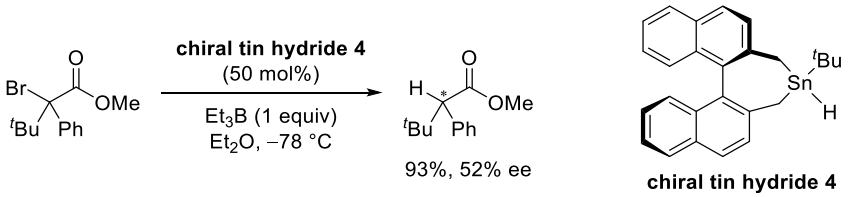


**Scheme 4.** Catalytic Enantioselective Hydrogen-Transfer from a Chiral Tin Hydride

### 1.1.3. Asymmetric Metal Catalysis via Radical Processes

Titanium has long been used mainly as a sacrificial reducing reagent for epoxides and carbonyl compounds. In 1999, Gansäuer and co-workers reported an enantioselective carbon-carbon bond-forming reaction via ring opening of *meso*-epoxides using a catalytic amount of optically-active titanocene **5** along with zinc (Scheme 5).[5] Moreover, in 1999, Nicholas *et al.* reported the first catalytic asymmetric pinacol coupling reaction of benzaldehyde with a chiral titanium complex **6** (Scheme 6).[6]

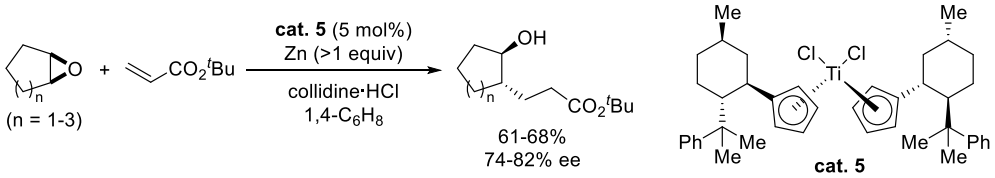


**Scheme 5.** Chiral Titanocene-Catalyzed Asymmetric Radical Addition from *meso*-Epoxides

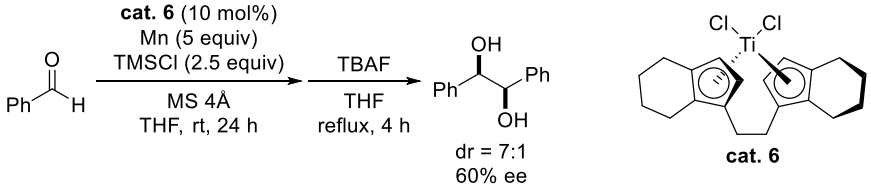


**Scheme 6.** Chiral Titanium-Catalyzed Enantioselective Pinacol Coupling Reaction

In 2008, Fu *et al.* developed catalytic enantioselective alkyl-alkyl Suzuki cross-coupling reaction via radical intermediates with the strategy of directing groups (Scheme 7).[7] In this reaction, the free radical species generated via the one-electron reduction by the nickel complex binds to the nickel center with the help of the directing group in the radical intermediate, resulting in highly enantioselective coupling reactions. Subsequently, various asymmetric nickel-catalyzed radical reactions utilizing directing groups were developed, mainly by the Fu group.[8]

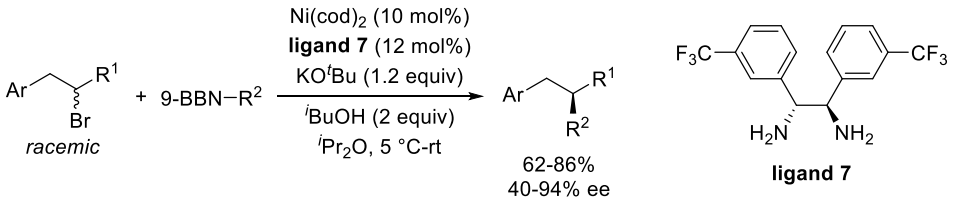


**Scheme 7.** Asymmetric Suzuki Cross-Coupling Reaction using the Directing Group Strategy

Zhang and co-workers demonstrated a highly stereoselective radical-mediated cyclization of diazo esters by exploiting a catalytic amount of cobalt complex **8** which has a chiral porphyrin ligand in 2015 (Scheme 8).[9] In this asymmetric metalloradical-catalyzed reaction, the radical substitution reaction between benzylic radicals generated by intramolecular hydrogen-atom abstraction and the Co(III)-alkyl complex yields optically-active cyclized products.

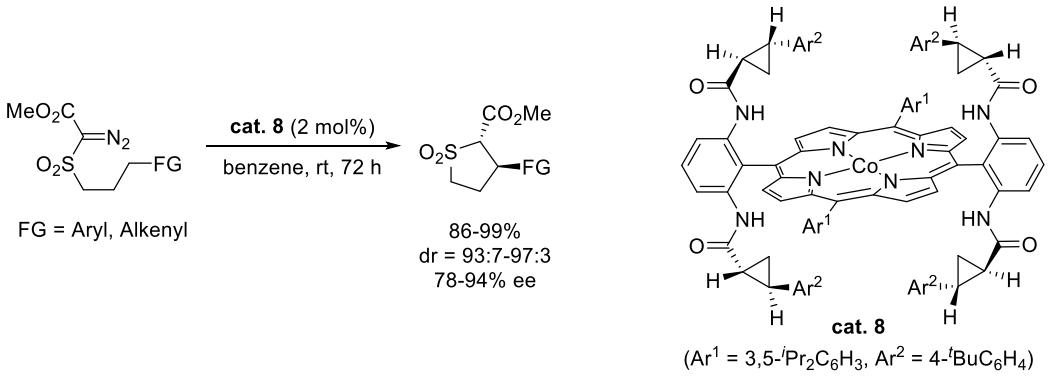


**Scheme 8.** Enantioselective Radical C–H Alkylation Reaction via Metalloradical Catalysis

## 1.1.4. Covalent Organocatalysis in Asymmetric Radical Reactions

Organocatalyzed enantioselective radical bond-forming reactions have undergone a major development with two representative works reported in 2007. Firstly, Sibi *et al.* reported an enantioselective α-oxyamination of aldehydes catalyzed by chiral imidazolidinone **9** (Scheme 9).[10a] Secondary, MacMillan and co-workers showed a similar chiral secondary amine **10**-catalyzed highly enantioselective α-allylation of aldehydes (Scheme 10).[10b] The key word in these studies is SOMO activation. They proposed that one-electron oxidation of an enamine generated from an aldehyde and a chiral amine by a photocatalyst with a sacrificial oxidant produces radical cation species, which undergo the stereoselective radical bond-forming reaction. Later, it was found that the reaction reported by Sibi did not proceed through the SOMO activation pathway, but through two-electron enamine catalysis.[11] With the above reports as a trigger, study on asymmetric reactions that combine stoichiometric amounts of sacrificial oxidants and enamine catalysis has been extensively carried out by MacMillan group.[12]

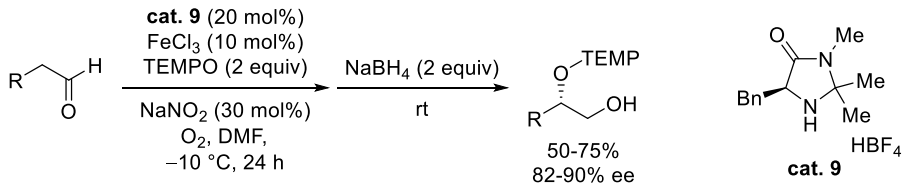


**Scheme 9.** Catalytic Enantioselective α-Oxyamination of Aldehydes

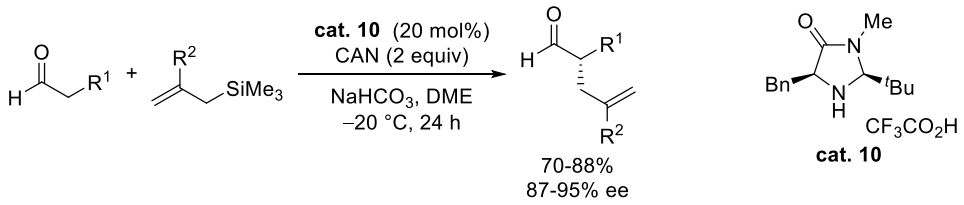


**Scheme 10.** Catalytic Asymmetric α-Allylation of Aldehydes via SOMO Activation

In 2013, Maruoka *et al.* reported an asymmetric radical cyclization reaction of aldehydes using chiral organotin hydride **11** as an radical catalyst (Scheme 11).[13] The system utilizes the addition of the tin radical to the carbonyl oxygen of the substrate to form the organotin alkoxide having a carboradical at its α-position. After the cyclization reaction, the intermediary benzylic radical abstracts hydrogen from **11** and the resulting tin alkoxide undergoes protonation with ethanol to afford the product in moderate stereoselectivity, where the catalyst is regenerated through reduction of the tin ethoxide by diphenylsilane.

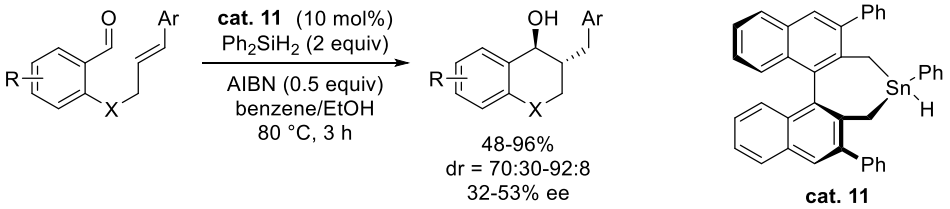


**Scheme 11.** Asymmetric Radical Cyclization Catalyzed by Organotin Hydride

## 1.2. Asymmetric Radical Reactions under Photocatalytic Conditions

The usefulness of light in organic chemical reactions has attracted a high degree of attention from the perspective of green chemistry, as it orients toward the employment of solar energy, an ideal resource. Furthermore, chemical species being generated by energy or electron transfer from photocatalysts are usually radical intermediates with open-shell electronic structures, which may lead to new chemical transformations that are not possible in ionic reactions. Here, the author will introduce asymmetric radical reactions under photocatalytic conditions, which have been developing rapidly in recent years.[14]

### 1.2.1. Covalent Organocatalytic Asymmetric Photoreactions

In 2008, MacMillan and Nicewictz reported the first direct enantioselective α-alkylation reaction of aliphatic aldehydes using photoredox catalyst, $[Ru(bpy)_3]Cl_2$, in combination with imidazolidinone organocatalyst **12** (Scheme 12).[15]

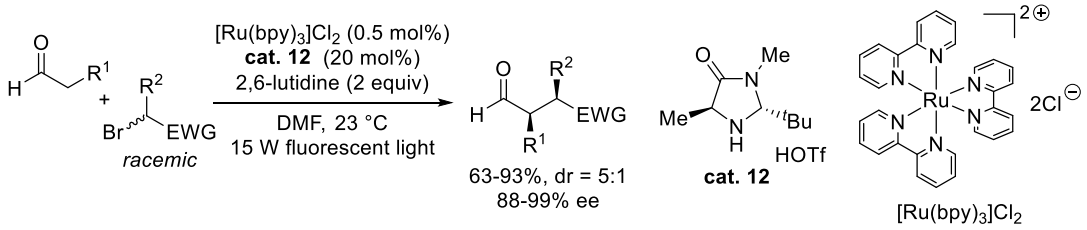


**Scheme 12.** Asymmetric α-Alkylation of Aldehydes under Photoredox Conditions

In 2012, Jang and co-workers introduced a system that combines iminium catalysis with the SOMO activation strategy, which was proposed by MacMillan in 2007,[10b] into asymmetric radical reactions under photoredox conditions (Scheme 13).[16a] Furthermore, in 2017, a chiral secondary amine- and photoinduced SOMO-catalyzed α-alkylation reaction of aldehydes was reported by MacMillan *et al.*, and it relies on a multi-catalytic system consisting of an organocatalyst **14**, an iridium photocatalyst, and a hydrogen atom transfer (HAT) catalyst (Scheme 14).[16b] In these systems, the 3π-enaminyl radical being produced by the photooxidation of the enamine is trapped by TEMPO or an olefin coupling partner, respectively, and facilitates stereoselective radical bond formations.

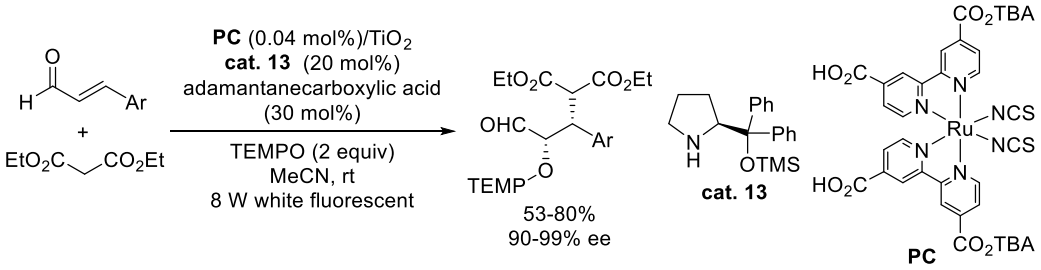


**Scheme 13.** Asymmetric Tandem Michael Addition/Oxyamination of Enals via Photo-SOMO Activation

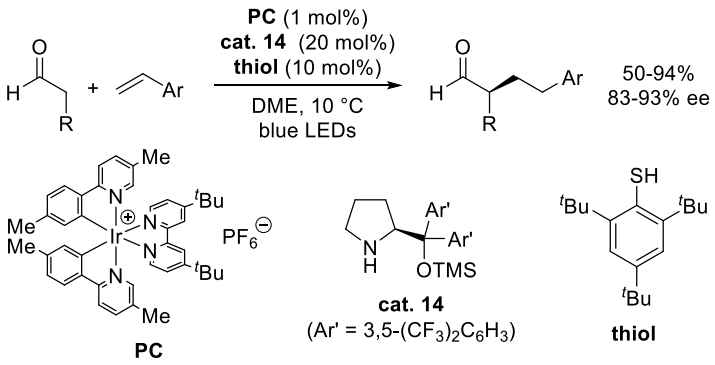


**Scheme 14.** Asymmetric α-Alkylation Reaction of Aldehydes via Photo-SOMO Activation

While the previously described reports by MacMillan and co-workers employ enamine or iminium species in the ground state,[15,16b] Melchiorre *et al.* found that certain iminium and enamine species can undergo photoexcitation to promote single electron transfer and generate free radical intermediates via formation of an electron donor-acceptor (EDA) complex. In the system reported in 2013, electron transfer is facilitated by light absorption of an EDA complex between an electron-deficient alkyl halide and an electron-rich chiral enamine intermediate (Scheme 15).[17] In 2017, the same group also reported the enantioselective β-alkylation of enals by radical species, in which an electron-deficient chiral iminium ion can act as a potent single-electron oxidant upon direct excitation by light irradiation (Scheme 16).[18]

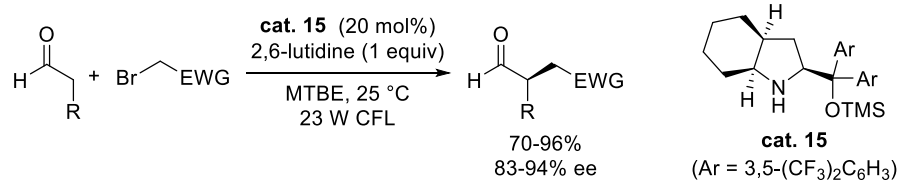


**Scheme 15.** Asymmetric Photochemical α-Alkylation of Aldehydes via an EDA Complex

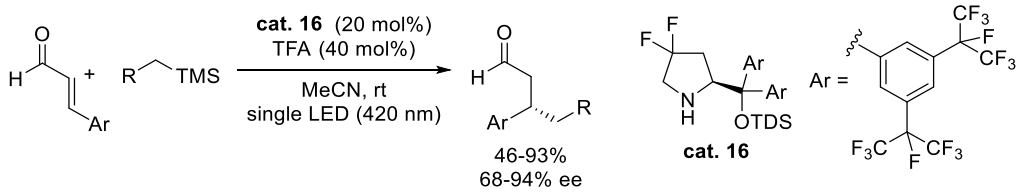


**Scheme 16.** Catalytic Asymmetric β-Alkylation of Enals through Excitation of Iminium Ions

As an asymmetric radical reaction using other covalent organocatalyst, an optically active thiyl radical-catalyzed stereoselective cyclization should be mentioned. In 2014, Maruoka and co-workers reported a highly diastereo- and enantioselective radical cycloaddition reaction exploiting a precisely designed chiral thiol **17** as a precatalyst (Scheme 17).[19] Although the reaction system does not associate with photocatalysis, they use light energy to generate a radical species that is served as an initiator.

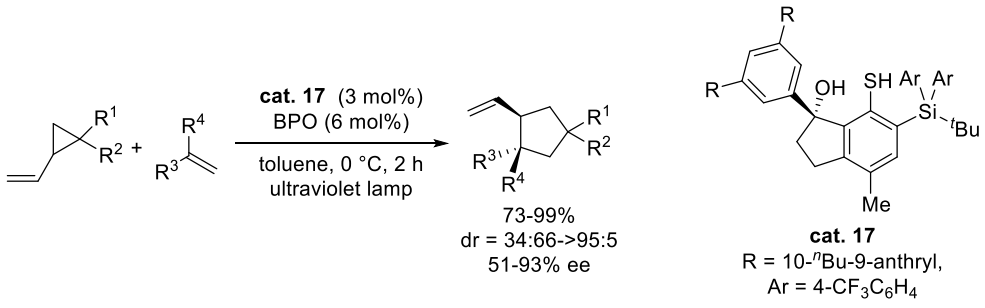


**Scheme 17.** Chiral Thiyl Radical-Catalyzed Asymmetric Cycloaddition Reaction

## 1.2.2. Chiral Lewis Acid Coordination in Photoreactions

Chiral Lewis acid-catalyzed asymmetric control of radical reactions has also been performed under photoreaction conditions. In 2010, Bach *et al.* reported an enantioselective intramolecular [2+2] photocycloaddition using $AlBr_3$-activated oxazaborolidine **18** as a chiral Lewis acid catalyst (Scheme 18).[20] However, due to the high energy light irradiation, the background reaction could not be suppressed and a substoichiometric amount of catalyst was required for attaining a highly enantioselective reaction.

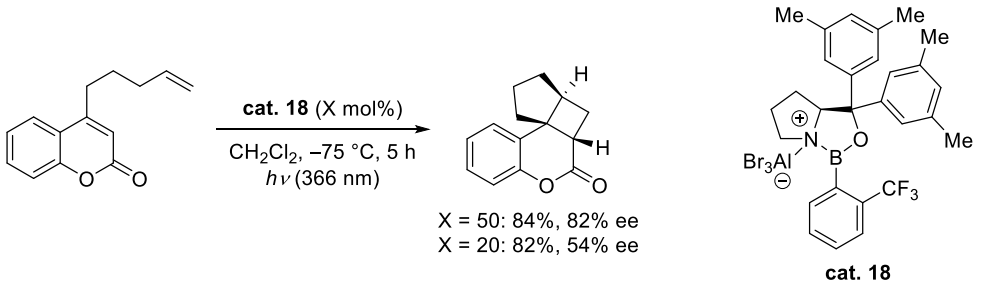


**Scheme 18.** Chiral Lewis Acid-Catalyzed Intramolecular [2+2] Photocycloaddition Reaction

In 2014, Yoon *et al.* combined the chiral Lewis acid-coordination strategy with photocatalysis to achieve an highly enantioselective radical cycloaddition reaction under mild conditions (Scheme 19).[21] Racemic background reaction was suppressed because the coordination of the Lewis acid to the substrate significantly accelerated a one-electron transfer from the photocatalyst.

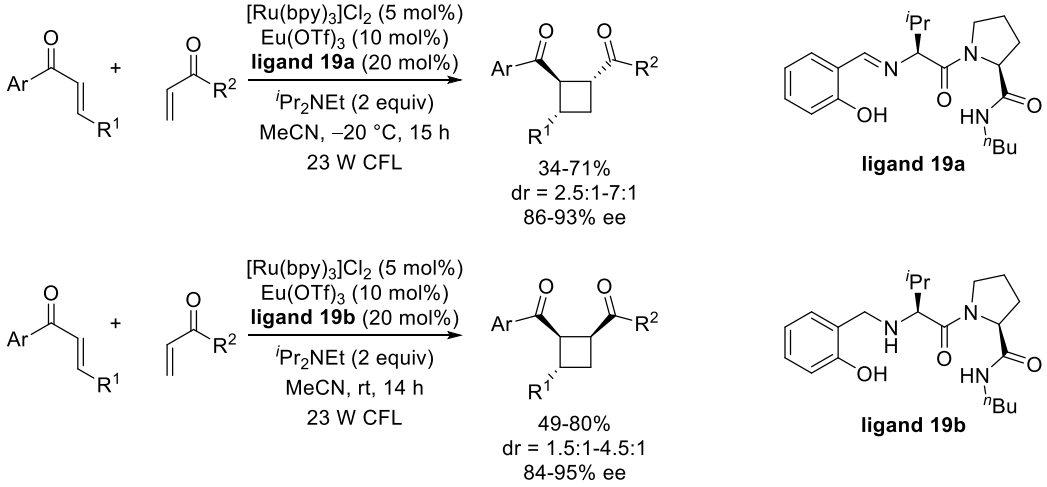


**Scheme 19.** Asymmetric Intramolecular [2+2] Photocycloaddition Reaction using Visible Light

A new strategy for enantioselective photoredox catalysis was reported by Meggers in 2014 (Scheme 20).[22] A chiral-at-metal iridium complex **20** simultaneously acted as a photoredox catalyst and a chiral Lewis acid.

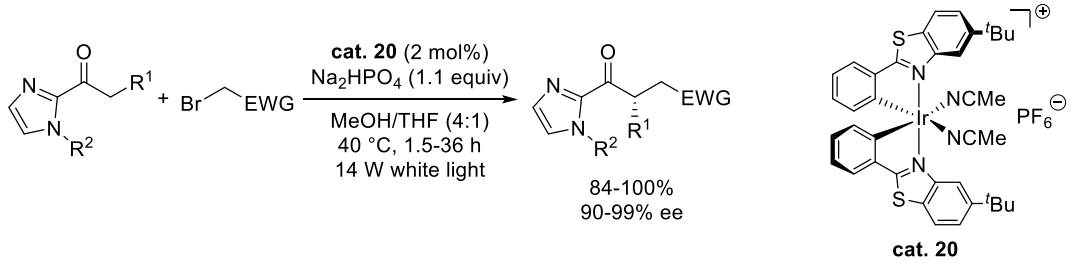


**Scheme 20.** Photocatalytic α-Alkylation of 2-Acyl Imidazoles using Chiral Iridium Complexes

## 1.2.3. Asymmetric Photocatalysis using Non-Covalent Interactions

### 1.2.3.1. Hydrogen-Bonding Templates in Asymmetric Photocatalysis

In 2005, Bach and co-workers demonstrated the first practical enantioselective photocatalytic reaction using organocatalyst **21** that was served as both a photosensitizer and a chiral hydrogen-bonding template (Scheme 21).[23a] Furthermore, the same group reported an enantioselective intramolecular [2+2] photocycloaddition catalyzed by an improved-chiral hydrogen-bonding organophotosensitizer **22** in 2009, which was promoted via an energy-transfer mechanism under ultraviolet irradiation (Scheme 22).[23b] These reports led to the active study of highly stereoselective photocatalytic reactions using various chiral hydrogen-bonding template catalysts.[24]

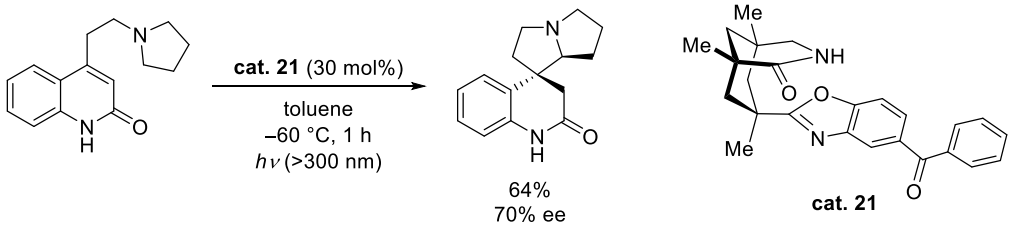


**Scheme 21.** Catalytic Enantioselective Photoreaction using Hydrogen-Bonding Templates

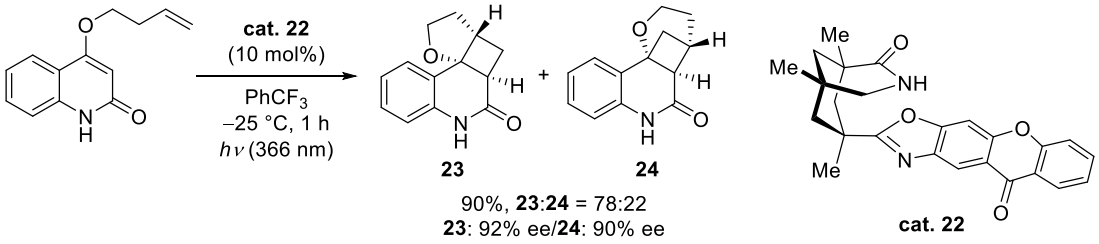


**Scheme 22.** Chiral Hydrogen-Bonding Templates-Catalyzed Asymmetric Photocycloaddition

### 1.2.3.2. Asymmetric Phase-Transfer Catalysis in Photoreactions

Chiral cations such as cinchona alkaloids-derived ammonium ions have been widely used for controlling anionic intermediates and their most prominent function is catalytic activity under

phase-transfer conditions.[25] In 2015, Melchiorre *et al.* demonstrated that chiral cationic phase-transfer catalyst **25** was effective in controlling an enantioselective radical perfluoroalkylation of β-ketoesters (Scheme 23).[26] Proposed reaction mechanism was that an enolate ion paired with the cinchonine-derived ammonium ion **25** forms an electron donor-acceptor complex with perfluoroalkyl iodide and subsequent white LED irradiation causes a one-electron transfer to produce the perfluoroalkyl radical, which reacts with another chiral ammonium enolate to furnish enantiomerically enriched products.[27]

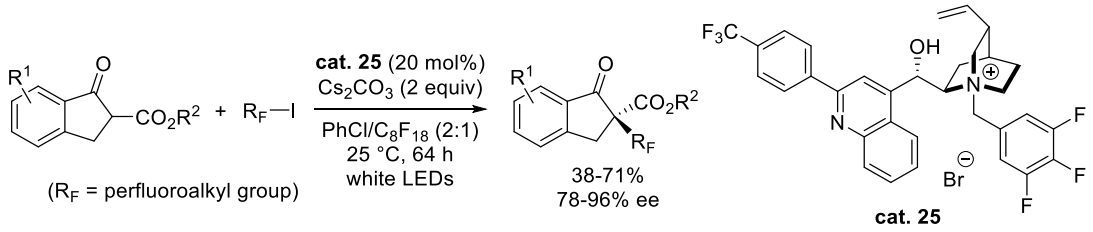


**Scheme 23.** Photo-Organocatalytic Asymmetric Perfluoroalkylation of Cyclic β-Ketoesters

### 1.2.3.3. Chiral Brønsted Acid Catalysis in Asymmetric Photoreactions

In 2013, the first example of asymmetric photocatalysis combined with a chiral Brønsted acid was reported by Knowles and co-workers as an enantioselective aza-pinacol coupling reaction (Scheme 24).[28] This highly stereoselective intramolecular cyclization of a ketone and a hydrazone functional groups has been attained by exploiting the hydrogen-bonding interaction between the chiral phosphate ion of **26** and the ketyl radical intermediate generated via a concerted proton-coupled electron transfer (PCET) .

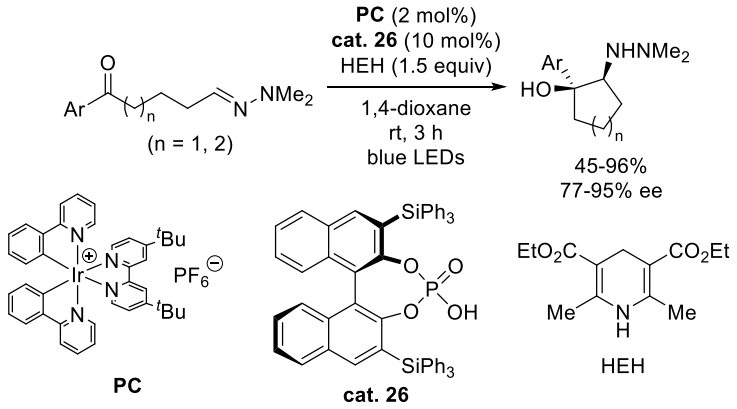


**Scheme 24.** Catalytic Asymmetric Aza-Pinacol Cyclization via a PCET Process

Ooi *et al.* established a highly stereoselective synthesis of 1,2-diamines via redox-neutral coupling of *N*-arylaminomethanes and *N*-Ms aromatic aldimines with the cooperation of a iridium photocatalyst and a chiral ionic Brønsted acid catalyst **27** under white LEDs irradiation in 2015 (Scheme 25).[29a] The enantio-determining step is proposed to be a radical-radical coupling reaction

between the neutral α-amino methyl radical and the radical anion of the imine recognized by the cationic chiral phosphonium salt. It was later demonstrated that a complementary electron transfer, the catalytic cycle initiated by oxidative quenching of the excited photosensitizer, was also feasible, suggesting that the order of the redox events is not critical for this highly enantioselective coupling.[29b]

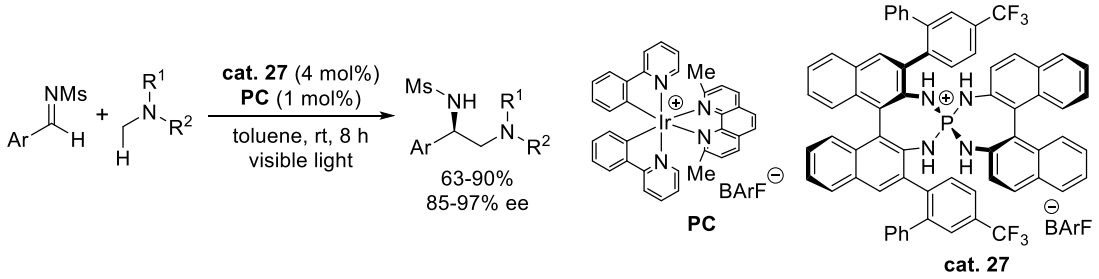


**Scheme 25.** Asymmetric α-Coupling of *N*-Arylaminomethanes with Imines

In 2018, Phipps and co-workers reported a catalytic asymmetric Minisci-type radical addition of *N*-acyl α-amino alkyl radicals generated from the corresponding redox-active esters to pyridines and quinolines by fusion of a photocatalyst and chiral Brønsted acid catalysts **28** (Scheme 26).[30a] At about the same time, a photocatalytic stereoselective radical coupling reaction between α-amino alkyl radicals derived from *N*-aryl amino acids and α-ketoradicals generated by one-electron reduction of α-bromo ketones was reported by Jiang and co-workers (Scheme 27).[30b] With these reports as a turning point, a lot of asymmetric radical reactions combining chiral phosphoric acid catalysts and photosensitizers have been reported.[31]

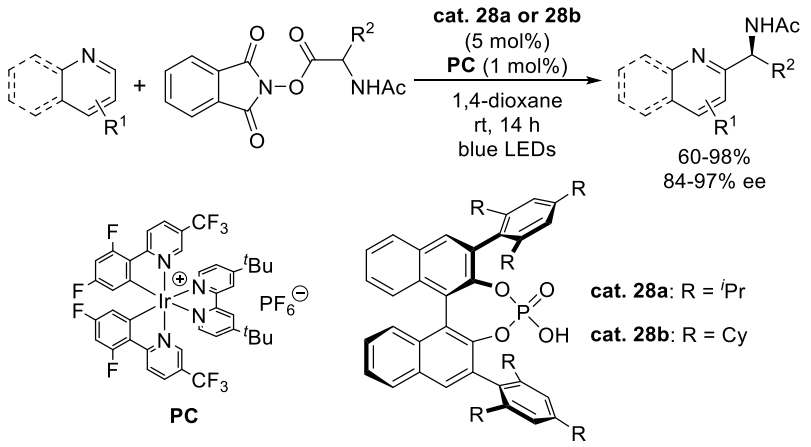


**Scheme 26.** Catalytic Asymmetric Minisci-Type Radical Addition under Photoredox Conditions

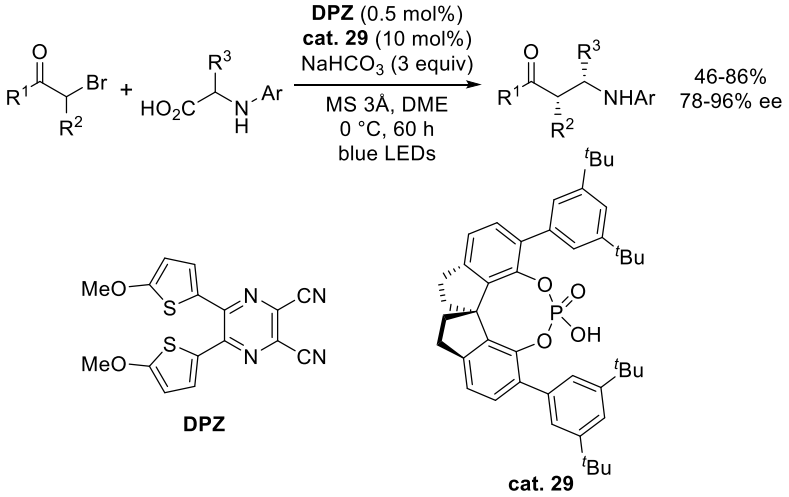


**Scheme 27.** Catalytic Enantioselective Photoredox Radical Coupling Reaction

## 1.2.3.4. Asymmetric Photoreactions using Chiral Anionic Catalysts

The first application of chiral anionic catalysts being aimed at the control of cationic radical intermediates under photocatalytic reaction condition was reported by Luo *et al.* in 2017 (Scheme 28).[32] They developed a moderately enantioselective intramolecular hydroetherification reaction using a chiral ion-pair photocatalyst **30** that consists of an acridinium ion as a photosensitizer and a chiral phosphate ion. In 2018, Nicewicz and co-workers demonstrated that a chiral *N*-triflyl phosphoramide anion and a pyrillium oxide salt could be used as an ion-paired photosensitizer **31** to induce moderate enantioselectivity in the Diels-Alder reaction via radical cation intermediates under visible light irradiation conditions (Scheme 29).[33]

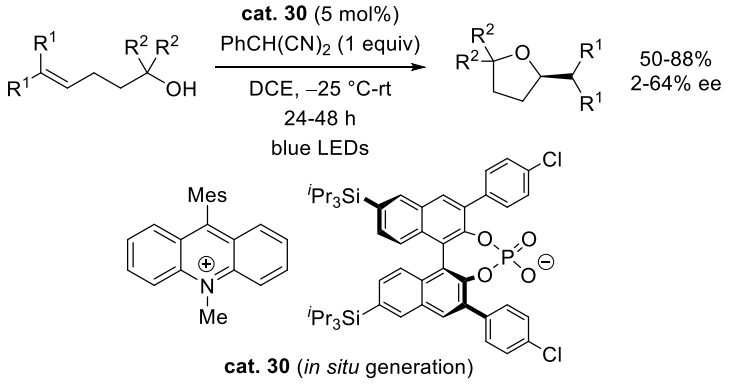


**Scheme 28.** Asymmetric Hydroetherification using Chiral Ion-Pair Photoredox Organocatalyst

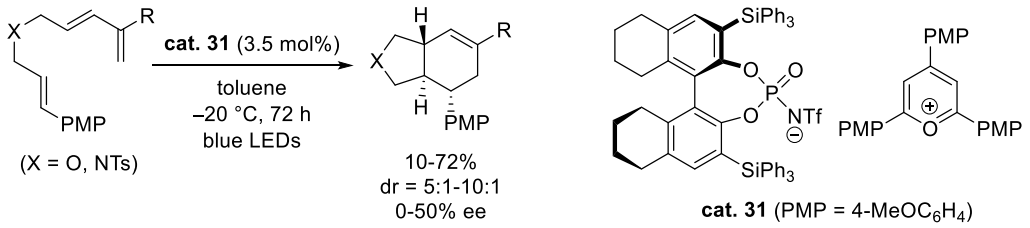


**Scheme 29.** Radical-Cation Diels-Alder Reaction Catalyzed by Chiral Pyrilium-*N*-triflyl Phosphoramide Salt

On the other hand, Knowles and co-workers showed that a distonic radical cation of indole derivatives generated via PCET could be precisely controlled by a chiral phosphate ion to afford chiral indoline derivatives in highly enantioselective manner (Scheme 30).[34]

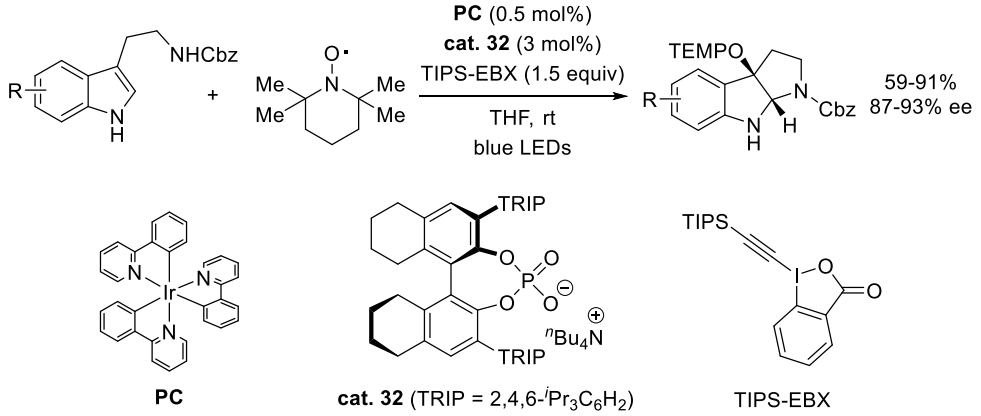


**Scheme 30.** Catalytic Control of Indole Radical Cations under Photoredox Conditions

In 2020, the author developed a highly stereoselective [3+2] radical photocycloaddition of a cyclopropyl urea and α-alkyl styrenes by using photocatalytically-active chiral ion pair **33** consisting of $Ir(dFCF_3ppy)_2(dtbbpy)^+$ and a chiral borate (Scheme 31).[35a] The key of the high enantioselectivity was proposed to be the directing group strategy for controlling a distonic radical cation intermediate through formation of hydrogen-bonding complex of the substrate and the chiral borate ion. Subsequently, asymmetric synthesis of 5-membered alicyclic β-amino acids under the similar photocatalytic system was also established by the same group in 2021 (Scheme 32).[35b] These reports indicate that the control of distonic radical-cation intermediates by chiral anions under photocatalytic reaction conditions is a practical methodology.

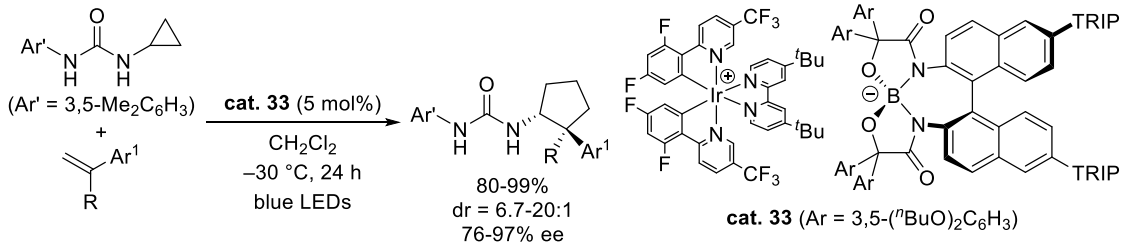


**Scheme 31.** Highly Stereoselective [3+2] Radical Cycloaddition Reaction under Asymmetric Photocatalysis

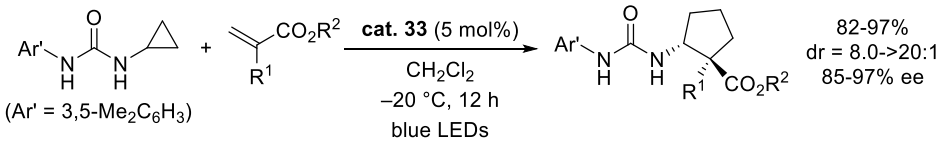


**Scheme 32.** Catalytic Asymmetric Synthesis of 5-membered alicyclic β-amino acids via [3+2] Photocycloaddition of α-Substituted Acrylates

Knowles group showed that the *N*-centered sulfonamidyl radical generated by PCET oxidation with the help of a chiral phosphate ion of **34** could be asymmetrically recognized by hydrogen-bonding interaction with the in situ-generated chiral phosphoric acid (Scheme 33).[36] Unlike the aforementioned system, this is not a catalytic control of radical cation species by chiral anions, but it provides a new guideline for controlling free radical species.

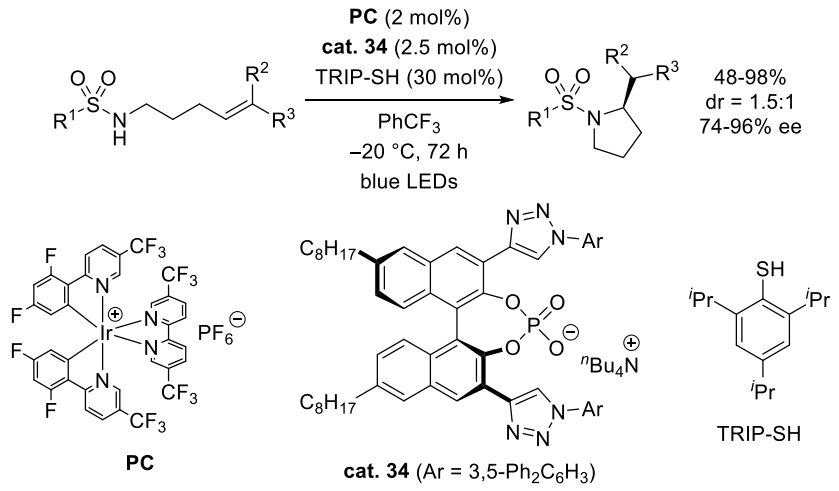


**Scheme 33.** Asymmetric Hydroamination of Alkenes under Photocatalytic Condition

## 1.3. Summary

As explained in the chapter 1, control of enantioselectivity in the photocatalytic radical bond formation processes is a premature and developing research field. In this doctoral thesis, the author developed highly stereoselective reactions by controlling distonic radical cation intermediates using a unique chiral ion-pair photocatalyst under photoredox reaction conditions. Through this doctoral research, which has provided new guidelines for catalytic stereocontrol methods in radical reactions, this field of studies will grow further.

## References


(1) (a) Sibi, M. P.; Porter, N. A. *Acc. Chem. Res.* **1999**, *32*, 163. (b) Sibi, M. P.; Manyem, S.; Zimmerman, J. *Chem. Rev.* **2003**, *103*, 3263.

(2) (a) Sibi, M. P.; Ji, J.; Wu, J. H., Gürtler, S.; Porter, N. A. *J. Am. Chem. Soc.* **1996**, *118*, 9200. (b) Sibi, M. P.; Ji, J. *J. Org. Chem.* **1997**, *62*, 3800.

(3) Haque, M. B.; Roberts, B. P. *Tetrahedron Lett.* **1996**, *37*, 9123.

(4) Blumenstein, M.; Schwarzkopf, K.; Metzger, J. O. *Angew. Chem. lnt. Ed. Engl.* **1997**, *36*, 235.

(5) Gansäuer, A.; Lauterbach, T.; Bluhm, H.; Noltemeyer, M. *Angew. Chem. Int. Ed.* **1999**, 38, 2909.

(6) Dunlap, M. S.; Nicholas, K. M. *Synth. Commun.* **1999**, *29*, 1097.

(7) Saito, B.; Fu, G. C. *J. Am. Chem. Soc.* **2008**, *130*, 6694.

(8) (a) Owston, N. A.; Fu, G. C. *J. Am. Chem. Soc.* **2010**, 132, 11908. (b) Lu, Z.; Wilsily, A.; Fu, G. C. *J. Am. Chem. Soc.* **2011**, *133*, 8154. (c) Wilsily, A.; Tramutola, F.; Owston, N. A.; Fu, G. C. *J. Am. Chem. Soc.* **2012**, *134*, 5794. (e) Jiang, X.; Gandelman, M. *J. Am. Chem. Soc.* **2015**, *137*, 2542. (f) Pezzetta, C.; Bonifazi, D.; Davidson, R. W. M. *Org. Lett.* **2019**, *21*, 8957.

(9) (a) Cui, X.; Xu, X.; Jin, L.-M.; Wojtas, L.; Zhang, X. P. *Chem. Sci.* **2015**, *6*, 1219. (b) Lu, H.; Dzik, W. I.; Xu, X.; Wojtas, L.; de Bruin, B.; Zhang, X. P. *J. Am. Chem. Soc.* **2011**, *133*, 8518.

(10) (a) Sibi, M. P.; Hasegawa, M. *J. Am. Chem. Soc.* **2007**, *129*, 4124. (b) Beeson, T. D.; Mastrachhio, A.; Hong, J.-B.; Ashton, K.; MacMillan, D. W. C. *Science* **2007**, *316*, 582.

(11) Van Humbeck, J. F.; Simonovich, S. P.; Knowles, R. R.; MacMillan, D. W. C. *J. Am. Chem. Soc.* **2010**, *132*, 10012.

(12) For selected examples of catalytic asymmetric α-functionalization of aldehydes via SOMO activation, see: (a) Jang, H.-Y.; Hong, J.-B.; MacMillan, D. W. C. *J. Am. Chem. Soc.* **2007**, *129*, 7004. (b) Kim, H.; MacMillan, D. W. C. *J. Am. Chem. Soc.* **2008**, *130*, 398. (c) Graham, T. H.; Jones, C. M.; Jui, N. T.; MacMillan, D. W. C. *J. Am. Chem. Soc.* **2008**, *130*, 16494. (d) Wilson, J. E.; Casarez, A. D.; MacMillan, D. W. C. *J. Am. Chem. Soc.* **2009**, *131*, 11332. (e) Conrad, J. C.; Kong, J.; Laforteza, B. N.; MacMillan, D. W. C. *J. Am. Chem. Soc.* **2009**, *131*, 11640. (f) Rendler, S.; MacMillan, D. W. C. *J. Am. Chem. Soc.* **2010**, *132*, 5027. (g) Pham, P. V.; Ashton, K.; MacMillan, D. W. C. *Chem. Sci.* **2011**, *2*, 1470. (h) Comito, R. J.; Finelli, F. G.; MacMillan, D. W. C. *J. Am. Chem. Soc.* **2013**, *135*, 9358.

(13) Shirakawa, S.; Usui, A.; Kan, S. B. J.; Maruoka, K. *Asian J. Org. Chem.* **2013**, *2*, 916.

(14) (a) Wang, C.; Lu, Z. *Org. Chem. Front.* **2015**, *2*, 179. (b) Meggers, E. *Chem. Commun.* **2015**, *51*, 3290. (c) Brimioulle, R.; Lenhart, D.; Maturi, M. M.; Bach, T. *Angew. Chem. Int. Ed.* **2015**, *54*, 3872. (d) Miyabe, H.; Kawashima, A.; Yoshioka, E.; Kohtani, S. *Chem. - Eur. J.* **2017**, *23*, 6225–6236. (e) Silvi, M.; Melchiorre, P. *Nature* **2018**, *554*, 41. (f) Garrido-Castro, A.

F.; Maestro, M. C.; Alemán, J. *Tetrahedron Lett.* **2018**, *59*, 1286. (g) Jiang, C.; Chen, W.; Zheng, W.-H.; Lu, H. *Org. Biomol. Chem.* **2019**, *17*, 8673. (h) Hong, B.-C. *Org. Biomol. Chem.* **2020**, *18*, 4298. (i) Saha, D. *Chem. - Asian J.* **2020**, *15*, 2129. (j) Rigotti, T.; Alemán, J. *Chem. Commun.* **2020**, *56*, 11169. (k) Proctor, R. S. J.; Colgan, A. C.; Phipps, R. J. *Nat. Chem.* **2020**, *12*, 990.

(15) Nicewicz, D. A.; MacMillan, D. W. C. *Science* **2008**, *322*, 77.

(16) (a) Yoon, H.-S.; Ho, X.-H.; Jang, J.; Lee, H.-J.; Kim, S.-J.; Jang, H.-Y. *Org. Lett.* **2012**, *14*, 3272. (b) Capacci, A. G.; Malinowski, J. T.; McAlpine, N. J.; Kuhne, J.; MacMillan, D. W. C. *Nat. Chem.* **2017**, *9*, 1073.

(17) Arceo, E.; Jurberg, I. D.; Álvarez-Fernández, A.; Melchiorre, P. *Nat. Chem.* **2013**, *5*, 750.

(18) Silvi, M.; Verrier, C.; Rey, Y. P.; Buzzetti, L.; Melchiorre, P. *Nat. Chem.* **2017**, *9*, 868.

(19) Hashimoto, T.; Kawamata, Y.; Maruoka, K. *Nat. Chem.* **2014**, *6*, 702

(20) Guo, H.; Herdtweck, E.; Bach, T. *Angew. Chem. Int. Ed.* **2010**, *49*, 7782.

(21) Du, J.; Skubi, K. L.; Schultz, D. M.; Yoon, T. P. *Science* **2014**, *344*, 392.

(22) Huo, H.; Shen, X.; Wang, C.; Zhang, L.; Röse, P.; Chen, L.-A.; Harms, K.; Marsch, M.; Hilt, G.; Meggers, E. *Nature* **2014**, *515*, 100.

(23) (a) Bauer , A.; Westkämper , F.; Grimme, S.; Bach, T. *Nature* **2005**, *436*, 1139. (b) Müller, C.; Bauer, A.; Bach, T. *Angew. Chem. Int. Ed.* **2009**, *48*, 6640.

(24) For selected examples of asymmetric photoreactions catalyzed by hydrogen-bonding templates, see: (a) Vallavoju, N.; Selvakumar, S.; Jockusch, S.; Sibi, M. P.; Sivaguru, J. *Angew. Chem. Int. Ed.* **2014**, *53*, 5604. (b) Alonso, R.; Bach, T. *Angew. Chem. Int. Ed.* **2014**, *53*, 4368. (c) Tröster, A.; Alonso, R.; Bauer, A.; Bach, T. *J. Am. Chem. Soc.* **2016**, *138*, 7808. (d) Skubi, K. L.; Kidd, J. B.; Jung, H.; Guzei, I. A.; Baik, M.-H.; Yoon, T. P. *J. Am. Chem. Soc.* **2017**, *139*, 17186. (e) Hölzl-Hobmeier, A.; Bauer, A.; Silva, A. V.; Huber, S. M.; Bannwarth, C.; Bach, T. *Nature* **2018**, *564*, 240.

(25) Shirakawa, S.; Maruoka, K. *Angew. Chem. Int. Ed.* **2013**, *52*, 4312.

(26) Woźniak, Ł.; Murphy, J. J.; Melchiorre, P. *J. Am. Chem. Soc.* **2015**, *137*, 5678.

(27) Yang, C.; Zhang, W.; Li, Y.-H.; Xue, X.-S.; Li, X.; Cheng, J.-P. *J. Org. Chem.* **2017**, *82*, 9321.

(28) Rono, L. J.; Yayla, H. G.; Wang, D. Y.; Armstrong, M. F.; Knowles, R. R. *J. Am. Chem. Soc.* **2013**, *135*, 17735.

(29) (a) Uraguchi, D.; Kinoshita, N.; Kizu, T.; Ooi, T. *J. Am. Chem. Soc.* **2015**, *137*, 13768. (b) Kizu, T.; Uraguchi, D.; Ooi, T. *J. Org. Chem.* **2016**, *81*, 6953.

(30) (a) Proctor, R. S. J.; Davis, H. J.; Phipps, R. J. *Science* **2018**, *360*, 419. (b) Li, J.; Kong, M.; Qiao, B.; Lee, R.; Zhao, X.; Jiang, Z. *Nat. Commun.* **2018**, *9*, 2445.

(31) For selected examples of asymmetric radical reactions combining chiral phosphoric acids and photocatalysts, see: (a) Liu, X.; Liu, Y.; Chai, G.; Qiao, B.; Zhao, X.; Jiang, Z. *Org. Lett.* **2018**,

*20*, 6298. (b) Liu, Y.; Liu, X.; Li, J.; Zhao, X.; Qiao, B.; Jiang, Z. *Chem. Sci.* **2018**, *9*, 8094. (c) Cao, K.; Tan, S. M.; Lee, R.; Yang, S.; Jia, H.; Zhao, X.; Qiao, B.; Jiang, Z. *J. Am. Chem. Soc.* **2019**, *141*, 5437. (d) Zheng, D.; Studer, A. *Angew. Chem. Int. Ed.* **2019**, *58*, 15803. (e) Feng, A.; Yang, Y.; Liu, Y.; Geng, C.; Zhu, R.; Zhang, D. *J. Org. Chem.* **2020**, *85*, 7207. (f) Yin, Y.; Li, Y.; Gonçalves, T. P.; Zhan, Q.; Wang, G.; Zhao, X.; Qiao, B.; Huang, K.-W.; Jiang, Z. *J. Am. Chem. Soc.* **2020**, *142*, 19451.

(32) Yang, Z.; Li, H.; Li, S.; Zhang, M.-T.; Luo, S. *Org. Chem. Front.* **2017**, *4*, 1037.

(33) Morse, P. D.; Nguyen, T. M.; Cruz, C. L.; Nicewicz, D. A. *Tetrahedron* **2018**, *74*, 3266.

(34) Gentry, E. C.; Rono, L. J.; Hale, M. E.; Matsuura, R.; Knowles, R. R. *J. Am. Chem. Soc.* **2018**, *140*, 3394.

(35) (a) Uraguchi, D.; Kimura, Y.; Ueoka, F.; Ooi, T. *J. Am. Chem. Soc.* **2020**, *142*, 19462. (b) Kimura, Y.; Uraguchi, D.; Ooi, T. *Org. Biomol. Chem.* **2021**, *19*, 1744.

(36) Roos, C. B.; Demaerel, J.; Graff, D. E.; Knowles, R. R. *J. Am. Chem. Soc.* **2020**, *142*, 5974.

# Chapter 2

## Urea as a Redox-Active Directing Group under Asymmetric Photocatalysis of Iridium-Chiral Borate Ion Pairs

**Abstract:**

The development of a photoinduced, highly diastereo- and enantioselective [3 + 2]-cycloaddition of *N*-cyclopropylurea with α-alkylstyrenes is reported. This asymmetric radical cycloaddition relies on the strategic placement of urea on cyclopropylamine as a redox-active directing group (DG) with anion-binding ability and the use of an ion pair, comprising an iridium polypyridyl complex and a weakly coordinating chiral borate ion, as a photocatalyst. The structure of the anion component of the catalyst governs reactivity, and pertinent structural modification of the borate ion enables high levels of catalytic activity and stereocontrol. This system tolerates a range of α-alkylstyrenes and hence offers rapid access to various aminocyclopentanes with contiguous tertiary and quaternary stereocenters, as the urea DG is readily removable.

## 2.1. Introduction

Directing groups (DGs) are commonly polar functional groups situated in the vicinity of the reaction site of the substrate and are expected to participate in attractive or repulsive nonbonding interactions with reagents or catalysts, which often plays a pivotal role in accelerating/retarding the ensuing bond formation, as well as dictating regio- and stereochemical outcomes.[1] The use of DGs is a traditional strategy, yet among the most reliable for attaining otherwise difficult reactivity and selectivity in metal-mediated/catalyzed transformations and other polar reactions to access structurally and stereochemically defined organic molecules (Figure 1a). In contrast, the utility of DGs in radical chemistry remains obscure. In fact, although chiral Lewis- and Brønsted-acid catalysis in establishing stereoselective radical reactions has significant implication for the effectiveness of DGs in controlling one-electron-mediated processes,[2] DGs have mainly been utilized for the development of transition metalcatalyzed asymmetric reactions involving radical intermediates.[3,4] In general, the intermolecular forces exploited in DG-assisted selective two-electron processes are deemed less effective when employing DGs to guide the reaction pathway and stereochemistry of highly reactive radical intermediates because they are apt to spontaneously engage in possible bondforming events without assistance (Figure 1b). While this perception mirrors the stringent difficulty in taming radical species for target bond construction, particularly in a catalytic stereoselective manner, the author envisioned that the judicious use of DGs to achieve control over the reactivity and/or selectivity of radical reactions would provide a powerful means to address this important and challenging problem. Considering the difficulty in the precise recognition of radical species by a chiral catalyst and the behavior of chiral acid catalysts in the asymmetric radical reactions,[2] the author sought to develop a system for the generation of a reactive radical intermediate in a molecular assembly built through nonbonding interactions between a chiral catalyst and a substrate bearing an appropriate DG, anticipating the subsequent bond formation to occur without destructing this preorganization. With the advantage of photoinduced generation of radical-ion species in mind, the author conceived a strategic use of DG for anchoring a photocatalyst (PC) to a substrate prior to electron transfer (Figure 1c).[5] For the pursuit of this possibility, the author regarded widely used cationic iridium (Ir)-polypyridyl complexes as a suitable class of PCs because of two considerations: (1) the requisite chiral information can be introduced into the structure of the pairing anion, which would not affect the photocatalytic activity of the PC;[6] (2) the installation of DGs with an anion-recognition ability onto the substrate would ensure its association with the PC. Assuming a case with an electron-rich substrate embedded with such DG functionality, the author reasoned that capturing the chiral anion component of the PC by the DG moiety would form a chiral supramolecular ion pair. Upon light irradiation, single-electron transfer (SET) from the substrate to the accompanying excited-state cationic Ir complex could

generate the corresponding radical-ion pair with a defined three-dimensional arrangement. This would enable the resultant radical cation to undergo ensuing stereoselective bond formation within the asymmetric environment created by the chiral anion.

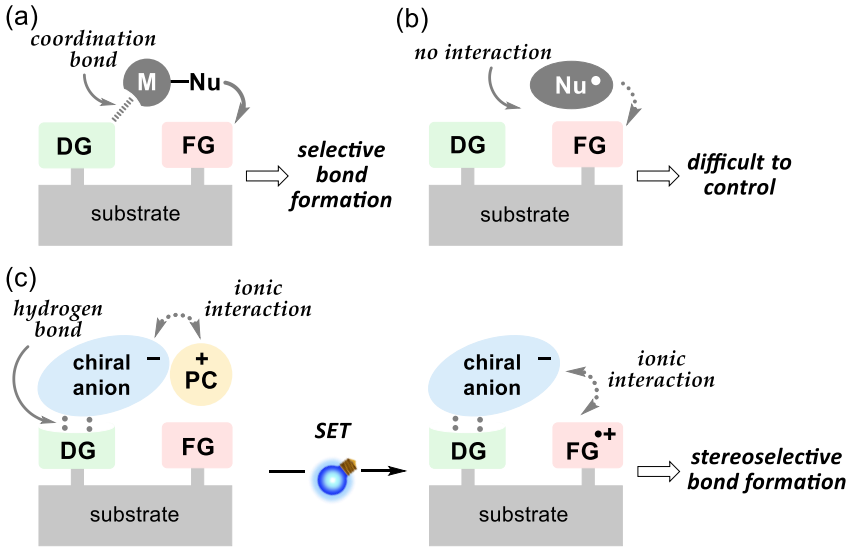


**Figure 1.** Directing-Group (DG) Approach for Stereoselective Transformation. (a) Schematic illustration of DG-Assisted, Metal (M) Reagent-Mediated Ionic Reaction. (b) Difficulty in Radical Reaction. (c) Working Hypothesis of DG Strategy in Photoredox System with Cationic Photocatalyst (PC)-Chiral Anion Ion Pair. FG = functional group to be transformed, Nu = nucleophilic com-ponent, SET = single-electron transfer.

Herein, the author reports the successful operation of this system using urea as an anion-recognizable, redox active DG, and a cationic Ir complex-chiral borate ion pair as a PC in achieving an efficient and highly diastereo- and enantioselective [3 + 2]-cycloaddition of cyclopropylamine with alkenes under visible-light irradiation.

## 2.2. Result and Discussion

To substantiate the hypothesis, the author chose the [3 + 2]-cycloaddition of cyclopropylamines with alkenes as a model reaction,[7−10] which is initiated by single-electron oxidation of the amine reactant, primarily because *N*-carbamoylation of the amine readily sets the urea functionality that is expected to act as an oxidizable DG with a distinct anion-binding capability. Importantly, the affinity of the urea moiety toward an anion would be increased in the corresponding radical cation generated via single-electron oxidation by an appropriate PC, such as an Ir-polypyridyl complex. As an anionic component of the PC, the author employed weakly coordinating chiral borate **1**[11,12] (Table 1 scheme) in anticipation that its negligible nucleophilicity would be beneficial for the pairing Ir complex to exert full potential as a PC,[13] while its characteristic as a hydrogen-bond acceptor would allow interaction with the urea moiety. A preparatory step of the presumed reaction pathway is the assembly of the photoactive Ir-chiral borate ion pair, [PC][**1**], and *N*-cyclopropylurea derivative **2** into the supramolecular ion pair [PC] [**1**⊂**2**] (Figure 2). The excitation of the Ir complex $[PC]^+$ with irradiation of visible light followed by SET leads to the generation of the radical-ion pair $[\mathbf{1}\subset\mathbf{2}]^{\bullet}$ with concomitant release of the reduced, noncharged Ir complex [PC]. In this assembly, the radical cation derived from **2** is considered to exist as a formal equilibrium mixture of N-radical cation and distonic radical cation,[14] and the latter would react with alkene **3**. The intermediary alkyl radical would undergo stereoselective five-*exo* cyclization under the guidance of accompanying **1** to afford aminocyclopentane **4** as a form of *N*-radical cation pairing with **1**. After single-electron reduction of the *N*-radical cation by the reduced Ir complex [PC], the desired product **4** is liberated via the transfer of chiral anion **1** to **2** to complete the catalytic cycle. An alternative chain process could also be operative if the *N*-radical cation of **4** acts as an oxidant of **2** to directly generate the key radical-ion pair $[1\subset2]^{\bullet}$ via simultaneous transfer of the hole and **1**, although the same transition-state structure would be involved in the stereo-determining step.

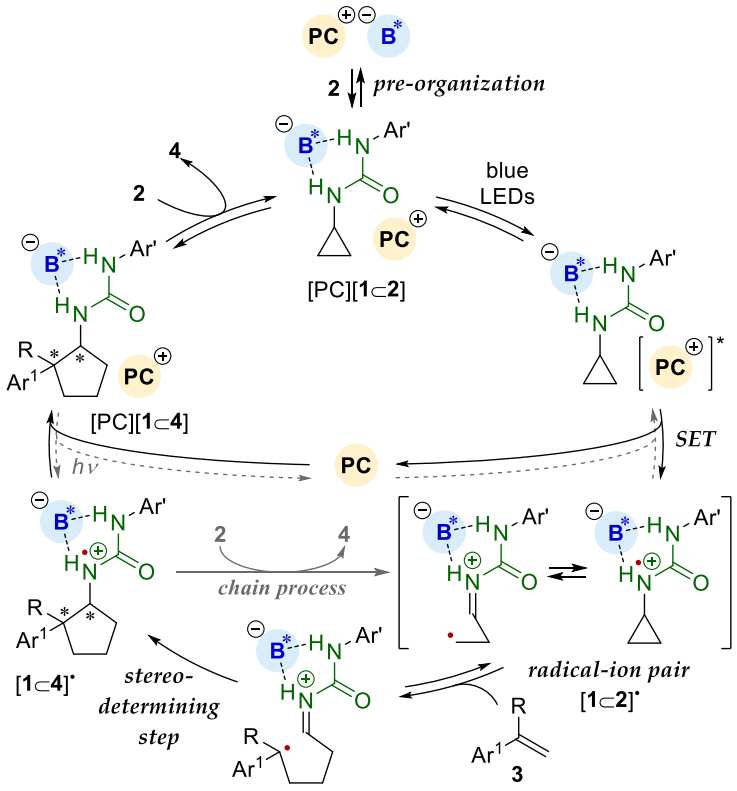


**Figure 2.** Proposed Catalytic Cycle. PC = photocatalyst (chromo-phore), B* = chiral borate ion **1**.

The validity of this mechanistic blueprint was initially assessed by attempting the cycloaddition of 3,5-xylyl cyclopropylurea (**2**) ($E^{ox}$ = 1.37 V vs saturated calomel electrode (SCE)) and α-methylstyrene (**3a**) with a catalytic amount of [*rac*-Ir(dFCF$_3$ppy)$_2$(dtbbpy)][**1a**] (*$E^{red}$ = 1.42 V vs SCE)[15] (5 mol %) in dichloromethane under irradiation with blue LEDs (470 nm) at −30 °C. After stirring for 24 h, the desired [3 + 2]-cycloadduct **4a** was isolated in 40% yield as a mixture of diastereomers (1.6:1), and a certain enantiomeric excess (ee) was detected (18% ee for the major diastereomer) (Table 1, entry 1). Interestingly, the parallel reaction with [*rac*-Ir(dFCF$_3$ppy)$_2$(dtbbpy)][PF$_6$] as the PC under otherwise similar conditions for obtaining racemic **4a** was very sluggish (<10% yield), suggesting that the property of the anionic component of the PC is tightly associated with the reaction efficiency. This observation prompted the author to evaluate the relationship between the anion structure and the catalytic activity of the iridium-based PC by examining the reaction with a series of iridium complexes possessing various anions. This revealed that the reactivity trend was indeed dependent on the anion characteristics (Experimental Section, Table S1). Considering the anion effect reported for ruthenium-based photocatalysis,[13] the author assumed that the observed reactivity difference could be ascribed to the stabilization of the excited-state iridium complex by the counterion and thus the author measured the fluorescence spectrum of each iridium complex. However, all the complexes exhibited essentially identical

spectra (Experimental Section, Figure S1), unlike the case with ruthenium complexes. Therefore, the author considered the influence of the ability of the anion to coordinate with the urea on reactivity and determined the association constants ($K_a$) of the anions with **2** by $^1$H NMR titration experiments (Experimental Section, Figure S2).[16] By plotting the $K_a$ values against cycloaddition conversion, an evident correlation was revealed (Figure 3). While the reaction with the iridium complex bearing a noncoordinating anion afforded very low conversion, the conversion gradually increased as the $K_a$ value increased, reaching a maximum when $K_a$ was approximately 60 $M^{-1}$, and then declined with further increases in $K_a$. Although elucidation of the origin of this profile should await detailed mechanistic studies, one possibility is that the equilibrium between the radical cation of **2** and the corresponding distonic radical cation would favor the distonic form by stabilization of the iminium ion through the formation of hydrogen bonds with the anion of PC. In fact, methylation of one or both of the nitrogen atoms in **2** inhibited the reaction to a significant extent, supporting the relevance of hydrogen-bonding interactions between the anion and **2** (Experimental Section, Table S2).

**Table 1.** Optimization of Reaction Conditions[a]

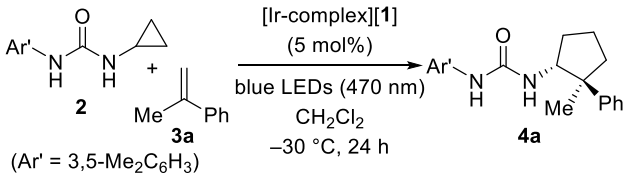


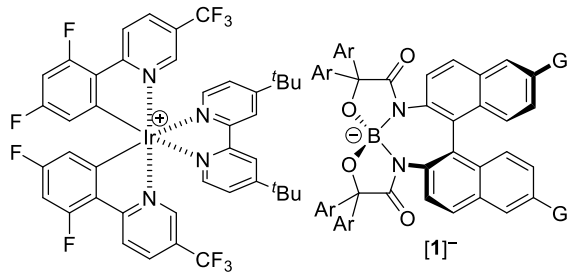


| entry | Ar | G | **1** | yield (%)[b] | dr[c] | ee (%)[d] |
|---|---|---|---|---|---|---|
| 1 | Ph | H | **1a** | 40 | 1.6:1 | 18 |
| 2 | 4-$MeOC_6H_4$ | H | **1b** | 53 | 2.4:1 | 16 |
| 3 | 3,5-$(MeO)_2C_6H_3$ | H | **1c** | 41 | 2.5:1 | 32 |
| 4 | 3,5-($^n$BuO)$_2C_6H_3$ | H | **1d** | 99 | 7.4:1 | 84 |
| 5 | 3,5-($^n$BuO)$_2C_6H_3$ | Ph | **1e** | 95 | 6.7:1 | 81 |
| 6 | 3,5-($^n$BuO)$_2C_6H_3$ | 2,4,6-$Me_3C_6H_2$ | **1f** | 99 | 9.9:1 | 90 |
| 7 | 3,5-($^n$BuO)$_2C_6H_3$ | 2,4,6-$^i$Pr$_3C_6H_2$ | **1g** | 95 | 12:1 | 92 |
| 8[e] | 3,5-($^n$BuO)$_2C_6H_3$ | 2,4,6-$^i$Pr$_3C_6H_2$ | **1g** | 98 | 12:1 | 93 |

[a] Unless otherwise noted, the reaction was performed with **2** (0.1 mmol), **3a** (0.5 mmol), and [*rac*-Ir(dFCF$_3$ppy)$_2$(dtbbpy)][**1**] (5 mol%) in $CH_2Cl_2$ (0.1 M) for 24 h under blue LEDs (470 nm) irradiation at –30 °C. [b] Isolated yield. [c] The diastereomeric ratio (dr) was determined by $^1$H NMR analysis of the crude aliquot. [d] The enantiomeric excess (ee) of the major diastereomer was determined by chiral HPLC. [e] [Δ-Ir(dFCF$_3$ppy)$_2$(dtbbpy)]$^+$ was used as a counterion of **1g**$^-$ instead of the corresponding racemate.

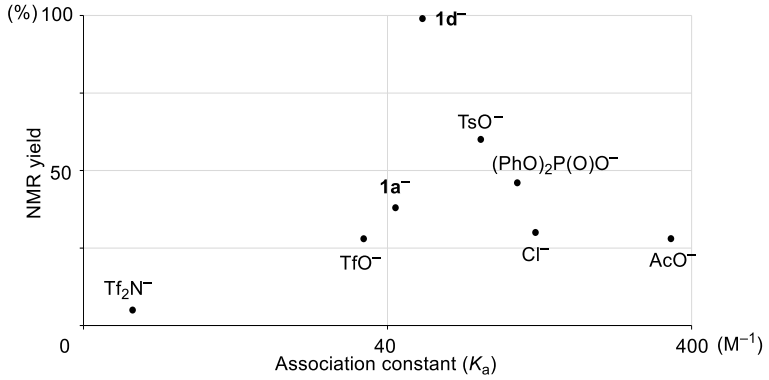


**Figure 3.** Anion Effect on the Correlation between Catalytic Efficiency of [Ir-complex]$^+$ and Association Constant with **2**.

With this information in mind, the author next pursued the structural modification of the borate ion of **1**, as the enantioselectivity of the **1a**-catalyzed reaction was insufficient. The strategy entailed the introduction of electron-donating groups, such as alkoxy groups, to the geminal aromatic substituents (Ar) with the expectation that it would lead to an improvement in both catalytic activity and stereoselectivity. While the effect of attaching 4-methoxyphenyl groups (**1b**) was marginal (entry 2), improved enantioselectivity was attained with **1c** having 3,5-dimethoxyphenyl groups (entry 3). Notably, 3,5-bis-*n*-butoxylphenyl-substituted **1d** exerted significantly higher catalytic activity and stereocontrolling ability, affording **4a** in near quantitative yield with 84% ee for the major diastereomer (entry 4). This distinct relationship between the borate-ion structure and the catalytic performance of the PC prompted the author to obtain the $K_a$ value of **1d**, which was determined to be 52 $M^{-1}$, slightly higher than that of **1a**, as expected. To further improve relative and absolute stereocontrol, the author continued to modify the borate ion by introducing aromatic substituents to the 6,6'-position of the binaphthyl backbone. The installation of sterically demanding 2,4,6-trimethylphenyl appendages (**1f**) was particularly beneficial, compared to that of simple phenyl groups (**1e**) (entries 5 and 6), and **1g**, consisting of a borate ion with 2,4,6-triisopropylphenyl groups, delivered a critical enhancement in diastereo- and enantioselectivity without affecting catalytic activity, enabling the isolation of **4a** in 95% yield with a diastereomeric ratio of 12:1 and 92% ee for the major isomer (entry 7). It should be noted that the chirality of the cationic iridium component played no part in the stereocontrol, as the respective use of *Δ*- and *Λ*-isomers of the iridium complex gave essentially the same results (entry 8 and Experimental Section, Table S2).

Having established the optimal conditions, the scope and limitation of this protocol were explored with a series of α-substituted styrenes. With respect to α-methylstyrenes, incorporation of substituted phenyl groups of different electronic and steric attributes was generally tolerated (Table 2, entries 1−8). Variation of α-alkyl substituents was also feasible (**3j**−**m**) without detrimental impact on the stereochemical outcome (entries 9−12). Moreover, α-alkylstyrenes bearing functional groups were amenable to the present photocatalytic system (entries 13−16). It is noteworthy that aliphatic conjugated diene **3r** was accommodated with a comparable degree of reactivity and selectivity (entry 17), while a certain decrease in enantiocontrol was inevitable in the reaction with simple styrene (**3s**) (entry 18).

**Table 2.** Reaction Scope[a]

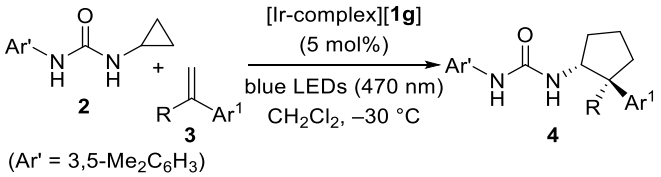


| entry | $Ar^1$, R | **3** | yield (%)[b] | dr[c] | ee (%)[d] | prod (**4**) |
|---|---|---|---|---|---|---|
| 1 | 4-$BrC_6H_4$, Me | **3b** | 98 | 8.4:1 | 94/91 | **4b** |
| 2 | 4-$FC_6H_4$, Me | **3c** | 99 | 6.7:1 | 94/90 | **4c** |
| 3[e] | 4-$Me_3SiC_6H_4$, Me | **3d** | 95 | 12:1 | 92 | **4d** |
| 4 | 4-pin$BC_6H_4$, Me | **3e** | 95 | 14:1 | 93 | **4e** |
| 5 | 3-$BrC_6H_4$, Me | **3f** | 94 | 16:1 | 93 | **4f** |
| 6 | 3-$MeC_6H_4$, Me | **3g** | 96 | 14:1 | 90 | **4g** |
| 7 | 3-$MeOC_6H_4$, Me | **3h** | 99 | 19:1 | 93 | **4h** |
| 8 | 2-$FC_6H_4$, Me | **3i** | 98 | >20:1 | 93 | **4i** |
| 9[e] | Ph, Et | **3j** | 98 | 13:1 | 94 | **4j** |
| 10 | Ph, $(CH_2)_5Me$ | **3k** | 94 | 11:1 | 97 | **4k** |
| 11 | Ph, $^i$Bu | **3l** | 96 | 11:1 | 90 | **4l** |
| 12 | Ph, $CH_2Ph$ | **3m** | 86 | >20:1 | 96 | **4m** |
| 13 | Ph, $(CH_2)_3CH{=}CH_2$ | **3n** | 94 | 13:1 | 96 | **4n** |
| 14 | Ph, $(CH_2)_2Cl$ | **3o** | 95 | >20:1 | 96 | **4o** |
| 15[e] | Ph, $(CH_2)_2OAc$ | **3p** | 80 | 8.3:1 | 88/47 | **4p** |
| 16[e] | Ph, $(CH_2)_2CO_2Me$ | **3q** | 81 | 7.5:1 | 92/48 | **4q** |
| 17 | 2-propenyl, Me | **3r** | 96 | 12:1 | 90 | **4r** |
| 18 | Ph, H | **3s** | 92 | 17:1 | 76 | **4s** |

[a] Unless otherwise noted, the reaction was performed with **2** (0.1 mmol), **3** (0.5 mmol), and [*rac*-Ir(dF$CF_3$ppy)$_2$(dtbbpy)][**1g**] (5 mol%) in $CH_2Cl_2$ (0.1 M) for 24 h under blue LEDs (470 nm) irradiation at –30 °C. [b] Isolated yield. [c] Dr was determined by $^1$H NMR analysis of the crude aliquot. [d] Ee was determined by chiral HPLC. [e] The reaction was conducted at –20 °C.

Finally, the author confirmed that the urea DG could be readily removed using a literature procedure to liberate the primary amine functionality (Scheme 1).[17] Thus, treatment of cycloadduct **4a** (92% ee) with diethylenetriamine at 130 °C for 19 h furnished aminocyclopentane **5** in 86% yield with complete preservation of enantiomeric purity (92% ee).[18]

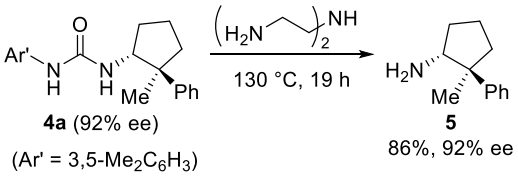


**Scheme 1.** Removal of DG

## 2.3. Conclusion

In conclusion, the author strategically utilizes urea as a redox-active DG with anion-binding ability to achieve photoinduced, highly diastereo- and enantioselective [3 + 2]-cycloaddition of cyclopropylamine with α-alkylstyrenes, which provides access to a series of aminocyclopentanes bearing stereochemically defined, vicinal tertiary and quaternary stereocenters. A key element was the use of an Ir-polypyridyl complex-chiral borate ion pair as the PC. This study clearly demonstrates the effectiveness of the DG approach for controlling radical-mediated bond formations and is expected to stimulate further research endeavors in this direction.

## 2.4. Experimental Section

**General Information:** Infrared spectra were recorded on a Shimadzu IRAffinity-1 spectrometer. $^{1}$H NMR spectra were recorded on a JEOL JNM-ECS400 (400 MHz), JEOL JNM-ECA500II (500 MHz), and JEOL JNM-ECA600II (600 MHz) spectrometers. Chemical shifts are reported in ppm from tetramethylsilane (0.0 ppm) resonance as the internal standard ((CD3)2CO and $CDCl_3$). Data are reported as follows: chemical shift, integration, multiplicity (s = singlet, d = doublet, t = triplet, q = quartet, quin = quintet, sex = sextet, sept = septet, m = multiplet, br = broad) and coupling constants (Hz). $^{13}$C NMR spectra were recorded on a JEOL JNM-ECS400 (101 MHz) spectrometer, JEOL JNM-ECA500II (126 MHz) spectrometer, and JEOL JNM-ECS600 (151 MHz) with complete proton decoupling. Chemical shifts are reported in ppm from the solvent resonance as the internal standard ((CD3)2CO; 29.84 ppm, $CDCl_3$; 77.16 ppm). $^{19}$F NMR spectra were recorded on a JEOL JNM-ECA500II (471 MHz) spectrometer. Chemical shifts are reported in ppm from benzotrifluoride (–64.0 ppm) resonance as the external standard. $^{11}$B NMR spectra were recorded on a JEOL JNM-ECA500II (161 MHz) spectrometer with complete proton decoupling. Chemical shifts are reported in ppm from $BF_3{\cdot}OEt_2$ resonance (0.0 ppm) as the external standard. Optical rotations were measured on a HORIBA SEPA-500 polarimeter. The high resolution mass spectra were measured on Thermo Fisher Scientific Exactive (ESI). Analytical thin layer chromatography (TLC) was performed on Merck precoated TLC plates (silica gel 60 $GF_{254}$, 0.25 mm). Preparative thin layer chromatography was performed on Wako precoated PLC plates (silica gel 70 $F_{254}$, 0.25 mm with concentrating zone 20 x 20 cm). Manual flash column chromatography was conducted on silica gel 60 (spherical, 40–50 μm; Kanto Chemical Co., Inc.), silica gel 60N (spherical, 40–50 μm; Kanto Chemical Co., Inc.), PSQ60AB (spherical, av. 55 μm; Fuji Silysia Chemical ltd.), and Silica gel 60 (Merck 1.09385.9929, 230–400 mesh). Automated flash column chromatography was performed using an Isolera Spektra instrument equipped with a Biotage SNAP Ultra 50 g cartridge. Recycling preparative high-performance liquid chromatography (HPLC) was performed using YMC HPLC LC-forte/R equipped with a silica gel column [ϕ 20 mm x 250 mm, YMC-Pack SIL SL12S05-2520WT]. Enantiomeric excesses were determined by HPLC analysis using chiral columns [ϕ 4.6 mm x 250 mm, DAICEL CHIRALPAK IA-3 (IA3), CHIRALPAK IB-3 (IB3), CHIRALPAK IB N-3 (IB N-3), and CHIRALPAK IC-3 (IC3), and CHIRALCEL OD-3 (OD3)] with hexane (H), 2-propanol (IPA), and ethanol (EtOH) as eluent. Cyclic voltammetry and square wave voltammetry were performed on an ALS/CHI 600E electrochemical analyzer. The voltammetric cell consisted of a glassy carbon electrode, a Pt wire counter electrode, and an $Ag/AgNO_3$ reference electrode. Stern-Volmer quenching experiments were conducted on a HORIBA FluoroMax-4P spectrometer.

Tetrahydrofurane (THF), dichloromethane ($CH_2Cl_2$), and acetonitrile (MeCN) were supplied from Kanto Chemical Co., Inc. as "Dehydrated" and further purified by passing through neutral alumina under nitrogen atmosphere. α-Alkylstyrenes were prepared by following the literature procedures.[19] Other simple chemicals were purchased and used as such.

**Additional Information**

**Table S1.** Anion Effect on the Catalytic Efficiency (Ar' = 3,5-$Me_2C_6H_3$)

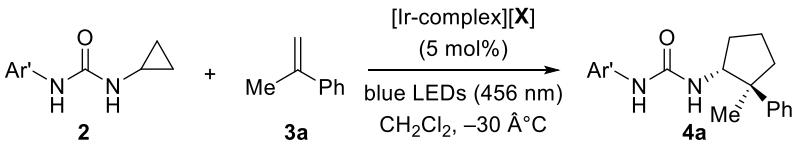


| entry | $\mathbf{X}^-$ | yield (%) | dr | $\beta$[11,20a] | Hydrogen Bond Basicity Index (HBI)[20b] | Association Constant ($K_a$) |
|---|---|---|---|---|---|---|
| 1 | $BzO^-$ | 25 | 1.3:1 | 15.1 | | |
| 2 | $AcO^-$ | 28 | 1.5:1 | 15.0 | 10 | 342±15 |
| 3 | $Cl^-$ | 30 | 1.4:1 | 12.1 | 6.5 | 123±8 |
| 4 | $(PhO)_2P(O)O^-$ | 46 | 1.4:1 | | | 107±8 |
| 5 | $TsO^-$ | 62 | 1.5:1 | | 4.3 | 81±3 |
| 6 | $\mathbf{1d}^-$ | 99 | 7.4:1 | | | 52±9 |
| 7 | $\mathbf{1a}^-$ | 38 | 1.6:1 | 7.6 | | 42±1 |
| 8 | $TfO^-$ | 28 | 1.5:1 | 9.4 | 3.4 | 33±8 |
| 9 | $PF_6^-$ | 10 | 1.1:1 | 7.0 | 3.2 | |
| 10 | $Tf_2N^-$ | 5 | 1.4:1 | 7.3 | | 5.8±0.5 |
| 11 | $BArF^-$ | 4 | 1.5:1 | | | |

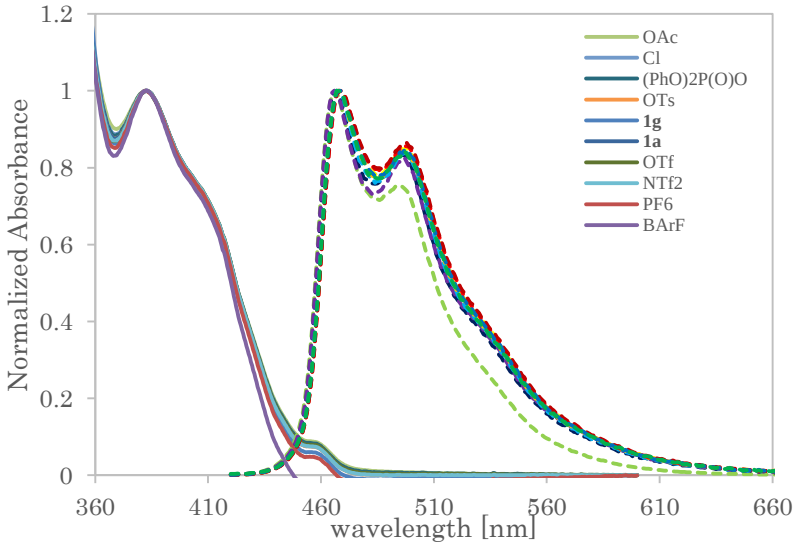


**Figure S1.** Absorption and Emission Spectra of [$Ir(dFCF_3ppy)_2(dtbbpy)$][**X**]

**Determination of Association Constant**

A solution of **2** in $CDCl_3$ (dried under activated MS4A) was prepared in the concentration of $3.0 \times 10^{-3}$ M. To the solution in a NMR tube (300 μL for $AcO^-$, $Cl^-$, $(PhO)_2P(O)O^-$, **1d**; 200 μL for $TsO^-$, $TfO^-$; 100 μL for **1a**, $Tf_2N^-$) was added a solution of $Bu_4N^+X^-$ (X = $AcO^-$ ($1.5 \times 10^{-2}$ M), $Cl^-$ ($1.5 \times 10^{-2}$ M), $(PhO)_2P(O)O^-$ ($3.0 \times 10^{-2}$ M), $TsO^-$ ($3.0 \times 10^{-2}$ M), **1d**$^-$ ($3.0 \times 10^{-2}$ M), **1a**$^-$ ($3.0 \times 10^{-2}$ M), $TfO^-$ ($3.0 \times 10^{-2}$ M), $Tf_2N^-$ ($6.0 \times 10^{-2}$ M)) in $CDCl_3$, followed by the further addition of $CDCl_3$ to adjust the total volume to 600 μL. $^1$H NMR spectra were recorded at 50 ºC. The resonance signal assigned to the N–H proton of the nitrogen atom connected to the cyclopropyl group was monitored to plot its chemical shift change (Δδ ppm) against the concentration of the anion. The association constant ($K_a$) was calculated from the obtained curves ($\Delta\delta$ N–H vs [**X**$^-$]) via nonlinear regression analysis using a simple 1:1 binding model, which was carried out with the Kaleidagraph program.[16]

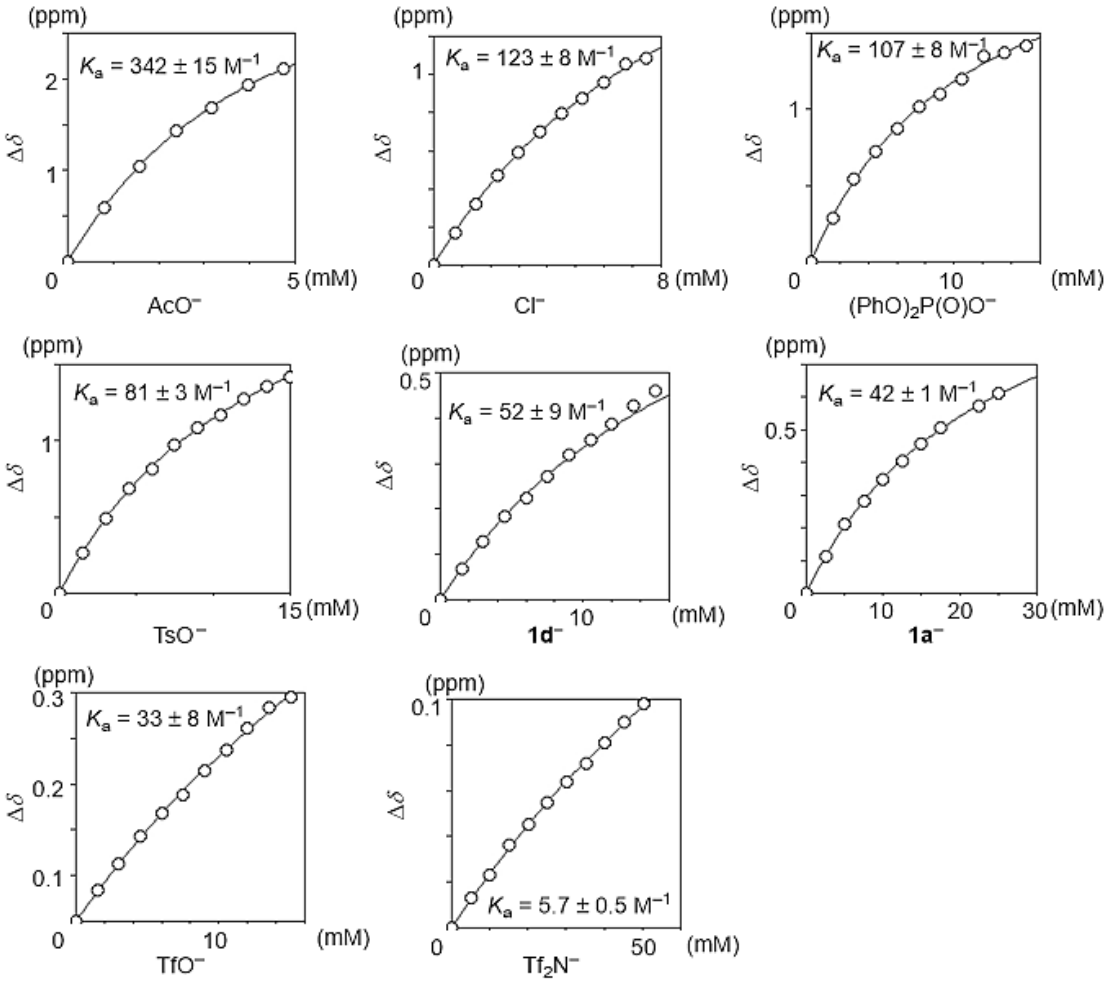


**Figure S2a** Determination of Association Constant

A solution of **4a** (major diastereomer) in $CDCl_3$ was prepared in the concentration of $3.0 \times 10^{-3}$ M. To the 300 μL of solution in a NMR tube was added a $3.0 \times 10^{-2}$ M solution of $Bu_4N^+$**1a**$^-$ in $CDCl_3$, followed by the further addition of $CDCl_3$ to adjust the total volume to 600 μL. $^1$H NMR spectra were recorded at 50 ºC. The resonance signal assigned to the N–H proton of the nitrogen atom connected to the cyclopropyl group was monitored to plot its chemical shift change (Δδ ppm) against the concentration of the anion. The association constant ($K_a$) was calculated from the obtained curves (Δ$\delta$ N–H vs [X$^-$]) via nonlinear regression analysis using a simple 1:1 binding model, which wa s carried out with the Kaleidagraph program.

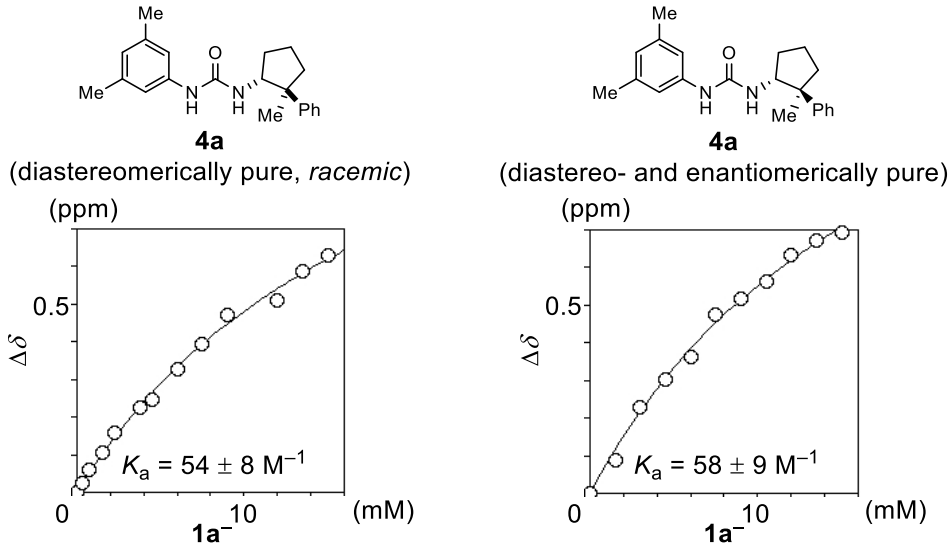


**Figure S2b** Determination of Association Constant of **4a** and **1a**$^-$

**Control Experiments (Table S2) (Ar' = 3,5-$Me_2C_6H_3$)**

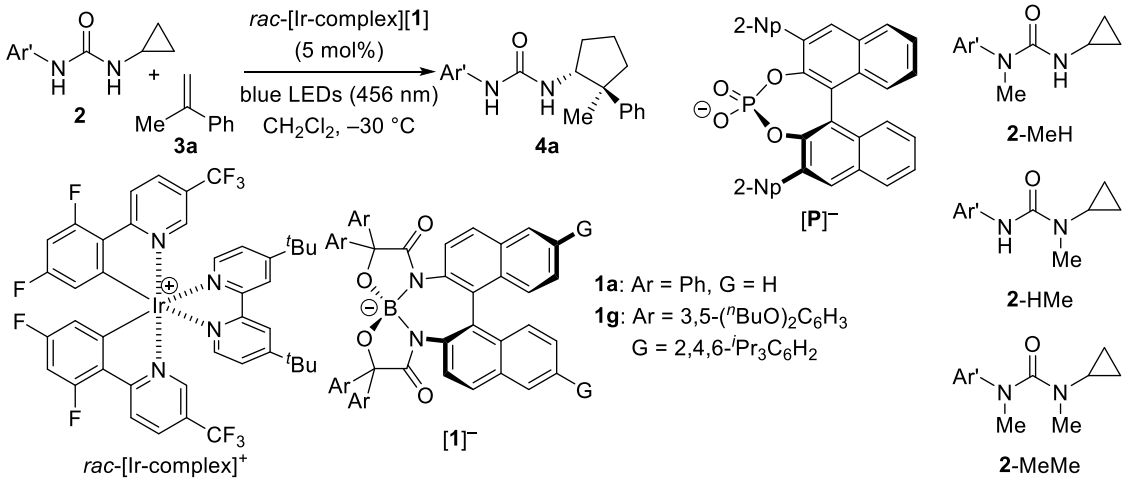


| entry | Change from the Standard Condition (Table 1 in the main part) | yield (%) | dr | ee (%) |
|---|---|---|---|---|
| 1 | no change (*rac*-[Ir-complex][**1g**]) | 95 | 12:1 | 92 |
| 2 | **2**-MeH was used instead of **2** (*rac*-[Ir-complex][**1a**]) | trace | | |
| 3 | **2**-HMe was used instead of **2** (*rac*-[Ir-complex][**1a**]) | 13 | 1.8:1 | 0/1 |
| 4 | **2**-MeMe was used instead of **2** (*rac*-[Ir-complex][**1a**]) | trace | | |
| 5 | under dark (*rac*-[Ir-complex][**1a**]) | 0 | | |
| 6 | $^nBu_4N$[**1a**] was used instead of *rac*-[Ir-complex][**1**] | 0 | | |
| 7 | Δ-[Ir-complex][**1g**] was used instead of *rac*-[Ir-complex][**1**] | 98 | 12:1 | 93 |
| 8 | Λ-[Ir-complex][**1g**] was used instead of *rac*-[Ir-complex][**1**] | 99 | 13:1 | 93 |
| 9 | *rac*-[Ir-complex][**P**] was used instead of *rac*-[Ir-complex][**1**] | 49 | 1.4:1 | –2/–2 |

**Cyclic Voltammetry and Square Wave Voltammetry**

Cyclic voltammetry and square wave voltammetry were carried out under $N_2$ with a sample solution of a concentration of 1.0 mM in MeCN containing tetrabutylammonium perchlorate ($^nBu_4N{\cdot}ClO_4$) as a supporting electrolyte (0.10 M). The scan rate was 100 $mV{\cdot}s^{-1}$ for cyclic voltammetry and 4 $mV{\cdot}s^{-1}$ for square wave voltammetry. The obtained potentials were calibrated to the saturated calomel electrode (SCE) scale with a ferrocene/ferrocenium ion couple. The reported potentials were taken at the peak top of the square wave voltammograms.

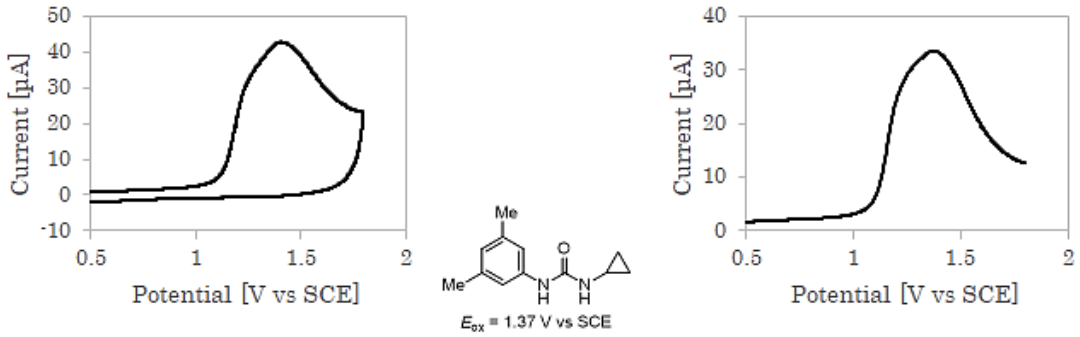


**Figure S3a** Cyclic voltammogram and square wave voltammogram of **2**.

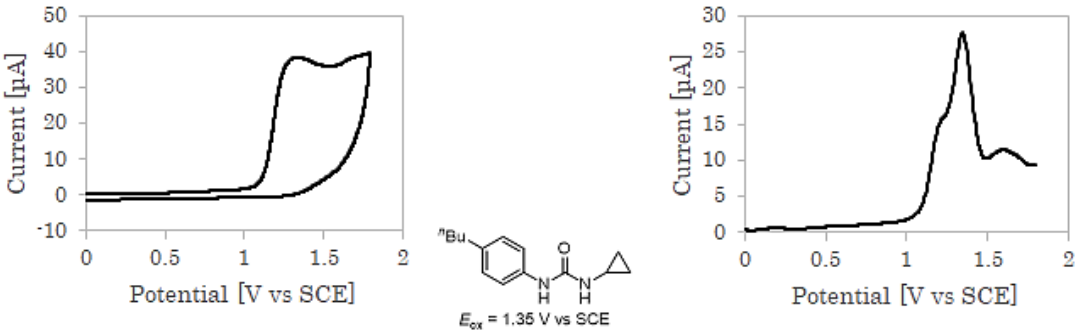


**Figure S3b** Cyclic voltammogram and square wave voltammogram of 4-$^n$Bu$C_6H_4$-urea**.**

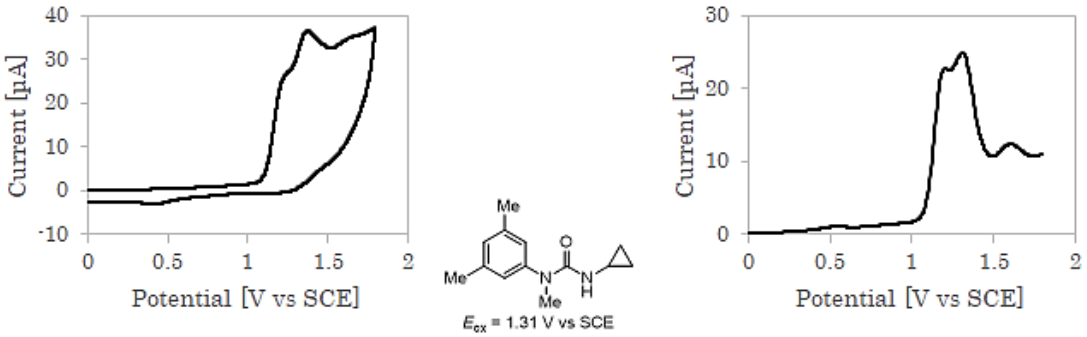


**Figure S3c** Cyclic voltammogram and square wave voltammogram of **2**-MeH.

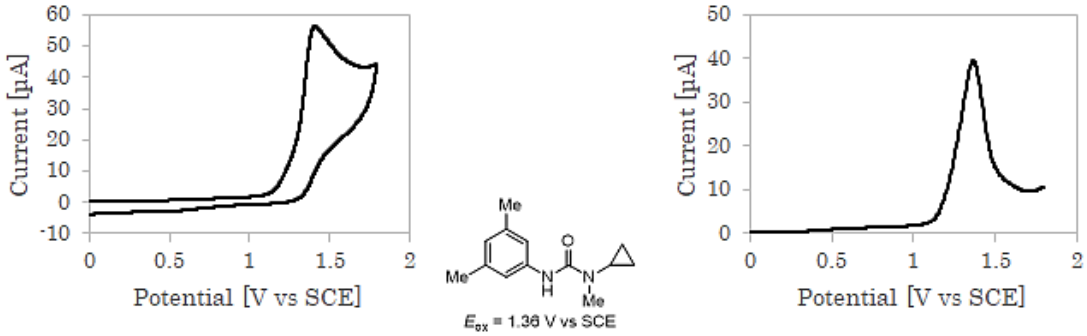


**Figure S3d** Cyclic voltammogram and square wave voltammogram of **2**-HMe.

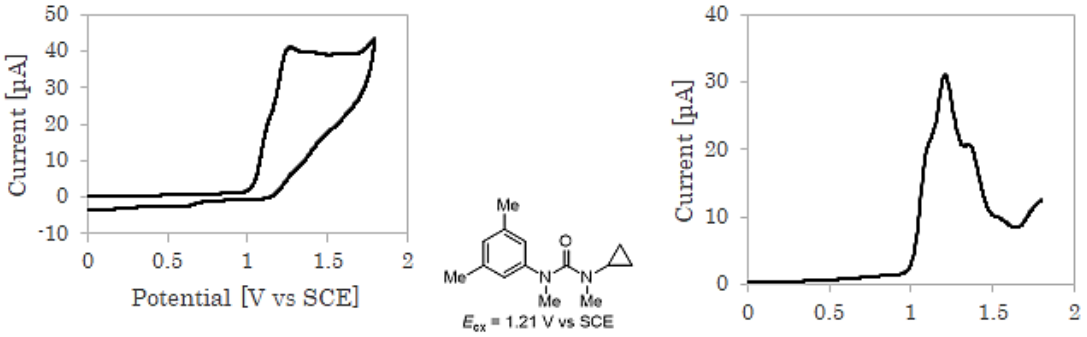


**Figure S3e** Cyclic voltammogram and square wave voltammogram of **2**-MeMe.

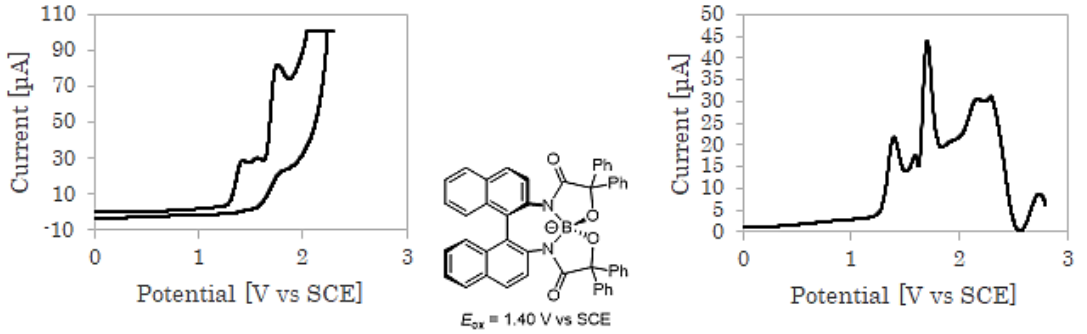


**Figure S3f** Cyclic voltammogram and square wave voltammogram of **1a**.

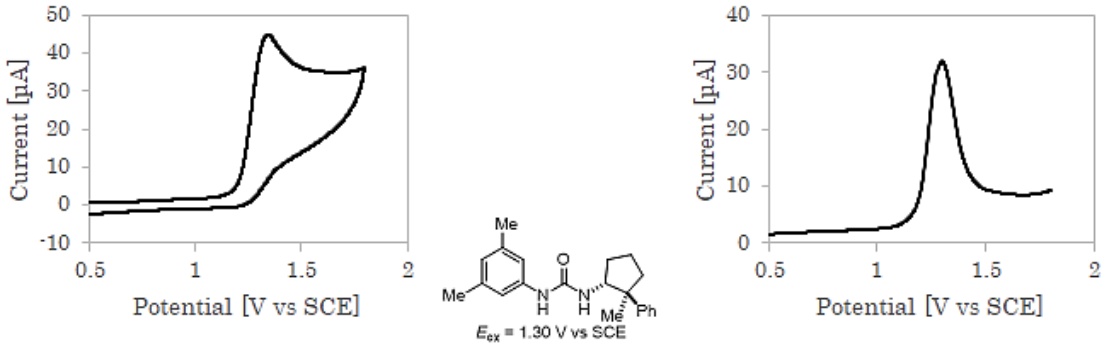


**Figure S3g** Cyclic voltammogram and square wave voltammogram of **4a** (major diastereomer)

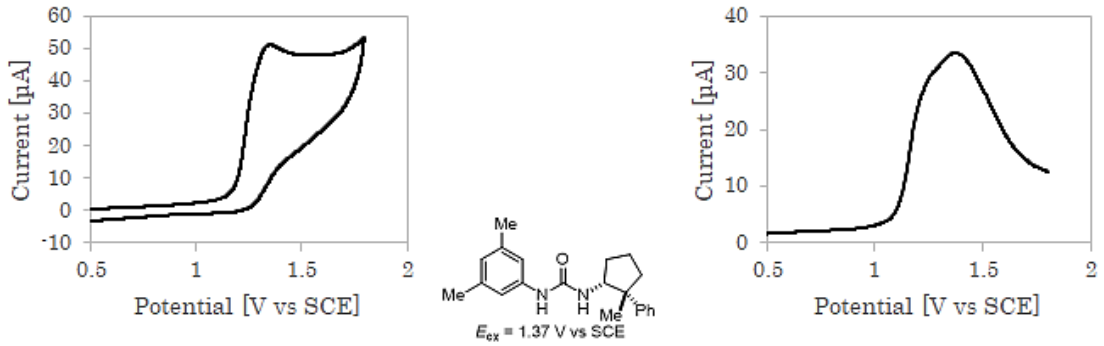


**Figure S3h** Cyclic voltammogram and square wave voltammogram of **4a** (minor diastereomer)

**Stern-Volmer Quenching Experiments**

1,2-Dichloroethane (DCE) solutions of [Ir(dFCF$_3$ppy)$_2$(dtbbpy)][**1g**] and 4-$^n$BuC$_6$H$_4$-urea were deaerated with argon (Ar) bubbling prior to each measurement. The emission from [Ir(dFCF$_3$ppy)$_2$(dtbbpy)][**1g**] was recorded at 470 nm upon excitation at 400 nm.

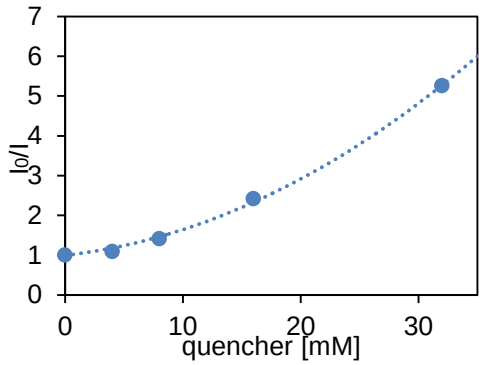


**Figure S4** Stern-Volmer quenching plots of [Ir(dFCF$_3$ppy)$_2$(dtbbpy)][**1g**] (10 μM in deaerated DCE) quenched with varying concentrations of 4-$^n$BuC$_6$H$_4$-urea in DCE.

**Light/Dark Experiment**

A solution of 1-cyclopropyl-3-(4-*n*-butylphenyl)urea (11.80 mg, 0.05 mmol), *rac*-[Ir-complex]·**1g** (6.80 mg, 0.0025 mmol), α-methylstyrene (**3a**) (162.0 μL, 1.25 mmol), and trimethylphenylsilane (3.51 mg, 0.023 mmol) in dichloromethane-$d_2$ (0.55 mL) was prepared in ϕ 5 mm NMR tube under Ar. After the solution was evacuated in vacuo and backfilled with Ar three times at 0 °C, the NMR tube was alternately placed in a reaction field at ambient temperature with fan under irradiation of blue LEDs (470 nm, approximate distance was 4 cm from the light source) and in a dark place at ambient temperature. The yield of the corresponding product of each time was determined by $^1$H NMR with trimethylphenylsilane as an internal standard.

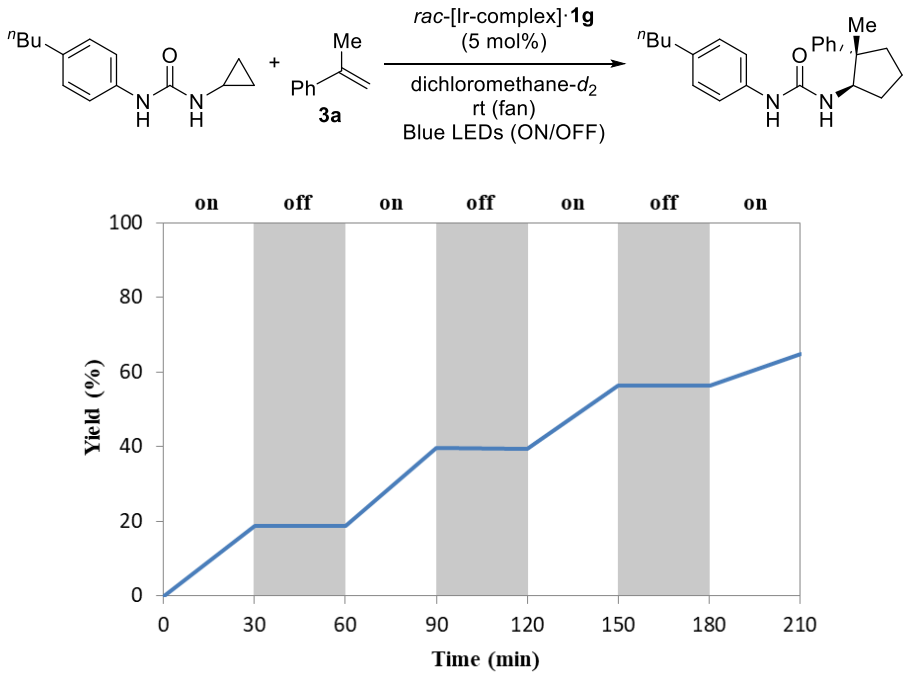


**Figure S5** Profile of the reaction with the light on/off over time.

**Measurement of Quantum Yield**

Photon flux was measured by Shimadzu-QYM-01. Irradiation was carried out with Asahi Spectra-MAX 303 equipped with band pass filter. A 1 $cm^2$ quartz cuvette was charged with a solution of 1-cyclopropyl-3-(4-*n*-butylphenyl)urea (58.1 mg, 0.25 mmol), *rac*-[Ir-complex]·**1g** (33.4 mg, 0.0125 mmol), and α-methylstyrene (**3a**) (162.0 μL, 1.25 mmol) in $CH_2Cl_2$ (2.5 mL). The solution was evacuated in vacuo and backfilled with Ar three times, and it was irradiated for 24 h. After evaporation to remove solvent, the yield of the corresponding product was determined by $^1H$ NMR with trimethylphenylsilane as an internal standard. Quantum yield ($\Phi$) was calculated by following formula.

$$\Phi = \frac{n_{22} \cdot N_A}{n_{ph}} \qquad \begin{bmatrix} \Phi\text{: quantum yield} \\ n_{22}\text{: amount of product [mol]} \\ N_A\text{: Avogadro constant } (6.02 \cdot 10^{23}\ \text{mol}^{-1}) \\ n_{ph}\text{: number of absorbed photons} \end{bmatrix}$$

$n_{22}$ = $2.03 \cdot 10^{-4}$, $n_{ph}$ = $7.70 \cdot 10^{20}$: $\boldsymbol{\Phi}$ = **0.16**

**Experimental Section:**

**Preparation and Characterization of Chiral Iridium Borates**

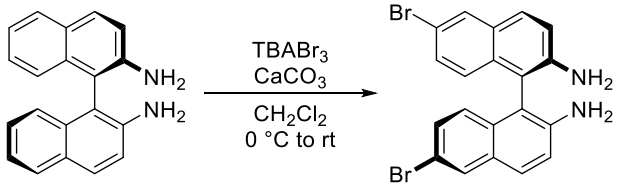


**Procedure for the Synthesis of (*R*)-6,6'-DibromoBINAM:** To a solution of (*R*)-1,1'-binaphthyl-2,2'-diamine (BINAM) (0.57 g, 2.0 mmol) in $CH_2Cl_2$ (20.0 mL) were added $CaCO_3$ (0.42 g, 4.2 mmol) and tetra-*n*-butylammonium tribromide ($TBABr_3$) (2.03 g, 4.2 mmol) at 0 °C under Ar atmosphere. After being stirred for 20 min, the mixture was warmed to ambient temperature and stirred for 1.5 h. The reaction was quenched by adding a saturated aqueous solution of $NH_4Cl$ and the aqueous phase was extracted with $CH_2Cl_2$ four times. The combined organic phases were washed with brine, dried over $Na_2SO_4$, filtered, and concentrated. Purification of the residue was performed by column chromatography on silica gel ($H/CH_2Cl_2$ = 2:1 to 1:10 as eluent) to afford (*R*)-6,6'-dibromoBINAM (0.75 g, 1.7 mmol, 85%) as a brown solid. The spectral data is consistent with that reported in the literature.[21]

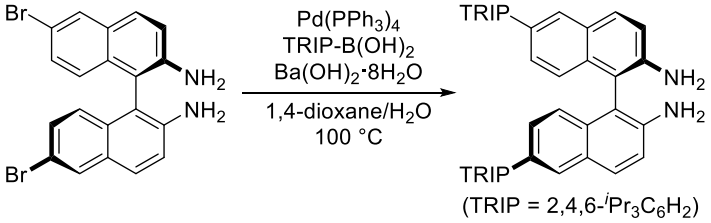


**Procedure for the Synthesis of (*R*)-6,6'-Bis(TRIP)BINAM:** A suspension of (*R*)-6,6'-dibromoBINAM (0.71 g, 1.6 mmol), TRIP-$B(OH)_2$ (TRIP = 2,4,6-$^i$Pr$_3$C$_6$H$_2$, 1.19 g, 4.8 mmol), $Pd(PPh_3)_4$ (92.5 mg, 0.08 mmol), and $Ba(OH)_2 \cdot 8H_2O$ (3.03 g, 9.6 mmol) in 1,4-dioxane (12.0 mL) and $H_2O$ (4.0 mL) was degassed and the whole reaction mixture was stirred for 40 h at 100 °C under Ar. The reaction mixture was cooled to ambient temperature and filtered through a pad of Celite overlaid with silica gel by the aid of ethyl acetate (EA). The filtrate was concentrated under vacuum to afford the crude residue. Purification of the residue was performed using Isolera automated flash column chromatography (5% to 25% EA/H as eluent) and the obtained material was further purified by Isolera automated flash column chromatography (33% to 80% $CH_2Cl_2$/H as eluent) to furnish (*R*)-6,6'-bis(TRIP)BINAM (0.83 g, 1.2 mmol, 76%) as a light brown solid. **(*R*)-6,6'-Bis(TRIP)BINAM:** $^1$H NMR (500 MHz, $CDCl_3$) δ 7.78 (2H, d, *J* = 8.0 Hz), 7.59 (2H, d, *J* = 1.7 Hz), 7.24 (2H, d, *J* = 8.0 Hz), 7.19 (2H, d, *J* = 8.7 Hz), 7.11 (2H, dd, *J* = 8.7, 1.7 Hz), 7.07 (4H, s), 3.80 (4H, brs), 2.95 (2H, sept, *J* = 6.9 Hz), 2.70 (4H, sept, *J* = 6.7 Hz), 1.32 (12H, d, *J* = 6.9 Hz), 1.12 (6H, d, *J* = 6.8 Hz), 1.11 (6H, d, *J* = 6.8 Hz), 1.06 (6H, d, *J* = 6.8 Hz), 1.02 (6H, d, *J* = 6.8 Hz);

$^{13}$C NMR (125 MHz, $CDCl_3$) $\delta$ 147.9, 147.2, 147.0, 142.7, 137.3, 134.9, 132.5, 129.6, 128.6, 128.4, 123.7, 120.7, 120.6, 118.6, 113.0, 34.4, 30.4$_1$, 30.3$_6$, 24.7, 24.6, 24.4$_0$, 24.3$_7$, 24.3; IR (film): 3479, 3379, 2952, 2868, 1609, 1285, 1457, 1382, 1362, 1336, 1316, 1289, 1247, 1056, 909 cm$^{-1}$; HRMS (ESI) Calcd for $C_{50}H_{61}N_2$ ([M+H]$^+$) 689.4829. Found 689.4828.

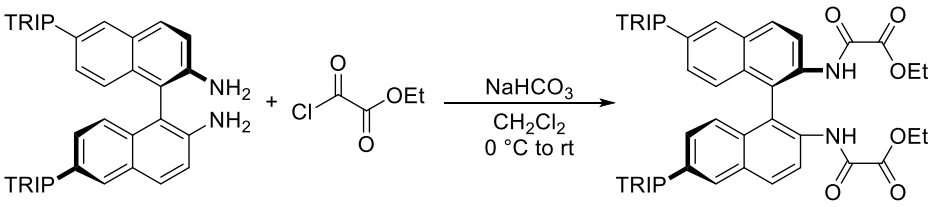


**Procedure for the Synthesis of (*R*)-6,6'-Bis(TRIP)-*N*,*N*'-bis(2-ethoxy-2-oxoacetyl)BINAM:** Following the literature procedure,[11] (*R*)-6,6'-bis(TRIP)-*N*,*N*'-bis(2-ethoxy-2-oxoacetyl)BINAM was synthesized in 95% yield (1.02 g, 1.1 mmol) as a white solid through purification by column chromatography on silica gel (H/EA = 30:1 to 3:1 as eluent). **(*R*)-6,6'-Bis(TRIP)-*N*,*N*'-bis(2-ethoxy-2-oxoacetyl)BINAM:** $^1$H NMR (400 MHz, $CDCl_3$) δ 8.80 (2H, d, *J* = 9.2 Hz), 8.67 (2H, brs), 8.12 (2H, d, *J* = 9.2 Hz), 7.82 (2H, d, *J* = 1.3 Hz), 7.37 (2H, d, *J* = 8.7 Hz), 7.27 (2H, dd, *J* = 8.7, 1.3 Hz), 7.09 (4H, s), 4.15 (4H, q, *J* = 7.0 Hz), 2.96 (2H, sept, *J* = 7.0 Hz), 2.67 (2H, sept, *J* = 6.8 Hz), 2.57 (2H, sept, *J* = 6.8 Hz), 1.32 (12H, d, *J* = 7.0 Hz), 1.21 (6H, t, *J* = 7.0 Hz), 1.14 (6H, d, *J* = 6.8 Hz), 1.11 (6H, d, *J* = 7.2 Hz), 1.03 (12H, d, *J* = 6.8 Hz); $^{13}$C NMR (101 MHz, $CDCl_3$) $\delta$ 160.0, 154.0, 148.5, 146.8, 146.7, 139.0, 136.4, 133.7, 131.5, 130.9, 130.7, 129.1, 124.7, 120.8, 120.1, 119.8, 63.5, 34.5, 30.6, 30.5, 24.5, 24.4, 24.3$_3$, 24.2$_9$, 24.2, 13.9; IR (film): 3356, 2957, 2866, 1711, 1593, 1521, 1489, 1458, 1362, 1283, 1180, 1017, 907, 877 cm$^{-1}$; HRMS (ESI) Calcd for $C_{58}H_{68}N_2O_6Na$ ([M+Na]$^+$) 911.4970. Found 911.4963.

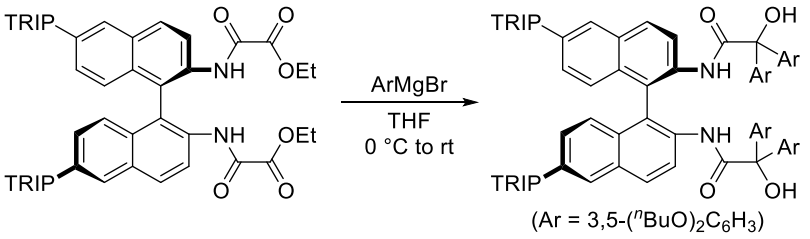


**Procedure for the Synthesis of (*R*)-6,6'-Bis(TRIP)-*N*,*N*'-bis(2,2-bis(3,5-di-*n*-butoxyphenyl)-2-hydroxyacetyl)BINAM:** The synthesis was implemented by following the literature procedure[11] and purification by column chromatography on silica gel (H/EA = 100:1 to 15:1 as eluent) afforded (*R*)-6,6'-bis(TRIP)- *N*,*N*'-bis(2,2-bis(3,5-di-*n*-butoxyphenyl)-2-hydroxyacetyl)
BINAM (1.68 g, 1.0 mmol, 91%) as a yellow solid.

**(*R*)-6,6'-Bis(TRIP)-*N*,*N*'-bis(2,2-bis(3,5-di-*n*-butoxyphenyl)-2-hydroxyacetyl)BINAM:** $^1$H NMR (500 MHz, $CDCl_3$) $\delta$ 8.67 (2H, d, *J* = 9.3 Hz), 8.08 (2H, brs), 7.92 (2H, d, *J* = 9.3 Hz), 7.68 (2H, s),

7.13 (2H, dd, *J* = 8.7, 1.3 Hz), 7.09 (2H, d, *J* = 8.7 Hz), 7.05 (4H, s), 6.40 (4H, d, *J* = 2.5 Hz), 6.27 (4H, d, *J* = 2.0 Hz), 6.25 (4H, dd, *J* = 2.5, 2.0 Hz), 3.82-3.74 (16H, m), 3.64 (2H, brs), 2.94 (2H, sept, *J* = 6.8 Hz), 2.61 (2H, sept, *J* = 6.9 Hz), 2.54 (2H, sept, *J* = 6.9 Hz), 1.67-1.61 (16H, m), 1.39 (16H, sept, *J* = 7.5 Hz), 1.30 (12H, d, *J* = 6.8 Hz), $1.08_1$ (6H, d, *J* = 7.0 Hz), $1.07_5$ (6H, d, *J* = 7.0 Hz), 0.97 (6H, d, *J* = 7.0 Hz), 0.97 (12H, t, *J* = 7.5 Hz), 0.83 (12H, t, *J* = 7.5 Hz), 0.86 (6H, d, *J* = 7.0 Hz); $^{13}$C NMR (125 MHz, $CDCl_3$) $\delta$ 171.9, $160.0_5$, $160.0_1$, 148.2, 146.8, 146.8, 144.2, 143.9, 137.9, 136.7, 134.4, 131.0, 130.2, 130.1, 128.8, 124.7, 120.7, 120.6, 120.3, 119.6, 106.2, 106.1, 100.8, 100.6, 81.6, $67.7_2$, $67.6_8$, 34.4, 31.4, 30.4, 24.5, 24.4, 24.2, 24.1, 19.4, $14.0_3$, $13.9_9$, one carbon atom was not found probably due to overlapping.; IR (film): 3351, 2956, 2870, 1694, 1593, 1486, 1443, 1381, 1286, 1163, 1072, 831 $cm^{-1}$; HRMS (ESI) Calcd for $C_{110}H_{143}N_2O_{12}$ ($[M-H]^-$) 1684.0647. Found 1684.0647.

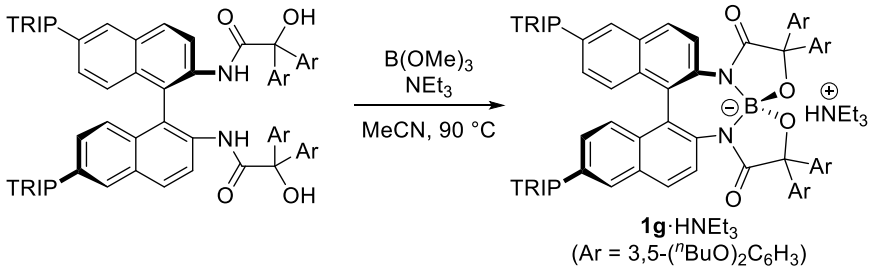


**Representative Procedure for the Synthesis of Triethylammonium Borate 1g·HNEt$_3$:** The synthesis was performed using a modified literature method.[11] A mixture of (*R*)-6,6'-bis(TRIP)-*N*,*N*'-bis(2,2-bis(3,5-di-*n*-butoxyphenyl)-2-hydroxyacetyl)BINAM (1.68 g, 1.0 mmol), $NEt_3$ (0.21 mL, 1.5 mmol), and $B(OMe)_3$ (0.12 mL, 1.1 mmol) in MeCN (10.0 mL) was stirred at 90 °C for 24 h. After cooling down to ambient temperature, the resulting mixture was concentrated in vacuo and the residual solid was purified by column chromatography on silica gel (H/EA = 20:1 to 1:3 as eluent) to furnish **1g**·$HNEt_3$ (1.61 g, 0.89 mmol, 89%) as an off-white solid. **1g·HNEt$_3$ (Ar = 3,5-($^n$BuO)$_2$C$_6$H$_3$):** $^1$H NMR (500 MHz, $CDCl_3$) $\delta$ 9.29 (1H, br), 7.85 (2H, d, *J* = 8.6 Hz), 7.81 (2H, d, *J* = 8.6 Hz), 7.57 (2H, s), 7.05 (2H, d, *J* = 1.5 Hz), 7.03 (2H, s), 7.00 (4H, s), 6.95 (2H, d, *J* = 8.6 Hz), 6.82 (2H, d, *J* = 8.6 Hz), 6.41 (4H, d, *J* = 1.5 Hz), 6.32 (2H, d, *J* = 1.5 Hz), 5.96 (2H, d, *J* = 1.5 Hz), 3.88 (8H, t, *J* = 6.8 Hz), 3.66 (4H, dt, *J* = 9.1, 6.8 Hz), 3.56 (4H, dt, *J* = 9.1, 6.8 Hz), 2.93 (2H, sept, *J* = 6.8 Hz), 2.57 (2H, sept, *J* = 6.8 Hz), 2.54 (2H, sept, *J* = 6.8 Hz), 2.35 (6H, qd, *J* = 6.8, 6.1 Hz), 1.72 (8H, quin, *J* = 6.8 Hz), 1.60 (8H, quin, *J* = 6.8 Hz), 1.44 (8H, sex, *J* = 6.8 Hz), 1.40 (8H, sex, *J* = 6.8 Hz), 1.30 (12H, d, *J* = 6.8 Hz), 1.12 (6H, d, *J* = 6.8 Hz), 1.06 (6H, d, *J* = 6.8 Hz), 0.95 (12H, t, *J* = 6.8 Hz), 0.94 (12H, d, *J* = 6.8 Hz), 0.91 (12H, dd, *J* = 6.9, 1.8 Hz), 0.60 (12H, t, *J* = 6.8 Hz); $^{13}$C NMR (126 MHz, $CDCl_3$) $\delta$ 177.1, 159.8, 159.1, 148.0, 147.5, 146.9, 146.8, 146.7, 146.5, 137.8, $137.0_5$, $136.9_7$, 132.2, 131.8, 129.7, 128.8, 128.0, 127.6, 127.4, 120.6, 106.1, 106.0, 100.5, 99.4, 85.0, 67.8, 67.4, 45.9, 34.4, $31.6_1$, $31.5_6$, 30.4, 30.3, 24.4, 24.3, $24.2_4$, $24.2_1$, $24.1_9$,

23.9, 19.5, 19.4, 14.1, 8.0, two carbon atoms were not found probably due to overlapping.; $^{11}$B NMR (160 MHz, $CDCl_3$) $\delta$ 10.9; IR (film): 2958, 2869, 1640, 1592, 1483, 1438, 1382, 1338, 1286, 1161, 1032, 907 $cm^{-1}$; HRMS (ESI) Calcd for $C_{110}H_{140}N_2O_{12}B^-$ ([M−HNEt$_3$]$^-$) 1692.0505. Found 1692.0428; $[\alpha]_D^{26}$ −116.1 (*c* = 13.3, $CHCl_3$).

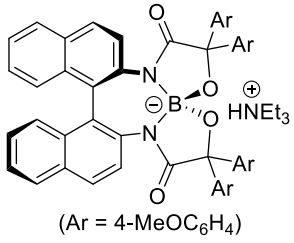


**1b·HNEt$_3$ (Ar = 4-MeOC$_6$H$_4$):** $^1$H NMR (500 MHz, $CDCl_3$) $\delta$ 9.45 (1H, br), 7.95 (2H, d, *J* = 7.9 Hz), 7.88 (2H, d, *J* = 7.9 Hz), 7.85 (4H, d, *J* = 8.8 Hz), 7.50 (2H, d, *J* = 7.9 Hz), 7.42 (2H, t, *J* = 7.9 Hz), 7.27 (2H, d, *J* = 7.9 Hz), 7.17 (2H, t, *J* = 7.9 Hz), 6.89 (4H, d, *J* = 8.8 Hz), 6.23 (4H, d, *J* = 8.8 Hz), 6.10 (4H, d, *J* = 8.8 Hz), 3.83 (6H, s), 3.58 (6H, s), 2.29 (6H, qd, *J* = 7.4, 4.8 Hz), 0.63 (9H, t, *J* = 7.4 Hz); $^{13}$C NMR (126 MHz, $CDCl_3$) $\delta$ 178.3, 158.6, 158.0, 138.8, 138.6, 135.9, 133.5, 132.5, 130.6, 129.1, 128.8, 128.7, 128.3, 128.0, 127.5, 125.7, 125.1, 113.0, 112.6, 85.0, 55.5, 55.3, 46.0, 8.2; $^{11}$B NMR (160 MHz, $CDCl_3$) $\delta$ 10.7; IR (film): 3004, 1639, 1506, 1466, 1400, 1300, 1245, 1173, 1028, 830 $cm^{-1}$; HRMS (ESI) Calcd for $C_{52}H_{40}N_2O_8B^-$ ([M−HNEt$_3$]$^-$) 831.2883. Found 831.2875; $[\alpha]_D^{26}$ −218.4 (*c* = 10.1, $CHCl_3$).

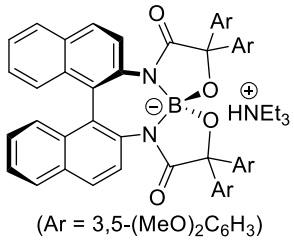


**1c·HNEt$_3$ (Ar = 3,5-(MeO)$_2$C$_6$H$_3$):** $^1$H NMR (500 MHz, $CDCl_3$) $\delta$ 9.29 (1H, br), 7.82 (2H, d, *J* = 8.3 Hz), 7.73 (2H, d, *J* = 8.3 Hz), 7.48 (2H, d, *J* = 8.3 Hz), 7.34 (2H, ddd, *J* = 8.3, 6.4, 1.5 Hz), 7.12 (4H, d, *J* = 2.3 Hz), 7.10 (2H, d, *J* = 8.3 Hz), 7.07 (2H, ddd, *J* = 8.3, 6.4, 1.5 Hz), 6.34 (2H, t, *J* = 2.3 Hz), 6.01 (4H, d, *J* = 2.3 Hz), 5.99 (2H, t, *J* = 2.3 Hz), 3.76 (12H, s), 3.26 (12H, s), 2.35 (6H, qdd, *J* = 7.2, 4.9, 1.9 Hz), 0.62 (9H, t, *J* = 7.2 Hz); $^{13}$C NMR (126 MHz, $CDCl_3$) $\delta$ 177.1, 160.1, 159.7, 147.8, 146.9, 138.1, 133.4, 132.5, 130.0, 128.9, 128.4, 127.5, 127.4, 125.3, 124.8, 105.8, 105.7, 99.0$_9$, 99.0$_0$, 85.3, 55.5, 55.1, 46.1, 8.2; $^{11}$B NMR (160 MHz, $CDCl_3$) $\delta$ 10.8; IR (film): 2943, 1641, 1593, 1460, 1409, 1313, 1201, 1144, 1040, 924 $cm^{-1}$; HRMS (ESI) Calcd for $C_{56}H_{48}N_2O_{12}B^-$ ([M−HNEt$_3$]$^-$) 951.3295. Found 951.3295; $[\alpha]_D^{23}$ −203.5 (*c* = 8.3, $CHCl_3$).

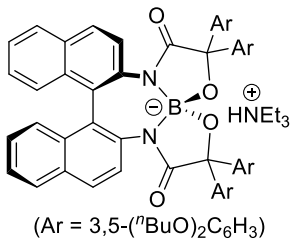


**1d·HNEt$_3$ (Ar = 3,5-($^n$BuO)$_2$C$_6$H$_3$):** $^1$H NMR (500 MHz, $CDCl_3$) $\delta$ 9.41 (1H, br), 7.77 (2H, d, *J* = 8.3 Hz), 7.65 (2H, d, *J* = 8.3 Hz), 7.40 (2H, d, *J* = 8.3 Hz), 7.30 (2H, ddd, *J* = 8.3, 6.5, 1.8 Hz), 7.07 (2H, d, *J* = 8.3 Hz), 7.06-7.01 (2H, m), 7.04 (4H, d, *J* = 2.3 Hz), 6.31 (2H, t, *J* = 2.3 Hz), 6.12 (4H, d, *J* = 2.3 Hz), 5.99 (2H, t, *J* = 2.3 Hz), 3.92 (8H, t, *J* = 7.5 Hz), 3.47 (4H, dt, *J* = 9.3, 7.5 Hz), 3.34 (4H, dt, *J* = 9.3, 7.5 Hz), 2.38 (6H, qdd, *J* = 7.3, 4.5, 2.9 Hz), 1.69 (8H, quin, *J* = 7.5 Hz), 1.54 (8H, quin-d, *J* = 7.5, 2.1 Hz),

1.42 (8H, sex, $J$ = 7.5 Hz), 1.33 (8H, sex-d, $J$ = 7.5, 2.1 Hz), 0.92 (12H, t, $J$ = 7.5 Hz), 0.91 (12H, t, $J$ = 7.5 Hz), 0.65 (9H, t, $J$ = 7.3 Hz); $^{13}$C NMR (126 MHz, $CDCl_3$) $\delta$ 176.9, 159.6, 159.2, 147.2, 138.1, 133.3, 132.2, 130.1, 128.7, 128.2, 127.6, 127.4, 125.0, 124.6, 106.1, 105.9, 100.1, 99.7, 85.2, 67.8, 67.3, 46.0, 31.6, 31.5, $19.4_2$, $19.3_9$, 14.1, 8.2, two carbon atoms were not found probably due to overlapping.; $^{11}$B NMR (160 MHz, $CDCl_3$) $\delta$ 10.8; IR (film): 2955, 2874, 1639, 1589, 1509, 1437, 1384, 1289, 1153, 1027, 817 cm$^{-1}$; HRMS (ESI) Calcd for $C_{80}H_{96}N_2O_{12}B^-$ ([M−HNEt$_3$]$^-$) 1287.7062. Found 1287.7048; $[\alpha]_D^{26}$ −132.7 ($c$ = 10.5, $CHCl_3$).

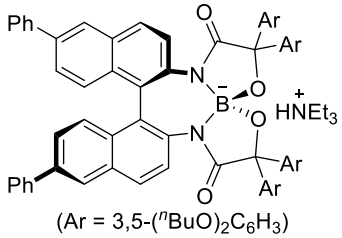


**1e·HNEt$_3$ (Ar = 3,5-($^n$BuO)$_2$C$_6$H$_3$):** $^1$H NMR (600 MHz, $CDCl_3$) $\delta$ 9.32 (1H, br), 8.01 (2H, d, $J$ = 1.8 Hz), 7.69 (4H, d, $J$ = 7.6 Hz), 7.67 (2H, d, $J$ = 8.9 Hz), 7.43 (4H, t, $J$ = 7.6 Hz), 7.39 (2H, dd, $J$ = 8.9, 1.8 Hz), 7.38 (2H, d, $J$ = 8.9 Hz), 7.33 (2H, t, $J$ = 7.6 Hz), 7.18 (2H, d, $J$ = 8.9 Hz), 7.00 (4H, d, $J$ = 2.2 Hz), 6.32 (2H, t, $J$ = 2.2 Hz), 6.10 (4H, d, $J$ = 2.2 Hz), 6.00 (2H, t, $J$ = 2.2 Hz), 3.90 (8H, t, $J$ = 7.1 Hz), 3.43 (4H, dt, $J$ = 9.1, 7.1 Hz), 3.30 (4H, dt, $J$ = 9.1, 7.1 Hz), 2.46-2.35 (6H, m), 1.67 (8H, quin, $J$ = 7.1 Hz), 1.42 (8H, sex, $J$ = 7.1 Hz), 1.39 (8H, sex, $J$ = 7.1 Hz), 1.26-1.18 (8H, m), 0.90 (12H, t, $J$ = 7.1 Hz), 0.77 (12H, t, $J$ = 7.1 Hz), 0.67 (9H, t, $J$ = 7.5 Hz); $^{13}$C NMR (126 MHz, $CDCl_3$) $\delta$ 177.1, 159.6, 159.2, 147.1, 146.9, 140.5, 137.9, 136.9, 132.6, 132.5, 129.9, 129.1, 128.9, 128.2, 127.5, 127.4, 127.1, 125.8, 124.6, 106.3, 106.0, 100.0, 99.8, 85.5, 67.9, 67.4, 46.2, 31.5, 31.4, $19.3_3$, $19.2_5$, 14.0, 13.9, 8.2; $^{11}$B NMR (160 MHz, $CDCl_3$) $\delta$ 10.7; IR (film): 2959, 2863, 1640, 1590, 1493, 1440, 1380, 1288, 1160, 1017 cm$^{-1}$; HRMS (ESI) Calcd for $C_{98}H_{116}N_2O_{12}B^-$ ([M−HNEt$_3$]$^-$) 1439.7688. Found 1439.7643; $[\alpha]_D^{24}$ −159.4 ($c$ = 13.9, $CHCl_3$).

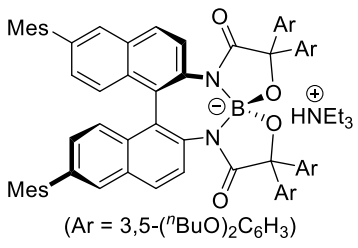


**1f·HNEt$_3$ (Mes = 2,4,6-Me$_3$C$_6$H$_2$, Ar = 3,5-($^n$BuO)$_2$C$_6$H$_3$):** $^1$H NMR (500 MHz, $CDCl_3$) $\delta$ 9.31 (1H, br), 7.78 (2H, d, $J$ = 8.3 Hz), 7.75 (2H, d, $J$ = 8.3 Hz), 7.53 (2H, d, $J$ = 1.8 Hz), 7.03 (4H, d, $J$ = 2.3 Hz), 7.01 (2H, d, $J$ = 8.3 Hz), 6.93 (4H, s), 6.79 (2H, dd, $J$ = 8.3, 1.8 Hz), 6.31 (6H, d, $J$ = 2.3 Hz), 5.95 (2H, t, $J$ = 2.3 Hz), 3.88 (8H, t, $J$ = 7.0 Hz), 3.62 (4H, dt, $J$ = 9.4, 7.0 Hz), 3.53 (4H, dt, $J$ = 9.4, 7.0 Hz), 2.39-2.31 (6H, m), 2.32 (6H, s), 1.98 (6H, s), 1.94 (6H, s), 1.71 (8H, quin, $J$ = 7.0 Hz), 1.58 (8H, quin-d, $J$ = 7.0, 1.6 Hz), 1.44 (8H, sex, $J$ = 7.0 Hz), 1.37 (8H, sex, $J$ = 7.0 Hz), 0.94 (12H, t, $J$ = 7.0 Hz), 0.90 (12H, t, $J$ = 7.0 Hz), 0.61 (9H, t, $J$ = 7.3 Hz); $^{13}$C NMR (151 MHz, $CDCl_3$) $\delta$ $177.3, 159.7, 159.1, 147.2_4, 147.1_9$, 138.8, 138.0, 137.2, 136.7, 136.3, 135.9, 132.2, 129.8, 128.7, 128.3, 128.2, 128.0, 127.8, 127.6, 127.0, 106.2, 106.1, 100.5, 99.4, 85.1, 67.8, 67.4, 46.0, 31.6, 31.5, 21.2, 20.9, 20.8, 19.4, 14.1, 14.0, 8.2, two carbon atoms were not found probably due to overlapping.; $^{11}$B NMR (160 MHz, $CDCl_3$) $\delta$ 11.0; IR (film): 2931, 2864, 1639, 1591, 1437, 1384,

1337, 1287, 1162, 1036 $cm^{-1}$; HRMS (ESI) Calcd for $C_{98}H_{116}N_2O_{12}B^-$ ($[M-HNEt_3]^-$) 1523.8627. Found 1523.8589; $[\alpha]_D^{26}$ −106.4 (*c* = 20.7, $CHCl_3$).

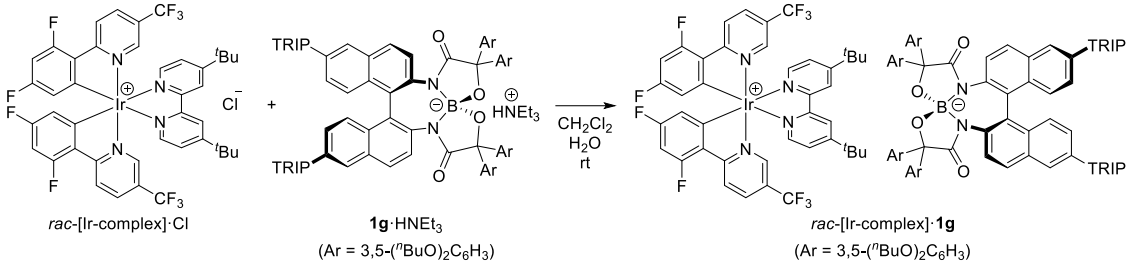


**Representative Procedure for the Preparation of Chiral Iridium Borate *rac*-[Ir-complex]·1g:** A solution of iridium chloride [*rac*-Ir]·Cl (0.11 g, 0.11 mmol)[22] and **1g**·$HNEt_3$ (0.20 g, 0.11 mmol) in $CH_2Cl_2$ (20.0 mL) was vigorously washed with distilled water (25.0 mL) four times. After the combined organic phases were dried over $Na_2SO_4$, concentration under vacuum afforded [*rac*-Ir]·**1g** (0.30 g, 0.11 mmol) as an yellow solid, which was used as a catalyst for the asymmetric [3+2] radical cycloaddition reaction without further purification.

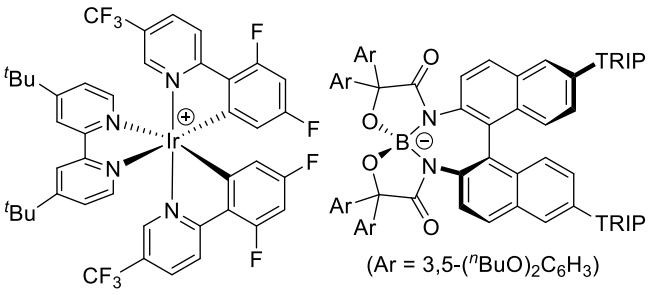


**Δ-[Ir-complex]·1g:** Prepared from enantiomerically pure iridium chloride *Δ*-[Ir(dFCF$_3$ppy)$_2$(dtbbpy)]·Cl (see below). $^1$H NMR (500 MHz, $CDCl_3$) $\delta$ 8.41 (2H, dd, $J_{H\text{-}H}$ = 9.0 Hz, $J_{H\text{-}F}$ = 2.5 Hz), 8.37 (2H, d, *J* = 1.3 Hz), 7.98 (2H, dd, *J* = 9.0, 1.2 Hz), 7.94 (2H, d, *J* = 5.7 Hz), 7.86 (2H, d, *J* = 8.6 Hz), 7.73 (2H, d, *J* = 8.6 Hz), 7.63 (2H, dd, *J* = 5.7, 1.3 Hz), 7.49 (2H, d, *J* = 1.2 Hz), 7.30 (2H, s), 7.17 (4H, d, *J* = 2.1 Hz), 7.04 (2H, s), 7.01 (2H, s), 6.99 (2H, d, *J* = 8.6 Hz), 6.76 (2H, dd, *J* = 8.6, 2.1 Hz), 6.66 (2H, ddd, $J_{H\text{-}F}$ = 11.6, 9.1 Hz, $J_{H\text{-}H}$ = 2.3 Hz), 6.55 (4H, d, *J* = 2.1 Hz), 6.02 (2H, t, *J* = 2.1 Hz), 5.88 (2H, t, *J* = 2.1 Hz), 5.62 (2H, dd, $J_{H\text{-}F}$ = 7.8 Hz, $J_{H\text{-}H}$ = 2.3 Hz), 3.86-3.78 (8H, m), 3.62 (4H, dt, *J* = 9.3, 6.8 Hz), 3.52 (4H, dt, *J* = 9.3, 6.8 Hz), 2.92 (2H, sept, *J* = 6.8 Hz), 2.65 (2H, sept, *J* = 6.8 Hz), 2.58 (2H, sept, *J* = 6.8 Hz), 1.62 (8H, quin, *J* = 6.8 Hz), 1.53 (8H, quin, *J* = 6.8 Hz), 1.40 (18H, s), 1.42-1.30 (16H, m), 1.29 (12H, d, *J* = 6.8 Hz), 1.10 (6H, d, *J* = 6.8 Hz), 1.04 (6H, d, *J* = 6.8 Hz), 0.96 (6H, d, *J* = 6.8 Hz), 0.92-0.84 (30H, m); $^{13}$C NMR (126 MHz, $CDCl_3$) $\delta$ 176.9, 168.0 (d, $J_{C\text{-}F}$ = 4.8 Hz), 166.6, 165.1 (dd, $J_{C\text{-}F}$ = 262.5, 13.4 Hz), 162.8 (dd, $J_{C\text{-}F}$ = 266.1, 12.7 Hz), 159.3, 158.7, 155.3, 153.9 (d, $J_{C\text{-}F}$ = 7.3 Hz), 150.7, 148.7, 147.5, 147.4, 147.1, 147.0, 144.2 (d, $J_{C\text{-}F}$ = 4.8 Hz), 138.5, 137.8, 137.1, 136.0, 132.5, 131.6, 130.0, 128.2, 127.7, 127.5, 127.0, 126.9, 126.4, 125.9 (q, $J_{C\text{-}F}$ = 35.2 Hz), 124.3 (d, $J_{C\text{-}F}$ = 21.8 Hz), 121.7 (q, $J_{C\text{-}F}$ = 273.3 Hz), 121.6, 120.5, 120.3, 114.2 (d, $J_{C\text{-}F}$ = 16.9 Hz), 106.2, 106.0, 100.4$_1$, 100.3$_7$ (t, $J_{C\text{-}F}$ = 26.0 Hz), 100.0,

84.9, 67.5, 67.3, 36.2, 34.4, 31.7, 31.6, 30.3, 24.5, 24.4, 24.3, $24.2_4$, $24.2_0$, 23.9, 19.5, 19.4, 14.1, three carbon atoms were not found probably due to overlapping.; $^{19}$F NMR (470 MHz, $CDCl_3$) $\delta$ −62.7, –100.7, –104.5; $^{11}$B NMR (160 MHz, $CDCl_3$) $\delta$ 10.9; IR (film): 2959, 2868, 1653, 1591, 1482, 1235, 1382, 1328, 1297, 1251, 1138, 1109, 1088, 988, 905 cm$^{-1}$; $[\alpha]_D^{24}$ −214.4 ($c$ = 10.0, $CHCl_3$).

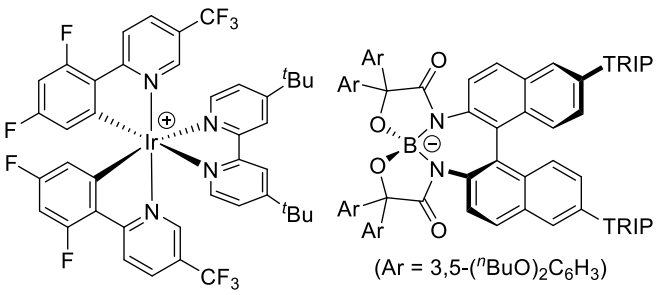


**Λ-[Ir-complex]·1g:** Prepared from enantiomerically pure iridium chloride *Λ*-[Ir(dFCF$_3$ppy)$_2$(dtbbpy)]·Cl (see below). $^1$H NMR (500 MHz, $CDCl_3$) $\delta$ 8.41 (2H, dd, $J_{H\text{-}H}$ = 8.8 Hz, $J_{H\text{-}F}$ = 2.8 Hz), 8.38 (2H, d, $J$ = 1.3 Hz), 7.98 (2H, dd, $J$ = 8.8, 1.3 Hz), 7.94 (2H, d, $J$ = 5.8 Hz), 7.86 (2H, d, $J$ = 8.7 Hz), 7.73 (2H, d, $J$ = 8.7 Hz), 7.63 (2H, dd, $J$ = 5.8, 1.3 Hz), 7.49 (2H, s), 7.30 (2H, s), 7.14 (4H, d, $J$ = 2.2 Hz), 7.04 (2H, s), 7.00 (2H, s), 6.98 (2H, d, $J$ = 8.7 Hz), 6.76 (2H, dd, $J$ = 8.7, 1.3 Hz), 6.64 (2H, ddd, $J_{H\text{-}F}$ = 11.6, 9.1 Hz, $J_{H\text{-}H}$ = 2.3 Hz), 6.54 (4H, d, $J$ = 2.2 Hz), 6.07 (2H, t, $J$ = 2.2 Hz), 5.89 (2H, t, $J$ = 2.2 Hz), 5.61 (2H, dd, $J_{H\text{-}F}$ = 8.0 Hz, $J_{H\text{-}H}$ = 2.3 Hz), 3.82 (8H, t, $J$ = 6.8 Hz), 3.61 (4H, dt, $J$ = 9.2, 6.8 Hz), 3.52 (4H, dt, $J$ = 9.2, 6.8 Hz), 2.92 (2H, sept, $J$ = 6.8 Hz), 2.65 (2H, sept, $J$ = 6.8 Hz), 2.57 (2H, sept, $J$ = 6.8 Hz), 1.62 (8H, quin, $J$ = 6.8 Hz), 1.53 (8H, quin, $J$ = 6.8 Hz), 1.39 (18H, s), 1.41-1.32 (16H, m), 1.29 (12H, d, $J$ = 6.8 Hz), 1.11 (6H, d, $J$ = 6.8 Hz), 1.04 (6H, d, $J$ = 6.8 Hz), 0.96 (6H, d, $J$ = 6.8 Hz), 0.91-0.84 (30H, m); $^{13}$C NMR (126 MHz, $CDCl_3$) $\delta$ 176.9, 168.0 (d, $J_{C\text{-}F}$ = 7.2 Hz), 166.7, 165.1 (dd, $J_{C\text{-}F}$ = 262.5, 12.7 Hz), 162.8 (dd, $J_{C\text{-}F}$ = 287.2, 13.7 Hz), 159.3, 158.7, 155.3, 154.0 (d, $J_{C\text{-}F}$ = 7.3 Hz), 150.7, 148.7, 147.5, 147.4, 147.1, 146.9, 144.2 (d, $J_{C\text{-}F}$ = 3.7 Hz), 138.5, 137.8, 137.0, 136.0, 132.5, 131.6, 130.0, $128.2_1$, $128.1_7$, 127.8, 127.6, 127.0, 126.8, 126.3, 125.9 (q, $J_{C\text{-}F}$ = 35.2 Hz), 124.3 (d, $J_{C\text{-}F}$ = 20.5 Hz), $121.7_2$, $121.7_0$ (q, $J_{C\text{-}F}$ = 273.3 Hz), 120.5, 120.3, 114.2 (d, $J_{C\text{-}F}$ = 18.1 Hz), 106.3, 106.0, 100.5, 100.4 (t, $J_{C\text{-}F}$ = 26.0 Hz), 100.0, 85.0, 67.5, 67.2, 36.2, 34.4, 31.7, 31.6, 30.3, 24.5, 24.4, 24.3, $24.2_4$, $24.1_9$, 23.9, 19.5, 19.4, 14.1, two carbon atoms were not found probably due to overlapping.; $^{19}$F NMR (470 MHz, $CDCl_3$) $\delta$ −62.8, –100.7, –104.6; $^{11}$B NMR (160 MHz, $CDCl_3$) $\delta$ 10.9; IR (film): 2959, 2869, 1659, 1599, 1482, 1382, 1327, 1295, 1140, 1109, 991, 907 cm$^{-1}$; $[\alpha]_D^{24}$ +107.7 ($c$ = 9.6, $CHCl_3$).

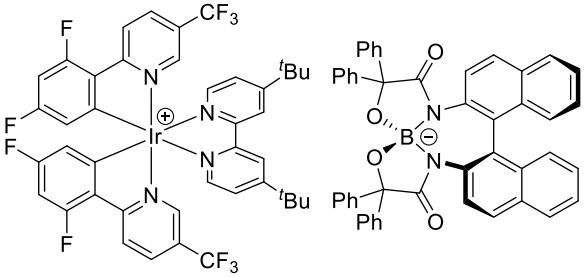


***rac*-[Ir-complex]·1a:** Triethylammonium borate **1a**·HNEt$_3$ was prepared by following the literature procedure.[11] $^1$H NMR (500 MHz, $CDCl_3$) *mixture of diastereomers* $\delta$ 8.43 (1H, dd, $J_{H\text{-}H}$ = 8.8 Hz, $J_{H\text{-}F}$ = 2.6 Hz), 8.40 (1H, dd, $J_{H\text{-}H}$ = 8.8 Hz, $J_{H\text{-}F}$ = 2.6 Hz), 8.32

(1H, d, $J$ = 1.9 Hz), 8.31 (1H, d, $J$ = 1.9 Hz), 8.08 (4H, d, $J$ = 7.8 Hz), 7.98 (1H, dd, $J$ = 8.8, 1.9 Hz), 7.95 (1H, dd, $J$ = 8.8, 1.9 Hz), 7.89 (1H, d, $J$ = 5.8 Hz), $7.87_3$ (1H, d, $J$ = 5.8 Hz), $7.86_9$ (2H, d, $J$ = 7.8 Hz), 7.75 (2H, d, $J$ = 7.8 Hz), 7.59 (1H, dd, $J$ = 5.8, 1.9 Hz), 7.52 (1H, dd, $J$ = 5.8, 1.9 Hz), 7.45 (2H, d, $J$ = 7.8 Hz), 7.34 (2H, ddd, $J$ = 7.8, 7.9, 1.3 Hz), 7.32 (2H, d, $J$ = 7.8 Hz), 7.30 (2H, s), 7.26 (4H, t, $J$ = 7.8 Hz), 7.15 (2H, t, $J$ = 7.8 Hz), 7.10 (2H, ddd, $J$ = 7.8, 7.0, 1.3 Hz), 6.71 (2H, t, $J$ = 7.8 Hz), 6.64 (2H, ddd, $J_{H\text{-}F}$ = 12.1, 9.3 Hz, $J_{H\text{-}H}$ = 2.3 Hz), 6.61 (1H, ddd, $J_{H\text{-}F}$ = 12.1, 9.3 Hz, $J_{H\text{-}H}$ = 2.3 Hz), 6.46 (4H, t, $J$ = 7.8 Hz), 6.32 (4H, dd, $J$ = 7.8, 1.3 Hz), 5.60 (2H, dd, $J_{H\text{-}F}$ = 8.0 Hz, $J_{H\text{-}H}$ = 2.3 Hz), 1.36 (18H, s); $^{13}$C NMR (151 MHz, $CDCl_3$) *mixture of diastereomers* $\delta$ 177.1, $168.0_5$ (d, $J_{C\text{-}F}$ = 5.7 Hz), $168.0_2$ (d, $J_{C\text{-}F}$ = 4.4 Hz), $166.6_5$, $166.5_6$, 165.1 (dd, $J_{C\text{-}F}$ = 262.4, 5.1 Hz), 165.0 (dd, $J_{C\text{-}F}$ = 265.3, 4.3 Hz), 162.8 (dd, $J_{C\text{-}F}$ = 264.6, 4.4 Hz), 162.7 (dd, $J_{C\text{-}F}$ = 265.2, 5.1 Hz), $155.1_3$, $155.0_8$, 153.9, 150.7, 150.5, 146.8, 144.5, 144.1 (d, $J_{C\text{-}F}$ = 4.4 Hz), 139.2, 137.1, 137.0, 133.9, 132.3, 131.0, 128.5, $128.2_0$, $128.1_6$, 128.0, 127.7, 127.1, $127.0_0$, $126.9_5$, 126.9, 126.4, 126.3, 126.0, $125.9_4$ (q, $J_{C\text{-}F}$ = 34.6 Hz), $125.8_8$ (q, $J_{C\text{-}F}$ = 33.2 Hz), 125.6, 125.1, 124.4, 124.3 (d, $J_{C\text{-}F}$ = 20.9 Hz), 121.6 (q, $J_{C\text{-}F}$ = 274.0 Hz), 121.5, 121.4, $114.0_9$ (d, $J_{C\text{-}F}$ = 18.9 Hz), $114.0_6$ (d, $J_{C\text{-}F}$ = 17.4 Hz), 100.4 (t, $J_{C\text{-}F}$ = 26.7 Hz), 100.3 (t, $J_{C\text{-}F}$ = 26.7 Hz), 85.4, 36.2, 36.1, 30.3, 26 carbon atoms were not found probably due to overlapping.; $^{19}$F NMR (470 MHz, $CDCl_3$) *mixture of diastereomers* $\delta$ −62.8, −100.4, −100.7, −104.6, −104.7, one fluorine atom was not found probably due to overlapping.; $^{11}$B NMR (160 MHz, $CDCl_3$) *mixture of diastereomers* $\delta$ 10.8 (overlapped); IR (film): 3069, 1661, 1601, 1577, 1492, 1395, 1329, 1299, 1143, 1110, 1090, 1023, 993, 850 cm$^{-1}$.

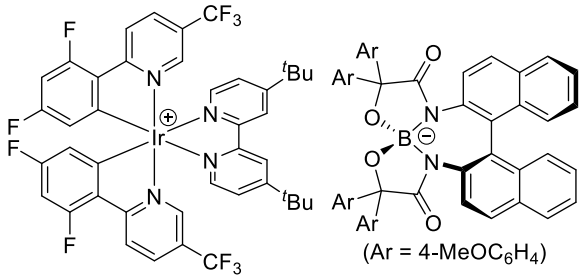


***rac*-[Ir-complex]·1b (Ar = 4-MeOC$_6$H$_4$):** $^1$H NMR (500 MHz, $CDCl_3$) *mixture of diastereomers* $\delta$ 8.41 (1H, dd, $J_{H\text{-}H}$ = 9.3 Hz, $J_{H\text{-}F}$ = 2.3 Hz), 8.39 (1H, dd, $J_{H\text{-}H}$ = 9.3 Hz, $J_{H\text{-}F}$ = 2.3 Hz), 8.32 (2H, s), 7.95 (2H, d, $J$ = 9.3 Hz), 7.94 (4H, d, $J$ = 9.0 Hz), 7.89 (1H, d, $J$ = 5.8 Hz), 7.87 (1H, d, $J$ = 5.8 Hz), 7.85 (2H, d, $J$ = 7.8 Hz), 7.76 (2H, d, $J$ = 7.8 Hz), 7.59 (1H, dd, $J$ = 5.8, 1.5 Hz), 7.54 (1H, dd, $J$ = 5.8, 1.5 Hz), 7.45 (2H, d, $J$ = 7.8 Hz), 7.32 (2H, t, $J$ = 7.8 Hz), $7.30_4$ (2H, d, $J$ = 7.8 Hz), $7.29_6$ (1H, s), 7.29 (1H, s), 7.07 (2H, t, $J$ = 7.8 Hz), 6.80 (4H, d, $J$ = 9.0 Hz), 6.64 (1H, ddd, $J_{H\text{-}F}$ = 9.0, 6.3 Hz, $J_{H\text{-}H}$ = 2.5 Hz), 6.61 (1H, ddd, $J_{H\text{-}F}$ = 9.0, 6.3 Hz, $J_{H\text{-}H}$ = 2.5 Hz), 6.22 (4H, d, $J$ = 9.0 Hz), 5.99 (4H, d, $J$ = 9.0 Hz), 5.60 (2H, d, $J_{H\text{-}F}$ = 8.0 Hz), 3.76 (6H, s), 3.52 (6H, s), 1.36 (9H, s), 1.35 (9H, s); $^{13}$C NMR (126 MHz, $CDCl_3$) *mixture of diastereomers* $\delta$ 177.5, 168.0 (d, $J_{C\text{-}F}$ = 6.0 Hz), $166.6_1$, $166.5_7$, 165.0 (dd, $J_{C\text{-}F}$ = 263.7, 12.1 Hz), 162.7 (dd, $J_{C\text{-}F}$ = 265.5, 12.7 Hz), 158.1, 157.4, $155.1_8$, $155.1_6$, 153.9 (d, $J_{C\text{-}F}$ = 6.0 Hz), $150.5_8$, $150.5_5$, 144.2, 139.6, 139.2, 137.1, 133.8, 132.3, 131.0, 128.9, 128.8, 128.5, 128.3, 128.1, 127.6, 126.9, 126.3, 125.9 (q, $J_{C\text{-}F}$ = 34.5 Hz), 125.2, 124.4, 124.3 (d, $J_{C\text{-}F}$ = 20.5 Hz), $121.6_4$ (q, $J_{C\text{-}F}$ = 273.3 Hz), $121.6_3$, $121.5_8$, 114.1

(d, $J_{C\text{-}F}$ = 18.1 Hz), 112.6, 112.4, 100.4 (t, $J_{C\text{-}F}$ = 26.6 Hz), 100.3 (t, $J_{C\text{-}F}$ = 26.6 Hz), 84.7, 55.3, 55.0, 36.2, 30.3, 37 carbon atoms were not found probably due to overlapping.; $^{19}$F NMR (470 MHz, $CDCl_3$) *mixture of diastereomers* $\delta$ −62.7, −100.6, −100.7, −104.6, two fluorine atoms were not found probably due to overlapping.; $^{11}$B NMR (160 MHz, $CDCl_3$) *mixture of diastereomers* $\delta$ 10.7 (overlapped); IR (film): 3056, 2958, 1654, 1601, 1506, 1464, 1386, 1327, 1296, 1241, 1168, 1139, 1108, 1019 cm$^{-1}$.

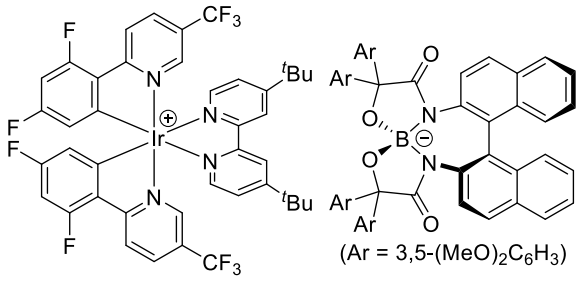


***rac*-[Ir-complex]·1c (Ar = 3,5-(MeO)$_2$C$_6$H$_3$):** $^1$H NMR (500 MHz, $CDCl_3$) *mixture of diastereomers* $\delta$ 8.38 (1H, dd, $J_{H\text{-}H}$ = 8.8 Hz, $J_{H\text{-}F}$ = 3.0 Hz), 8.34 (1H, dd, $J_{H\text{-}H}$ = 8.8 Hz, $J_{H\text{-}F}$ = 3.0 Hz), 8.33 (1H, s), 8.31 (1H, s), 7.94 (2H, d, $J$ = 8.8 Hz), 7.93 (1H, d, $J$ = 6.0 Hz), 7.91 (1H, d, $J$ = 6.0 Hz), 7.73 (2H, d, $J$ = 8.0 Hz), 7.60$_9$ (1H, d, $J$ = 6.0 Hz), 7.60$_7$ (2H, d, $J$ = 8.0 Hz), 7.55 (1H, d, $J$ = 6.0 Hz), 7.42 (2H, d, $J$ = 8.0 Hz), 7.32 (2H, s), 7.27 (4H, d, $J$ = 2.0 Hz), 7.24 (2H, t, $J$ = 8.0 Hz), 7.13 (2H, d, $J$ = 8.0 Hz), 6.98 (2H, t, $J$ = 8.0 Hz), 6.63 (2H, t, $J_{H\text{-}F}$ = 10.5 Hz), 6.16 (2H, t, $J$ = 2.0 Hz), 6.11 (4H, d, $J$ = 2.0 Hz), 5.87 (2H, t, $J$ = 2.0 Hz), 5.61 (2H, d, $J_{H\text{-}F}$ = 8.0 Hz), 3.70 (12H, s), 3.07 (12H, s), 1.36 (9H, s), 1.35 (9H, s); $^{13}$C NMR (126 MHz, $CDCl_3$) *mixture of diastereomers* $\delta$ 176.3, 168.0 (d, $J_{C\text{-}F}$ = 6.0 Hz), 166.6$_2$, 166.5$_6$, 165.0 (dd, $J_{C\text{-}F}$ = 263.1, 12.7 Hz), 162.7 (dd, $J_{C\text{-}F}$ = 265.5, 12.7 Hz), 159.7, 159.3, 155.2$_0$, 155.1$_5$, 153.9 (d, $J_{C\text{-}F}$ = 7.3 Hz), 150.7, 150.6, 148.6, 148.2, 144.2, 138.8, 137.0, 136.9, 133.6, 132.2, 130.3, 128.2, 128.1, 127.8$_1$, 127.7$_7$, 126.8, 126.3, 125.9 (q, $J_{C\text{-}F}$ = 35.1 Hz), 125.8 (q, $J_{C\text{-}F}$ = 34.5 Hz), 124.6, 124.2$_4$ (d, $J_{C\text{-}F}$ = 21.8 Hz), 124.2$_1$ (d, $J_{C\text{-}F}$ = 20.7 Hz), 124.1, 121.7 (q, $J_{C\text{-}F}$ = 272.9 Hz), 121.5, 121.4, 114.1 (d, $J_{C\text{-}F}$ = 18.1 Hz), 105.7, 105.4, 100.3 (t, $J_{C\text{-}F}$ = 26.6 Hz), 99.6, 99.4, 85.2, 55.4, 54.7, 36.1$_3$, 36.1$_0$, 30.2, 33 carbon atoms were not found probably due to overlapping.; $^{19}$F NMR (470 MHz, $CDCl_3$) *mixture of diastereomers* $\delta$ −62.8, −100.7, −100.8, −104.5, two fluorine atoms were not found probably due to overlapping.; $^{11}$B NMR (160 MHz, $CDCl_3$) *mixture of diastereomers* $\delta$ 10.8 (overlapped); IR (film): 2937, 2834, 1653, 1591, 1457, 1384, 1328, 1296, 1251, 1204, 1139, 1090, 1044, 903 cm$^{-1}$.

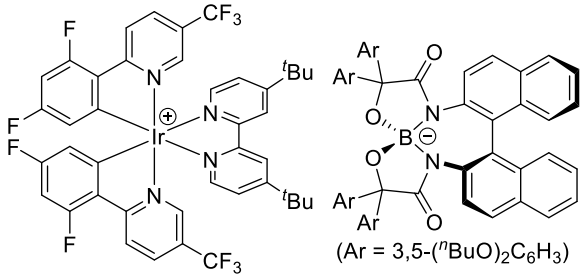


***rac*-[Ir-complex]·1d (Ar = 3,5-($^n$BuO)$_2$C$_6$H$_3$):** $^1$H NMR (500 MHz, $CDCl_3$) *mixture of diastereomers* $\delta$ 8.38 (1H, dd, $J_{H\text{-}H}$ = 8.8 Hz, $J_{H\text{-}F}$ = 2.7 Hz), 8.35 (1H, dd, $J_{H\text{-}H}$ = 8.8 Hz, $J_{H\text{-}F}$ = 2.7 Hz), 8.34 (1H, d, $J$ = 1.8 Hz), 8.32 (1H, d, $J$ = 1.8 Hz), 7.95 (1H, dd, $J$ = 8.8, 1.8 Hz), 7.94 (1H, d, $J$ = 6.3 Hz), 7.93 (1H, d, $J$ = 6.3 Hz), 7.91 (1H, dd, $J$ = 8.8, 1.8 Hz),

7.68 (2H, d, $J$ = 8.0 Hz), 7.64 (1H, dd, $J$ = 6.3, 1.8 Hz), 7.59 (1H, dd, $J$ = 6.3, 1.8 Hz), 7.51 (2H, d, $J$ = 8.0 Hz), 7.33 (2H, d, $J$ = 8.0 Hz), 7.29 (2H, brs), $7.20_4$ (2H, t, $J$ = 8.0 Hz), $7.19_7$ (4H, d, $J$ = 2.3 Hz), 7.10 (2H, d, $J$ = 8.0 Hz), 6.96 (2H, t, $J$ = 8.0 Hz), 6.65 (1H, ddd, $J_{H\text{-}F}$ = 8.9, 6.3 Hz, $J_{H\text{-}H}$ = 2.5 Hz), 6.63 (1H, ddd, $J_{H\text{-}F}$ = 8.9, 6.3 Hz, $J_{H\text{-}H}$ = 2.5 Hz), 6.23 (4H, d, $J$ = 2.3 Hz), 6.13 (2H, t, $J$ = 2.3 Hz), 5.89 (2H, t, $J$ = 2.3 Hz), 5.61 (1H, dd, $J_{H\text{-}F}$ = 7.8 Hz, $J_{H\text{-}H}$ = 2.5 Hz), 5.60 (1H, dd, $J_{H\text{-}F}$ = 7.8 Hz, $J_{H\text{-}H}$ = 2.5 Hz), 3.90 (4H, dt, $J$ = 13.8, 7.1 Hz), 3.88 (4H, dt, $J$ = 13.8, 7.1 Hz), 3.39 (4H, dt, $J$ = 9.3, 7.1 Hz), 3.12 (4H, dt, $J$ = 9.3, 7.1 Hz), 1.62 (8H, quin, $J$ = 7.1 Hz), $1.44_3$ (4H, quin, $J$ = 7.1 Hz), $1.43_8$ (4H, quin, $J$ = 7.1 Hz), 1.40 (9H, s), 1.39 (9H, s), 1.36 (8H, sex, $J$ = 7.1 Hz), 1.28 (4H, sex, $J$ = 7.1 Hz), 1.27 (4H, sex, $J$ = 7.1 Hz), 0.86 (12H, t, $J$ = 7.1 Hz), 0.85 (12H, t, $J$ = 7.1 Hz); $^{13}$C NMR (126 MHz, $CDCl_3$) *mixture of diastereomers* $\delta$ 176.4, 168.1, 166.7, 166.6, 165.1 (dd, $J_{C\text{-}F}$ = 263.1, 12.7 Hz), 162.8 (dd, $J_{C\text{-}F}$ = 265.5, 13.9 Hz), 159.2, 158.9, 155.3, 155.2, 153.9 (d, $J_{C\text{-}F}$ = 7.2 Hz), 150.8, 150.7, 148.4, 148.2, 144.1 (d, $J_{C\text{-}F}$ = 3.7 Hz), 138.9, 137.0, 136.9, 133.5, 132.0, 130.4, $128.1_2$, $128.0_5$, 127.9, 127.8, 126.9, 126.3, 126.0 (q, $J_{C\text{-}F}$ = 35.1 Hz), 125.9 (q, $J_{C\text{-}F}$ = 33.9 Hz), 124.4, 124.2 (d, $J_{C\text{-}F}$ = 7.3 Hz), 123.9, 121.7 (q, $J_{C\text{-}F}$ = 273.0 Hz), 121.6, 121.5, 114.1 (d, $J_{C\text{-}F}$ = 19.4 Hz), 106.2, 105.8, 100.4 (t, $J_{C\text{-}F}$ = 28.4 Hz), $100.2_2$, $100.1_5$, 85.2, 67.6, 67.0, $36.2_3$, $36.2_0$, 31.7, 31.6, 30.3, 19.4, 19.3, $14.1_0$, $14.0_6$, 40 carbon atoms were not found probably due to overlapping.; $^{19}$F NMR (470 MHz, $CDCl_3$) *mixture of diastereomers* $\delta$ −62.8, −100.6, −100.7, −104.5, two fluorine atoms were not found probably due to overlapping.; $^{11}$B NMR (160 MHz, $CDCl_3$) *mixture of diastereomers* $\delta$ 10.8 (overlapped); IR (film): 2958, 2868, 1659, 1592, 1464, 1435, 1382, 1328, 1297, 1252, 1135, 1109, 1049, 847 cm$^{-1}$.

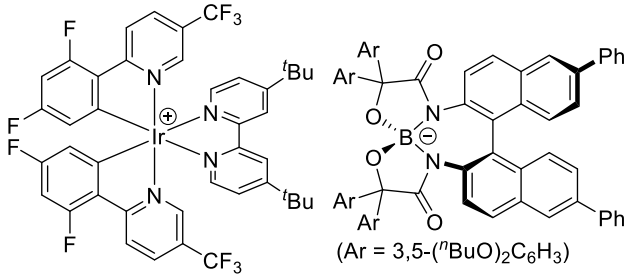


***rac*-[Ir-complex]·1e (Ar = 3,5-($^n$BuO)$_2$C$_6$H$_3$):** $^1$H NMR (600 MHz, $CDCl_3$) *mixture of diastereomers* $\delta$ 8.38 (1H, dd, $J_{H\text{-}H}$ = 9.3 Hz, $J_{H\text{-}F}$ = 2.1 Hz), 8.36 (1H, dd, $J_{H\text{-}H}$ = 9.3 Hz, $J_{H\text{-}F}$ = 2.1 Hz), 8.35 (1H, s), 8.33 (1H, s), 7.95 (2H, d, $J$ = 1.8 Hz), 7.95-7.90 (4H, m), 7.69 (4H, d, $J$ = 8.0 Hz), 7.62 (1H, dd, $J$ = 6.0, 1.5 Hz), 7.60 (2H, d, $J$ = 8.0 Hz), 7.57 (2H, dd, $J$ = 6.0, 1.5 Hz), 7.40 (4H, t, $J$ = 8.0 Hz), 7.38 (2H, d, $J$ = 8.0 Hz), 7.31 (2H, dd, $J$ = 8.0, 1.8 Hz), 7.29 (2H, t, $J$ = 8.0 Hz), 7.29 (2H, s), 7.23 (2H, d, $J$ = 8.0 Hz), 7.21 (4H, d, $J$ = 2.3 Hz), 6.63 (1H, ddd, $J_{H\text{-}F}$ = 12.0, 9.6 Hz, $J_{H\text{-}H}$ = 2.3 Hz), 6.61 (1H, ddd, $J_{H\text{-}F}$ = 12.0, 9.6 Hz, $J_{H\text{-}H}$ = 2.3 Hz), 6.25 (4H, d, $J$ = 2.3 Hz), 6.15 (2H, t, $J$ = 2.3 Hz), 5.91 (2H, t, $J$ = 2.3 Hz), 5.60 (1H, dd, $J_{H\text{-}F}$ = 7.1 Hz, $J_{H\text{-}H}$ = 2.3 Hz), 5.59 (1H, dd, $J_{H\text{-}F}$ = 7.1 Hz, $J_{H\text{-}H}$ = 2.3 Hz), 3.93-3.86 (8H, m), 3.39 (4H, dt, $J$ = 9.1, 7.0 Hz), 3.17 (4H, dt, $J$ = 9.1, 7.0 Hz), 1.62 (8H, quin, $J$ = 7.0 Hz), 1.39-1.32 (16H, m), 1.38 (9H, s), 1.37 (9H, s), 1.20 (4H, sex, $J$ = 7.0 Hz), 1.17 (4H, sex, $J$ = 7.0 Hz), 0.86 (12H, t, $J$ = 7.0 Hz), 0.73 (12H, t, $J$ = 7.0 Hz); $^{13}$C NMR (151 MHz, $CDCl_3$) *mixture of diastereomers* $\delta$ 176.6, 168.1,

166.7, 166.6, 165.1 (dd, $J_{C\text{-}F}$ = 263.8, 13.0 Hz), 163.6 (dd, $J_{C\text{-}F}$ = 263.8, 13.0 Hz), 160.1, 159.2, 158.9, 155.3, 155.2, 153.9 (d, $J_{C\text{-}F}$ = 4.4 Hz), 150.8, 150.7, 148.2, 148.1, 144.2 (d, $J_{C\text{-}F}$ = 2.9 Hz), 141.1, 139.1, 137.0$_1$, 136.9$_6$, 136.0, 132.8, 132.4, 130.3, 128.7, 128.5, 128.3, 127.2, 126.9$_2$, 126.8$_7$, 126.3, 125.9$_4$ (q, $J_{C\text{-}F}$ = 34.6 Hz), 125.9$_0$ (q, $J_{C\text{-}F}$ = 34.7 Hz), 125.5, 124.3 (d, $J_{C\text{-}F}$ = 21.6 Hz), 123.9, 121.8 (q, $J_{C\text{-}F}$ = 271.8 Hz), 121.7, 121.5, 114.1 (d, $J_{C\text{-}F}$ = 17.4 Hz), 106.2, 105.8, 100.4 (t, $J_{C\text{-}F}$ = 27.6 Hz), 100.3, 100.2, 85.3, 67.6, 67.1, 36.2$_0$, 36.1$_9$, 31.6, 31.5, 30.3, 19.4, 19.3, 14.1, 13.9, 44 carbon atoms were not found probably due to overlapping.; $^{19}$F NMR (470 MHz, $CDCl_3$) *mixture of diastereomers* $\delta$ −62.8, −100.6, −104.5, three fluorine atoms were not found probably due to overlapping.; $^{11}$B NMR (160 MHz, $CDCl_3$) *mixture of diastereomers* $\delta$ 10.8 (overlapped); IR (film): 2956, 2867, 1658, 1587, 1443, 1382, 1327, 1296, 1136, 1034, 991, 909 cm$^{-1}$.

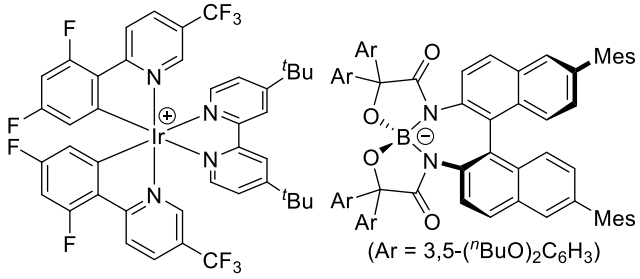


***rac*-[Ir-complex]·1f (Mes = 2,4,6-Me$_3$C$_6$H$_2$, Ar = 3,5-($^n$BuO)$_2$C$_6$H$_3$):** $^1$H NMR (600 MHz, $CDCl_3$) *mixture of diastereomers* $\delta$ 8.41-8.35 (4H, m), 7.95 (1H, d, $J$ = 8.1 Hz), 7.94 (1H, d, $J$ = 8.1 Hz), 7.93 (1H, d, $J$ = 6.3 Hz), 7.92 (1H, d, $J$ = 6.3 Hz), 7.75 (2H, d, $J$ = 8.4 Hz), 7.67 (2H, d, $J$ = 8.4 Hz), 7.61 (1H, d, $J$ = 6.3 Hz), 7.60 (1H, d, $J$ = 6.3 Hz), 7.44 (2H, s), 7.29 (2H, s), 7.18 (4H, s), 7.02 (2H, d, $J$ = 8.4 Hz), 6.90 (4H, s), 6.70 (2H, d, $J$ = 8.4 Hz), 6.63 (1H, t, $J_{H\text{-}F}$ = 10.0 Hz), 6.60 (1H, t, $J_{H\text{-}F}$ = 10.0 Hz), 6.47 (4H, s), 6.08 (2H, s), 5.84 (2H, s), 5.61 (1H, d, $J_{H\text{-}F}$ = 10.0 Hz), 5.59 (1H, d, $J_{H\text{-}F}$ = 10.0 Hz), 3.84 (8H, t, $J$ = 6.6 Hz), 3.54 (4H, dt, $J$ = 9.0, 7.2 Hz), 3.49 (4H, dt, $J$ = 9.0, 7.2 Hz), 2.31 (6H, s), 1.96 (6H, s), 1.95 (6H, s), 1.62 (8H, quin, $J$ = 7.2 Hz), 1.50 (8H, quin, $J$ = 7.2 Hz), 1.39 (9H, s), 1.38 (9H, s), 1.37 (8H, sex, $J$ = 7.2 Hz), 1.32 (8H, sex, $J$ = 7.2 Hz), 0.87 (12H, t, $J$ = 7.2 Hz), 0.84 (12H, t, $J$ = 7.2 Hz); $^{13}$C NMR (151 MHz, $CDCl_3$) $\delta$ 176.8, 168.0, 166.6, 165.0 (dd, $J_{C\text{-}F}$ = 263.9, 10.8 Hz), 162.7 (dd, $J_{C\text{-}F}$ = 264.6, 13.0 Hz), 159.3, 158.7, 155.3, 153.9 (d, $J_{C\text{-}F}$ = 7.2 Hz), 150.7$_1$, 150.6$_9$, 148.5, 147.8, 144.1 (d, $J_{C\text{-}F}$ = 2.9 Hz), 139.4, 138.7, 137.1, 137.0, 136.5, 136.4, 136.2$_2$, 136.1$_6$, 132.6, 131.9, 130.2, 128.5, 128.1, 128.0$_4$, 127.9$_6$, 127.8, 127.4, 126.9, 126.8, 126.3, 126.2, 125.9 (q, $J_{C\text{-}F}$ = 125.9 Hz), 124.3 (d, $J_{C\text{-}F}$ = 21.7 Hz), 121.7 (q, $J_{C\text{-}F}$ = 271.8 Hz), 121.6, 114.1 (d, $J_{C\text{-}F}$ = 17.4 Hz), 114.0 (d, $J_{C\text{-}F}$ = 17.4 Hz), 106.3, 106.0, 100.4, 100.3 (t, $J_{C\text{-}F}$ = 34.7 Hz), 100.0, 85.0, 67.6, 67.2, 36.2, 31.7, 31.5, 30.3, 21.1, 21.0, 20.7, 19.3$_8$, 19.3$_5$, 14.1, 14.0, 52 carbon atoms were not found probably due to overlapping.; $^{19}$F NMR (470 MHz, $CDCl_3$) *mixture of diastereomers* $\delta$ −62.8, –100.6$_8$, –100.7$_4$, –104.5, two fluorine atoms were not found probably due to overlapping.; $^{11}$B NMR (160 MHz, $CDCl_3$) *mixture of diastereomers* $\delta$ 10.9 (overlapped); IR (film): 2963, 2870, 1659, 1592, 1485, 1434, 1393, 1328, 1297, 1146, 1048, 912 cm$^{-1}$.

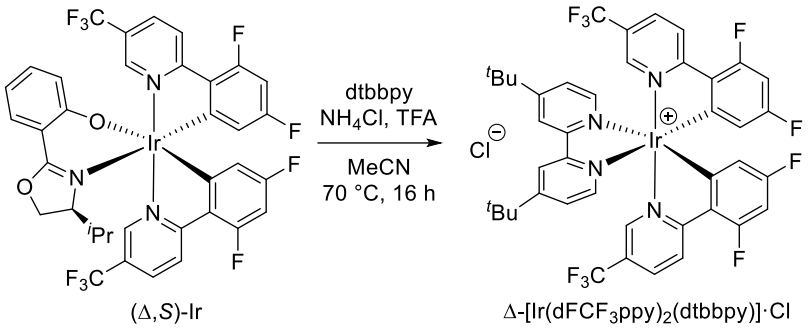


(Δ,*S*)-Ir  Δ-[Ir(dFCF$_3$ppy)$_2$(dtbbpy)]·Cl

**Procedure for the Synthesis of Enantiomerically Pure Iridium Chloride:** To a solution of the resolved neutral iridium complex (Δ,*S*)-**Ir** (0.11 g, 0.10 mmol),[23] dtbbpy (0.090 g, 0.33 mmol), and $NH_4Cl$ (0.033 g, 0.62 mmol) in MeCN (12.0 mL) was added TFA (0.046 mL, 0.61 mmol), and the resulting solution was stirred at 70 °C under Ar. After being stirred for 16 h, the mixture was cooled and concentrated in vacuo. The residual solid was dissolved into $CH_2Cl_2$ and the resulting solution was washed with water and brine. The organic phase was dried over $Na_2SO_4$ and concentrated. The crude residue was purified by column chromatography on silica gel ($CH_2Cl_2$/MeOH = 100:1 to 10:1 as eluent) to furnish Δ-[Ir(dFCF$_3$ppy)$_2$(dtbbpy)]·Cl (0.11 g, 0.11 mmol, 89%) as an yellow solid. **Δ-[Ir(dFCF$_3$ppy)$_2$(dtbbpy)]·Cl:** $^1$H NMR (500 MHz, $CDCl_3$) $\delta$ 9.84 (2H, s), 8.48 (2H, dd, $J$ = 8.8, 3.0 Hz), 8.05 (2H, dd, $J$ = 8.8, 1.5 Hz), 7.82 (2H, d, $J$ = 6.0 Hz), 7.56 (2H, dd, $J$ = 6.0, 1.8 Hz), 7.42 (2H, s), 6.64 (2H, ddd, $J_{H\text{-}F}$ = 11.9, 9.1 Hz, $J_{H\text{-}H}$ = 2.4 Hz), 5.64 (2H, dd, $J_{H\text{-}F}$ = 8.0 Hz, $J_{H\text{-}H}$ = 2.4 Hz), 1.58 (18H, s); $[\alpha]_D^{24}$ −307.4 ($c$ = 10.0, MeOH).

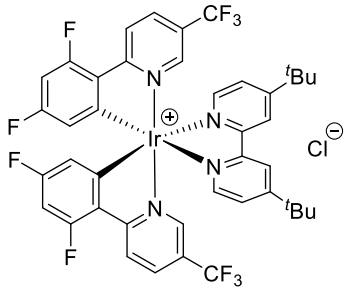

**Λ-[Ir(dFCF$_3$ppy)$_2$(dtbbpy)]·Cl:** According to the above procedure, the title compound was prepared with (Λ,*S*)-**Ir** as a precursor.[23] $[\alpha]_D^{24}$ +349.2 ($c$ = 10.1, MeOH).

**Preparation and Characterization of 1-Cyclopropyl-3-(3,5-dimethylphenyl)urea (2)**

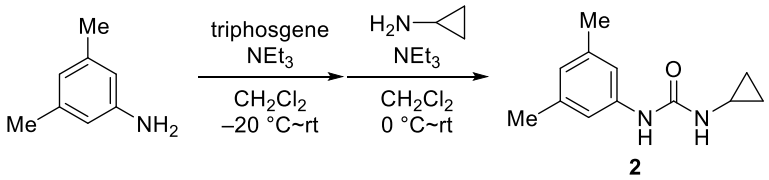


**2**

**Procedure for the Synthesis of 1-Cyclopropyl-3-(3,5-dimethylphenyl)urea (2):** A solution of 3,5-dimethylaniline (0.75 mL, 6.0 mmol) in $CH_2Cl_2$ (6.0 mL) was added to a $CH_2Cl_2$ solution of triphosgene (0.89 g, 3.0 mmol, 40.0 mL) and $NEt_3$ (0.83 mL, 6.0 mmol) at −20 °C under Ar atmosphere. After being stirred for 15 min, the mixture was warmed to ambient temperature and stirred for 3 h. All volatiles were then removed under reduced pressure. The residual solid was dissolved into $CH_2Cl_2$ (10.0 mL) and the resulting solution was added to a solution of cyclopropylamine (0.50 mL, 7.2 mmol) and $NEt_3$ (0.83 mL, 6.0 mmol) in $CH_2Cl_2$ (30.0 mL) at 0 °C under Ar atmosphere. The mixture was allowed to warm to ambient temperature and stirred for 12 h. The resulting mixture was quenched by the addition of $H_2O$ and the aqueous phase was extracted with $CHCl_3$ twice. The combined organic phases were dried over $Na_2SO_4$, filtered, and concentrated. Purification of the residue was performed by column chromatography on silica gel (H/$CHCl_3$/EA = 5:1:1 to 1:1:1 as eluent) to afford **2** (1.16 g, 5.7 mmol, 95%) as a white solid. **1-Cyclopropyl-3-(3,5-dimethylphenyl)urea (2):** $^1$H NMR (500 MHz, $(CD_3)_2CO$) δ 7.57 (1H, br), 7.13 (2H, s), 6.57 (1H, s), 5.85 (1H, br), 2.61 (1H, quind, *J* = 6.5, 3.2 Hz), 2.21 (6H, s), 0.73-0.63 (2H, m), 0.51-0.42 (2H, m); $^{13}$C NMR (126 MHz, $(CD_3)_2CO$) *δ* 156.7, 141.3, 138.7, 124.0, 117.0, 23.3, 21.5, 7.2; IR (KBr): 3328, 3021, 2915, 1649, 1617, 1576, 1334, 1278, 1229, 1189, 835 cm$^{-1}$; HRMS (ESI) Calcd for $C_{12}H_{16}N_2ONa$ ($[M+Na]^+$) 227.1155. Found 227.1150.

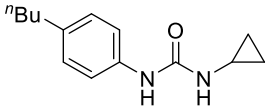


**1-Cyclopropyl-3-(4-*n*-butylphenyl)urea:** According to the above procedure, the title compound was prepared with 4-*n*-butylaniline as a precursor. $^1$H NMR (500 MHz, $CDCl_3$) δ 7.25 (1H, br), 7.24 (2H, d, *J* = 8.0 Hz), 7.07 (2H, d, *J* = 8.0 Hz), 5.46 (1H, br), 5.85 (1H, br), 2.59-2.51 (1H, m), 2.54 (2H, t, *J* = 7.5 Hz), 1.55 (2H, quin, *J* = 7.5 Hz), 1.33 (2H, sex, *J* = 7.5 Hz), 0.91 (3H, t, *J* = 7.5 Hz), 0.79-0.69 (2H, m), 0.60-0.51 (2H, m); $^{13}$C NMR (126 MHz, $CDCl_3$) *δ* 157.3, 138.1, 136.3, 129.0, 120.5, 35.1, 33.8, 22.7, 22.4, 14.1, 7.4; IR (film): 3299, 2931, 2852, 1640, 1595, 1549, 1411, 1305, 1240, 1206, 1019, 830 cm$^{-1}$; HRMS (ESI) Calcd for $C_{14}H_{20}N_2ONa$ ($[M+Na]^+$) 255.1468. Found 255.1467.

**Asymmetric [3+2] Radical Cycloaddition Reaction**

**Representative Procedure for the Asymmetric [3+2] Radical Cycloaddition Reaction**

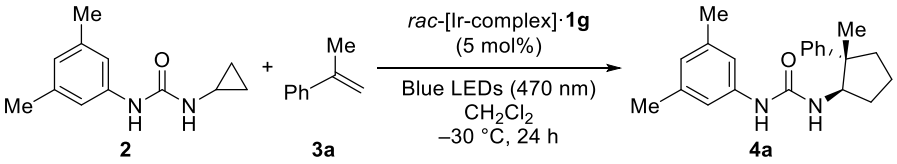


To a solution of 1-cyclopropyl-3-(3,5-dimethylphenyl)urea (**2**) (20.4 mg, 0.10 mmol) and *rac*-[Ir-complex]·**1g** (13.4 mg, 0.0050 mmol) in $CH_2Cl_2$ (1.0 mL) was added **3a** (59.1 mg, 0.50 mmol) under Ar atmosphere. The suspension was then subjected to freeze-pump-thaw process (1 cycle) and backfilled with Ar. The reaction mixture was illuminated with blue LEDs (470 nm) at −30 °C for 24 h. After exposing to air, the reaction mixture was concentrated to give the crude residue, which was analyzed by $^1$H NMR (500 MHz) to determine the diastereomeric ratio of the product. Purification of the residue by column chromatography on silica gel ($H/Et_2O$ = 3:1 to 1:1 as eluent) afforded **4a** (30.7 mg, 0.095 mmol, 95%) as a mixture of diastereomers. Enantiomeric excess of the major diastereomer of **4a** was determined by HPLC analysis on chiral stationary phase. **4a**: HPLC IB3, H/EtOH = 95:5, flow rate = 1.0 mL/min, 30 °C, λ = 254 nm, 9.9 min (minor diastereomer), 10.8 min (major enantiomer of major diastereomer), 18.1 min (minor diastereomer), 28.1 min (minor enantiomer of major diastereomer); $^1$H NMR (500 MHz, $(CD_3)_2CO$) major diastereomer $\delta$ 7.81 (1H, br), 7.48 (2H, d, $J$ = 7.4 Hz), 7.27 (2H, t, $J$ = 7.4 Hz), 7.14 (1H, t, $J$ = 7.4 Hz), 7.08 (2H, s), 6.55 (1H, s), 5.85 (1H, brd, $J$ = 8.5 Hz), 4.56 (1H, q, $J$ = 8.5 Hz), 2.19 (6H, s), 2.13 (1H, dddd, $J$ = 13.0, 8.5, 8.0, 4.8 Hz), 1.99 (1H, ddd, $J$ = 13.0, 9.5, 8.0 Hz), 1.86 (1H, ddd, $J$ = 13.0, 9.0, 4.8 Hz), 1.77 (1H, ddtd, $J$ = 13.0, 10.5, 8.0, 4.8 Hz), 1.66 (1H, ddddd, $J$ = 13.0, 9.5, 9.0, 6.5, 4.8 Hz), 1.56 (1H, dddd, $J$ = 13.0, 10.5, 8.5, 6.5 Hz), 1.28 (3H, s); $^{13}$C NMR (126 MHz, $(CD_3)_2CO$) major diastereomer $\delta$ 155.9, 149.6, 141.3, 138.7, 128.9, 126.8, 126.5, 123.9, 116.7, 58.3, 48.8, 39.7, 31.9, 22.9, 21.5, 20.4; IR (film): 3322, 2956, 2875, 1641, 1613, 1553, 1443, 1376, 1329, 1270, 1223, 1029, 837 cm$^{-1}$; HRMS (ESI) Calcd for $C_{21}H_{26}ON_2Na^+$ ([M+Na]$^+$) 345.1937. Found 345.1936.

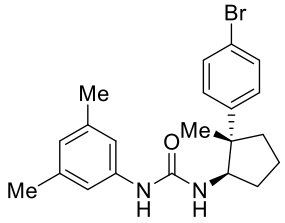


**4b**: HPLC IA3, H/$^i$PrOH = 10:1, flow rate = 1.0 mL/min, 30 °C, λ = 254 nm, 8.5 min (minor diastereomer), 10.4 min (major enantiomer of major diastereomer), 19.3 min (minor diastereomer), 31.9 min (minor enantiomer of major diastereomer); $^1$H NMR (500 MHz, $(CD_3)_2CO$) major diastereomer $\delta$ 7.83 (1H, br), 7.45-7.40 (4H, m), 7.06 (2H, s), 6.56 (1H, s), 5.87 (1H, brd, $J$ = 8.7 Hz), 4.51 (1H, q, $J$ = 8.7 Hz), 2.19 (6H, s), 2.17-2.07 (1H, m), 2.00-1.91 (1H, m), 1.89-1.81 (1H, m), 1.81-1.70 (1H, m), 1.70-1.59 (1H, m), 1.59-1.49 (1H, m), 1.26 (3H, s); $^{13}$C NMR (126 MHz, $(CD_3)_2CO$) major diastereomer $\delta$ 155.9, 149.1, 141.2, 138.8, 131.9, 129.1, 124.0, 119.9, 116.8, 58.3, 48.6, 39.7, 31.8, 22.6, 21.5, 20.3; IR (film): 3328, 2957, 2865, 1702, 1637, 1614, 1554, 1472, 1331, 1226, 1077, 1031, 1007, 821 cm$^{-1}$; HRMS (ESI) Calcd for

$C_{21}H_{25}ON_2{}^{79}BrNa^+$ ([M+Na]$^+$) 423.1042. Found 423.1030.

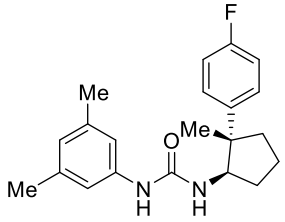

**4c**: HPLC IA3, H/$^i$PrOH = 93.5:6.5, flow rate = 1.0 mL/min, 30 °C, λ = 254 nm, 11.6 min (minor diastereomer), 13.6 min (major enantiomer of major diastereomer), 27.4 min (minor diastereomer), 54.6 min (minor enantiomer of major diastereomer); $^1$H NMR (500 MHz, $(CD_3)_2CO$) major diastereomer $\delta$ 7.83 (1H, br), 7.50 (2H, dd, $J_{H\text{-}H}$ = 9.0 Hz, $J_{H\text{-}F}$ = 5.5 Hz), 7.07 (2H, s), 7.01 (2H, dd, $J_{H\text{-}H}$ = 9.0 Hz, $J_{H\text{-}F}$ = 9.0 Hz), 6.56 (1H, s), 5.86 (1H, br), 4.52 (1H, q, $J$ = 8.7 Hz), 2.19 (6H, s), 2.13 (1H, dtd, $J$ = 13.0, 8.0, 4.5 Hz), 1.96 (1H, ddd, $J$ = 13.0, 9.0, 8.3 Hz), 1.86 (1H, ddd, $J$ = 13.0, 8.3, 4.5 Hz), 1.81-70 (1H, m), 1.70-1.60 (1H, m), 1.60-1.50 (1H, m), 1.27 (3H, s); $^{13}$C NMR (126 MHz, $(CD_3)_2CO$) major diastereomer $\delta$ 161.8 (d, $J_{C\text{-}F}$ = 241.9 Hz), 155.9, 145.7, 141.3, 138.8, 128.7 (d, $J_{C\text{-}F}$ = 8.4 Hz), 124.0, 116.8, 115.3 (d, $J_{C\text{-}F}$ = 20.5 Hz), 58.3, 48.4, 39.9, 31.9, 22.9, 21.5, 20.3; $^{19}$F NMR (471 MHz, $(CD_3)_2CO$) major diastereomer $\delta$ –119.3; IR (film): 3335, 2963, 2870, 1640, 1613, 1554, 1506, 1473, 1330, 1232, 1163, 1016, 831 cm$^{-1}$; HRMS (ESI) Calcd for $C_{21}H_{26}ON_2F^+$ ([M+H]$^+$) 341.2024. Found 341.2020.

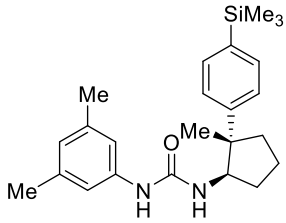

**4d**: HPLC IB3, H/$^i$PrOH = 10:1, flow rate = 1.0 mL/min, 30 °C, λ = 254 nm, 9.7 min (major enantiomer of major diastereomer), 11.2 min (minor diastereomer), 34.5 min (minor diastereomer), 42.7 min (minor enantiomer of major diastereomer); $^1$H NMR (500 MHz, $(CD_3)_2CO$) major diastereomer $\delta$ 7.74 (1H, br), 7.48 (2H, d, $J$ = 8.3 Hz), 7.45 (2H, d, $J$ = 8.3 Hz), 7.09 (2H, s), 6.55 (1H, s), 5.77 (1H, brd, $J$ = 9.0 Hz), 4.57 (1H, q, $J$ = 9.0 Hz), 2.20 (6H, s), 2.19-2.11 (1H, m), 1.99 (1H, dt, $J$ = 13.0, 8.5 Hz), 1.87 (1H, ddd, $J$ = 13.0, 8.5, 4.5 Hz), 1.83-1.73 (1H, m), 1.73-1.61 (1H, m), 1.57 (1H, dddd, $J$ = 13.0, 10.0, 8.5, 6.5 Hz), 1.29 (3H, s), 0.23 (9H, s); $^{13}$C NMR (126 MHz, $(CD_3)_2CO$) major diastereomer $\delta$ 155.9, 150.3, 141.3, 138.8, 137.6, 134.1, 126.3, 123.9, 116.7, 58.2, 48.7, 39.8, 32.0, 22.8, 21.5, 20.4, –1.0; IR (film): 3329, 2953, 2876, 1614, 1639, 1560, 1457, 1330, 1246, 1029, 816 cm$^{-1}$; HRMS (ESI) Calcd for $C_{24}H_{34}ON_2SiNa^+$ ([M+Na]$^+$) 417.2333. Found 417.2325.

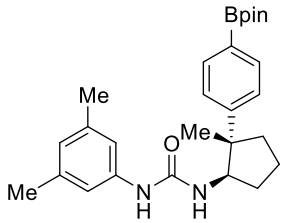

**4e**: HPLC IB3, H/$^i$PrOH = 10:1, flow rate = 1.0 mL/min, 30 °C, λ = 254 nm, 10.7 min (minor diastereomer), 11.6 min (major enantiomer of major diastereomer), 35.4 min (minor diastereomer), 48.8 min (minor enantiomer of major diastereomer); $^1$H NMR (500 MHz, $(CD_3)_2CO$) major diastereomer $\delta$ 7.68 (1H, br), 7.68 (2H, d, $J$ = 8.5 Hz), 7.51 (2H, d, $J$ = 8.5 Hz), 7.07 (2H, s), 6.55 (1H, s), 5.74 (1H, brd, $J$ = 8.5 Hz), 4.56 (1H, q, $J$ = 8.5 Hz), 2.20 (6H, s), 2.13 (1H, dddd, $J$ = 13.0, 9.5, 8.5, 4.8 Hz), 2.08-2.02 (1H, m), 1.86 (1H, ddd, $J$ = 13.0, 8.7, 4.8

Hz), 1.84-1.75 (1H, m), 1.74-1.65 (1H, m), 1.57 (1H, dddd, *J* = 13.0, 10.5, 8.5, 6.5 Hz), 1.32 (12H, s), 1.30 (3H, s); $^{13}$C NMR (126 MHz, $(CD_3)_2CO$) major diastereomer $\delta$ 155.9, 152.9, 141.3, 138.7, 135.5, 126.2, 123.9, 116.7, 84.3, 58.5, 49.1, 39.5, 31.9, 25.2, 22.6, 21.5, 20.5, one carbon atom was not found due to quadrupolar broadening; $^{11}$B NMR (160 MHz, $(CD_3)_2CO$) major diastereomer $\delta$ 29.9; IR (film): 3341, 2979, 2875, 1642, 1612, 1563, 1470, 1399, 1360, 1322, 1270, 1241, 1143, 1090, 1019, 963, 835 cm$^{-1}$; HRMS (ESI) Calcd for $C_{27}H_{27}O_3N_2BNa^+$ ([M+Na]$^+$) 471.2789. Found 471.2785.

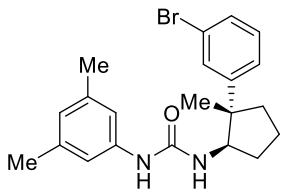


**4f**: HPLC IC3, H/$^i$PrOH = 10:1, flow rate = 1.0 mL/min, 30 °C, λ = 254 nm, 13.3 min (major enantiomer of major diastereomer), 16.2 min (minor diastereomer), 18.1 min (minor enantiomer of major diastereomer), 20.0 min (minor diastereomer); $^1$H NMR (500 MHz, $(CD_3)_2CO$) major diastereomer $\delta$ 7.79 (1H, br), 7.67 (1H, t, *J* = 2.0 Hz), 7.50 (1H, ddd, *J* = 8.0, 2.0, 1.0 Hz), 7.34 (1H, ddd, *J* = 8.0, 2.0, 1.0 Hz), 7.24 (1H, t, *J* = 8.0 Hz), 7.08 (2H, s), 6.56 (1H, s), 5.80 (1H, brd, *J* = 8.5 Hz), 4.53 (1H, q, *J* = 8.5 Hz), 2.20 (6H, s), 2.15 (1H, dddd, *J* = 13.0, 8.5, 8.0, 4.8 Hz), 2.00 (1H, ddd, *J* = 13.0, 9.5, 8.0 Hz), 1.89 (1H, ddd, *J* = 13.0, 9.0, 4.8 Hz), 1.79 (1H, ddtd, *J* = 13.0, 10.5, 8.0, 4.8 Hz), 1.69 (1H, ddddd, *J* = 13.0, 9.5, 9.0, 6.5, 4.8 Hz), 1.57 (1H, dddd, *J* = 13.0, 10.5, 8.5, 6.5 Hz), 1.29 (3H, s); $^{13}$C NMR (126 MHz, $(CD_3)_2CO$) major diastereomer $\delta$ 155.8, 152.6, 141.2, 138.7, 130.9, 130.1, 129.6, 125.9, 124.0, 122.8, 116.8, 58.2, 48.9, 39.6, 31.8, 22.6, 21.5, 20.3; IR (film): 3322, 2958, 2874, 1640, 1614, 1548, 1469, 1378, 1271, 1232, 1078, 1037, 995, 835 cm$^{-1}$; HRMS (ESI) Calcd for $C_{21}H_{25}ON_2{}^{79}BrNa^+$ ([M+Na]$^+$) 423.1042. Found 423.1037.

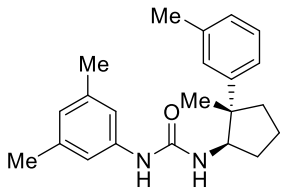


**4g**: HPLC IB3, H/EtOH = 96:4, flow rate = 1.0 mL/min, 30 °C, λ = 254 nm, 10.3 min (minor diastereomer), 11.6 min (major enantiomer of major diastereomer), 19.8 min (minor diastereomer), 25.6 min (minor enantiomer of major diastereomer); $^1$H NMR (500 MHz, $(CD_3)_2CO$) major diastereomer $\delta$ 7.70 (1H, br), 7.31 (1H, s), 7.28 (1H, d, *J* = 7.5 Hz), 7.15 (1H, t, *J* = 7.5 Hz), 7.08 (2H, s), 6.96 (1H, d, *J* = 7.5 Hz), 6.55 (1H, s), 5.75 (1H, brd, *J* = 8.5 Hz), 4.53 (1H, q, *J* = 8.5 Hz), 2.29 (3H, s), 2.20 (6H, s), 2.13 (1H, dddd, *J* = 13.0, 9.0, 8.0, 4.5 Hz), 2.01 (1H, ddd, *J* = 13.0, 9.0, 6.5 Hz), 1.84 (1H, ddd, *J* = 13.0, 9.0, 4.5 Hz), 1.83-1.73 (1H, m), 1.72-1.62 (1H, m), 1.55 (1H, dddd, *J* = 13.0, 10.5, 9.0, 6.5 Hz), 1.28 (3H, s); $^{13}$C NMR (126 MHz, $(CD_3)_2CO$) major diastereomer $\delta$ 155.9, 149.5, 141.4, 138.7, 138.1, 128.8, 127.6, 127.2, 123.9, 123.8, 116.7, 58.5, 48.8, 39.7, 31.9, 22.9, 21.7, 21.5, 20.4; IR (film): 3324, 2962, 2858, 1640, 1609, 1552, 1445, 1376, 1327, 1271, 1230, 1037, 839 cm$^{-1}$; HRMS (ESI) Calcd for $C_{22}H_{28}ON_2Na^+$ ([M+Na]$^+$) 359.2094. Found 359.2090.

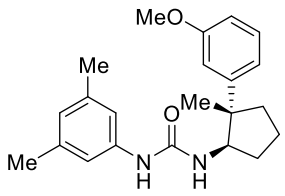

**4h**: HPLC IC3, H/$^{i}$PrOH = 10:1, flow rate = 1.0 mL/min, 30 °C, λ = 254 nm, 21.1 min (minor diastereomer), 24.6 min (major enantiomer of major diastereomer), 27.4 min (minor diastereomer), 31.3 min (minor enantiomer of major diastereomer); $^{1}$H NMR (500 MHz, $(CD_3)_2CO$) major diastereomer $\delta$ 7.72 (1H, br), 7.19 (1H, t, $J$ = 8.0 Hz), 7.09 (1H, t, $J$ = 2.5 Hz), 7.08 (2H, s), 7.04 (1H, ddd, $J$ = 8.0, 2.5, 1.0 Hz), 6.72 (1H, ddd, $J$ = 8.0, 2.5, 1.0 Hz), 6.55 (1H, s), 5.75 (1H, brd, $J$ = 8.8 Hz), 4.56 (1H, q, $J$ = 8.8 Hz), 3.75 (3H, s), 2.20 (6H, s), 2.15 (1H, dddd, $J$ = 13.0, 8.5, 8.0, 4.5 Hz), 1.99 (1H, ddd, $J$ = 13.0, 9.0, 8.0 Hz), 1.87 (1H, ddd, $J$ = 13.0, 9.0, 4.5 Hz), 1.78 (1H, ddtd, $J$ = 13.0, 10.5, 8.0, 4.5 Hz), 1.68 (1H, dtdd, $J$ = 13.0, 9.0, 6.5, 4.5 Hz), 1.57 (1H, dddd, $J$ = 13.0, 10.5, 8.5, 6.5 Hz), 1.28 (3H, s); $^{13}$C NMR (126 MHz, $(CD_3)_2CO$) major diastereomer $\delta$ 160.6, 155.9, 151.3, 141.3, 138.8, 129.8, 123.9, 119.2, 116.7, 112.9, 111.6, 58.2, 55.3, 48.8, 39.8, 31.9, 22.9, 21.5, 20.3; IR (film): 3327, 2958, 2876, 1641, 1608, 1559, 1428, 1329, 1268, 1220, 1042, 836 cm$^{-1}$; HRMS (ESI) Calcd for $C_{22}H_{28}O_2N_2Na^+$ ([M+Na]$^+$) 375.2043. Found 375.2038.

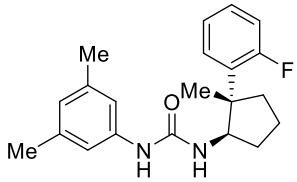

**4i**: HPLC IC3, H/EtOH = 97:3, flow rate = 1.0 mL/min, 30 °C, λ = 254 nm, 15.3 min (major enantiomer of major diastereomer), 18.8 min (minor enantiomer of major diastereomer), 30.9 min (minor diastereomer), 45.3 min (minor diastereomer); $^{1}$H NMR (500 MHz, $(CD_3)_2CO$) major diastereomer $\delta$ 7.83 (1H, br), 7.56 (1H, t, $J$ = 8.5 Hz), 7.21 (1H, tdd, $J_{H\text{-}H}$ = 8.5, 2.5 Hz, $J_{H\text{-}F}$ = 5.5 Hz), 7.09 (2H, s), 7.09-7.01 (2H, m), 6.56 (1H, s), 5.84 (1H, brd, $J$ = 9.0 Hz), 4.76 (1H, q, $J$ = 9.0 Hz), 2.19 (6H, s), 2.17-2.09 (2H, m), 1.94-1.84 (1H, m), 1.82-1.70 (1H, m), 1.70-1.53 (2H, m), 1.32 (3H, s); $^{13}$C NMR (126 MHz, $(CD_3)_2CO$) major diastereomer $\delta$ 162.6 (d, $J_{C\text{-}F}$ = 245.4 Hz), 155.8, 141.3, 138.8, 136.3 (d, $J_{C\text{-}F}$ = 12.1 Hz), 128.7 (d, $J_{C\text{-}F}$ = 8.5 Hz), 128.5 (d, $J_{C\text{-}F}$ = 4.8 Hz), 124.9 (d, $J_{C\text{-}F}$ = 2.4 Hz), 124.0, 116.7$_2$, 116.7$_1$ (d, $J_{C\text{-}F}$ = 24.1 Hz), 57.1, 46.8, 38.6, 31.4, 21.5, 20.8, 19.9; $^{19}$F NMR (471 MHz, $(CD_3)_2CO$) major diastereomer $\delta$ –111.0; IR (film): 3326, 2960, 2921, 2871, 1640, 1613, 1556, 1489, 1443, 1330, 1207, 1039, 937, 838 cm$^{-1}$; HRMS (ESI) Calcd for $C_{21}H_{25}ON_2FNa^+$ ([M+Na]$^+$) 363.1843. Found 363.1839.

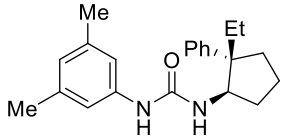

**4j**: HPLC IB3, H/$^{i}$PrOH = 10:1, flow rate = 1.0 mL/min, 30 °C, λ = 254 nm, 12.5 min (minor diastereomer), 14.1 min (major enantiomer of major diastereomer), 43.2 min (minor diastereomer), 45.6 min (minor enantiomer of major diastereomer); $^{1}$H NMR (500 MHz, $(CD_3)_2CO$) major diastereomer $\delta$ 7.87 (1H, br), 7.47 (2H, d, $J$ = 7.8 Hz), 7.29 (2H, t, $J$ = 7.8 Hz), 7.16 (1H, t, $J$ = 7.8 Hz), 7.12 (2H, s), 6.57 (1H, s), 6.01 (1H, brd, $J$ = 9.3 Hz), 4.52 (1H, ddd, $J$ = 9.3, 7.3, 4.5 Hz), 2.33-2.22 (1H, m), 2.20 (6H, s), 1.93-1.85 (2H, m), 1.77-1.57 (4H, m), 1.50-1.42 (1H, m), 0.55 (3H,

t, $J$ = 7.5 Hz); $^{13}$C NMR (126 MHz, $(CD_3)_2CO$) major diastereomer $\delta$ 156.0, 147.1, 141.4, 138.8, 128.9, 127.6, 126.5, 123.9, 116.8, 60.2, 54.9, 33.2, 32.2, 21.5, 21.2, 9.7, one carbon atom was not found probably due to overlapping; IR (film): 3320, 2959, 2876, 1634, 1614, 1554, 1456, 1329, 1269, 1227, 1063, 835 cm$^{-1}$; HRMS (ESI) Calcd for $C_{22}H_{28}ON_2Na^+$ ([M+Na]$^+$) 359.2094. Found 359.2086.

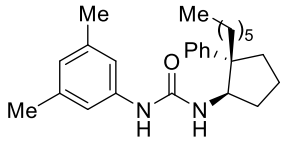

**4k**: HPLC IA3, H/$^i$PrOH = 10:1, flow rate = 1.0 mL/min, 30 °C, λ = 254 nm, 6.7 min (minor diastereomer), 7.4 min (major enantiomer of major diastereomer), 15.0 min (minor diastereomer), 33.9 min (minor enantiomer of major diastereomer); $^1$H NMR (400 MHz, $(CD_3)_2CO$) major diastereomer $\delta$ 7.82 (1H, br), 7.47 (2H, d, $J$ = 7.2 Hz), 7.29 (2H, t, $J$ = 7.2 Hz), 7.16 (1H, t, $J$ = 7.2 Hz), 7.11 (2H, s), 6.57 (1H, s), 6.00 (1H, br), 4.52 (1H, ddd, $J$ = 8.8, 7.4, 4.7 Hz), 2.37-2.22 (1H, m), 2.20 (6H, s), 1.95-1.82 (2H, m), 1.82-1.69 (2H, m), 1.69-1.58 (2H, m), 1.52-1.42 (1H, m), 1.24-0.97 (8H, m), 0.78 (3H, t, $J$ = 6.8 Hz); $^{13}$C NMR (126 MHz, $(CD_3)_2CO$) major diastereomer $\delta$ 156.0, 147.5, 141.4, 138.8, 128.9, 127.4, 126.5, 123.9, 116.8, 60.3, 54.3, 37.5, 33.8, 32.5, 32.2, 30.8, 25.8, 23.2, 21.5, 21.2, 14.3; IR (film): 3330, 2953, 2937, 2868, 1640, 1614, 1563, 1446, 1269, 1232, 1034, 838 cm$^{-1}$; HRMS (ESI) Calcd for $C_{26}H_{36}ON_2Na^+$ ([M+Na]$^+$) 415.2720. Found 415.2713.

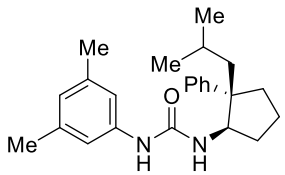

**4l**: HPLC IA3, H/$^i$PrOH = 10:1, flow rate = 1.0 mL/min, 30 °C, λ = 254 nm, 6.9 min (minor diastereomer), 7.8 min (major enantiomer of major diastereomer), 18.2 min (minor diastereomer), 30.0 min (minor enantiomer of major diastereomer); $^1$H NMR (500 MHz, $(CD_3)_2CO$) major diastereomer $\delta$ 7.87 (1H, br), 7.49 (2H, d, $J$ = 7.5 Hz), 7.29 (2H, t, $J$ = 7.5 Hz), 7.17 (1H, t, $J$ = 7.5 Hz), 7.13 (2H, s), 6.57 (1H, s), 6.03 (1H, brd, $J$ = 9.8 Hz), 4.49 (1H, ddd, $J$ = 9.8, 6.5, 3.0 Hz), 2.43 (1H, t, $J$ = 8.5 Hz), 2.21 (6H, s), 1.97 (1H, dd, $J$ = 13.8, 5.3 Hz), 1.81-1.72 (3H, m), 1.72-1.61 (1H, m), 1.54 (1H, dd, $J$ = 13.8, 7.0 Hz), 1.47-1.37 (1H, m), 1.33-1.23 (1H, m), 0.74 (3H, d, $J$ = 7.0 Hz), 0.49 (3H, d, $J$ = 7.0 Hz); $^{13}$C NMR (126 MHz, $(CD_3)_2CO$) major diastereomer $\delta$ 156.1, 147.4, 141.4, 128.9, 127.5, 126.6, 123.9, 116.8, 61.5, 54.8, 46.4, 33.7, 31.6, 25.9, 25.0, 24.8, 21.5$_4$, 21.5$_0$, one carbon atom was not found probably due to overlapping; IR (film): 3325, 2944, 2867, 1640, 1613, 1560, 1444, 1329, 1271, 1234, 1166, 1033, 834 cm$^{-1}$; HRMS (ESI) Calcd for $C_{24}H_{32}ON_2Na^+$ ([M+Na]$^+$) 387.2407. Found 387.2404.

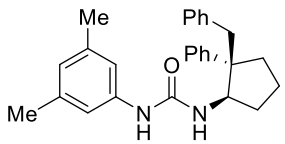

**4m**: HPLC IB3, H/EtOH = 95:5, flow rate = 1.0 mL/min, 30 °C, λ = 254 nm, 10.7 min (minor diastereomer), 14.3 min (major enantiomer of major diastereomer), 19.0 min (minor diastereomer), 29.7 min (minor enantiomer of major diastereomer); $^1$H NMR (500 MHz, $(CD_3)_2CO$)

major diastereomer $\delta$ 7.85 (1H, br), 7.33 (2H, d, $J$ = 7.3 Hz), 7.23 (2H, t, $J$ = 7.3 Hz), 7.16 (2H, s), 7.16 (1H, t, $J$ = 7.3 Hz), 7.03 (1H, t, $J$ = 7.3 Hz), 6.99 (2H, t, $J$ = 7.3 Hz), 6.61 (1H, s), 6.59 (2H, d, $J$ = 7.3 Hz), 6.15 (1H, brd, $J$ = 9.3 Hz), 4.66 (1H, ddd, $J$ = 9.3, 7.8, 5.0 Hz), 3.18 (1H, d, $J$ = 8.3 Hz), 2.94 (1H, d, $J$ = 8.3 Hz), 2.22 (6H, s), 2.05-1.92 (2H, m), 1.92-1.79 (2H, m), 1.68-1.53 (2H, m); $^{13}$C NMR (126 MHz, $(CD_3)_2CO$) major diastereomer $\delta$ 156.2, 146.6, 141.3, 139.7, 138.8, 130.8, 128.6, 128.1, 128.0, 126.7, 126.5, 124.1, 116.9, 60.6, 55.4, 43.5, 32.8, 32.1, 21.5, 20.8; IR (film): 3330, 2919, 2867, 1700, 1640, 1613, 1548, 1445, 1337, 1270, 1233, 1029, 840 cm$^{-1}$; HRMS (ESI) Calcd for $C_{27}H_{30}ON_2Na^+$ ([M+Na]$^+$) 421.2250. Found 421.2237.

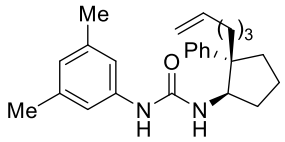


**4n**: HPLC IA3, H/$^i$PrOH = 10:1, flow rate = 1.0 mL/min, 30 °C, λ = 254 nm, 7.2 min (minor diastereomer), 8.3 min (major enantiomer of major diastereomer), 18.6 min (minor diastereomer), 31.8 min (minor enantiomer of major diastereomer); $^1$H NMR (500 MHz, $(CD_3)_2CO$) major diastereomer $\delta$ 7.75 (1H, br), 7.48 (2H, d, $J$ = 7.5 Hz), 7.30 (2H, t, $J$ = 7.5 Hz), 7.17 (1H, t, $J$ = 7.5 Hz), 7.12 (2H, s), 6.57 (1H, s), 5.93 (1H, brd, $J$ = 9.5 Hz), 5.65 (1H, ddt, $J$ = 17.0, 10.0, 6.5 Hz), 4.84 (1H, ddt, $J$ = 17.0, 2.5, 1.5 Hz), 4.80 (1H, ddt, $J$ = 10.0, 2.5, 1.0 Hz), 4.52 (1H, ddd, $J$ = 9.5, 7.5, 5.0 Hz), 2.36-2.28 (1H, m), 2.21 (6H, s), 1.94-1.80 (4H, m), 1.80-1.70 (2H, m), 1.70-1.58 (2H, m), 1.47 (1H, ddt, $J$ = 13.0, 9.3, 5.0 Hz), 1.14 (1H, tddd, $J$ = 13.0, 8.3, 6.5, 5.0 Hz), 0.95 (1H, tddd, $J$ = 13.0, 8.5, 6.5, 5.0 Hz); $^{13}$C NMR (126 MHz, $(CD_3)_2CO$) major diastereomer $\delta$ 156.0, 147.4, 141.4, 139.6, 138.8, 128.9, 127.4, 126.5, 123.9, 116.8, 114.6, 60.2, 54.3, 37.1, 35.1, 33.8, 32.1, 25.4, 21.5, 21.2; IR (film): 3351, 2938, 2864, 1695, 1641, 1613, 1555, 1446, 1330, 1243, 1029, 909, 834 cm$^{-1}$; HRMS (ESI) Calcd for $C_{25}H_{32}ON_2Na^+$ ([M+Na]$^+$) 399.2407. Found 399.2405.

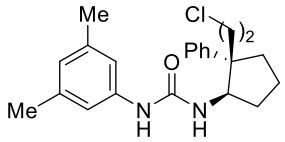


**4o**: HPLC IB3, H/EtOH = 94:6, flow rate = 1.0 mL/min, 30 °C, λ = 254 nm, 9.8 min (major enantiomer of major diastereomer), 10.8 min (minor diastereomer), 20.1 min (minor enantiomer of major diastereomer), 26.8 min (minor diastereomer); $^1$H NMR (500 MHz, $(CD_3)_2CO$) major diastereomer $\delta$ 7.78 (1H, br), 7.52 (2H, d, $J$ = 7.8 Hz), 7.35 (2H, t, $J$ = 7.8 Hz), 7.23 (1H, t, $J$ = 7.8 Hz), 7.13 (2H, s), 6.58 (1H, s), 6.02 (1H, brd, $J$ = 9.5 Hz), 4.58 (1H, dt, $J$ = 9.5, 5.0 Hz), 3.24 (1H, td, $J$ = 11.0, 5.0 Hz), 3.11 (1H, td, $J$ = 11.0, 5.0 Hz), 2.46-2.38 (2H, m), 2.22 (6H, s), 2.12 (1H, ddt, $J$ = 13.5, 11.0, 5.0 Hz), 1.87 (1H, tq, $J$ = 10.0, 5.0 Hz), 1.84-1.75 (2H, m), 1.70-1.60 (1H, m), 1.49 (1H, dtd, $J$ = 13.0, 9.0, 5.0 Hz); $^{13}$C NMR (126 MHz, $(CD_3)_2CO$) major diastereomer $\delta$ 156.0, 145.6, 141.3, 138.8, 129.3, 127.3, 127.2, 124.1, 117.1, 60.3, 54.4, 42.6, 41.7, 33.7, 31.6, 21.5, 21.4; IR (film): 3328, 2961, 2875, 1698, 1640, 1614, 1561, 1445, 1329, 1242, 1034, 837 cm$^{-1}$; HRMS (ESI) Calcd for $C_{22}H_{27}ON_2{}^{35}ClNa^+$ ([M+Na]$^+$) 393.1704. Found 393.1696.

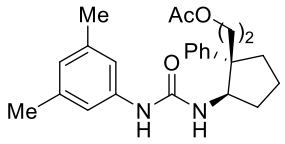

**4p**: HPLC IB3, H/$^{i}$PrOH = 85:15, flow rate = 1.0 mL/min, 30 °C, λ = 254 nm, 8.4 min (major enantiomer of major diastereomer), 11.1 min (minor diastereomer), 17.7 min (minor enantiomer of major diastereomer), 43.5 min (minor diastereomer); $^{1}$H NMR (500 MHz, $(CD_3)_2CO$) major diastereomer $\delta$ 7.80 (1H, br), 7.51 (2H, d, $J$ = 7.5 Hz), 7.33 (2H, t, $J$ = 7.5 Hz), 7.20 (1H, t, $J$ = 7.5 Hz), 7.13 (2H, s), 6.58 (1H, s), 6.03 (1H, br), 4.54 (1H, ddd, $J$ = 9.5, 7.5, 4.0 Hz), 3.77 (1H, ddd, $J$ = 11.0, 9.5, 6.5 Hz), 3.62 (1H, ddd, $J$ = 11.0, 9.5, 5.5 Hz), 2.45-2.37 (1H, m), 2.28 (1H, ddd, $J$ = 13.8, 9.5, 5.5 Hz), 2.22 (6H, s), 1.98 (1H, ddd, $J$ = 13.8, 9.5, 6.5 Hz), 1.88-1.74 (3H, m), 1.82 (3H, s), 1.73-1.62 (1H, m), 1.52-1.41 (1H, m); $^{13}$C NMR (126 MHz, $(CD_3)_2CO$) major diastereomer $\delta$ 170.8, 156.0, 146.3, 141.4, 138.8, 129.2, 127.3, 127.0, 124.0, 116.8, 62.7, 60.9, 35.3, 36.5, 33.5, 31.5, 21.5, 20.7; IR (film): 3329, 2949, 2879, 1737, 1641, 1613, 1551, 1445, 1365, 1230, 1031, 836 cm$^{-1}$; HRMS (ESI) Calcd for $C_{24}H_{30}O_3N_2Na^+$ ([M+Na]$^+$) 417.2149. Found 417.2142.

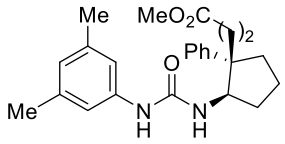

**4q**: HPLC IA3, H/$^{i}$PrOH = 10:1, flow rate = 1.0 mL/min, 30 °C, λ = 254 nm, 10.0 min (major enantiomer of major diastereomer), 14.9 min (minor diastereomer), 31.3 min (minor enantiomer of major diastereomer), 36.7 min (minor diastereomer); $^{1}$H NMR (500 MHz, $(CD_3)_2CO$) major diastereomer $\delta$ 7.80 (1H, br), 7.49 (2H, d, $J$ = 7.8 Hz), 7.32 (2H, t, $J$ = 7.8 Hz), 7.20 (1H, t, $J$ = 7.8 Hz), 7.12 (2H, s), 6.57 (1H, s), 5.99 (1H, brd, $J$ = 9.0 Hz), 4.56 (1H, ddd, $J$ = 9.0, 7.5, 4.5 Hz), 3.48 (3H, s), 2.35-2.26 (1H, m), 2.25-2.14 (1H, m), 2.21 (6H, s), 2.04-1.82 (4H, m), 1.80-1.71 (2H, m), 1.68-1.57 (1H, m), 1.53-1.45 (m); $^{13}$C NMR (126 MHz, $(CD_3)_2CO$) major diastereomer $\delta$ 174.2, 155.9, 146.4, 141.4, 138.8, 129.1, 127.5, 126.9, 123.9, 116.8, 59.9, 53.9, 51.5, 33.6, 32.7, 32.1, 30.8, 21.5, 21.2; IR (film): 3324, 2924, 2873, 1737, 1638, 1614, 1555, 1435, 1271, 1219, 1154, 1030, 835 cm$^{-1}$; HRMS (ESI) Calcd for $C_{24}H_{30}O_3N_2Na^+$ ([M+Na]$^+$) 417.2149. Found 417.2132.

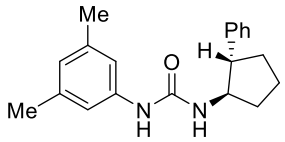

**4r**: HPLC OD3, H/$^{i}$PrOH = 88:12, flow rate = 1.0 mL/min, λ = 254 nm, 12.9 min (major enantiomer of major diastereomer), 15.0 min (minor diastereomer), 29.6 min (minor diastereomer), 40.8 min (minor enantiomer of major diastereomer); $^{1}$H NMR (500 MHz, $CDCl_3$) major diastereomer $\delta$ 7.25 (2H, t, $J$ = 7.0 Hz), 7.19 (2H, d, $J$ = 7.0 Hz), 7.16 (1H, t, $J$ = 7.0 Hz), 6.87 (1H, brs), 6.71 (2H, brs), 6.61 (1H, s), 5.45 (1H, brd, $J$ = 8.0 Hz), 4.10 (1H, quin, $J$ = 8.0 Hz), 2.67 (1H, q, $J$ = 9.0 Hz), 2.25 (1H, ddt, $J$ = 13.0, 8.5, 7.5 Hz), 2.16 (6H, s), 2.11-2.02 (1H, m), 1.76-1.62 (3H, m), 1.43 (1H, dq, $J$ = 13.0, 8.5 Hz); $^{13}$C NMR (126 MHz, $CDCl_3$) major diastereomer $\delta$ 156.2, 143.0, 138.7, 128.7, 127.5, 126.6, 125.0, 118.3, 58.5, 52.2, 33.5, 33.0, 22.3, 21.4, one carbon atom was not found probably due to overlapping; IR (film): 3323, 2958, 2911, 2856, 1640, 1613, 1559, 1450, 1377, 1331, 1274, 1231, 1077, 1032, 910, 836 cm$^{-1}$; HRMS (ESI) Calcd for $C_{20}H_{24}ON_2Na^+$

([M+Na]$^+$) 331.1781. Found 331.1760.

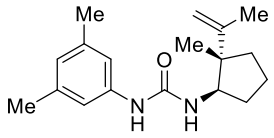

**4s**: HPLC IB N-3, H/$^i$PrOH = 10:1, flow rate = 1.0 mL/min, λ = 254 nm, 13.1 min (major enantiomer of major diastereomer), 15.0 min (minor diastereomer), 31.1 min (minor diastereomer), 70.4 min (minor enantiomer of major diastereomer); $^1$H NMR (500 MHz, $(CD_3)_2CO$) major diastereomer $\delta$7.75 (1H, br), 7.06 (2H, s), 6.54 (1H, s), 5.62 (1H, brd, $J$ = 9.0 Hz), 4.86 (1H, d, $J$ = 1.1 Hz), 4.73 (1H, t, $J$ = 1.1 Hz), 4.34 (1H, q, $J$ = 9.0 Hz), 2.19 (6H, s), 2.09 (1H, dddd, $J$ = 13.5, 9.0, 8.3, 5.0 Hz), 1.82 (1H, ddd, $J$ = 13.0, 9.8, 8.0 Hz), 1.80 (3H, d, $J$ = 1.1 Hz), 1.74-1.64 (1H, m), 1.60 (1H, ddddd, $J$ = 13.5, 9.8, 7.0, 5.0, 3.5 Hz), 1.54-1.45 (2H, m), 1.05 (3H, s); $^{13}$C NMR (126 MHz, $(CD_3)_2CO$) major diastereomer $\delta$ 155.7, 151.6, 141.5, 138.7, 123.8, 116.7, 110.1, 56.1, 49.6, 37.3, 31.7, 21.5, 20.2, 20.1, 19.6; IR (film): 3335, 2940, 2866, 1642, 1614, 1558, 1458, 1376, 1326, 1272, 1222, 1129, 893, 836 cm$^{-1}$; HRMS (ESI) Calcd for $C_{18}H_{26}ON_2Na^+$ ([M+Na]$^+$) 309.1937. Found 309.1934.

**Deprotection and Sulfonylation of 4a**

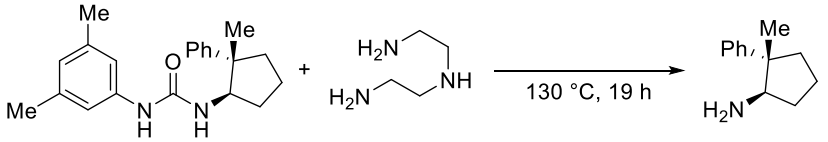


**4a** (dr = 12:1)
92% ee (major diastereomer)

**5** (dr = 11:1)

**Removal of Urea to Give Aminocyclopentane 5:** According to the literature method,[17] a mixture of urea **4a** (30.3 mg, 0.093 mmol) and diethylenetriamine (61.0 μL, 0.56 mmol) was stirred at 130 °C for 19 h in a test tube sealed with a screw cap. The resulting mixture was cooled to ambient temperature and directly purified by column chromatography on silica gel ($CH_2Cl_2$/MeOH = 100:1 to 10:1 as eluent) to give **5** (14.0 mg, 0.080 mmol, 86%) as a mixture of diastereomers. Preservation of the enantiomeric excess was confirmed after subsequent sulfonylation (see below). **5:** $^1$H NMR (500 MHz, $CDCl_3$) major diastereomer $\delta$ 7.41 (2H, d, $J$ = 7.5 Hz), 7.32 (2H, t, $J$ = 7.5 Hz), 7.19 (1H, t, $J$ = 7.5 Hz), 3.41 (1H, dd, $J$ = 9.5, 8.0 Hz), 2.13-2.00 (2H, m), 1.87-1.67 (3H, m), 1.55-1.37 (3H, m), 1.24 (3H, s); $^{13}$C NMR (126 MHz, $CDCl_3$) major diastereomer $\delta$ 148.7, 128.4, 126.0, 125.8, 62.1, 48.5, 39.5, 32.8, 19.9, 19.4; IR (film): 3375, 2949, 2870, 1685, 1599, 1495, 1444, 1375, 1274, 1029 cm$^{-1}$; HRMS (ESI) Calcd for $C_{12}H_{18}N^+$ ([M+H]$^+$) 176.1434. Found 176.1429.

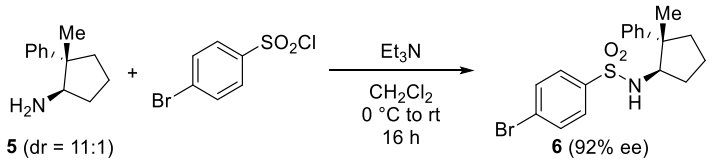


**Sulfonylation of Aminocyclopentane 5 to Give Sulfonamide 6:** To a solution of **5** (12.1 mg, 0.069 mmol) in $CH_2Cl_2$ (0.35 mL) were added $NEt_3$ (19.5 µL, 0.14 mmol) and a solution of 4-$BrC_6H_4SO_2Cl$ (22.7 mg, 0.090 mmol) in $CH_2Cl_2$ (0.50 mL) at 0 °C. The mixture was allowed to warm to ambient temperature and stirred there for 16 h. The reaction was quenched by adding a saturated aqueous solution of $NH_4Cl$ and the aqueous phase was extracted with $CH_2Cl_2$ three times. The combined organic phases were dried over $Na_2SO_4$ and filtered. All volatiles were removed under reduced pressure to give the crude residue. Purification of the residue was performed by using preparative thin layer chromatography on silica gel ($CH_2Cl_2$/H = 5:1 as eluent) to give **6** (18.7 mg, 0.047 mmol, 69%) as a single diastereomer. Enantiomeric excess of **6** was determined by HPLC analysis on chiral stationary phase. **6**: HPLC IA3, H/$^i$PrOH = 10:1, flow rate = 0.5 mL/min, 30 °C, λ = 254 nm, 21.5 min (major enantiomer), 24.5 min (minor enantiomer); $^1$H NMR (500 MHz, $CDCl_3$) major diastereomer $\delta$ 7.47 (2H, d, $J$ = 8.8 Hz), 7.44 (2H, d, $J$ = 8.8 Hz), 7.20-7.14 (5H, m), 4.74 (1H, d, $J$ = 8.5 Hz), 3.79 (1H, q, $J$ = 8.5 Hz), 2.08 (1H, dtd, $J$ = 13.0, 8.5, 4.5 Hz), 2.00-1.97 (1H, m), 1.54 (1H, dddd, $J$ = 13.0, 10.0, 8.5, 6.5 Hz), 1.82-1.61 (3H, m), 1.23 (3H, s); $^{13}$C NMR (126 MHz, $CDCl_3$) major diastereomer $\delta$ 146.5, 139.6, 132.2, 128.6, 128.4, 127.4, 126.2, 125.8, 63.5, 48.0, 39.4, 31.6, 20.4, 20.1; IR (film): 3307, 1575, 1437, 1385, 1338, 1316, 1162, 1089, 902 cm$^{-1}$; HRMS (ESI) Calcd for $C_{18}H_{19}NO_2SBr^-$ ([M−H]$^-$) 392.0325. Found 392.0322.

**Crystallographic Analysis**

**Crystallographic Structure Determination of 6:** The single crystal, which was obtained by the procedure described below, was mounted on MicroMesh. Data of X-ray diffraction were collected at 123 K on a Rigaku FR-X with Pilatus diffractometer with fine-focus sealed tube Mo/Kα radiation (λ = 0.71075 Å). An absorption correction was made using Crystal Clear. The structure was solved by direct methods and Fourier syntheses, and refined by full-matrix least squares on $F^2$ by using SHELXL-2014.[24] All non-hydrogen atoms were refined with anisotropic displacement parameters. Hydrogen atom bonded to the nitrogen atom was located from a difference synthesis, and its coordinates and isotropic thermal parameters were refined. The other hydrogen atoms were placed in calculated positions and their isotropic thermal parameters were refined.

**Recrystallization of 6:** Recrystallization was performed by using a $H/CH_2Cl_2$ solvent system at ambient temperature to afford single crystals of **6**. The crystallographic data are summarized in Table S3 and the ORTEP diagram is shown in Figure S6.

**Table S3.** Crystal data and structure refinement for **6** (CCDC 2026052).

| | | |
|---|---|---|
| Empirical formula | $C_{18}H_{20}BrNOS$ | |
| Formula weight | 394.32 | |
| Temperature | 123(2) K | |
| Wavelength | 0.71075 Å | |
| Crystal system | Orthorhombic | |
| Space group | P2(1)2(1)2(1) | |
| Unit cell dimensions | a = 9.5693(7) Å | α = 90°. |
| | b = 9.6039(8) Å | β = 90°. |
| | c = 18.6341(15) Å | γ = 90°. |
| Volume | 1712.5(2) $Å^3$ | |
| Z | 4 | |
| Density (calculated) | 1.529 $Mg/m^3$ | |
| Absorption coefficient | 2.531 $mm^{-1}$ | |
| F(000) | 808 | |
| Crystal size | 0.100 x 0.050 x 0.020 $mm^3$ | |
| Theta range for data collection | 3.005 to 25.493°. | |
| Index ranges | −11<=h<=11, −11<=k<=11, −22<=l<=22 | |
| Reflections collected | 26055 | |
| Independent reflections | 3194 [R(int) = 0.0303] | |
| Completeness to theta = 25.242° | 99.8 % | |
| Absorption correction | Semi-empirical from equivalents | |
| Max. and min. transmission | 1.000 and 0.894 | |
| Refinement method | Full-matrix least-squares on $F^2$ | |
| Data / restraints / parameters | 3194 / 0 / 213 | |
| Goodness-of-fit on $F^2$ | 0.972 | |
| Final R indices [I>2sigma(I)] | $R_1$ = 0.0180, $wR_2$ = 0.0385 | |
| R indices (all data) | $R_1$ = 0.0218, $wR_2$ = 0.0391 | |
| Absolute structure parameter | 0.002(2) | |
| Extinction coefficient | 0 | |
| Largest diff. peak and hole | 0.474 and −0.247 $e.Å^{-3}$ | |

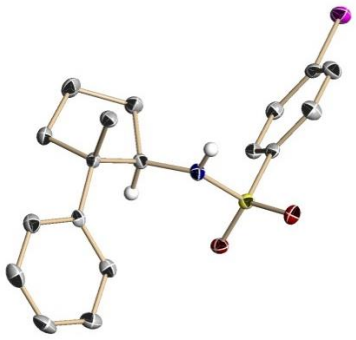

**Figure S6.** Molecular structure of **6**. The thermal ellipsoids of non-hydrogen atoms are shown at the 50% probability level. Calculated hydrogen atoms except them attached to nitrogen and stereogenic carbon are omitted for clarity. Blue = nitrogen, red = oxygen, gray = carbon, yellow = sulfur, purple = bromine.

## References and Notes


(1) (a) Hoveyda, A. H.; Evans, D. A.; Fu, G. C. *Chem. Rev.* **1993**, *93*, 1307. (b) Breit, B.; Schmidt, Y. *Chem. Rev.* **2008**, *108*, 2928. (c) Rousseau, G.; Breit, B. *Angew. Chem. Int. Ed.* **2011**, *50*, 2450. (d) Bhadra, S.; Yamamoto, H. *Chem. Rev.* **2018**, *118*, 3391. (e) Sambiagio, C.; Schönbauer, D.; Blieck, R.; Dao-Huy, T.; Pototschnig, G.; Schaaf, P.; Wiesinger, T.; Zia, M. F.; Wencel-Delord, J.; Besset, T.; Maes, B. U. W.; Schnürch, M. *Chem. Soc. Rev.* **2018**, *47*, 6603. (f) St John-Campbell, S.; Bull, J. A. *Org. Biomol. Chem.* **2018**, *16*, 4582. (g) Bag, D.; Verma, P. K.; Sawant, S. D. *Chem. - Asian J.* **2020**, *15*, 3225.

(2) (a) Sibi, M. P.; Manyem, S.; Zimmerman, J. *Chem. Rev.* **2003**, *103*, 3263. (b) Wang, C.; Lu, Z. *Org. Chem. Front.* **2015**, *2*, 179. (c) Meggers, E. *Chem. Commun.* **2015**, *51*, 3290. (d) Brimioulle, R.; Lenhart, D.; Maturi, M. M.; Bach, T. *Angew. Chem., Int. Ed.* **2015**, *54*, 3872. (e) Lu, Q.; Glorius, F. *Angew. Chem., Int. Ed.* **2017**, *56*, 49. (f) Miyabe, H.; Kawashima, A.; Yoshioka, E.; Kohtani, S. *Chem. - Eur. J.* **2017**, *23*, 6225. (g) Silvi, M.; Melchiorre, P. *Nature* **2018**, *554*, 41. (h) Garrido-Castro, A. F.; Maestro, M. C.; Alemán, J. *Tetrahedron Lett.* **2018**, *59*, 1286. (i) Jiang, C.; Chen, W.; Zheng, W.-H.; Lu, H. *Org. Biomol. Chem.* **2019**, *17*, 8673. (j) Hong, B.-C. *Org. Biomol. Chem.* **2020**, *18*, 4298. (k) Saha, D. *Chem. - Asian J.* **2020**, *15*, 2129. (l) Rigotti, T.; Alemán, J. *Chem. Commun.* **2020**, *56*, 11169.

(3) For seminal studies on the exploitation of directing groups in the development of nickel-catalyzed asymmetric coupling reactions, see: (a) Saito, B.; Fu, G. C. *J. Am. Chem. Soc.* **2008**, *130*, 6694. (b) Owston, N. A.; Fu, G. C. *J. Am. Chem. Soc.* **2010**, *132*, 11908. (c) Lu, Z.; Wilsily, A.; Fu, G. C. *J. Am. Chem. Soc.* **2011**, *133*, 8154. (d) Wilsily, A.; Tramutola, F.; Owston, N. A.; Fu, G. C. *J. Am. Chem. Soc.* **2012**, *134*, 5794. (e) Jiang, X.; Gandelman, M. *J. Am. Chem. Soc.* **2015**, *137*, 2542. (f) Pezzetta, C.; Bonifazi, D.; Davidson, R. W. M. *Org. Lett.* **2019**, *21*, 8957.

(4) For contributions that utilize the directing effect of urea for catalytic stereocontrol in radical-based reactions, see: (a) Lin, J.-S.; Dong, X.-Y.; Li, T.-T.; Jiang, N.-C.; Tan, B.; Liu, X.-Y. *J. Am. Chem. Soc.* **2016**, *138*, 9357. (b) Wang, F.-L.; Dong, X.-Y.; Lin, J.-S.; Zeng, Y.; Jiao, G.-Y.; Gu, Q.-S.; Guo, X.-Q.; Ma, C.-L.; Liu, X.-Y. *Chem.* **2017**, *3*, 979.

(5) (a) Burg, F.; Bach, T. *J. Org. Chem.* **2019**, *84*, 8815. (b) Huang, X.; Meggers, E. *Acc. Chem. Res.* **2019**, *52*, 833.

(6) (a) Yang, Z.; Li, H.; Li, S.; Zhang, M.-T.; Luo, S. *Org. Chem. Front.* **2017**, *4*, 1037. (b) Morse, P. D.; Nguyen, T. M.; Cruz, C. L.; Nicewicz, D. A. Tetrahedron **2018**, *74*, 3266.

(7) (a) Maity, S.; Zhu, M.; Shinabery, R. S.; Zheng, N. *Angew. Chem., Int. Ed.* **2012**, 51, 222. (b) Cai, Y.; Wang, J.; Zhang, Y.; Li, Z.; Hu, D.; Zheng, N.; Chen, H. *J. Am. Chem. Soc.* **2017**, *139*, 12259. (c) Staveness, D.; Collins, J. L., III; McAtee, R. C.; Stephenson, C. R. J. *Angew.*

*Chem., Int. Ed.* **2019**, *58*, 19000. (d) Muriel, B.; Gagnebin, A.; Waser, J. *Chem. Sci.* **2019**, *10*, 10716.

(8) (a) Yu, X.-Y.; Chen, J.-R.; Xiao, W.-J. *Chem. Rev.* **2020**, DOI: 10.1021/acs.chemrev.0c00030. (b) Zhang, T.; Zhang, Y.; Das, S. *ChemCatChem* 2020, *12*, 6173.

(9) (a) de Nanteuil, F.; De Simone, F.; Frei, R.; Benfatti, F.; Serrano, E.; Waser, J. *Chem. Commun.* **2014**, *50*, 10912. (b) Rassadin, V. A.; Six, Y. *Tetrahedron* **2016**, *72*, 4701. (c) Xuan, J.; He, X.-K.; Xiao, W.-J. *Chem. Soc. Rev.* **2020**, *49*, 2546. (d) Sokolova, O. O.; Bower, J. F. *Chem. Rev.* **2020**, DOI: 10.1021/acs.chemrev.0c00166. (e) Pirenne, V.; Muriel, B.; Waser, J. *Chem. Rev.* **2020**, DOI: 10.1021/acs.chemrev.0c00109.

(10) For pioneering studies on the related asymmetric [3 + 2]-photocycloadditions that proceed via an opposite redox cycle, see: (a) Amador, A. G.; Sherbrook, E. M.; Yoon, T. P. *J. Am. Chem. Soc.* **2016**, *138*, 4722. (b) Huang, X.; Lin, J.; Shen, T.; Harms, K.; Marchini, M.; Ceroni, P.; Meggers, E. *Angew. Chem., Int. Ed.* **2018**, *57*, 5454.

(11) Uraguchi, D.; Ueoka, F.; Tanaka, N.; Kizu, T.; Takahashi, W.; Ooi, T. *Angew. Chem., Int. Ed.* **2020**, *59*, 11456.

(12) (a) Riddlestone, I. M.; Kraft, A.; Schaefer, J.; Krossing, I. *Angew. Chem. Int. Ed.* **2018**, *57*, 13982. (b) Strauss, S. H. *Chem. Rev.* **1993**, *93*, 927. (c) Krossing, I.; Raabe, I. *Angew. Chem. Int. Ed.* **2004**, *43*, 2066.

(13) (a) Shida, N.; Imada, Y.; Nagahara, S.; Okada, Y.; Chiba, K. *Commun. Chem.* **2019**, *2*, 24. (b) Farney, E. P.; Chapman, S. J.; Swords, W. B.; Torelli, M. D.; Hamers, R. J.; Yoon, T. P. *J. Am. Chem. Soc.* **2019**, *141*, 6385.

(14) (a) Yates, B. F.; Bouma, W. J.; Radom, L. *Tetrahedron* **1986**, *42*, 6225. (b) Bjoernholm, T.; Hammerum, S.; Kuck, D. *J. Am. Chem. Soc.* **1988**, *110*, 3862. (c) Stirk, K. M.; Kiminkinen, L. K. M.; Kenttamaa, H. I. *Chem. Rev.* **1992**, *92*, 1649. (d) Hill, B. T.; Poutsma, J. C.; Chyall, L. J.; Hu, J.; Squires, R. R. *J. Am. Soc. Mass Spectrom.* **1999**, *10*, 896. (e) Tomazela, D. M.; Sabino, A. A.; Sparrapan, R.; Gozzo, F. C.; Eberlin, M. N. *J. Am. Soc. Mass Spectrom.* **2006**, *17*, 1014.

(15) Singh, A.; Teegardin, K.; Kelly, M.; Prasad, K. S.; Krishnan, S.; Weaver, J. D. *J. Organomet. Chem.* **2015**, *776*, 51.

(16) (a) Connors, K. A. Binding Constants, 1st ed.; John Wiley & Sons: New York, 1987; pp 189-215. (b) Kavallieratos, K.; Bertao, C. M.; Crabtree, R. H. *J. Org. Chem.* **1999**, *64*, 1675.

(17) Noshita, M.; Shimizu, Y.; Morimoto, H.; Ohshima, T. *Org. Lett.* **2016**, *18*, 6062.

(18) For the determination of the absolute configuration of **4a**, see the Experimental Section.

(19) Wang, Y.; Deng, L.; Mei, H.; Du, B.; Han, J.; Pan, Y. *Green Chem.* **2018**, *20*, 3444.

(20) (a) Pike, S. K.; Hutchinson, J. J.; Hunter, C. A. *J. Am. Chem. Soc.* **2017**, *139*, 6700. (b) Lu, Z.; Han, J.; Okoromoba, O. E.; Shimizu, N.; Amii, H.; Tormena, C. F.; Hammond, G. B.; Xu, B. *Org. Lett.* **2017**, *19*, 5848.

(21) Yan, P.; Millard, A. C.; Wei, M.; Loew, L. M. *J. Am. Chem. Soc.* **2006**, *128*, 11030.

(22) Rohe, S.; Morris, A. O.; McCallum, T.; Barriault, L. *Angew. Chem. Int. Ed.* **2018**, *57*, 15664.

(23) Skubi, K. L.; Kidd, J. B.; Jung, H.; Guzei, I. A.; Baik, M.-H.; Yoon, T. P. *J. Am. Chem. Soc.* **2017**, *139*, 17186.

(24) Sheldrick, G. M. *Acta Cryst.* **2015**, *C71*, 3.

# Chapter 3

# Catalytic Asymmetric Synthesis of 5-Membered Alicyclic α-Quaternary β-Amino Acids via [3 + 2]-Photocycloaddition of α-Substituted Acrylates

**Abstract:**

The photocatalytically active salt of a cationic iridium polypyridyl complex and a chiral borate is competent to promote a highly stereoselective [3+2]-cycloaddition of cyclopropylurea with α-substituted acrylates. This protocol provides straightforward access to a variety of stereochemically defined 5-membered alicyclic α-quaternary β-amino acids, useful building blocks of β-peptides and peptidomimetics.

## 3.1. Introduction

β-Amino acids, which are homologated variants of α-amino acids, constitute the basic structural components of β-peptides and peptidomimetics.[1,2] Chiral β-amino acid frameworks are frequently found in physiologically active compounds, including β-lactam antibiotics. Hence, greater attention has been paid to the utility of β-amino acids as intermediates toward more complex products than to their intrinsic pharmacological properties. Given this scenario, considerable efforts have been devoted to the development of synthetic methods to obtain acyclic and cyclic β-amino acids bearing substituents at various positions in a stereoselective manner.[3] Nevertheless, alicyclic β-amino acids, in which both the amino and carboxylic acid functionalities are vicinally attached to an aliphatic carbocycle, remain challenging targets due to the intrinsic difficulty associated with the simultaneous control of the absolute and relative stereochemistry of two adjacent stereocenters.[4] Among alicyclic β-amino acids, (1*R*,2*S*)-2-aminocyclopentanecarboxylic acid (*cispentacin*) and its derivatives are particularly important because of their physiological characteristics such as strong antibacterial activity as well as conformational rigidity beneficial for regulating the secondary and tertiary structures of peptides. Accordingly, several reliable protocols have been developed for their preparation;[5] however, catalytic asymmetric methodologies are very limited, and none of the available systems are applicable for the simultaneous construction of the primary structure and stereochemical integrity of α-quaternary congeners.[6,7] Here, the author describes the photocatalytic[8] approach to address this problem, thereby enabling a highly stereoselective assembly of 5-membered alicyclic α-quaternary β-amino acids and their derivatives.

## 3.2. Result and Discussion

Recently, the author developed an efficient asymmetric [3+2]-cycloaddition of cyclopropylamine with α-substituted styrenes under visible-light irradiation[9] based on the use of urea as a redox-active anion-recognizable directing group and an iridium-chiral borate ion pair [*rac*-Ir][**1**] as a photocatalyst (Figure 1).[10]

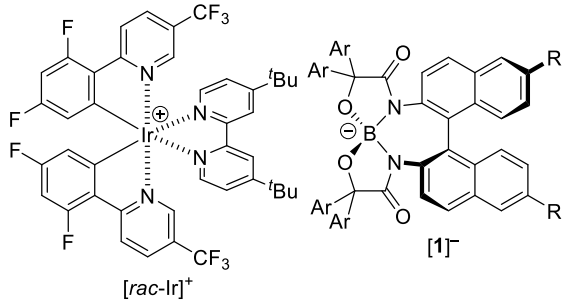


**Figure 1.** Structure of Chiral Iridium Borate

The key reactive intermediate in the stereoselective photocycloaddition is the cyclopropylurea-derived distonic radical cation, which acts as an electron-rich nucleophilic radical. The author thus speculated that if α-substituted acrylates[11] could be employed as electron-deficient acceptors for the distonic radical cation, this catalytic system would serve as a powerful tool for the asymmetric synthesis of 5-membered alicyclic α-quaternary β-amino acids. As an initial attempt to examine this possibility, a mixture of cyclopropylurea **2** and methyl methacrylate (**3a**) in dichloromethane was irradiated with a blue LED (470 nm) in the presence of [*rac*-Ir][**1a**] (5 mol%) at –30 °C for 12 h, which indeed resulted in the formation of the desired cycloadduct, the protected β-amino acid ester **4a**, in 79% yield with a diastereomeric ratio (dr) of 6.4:1 (Table 1, entry 1). The enantiomeric excess of the major diastereomer was determined to be 91%. Fortunately, the stereochemical outcome was improved to a satisfactory level upon increasing the substrate concentration and reaction temperature, and **4a** was obtained in 83% yield (dr = 15:1) with 94% ee for the major diastereomer (entry 2). Subsequent experiments performed with catalysts having borate ions **1** of different structures[10,12] revealed that the *n*-butoxy groups on the geminal aromatic substituents (Ar) of the 1,3,2-oxazaborolidin-4-one moiety were imperative for attaining high stereoselectivity (entries 3 and 4). The presence of 2,4,6-triisopropylphenyl (TRIP) groups at the 6,6'-positions of the binaphthyl backbone also appeared to be crucial for the present stereocontrol (entry 5).

**Table 1.** Optimization of Reaction Conditions[a]

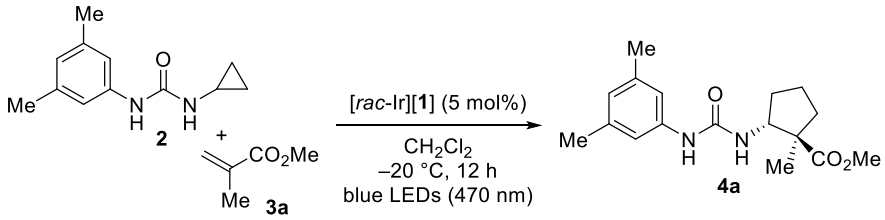


| entry | **1** (Ar, R) | yield (%)[b] | dr[c] | ee (%)[d] |
|---|---|---|---|---|
| 1[e] | **1a** (3,5-($^n$BuO)$_2$C$_6$H$_3$, TRIP) | 79 | 6.4:1 | 91 |
| 2 | **1a** | 83 | 15:1 | 94 |
| 3 | **1b** (3,5-($^n$Pent)$_2$C$_6$H$_3$, TRIP) | 62 | 1.4:1 | 35/*rac* |
| 4 | **1c** (3,5-(MeO)$_2$C$_6$H$_3$, TRIP) | 65 | 1.4:1 | 34/*rac* |
| 5 | **1d** (3,5-($^n$BuO)$_2$C$_6$H$_3$, H) | 81 | 5.6:1 | 56/*rac* |

[a] Unless otherwise noted, the reaction was performed with **2** (0.1 mmol), **3a** (0.5 mmol), and [*rac*-Ir(dFCF$_3$ppy)$_2$(dtbbpy)][**1**] (5 mol%) in $CH_2Cl_2$ (0.2 M) for 12 h under blue LEDs (470 nm) irradiation at –20 °C. [b] Isolated yield was reported. [c] Diastereomeric ratio (dr) was determined by $^1$H NMR analysis of the crude aliquot. [d] Enantiomeric excess (ee) was determined by chiral HPLC analysis using DAICEL CHIRALCEL OZ-3. [e] Reaction was performed in 0.1 M $CH_2Cl_2$ solution at –30 °C. TRIP = 2,4,6-$^i$Pr$_3$C$_6$H$_2$

Under the optimised reaction conditions, the scope of this asymmetric photocycloaddition was explored with various α-substituted acrylates **3** (Table 2). The straight-chain alkyl substituent could be elongated without affecting the stereochemical outcome (entries 1-3), and an excellent selectivity profile was also observed with acrylates bearing 4-*tert*-butylbenzyl and isobutyl groups at the α-position (entries 4 and 5). Various functional groups such as terminal olefins, chlorine, ethers, and esters were well tolerated, and the corresponding cycloadducts **4** were obtained with rigorous enantiocontrol, although the degree of diastereocontrol varied to a certain extent (entries 6-10). An acrylate with a redox-active *N*-Boc-protected indole moiety underwent smooth cycloaddition under the present photoredox conditions to afford the desired product **4l** in high chemical yield with moderate diastereoselectivity and good enantioselectivity (entry 11). When methyl acrylate was used as a radical acceptor, slight erosion of the enantiomeric excess was inevitable, while a satisfactory level of diastereoselectivity was attained (entry 12). The ester substituent of **3** could also be variable, and the steric hindrance caused a slight decrease in enantioselectivity (entries 13 and 14). The absolute configuration of **4** was assigned by analogy to that of **4e**, which was determined to be 1*R*,2*R* by single-crystal X-ray diffraction analysis (Figure 2).

**Table 2.** Reaction Scope[a]

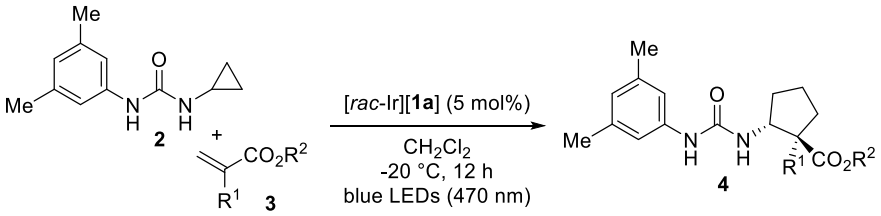


| entry | $R^1$ | $R^2$ | **3** | yield (%)[b] | dr[c] | ee (%)[d] | **4** |
|---|---|---|---|---|---|---|---|
| 1 | $Me(CH_2)_3$ | Me | **3b** | 90 | >20:1 | 96 | **4b** |
| 2 | $Me(CH_2)_9$ | Me | **3c** | 92 | >20:1 | 96 | **4c** |
| 3 | $Ph(CH_2)_3$ | Me | **3d** | 95 | >20:1 | 97 | **4d** |
| 4 | 4-$^t$Bu$C_6H_4CH_2$ | Me | **3e** | 97 | >20:1 | 95 | **4e** |
| 5 | $(Me)_2CHCH_2$ | Me | **3f** | 92 | >20:1 | 96 | **4f** |
| 6 | $CH_2$=$CH(CH_2)_3$ | Me | **3g** | 81 | 18:1 | 97 | **4g** |
| 7 | $Cl(CH_2)_3$ | Me | **3h** | 84 | >20:1 | 97 | **4h** |
| 8 | $^t$Bu$Me_2SiO(CH_2)_3$ | Me | **3i** | 93 | 9.2:1 | 93 | **4i** |
| 9 | $MeO(CH_2)_3$ | Me | **3j** | 84 | 13:1 | 94 | **4j** |
| 10 | $PhCOO(CH_2)_3$ | Me | **3k** | 82 | 8:1 | 94 | **4k** |
| 11 | (*N*-Boc-3-indolyl)$CH_2$ | Me | **3l** | 82 | 4:1 | 85 | **4l** |
| 12 | H | Me | **3m** | 85 | 11:1 | 85 | **4m** |
| 13 | Me | $^t$Bu | **3n** | 94 | 15:1 | 87 | **4n** |
| 14 | Me | $PhCH_2$ | **3o** | 95 | 12:1 | 93 | **4o** |

[a] The reaction was performed with **2** (0.1 mmol), **3** (0.5 mmol), and [*rac*-Ir(dF$CF_3$ppy)$_2$(dtbbpy)][**1a**] (5 mol%) in $CH_2Cl_2$ (0.2 M) for 12 h under blue LEDs (470 nm) irradiation at –20 °C. [b] Isolated yield was reported. [c] Dr was determined by $^1$H NMR analysis of the crude aliquot. [d] Ee was determined by chiral HPLC analysis.

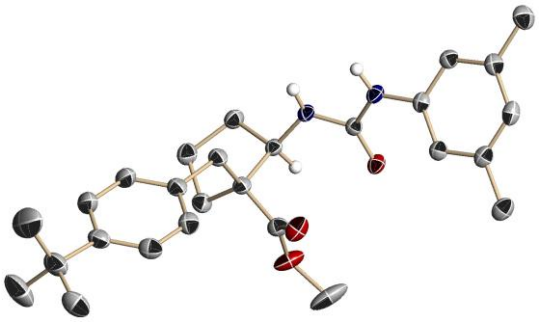

**Figure 2.** ORTEP Diagram of **4e** for Determination of the Absolute Stereochemistry*

*The thermal ellipsoids of non-hydrogen atoms are shown at the 50% probability level. Calculated hydrogen atoms except them attached to the stereogenic carbon are omitted for clarity. Blue = nitrogen, red = oxygen, gray = carbon.

The cycloadducts could be readily converted into the corresponding *N*-Boc-protected β-amino esters, as exemplified in Scheme 1. The initial saponification of the ester moiety of **4a** with NaOH in aqueous THF, followed by treatment with triamine at 120 °C, generated a free β-aminoacid.[13] Subsequent reactions with di-*tert*-butyl dicarbonate ($Boc_2O$) and trimethylsilyldiazomethane ($Me_3SiCHN_2$) were conducted sequentially at ambient temperature to isolate *N*-Boc methyl ester **5** in good yield. Conservation of the enantiomeric excess throughout these processes was confirmed by chiral HPLC analysis after replacing the Boc-protecting group of **5** with a 4-bromobenzenesulfonyl group (see the Experimental Section).

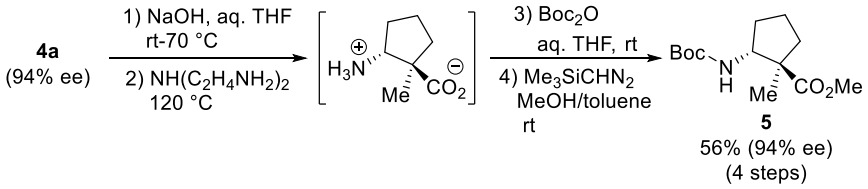


**Scheme 1.** Deprotection

## 3.3. Conclusion

In conclusion, the author established a straightforward procedure for the asymmetric synthesis of 5-membered alicyclic α-quaternary β-amino acids, which relies on the chiral iridium borate-catalysed [3+2]-photocycloaddition of cyclopropylurea with α-substituted acrylates. This photocatalytic protocol was applicable to a range of acrylates bearing different α-substituents, and the corresponding cycloadducts were obtained with high diastereo- and enantioselectivities. Since the presence of cyclic structures and quaternary carbon atoms in amino acids is known to restrict the conformational flexibility of peptides, increasing the accessibility of stereochemically defined alicyclic β-amino acids would pave the way for the development of novel functional β-peptides and peptidomimetics.

## 3.4. Experimental Section

**General Information:** Infrared spectra were recorded on a Shimadzu IRAffinity-1 spectrometer. $^{1}$H NMR spectra were recorded on a JEOL JNM-ECS400 (400 MHz) and JEOL JNM-ECA500II (500 MHz) spectrometers. Chemical shifts are reported in ppm from tetramethylsilane (0.0 ppm) resonance as the internal standard ($(CD_3)_2CO$ and $CDCl_3$). Data are reported as follows: chemical shift, integration, multiplicity (s = singlet, d = doublet, t = triplet, q = quartet, quin = quintet, sex = sextet, sept = septet, m = multiplet, br = broad) and coupling constants (Hz). $^{13}$C NMR spectra were recorded on a JEOL JNM-ECS400 (101 MHz), JEOL JNM-ECA500II (126 MHz), and JEOL JNM-ECS600 (151 MHz) spectrometers with complete proton decoupling. Chemical shifts are reported in ppm from the solvent resonance as the internal standard ($(CD_3)_2CO$; 29.84 ppm, $CDCl_3$; 77.16 ppm). $^{19}$F NMR spectra were recorded on a JEOL JNM-ECA500II (471 MHz) spectrometer. Chemical shifts are reported in ppm from benzotrifluoride (–64.0 ppm) resonance as the external standard. $^{11}$B NMR spectra were recorded on a JEOL JNM-ECA500II (161 MHz) spectrometer with complete proton decoupling. Chemical shifts are reported in ppm from $BF_3{\cdot}OEt_2$ resonance (0.0 ppm) as the external standard. Optical rotations were measured on a HORIBA SEPA-500 polarimeter. The high resolution mass spectra were measured on Thermo Fisher Scientific Exactive (ESI). Analytical thin layer chromatography (TLC) was performed on Merck precoated TLC plates (silica gel 60 $GF_{254}$, 0.25 mm). Manual flash column chromatography was conducted on silica gel 60N (spherical, 40–50 μm; Kanto Chemical Co., Inc.), PSQ60AB (spherical, av. 55 μm; Fuji Silysia Chemical ltd.), Silica gel 60 (Merck 1.09385.9929, 230–400 mesh), and CHROMATOREX NH-DM-2035 (spherical, av. 60 μm; Fuji Silysia Chemical ltd.). Enantiomeric excesses were determined by HPLC analysis using chiral columns [ϕ 4.6 mm x 250 mm, DAICEL CHIRALPAK IB-3 (IB3), CHIRALPAK IB N-3 (IBN3), CHIRALPAK IC-3 (IC3), and CHIRALCEL OZ-3 (OZ3)] with hexane (H), 2-propanol ($^{i}$PrOH), and ethanol (EtOH) as eluent.

Tetrahydrofurane (THF), dichloromethane ($CH_2Cl_2$), toluene, and acetonitrile (MeCN) were supplied from Kanto Chemical Co., Inc. as “Dehydrated” and further purified by passing through neutral alumina under nitrogen atmosphere. α-Substituted Methyl Acrylates were synthesized by following the literature procedures.[11b,14] Other simple chemicals were purchased and used as such.

**Experimental Section:**

**Characterization of a Chiral Iridium Borate [*rac*-Ir]·1 (TRIP = 2,4,6-$^{i}$Pr$_3$C$_6$H$_2$)**

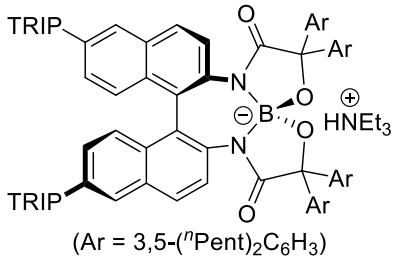


The synthesis was implemented by following the literature procedure[10,12] on 0.14 mmol scale and purification was performed by column chromatography on silica gel (ethyl acetate (EA)/H = 3:100 to 1:1 as eluent) to afford **1b·HNEt$_3$** (0.22 g, 0.12 mmol, 87%) as an off-white solid. **1b·HNEt$_3$ (Ar = 3,5-$^{n}$Pent$_2$C$_6$H$_3$):** $^{1}$H NMR (500 MHz, $CDCl_3$) $\delta$ 9.64 (1H, br), 7.87 (2H, d, $J$ = 9.0 Hz), 7.77 (2H, d, $J$ = 9.0 Hz), 7.66 (2H, s), 7.45 (4H, s), $7.05_3$ (2H, s), $7.04_8$ (2H, d, $J$ = 9.0 Hz), 7.04 (2H, s), 6.90 (2H, s), 6.86 (2H, d, $J$ = 9.0 Hz), 6.49 (2H, s), 6.33 (4H, s), 2.94 (2H, sept, $J$ = 6.9 Hz), 2.64 (2H, sept, $J$ = 6.9 Hz), 2.63-2.55 (2H, m), 2.58 (8H, t, $J$ = 7.3 Hz), 2.28-2.12 (6H, m), 2.10-2.01 (4H, m), 2.00-1.90 (4H, m), 1.59 (8H, quin, $J$ = 7.3 Hz), 1.39-1.31 (8H, m), 1.31-1.26 (16H, m), 1.30 (12H, d, $J$ = 6.9 Hz), 1.24 (8H, sex, $J$ = 7.3 Hz), 1.20-1.14 (8H, m), 1.13 (6H, d, $J$ = 6.9 Hz), 1.09 (6H, d, $J$ = 6.9 Hz), $0.93_3$ (6H, d, $J$ = 6.9 Hz), $0.92_6$ (6H, d, $J$ = 6.9 Hz), 0.85 (12H, t, $J$ = 7.3 Hz), 0.83 (12H, t, $J$ = 7.3 Hz), 0.61 (9H, t, $J$ = 7.5 Hz); $^{13}$C NMR (126 MHz, $CDCl_3$) $\delta$ 177.7, 148.0, 146.9, 146.5, 144.9, 144.2, 142.3, 141.3, 137.9, 137.2, 137.1, 132.4, 132.0, 130.2, 128.9, 128.0, $127.7_9$, $127.7_5$, 127.2, 126.9, 125.3, 125.2, $120.6_3$, $120.5_9$, 85.8, 45.7, 36.3, 35.7, 34.4, 31.8, 31.7, 31.5, 31.3, 30.4, 30.3, 24.6, 24.5, 24.4, $24.2_2$, $24.1_9$, 23.9, 22.7, 14.2, 8.2, two carbon atoms were not found probably due to overlapping.; $^{11}$B NMR (160 MHz, $CDCl_3$) $\delta$ 11.0; IR (film): 2927, 2855, 1635, 1590, 1487, 1409, 1396, 1122, 1063, 909 cm$^{-1}$; HRMS (ESI) Calcd for $C_{118}H_{156}N_2O_4B^-$ ([M−HNEt$_3$]$^-$) 1676.2153. Found 1676.2155; $[\alpha]_D^{22}$ −91.0 ($c$ = 5.4, $CHCl_3$).

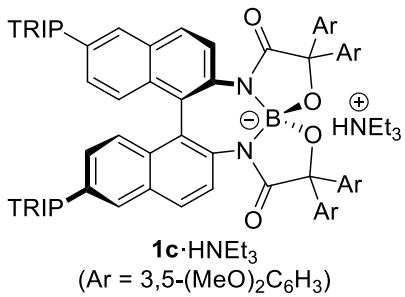


The synthesis was implemented by following the literature procedure[10,12] on 0.11 mmol scale and purification by column chromatography on silica gel (EA/H = 1:10 to 100:0 as eluent) afforded **1c**·HNEt$_3$ (0.15 g, 0.10 mmol, 93%) as an off-white solid. **1c·HNEt$_3$ (Ar = 3,5-(MeO)$_2$C$_6$H$_3$):** $^{1}$H NMR (500 MHz, $CDCl_3$) $\delta$ 9.08 (1H, br), 7.78 (2H, d, $J$ = 8.4 Hz), 7.68 (2H, d, $J$ = 8.4 Hz), 7.57 (2H, s), 7.03 (2H, s), 7.01 (2H, s), 6.97 (2H, d, $J$ = 8.4 Hz), 6.85 (2H, d, $J$ = 8.4 Hz), 6.78 (4H, s), 6.17 (2H, s), 6.13 (4H, s), 5.95 (2H, s), 3.47 (12H, s), 3.26 (12H, s), 2.92 (2H, sept, $J$ = 6.8 Hz), 2.55 (2H, sept, $J$ = 6.8 Hz), 2.49 (2H, sept, $J$ = 6.8 Hz), 2.43-2.33 (6H, m), 1.28 (12H, d, $J$ = 6.8 Hz), 1.11 (6H, d, $J$ = 6.8 Hz), 1.03 (6H, d, $J$ = 6.8 Hz), 0.90 (6H, d, $J$ = 6.8 Hz), 0.89 (6H, d, $J$ = 6.8 Hz), 0.61 (9H, t, $J$ = 7.3 Hz); $^{13}$C NMR (126 MHz, $CDCl_3$) $\delta$ 176.9, 160.6, 159.7, 148.1, 146.9, 146.4, 146.0, 137.6, 137.0, 136.8, 132.2, 129.7, 129.2, 128.1, 128.0, 127.4, 127.0, 120.7, 120.6, 105.9, 105.6, 99.0, 98.9, 85.6, 55.3, 55.1,

46.2, 34.4, 30.4, 24.5, $24.3_1$, $24.2_6$, $24.2_4$, $24.1_8$, 23.9, 8.1, two carbon atoms were not found probably due to overlapping.; $^{11}$B NMR (160 MHz, $CDCl_3$) $\delta$ 10.6; IR (film): 2959, 2906, 1651, 1591, 1452, 1414, 1343, 1288, 1142, 1038, 910 $cm^{-1}$; HRMS (ESI) Calcd for $C_{86}H_{92}N_2O_{12}B^-$ ($[M-HNEt_3]^-$) 1355.6738. Found 1355.6745; $[\alpha]_D^{22}$ −69.4 ($c$ = 6.0, $CHCl_3$).

**Representative Procedure for the Preparation of Chiral Iridium Borate [*rac*-Ir]·1**

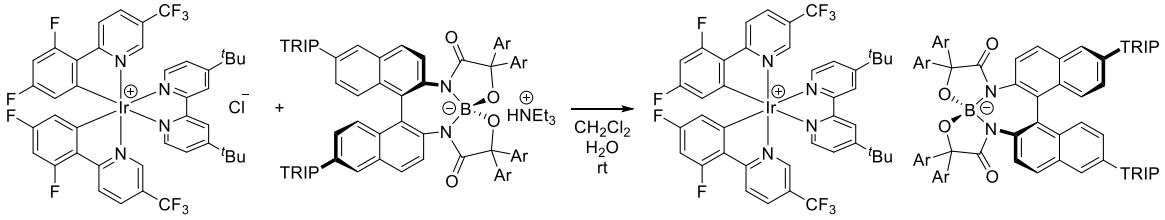


A solution of iridium chloride [*rac*-Ir]·Cl (47.6 mg, 0.047 mmol)[15] and **1b**·$HNEt_3$ (117.0 mg, 0.066 mmol) in $CH_2Cl_2$ (10.0 mL) was vigorously washed with distilled water (15.0 mL) four times. The organic phase was dried over $Na_2SO_4$ and concentrated under vacuum to afford [*rac*-Ir]·**1b** (0.17 g, 0.064 mmol) as an yellow solid, which was used as a catalyst for the asymmetric [3+2] radical cycloaddition reaction without further purification. **[*rac*-Ir]·1b (Ar = 3,5-$^n$Pent$_2$C$_6$H$_3$):** $^1$H NMR (500 MHz, $CDCl_3$) *mixture of diastereomers* $\delta$ 8.48 (1H, dd, $J_{H\text{-}H}$ = 8.6 Hz, $J_{H\text{-}F}$ = 2.0 Hz), 8.44 (1H, dd, $J_{H\text{-}H}$ = 8.6 Hz, $J_{H\text{-}F}$ = 2.0 Hz), 8.34 (2H, s), 8.01 (1H, d, $J$ = 8.6 Hz), 7.96 (1H, d, $J$ = 8.6 Hz), 7.92 (2H, d, $J$ = 5.7 Hz), 7.78 (4H, s), 7.77 (2H, d, $J$ = 8.8 Hz), 7.71 (2H, d, $J$ = 8.8 Hz), 7.63 (1H, dd, $J$ = 5.7, 1.5 Hz), 7.62 (2H, s), 7.59 (1H, dd, $J$ = 5.7, 1.5 Hz), 7.29 (2H, s), 7.20 (2H, d, $J$ = 8.8 Hz), 7.06 (2H, s), 7.04 (2H, s), 6.85 (2H, d, $J$ = 8.8 Hz), 6.82 (2H, s), 6.64 (1H, ddd, $J_{H\text{-}F}$ = 12.1, 9.3 Hz, $J_{H\text{-}H}$ = 2.3 Hz), 6.60 (1H, ddd, $J_{H\text{-}F}$ = 12.1, 9.3 Hz, $J_{H\text{-}H}$ = 2.3 Hz), 6.40 (2H, s), 6.20 (4H, s), 5.61 (1H, dd, $J_{H\text{-}F}$ = 7.9 Hz, $J_{H\text{-}H}$ = 2.3 Hz), 5.60 (1H, dd, $J_{H\text{-}F}$ = 7.9 Hz, $J_{H\text{-}H}$ = 2.3 Hz), 2.94 (2H, sept, $J$ = 6.8 Hz), 2.77 (2H, sept, $J$ = 6.8 Hz), 2.68 (2H, sept, $J$ = 6.8 Hz), 2.61 (8H, t, $J$ = 7.1 Hz), 2.00 (4H, dt, $J$ = 13.8, 7.1 Hz), 1.82 (4H, dt, $J$ = 13.8, 7.1 Hz), 1.61 (8H, quin, $J$ = 7.1 Hz), 1.41 (9H, s), 1.39 (9H, s), 1.35-1.30 (8H, m), 1.31 (12H, d, $J$ = 6.8 Hz), 1.30-1.24 (16H, m), 1.19 (8H, sex, $J$ = 7.1 Hz), 1.15-1.08 (8H, m), 1.13 (6H, d, $J$ = 6.8 Hz), 1.09 (6H, d, $J$ = 6.8 Hz), 0.96 (6H, d, $J$ = 6.8 Hz), 0.93 (6H, d, $J$ = 6.8 Hz), 0.83 (12H, t, $J$ = 7.1 Hz), 0.78 (12H, t, $J$ = 7.1 Hz); $^{13}$C NMR (126 MHz, $CDCl_3$) *mixture of diastereomers* $\delta$ 178.2, 168.1 (d, $J_{C\text{-}F}$ = 6.0 Hz), 166.7, 165.1 (ddd, $J_{C\text{-}F}$ = 263.0, 12.7, 3.7 Hz), 155.3, 153.8 (d, $J_{C\text{-}F}$ = 6.0 Hz), 150.7, 150.6, 147.5, 147.2, $146.9_2$, $146.9_0$, 144.5, 144.2 (d, $J_{C\text{-}F}$ = 4.9 Hz), 143.0, 140.8, 140.6, 139.4, 137.8, 137.2, 137.1, 136.2, 132.7, 131.9, 130.9, 128.6, 128.4, 128.3, 127.7, 127.6, 127.1, $126.9_0$, $126.8_6$, 126.4, 126.3, $126.0_3$ (q, $J_{C\text{-}F}$ = 35.1 Hz), $125.9_8$ (d, $J_{C\text{-}F}$ = 35.1 Hz), $125.9_4$, $125.8_9$, 125.8, $124.4_2$ (d, $J_{C\text{-}F}$ = 20.5 Hz), $124.3_5$ (d, $J_{C\text{-}F}$ = 20.7 Hz), 121.7 (q, $J_{C\text{-}F}$ = 273.3 Hz), 121.6, 120.5, 120.4, 114.1 (d, $J_{C\text{-}F}$ = 18.1 Hz), $100.4_2$ (t, $J_{C\text{-}F}$ = 26.6 Hz), $100.3_7$ (t, $J_{C\text{-}F}$ = 26.6 Hz), 85.4, 36.4, 36.2, 35.6, 34.4, 31.8, 31.6, 31.5, 31.3, 30.3, 24.8,

24.5, 24.4, 24.2$_3$, 24.1$_8$, 23.9, 27.8, 14.3, 14.2, 57 carbon atoms were not found probably due to overlapping.; $^{19}$F NMR (470 MHz, $CDCl_3$) *mixture of diastereomers* $\delta$ −62.8, −100.3, −100.5, −104.6, two fluorine atoms were not found probably due to overlapping.; $^{11}$B NMR (160 MHz, $CDCl_3$) *mixture of diastereomers* $\delta$ 11.0 (overlapped); IR (film): 2931, 1653, 1602, 1569, 1465, 1397, 1330, 1298, 1143, 1112, 1027, 903 cm$^{-1}$.

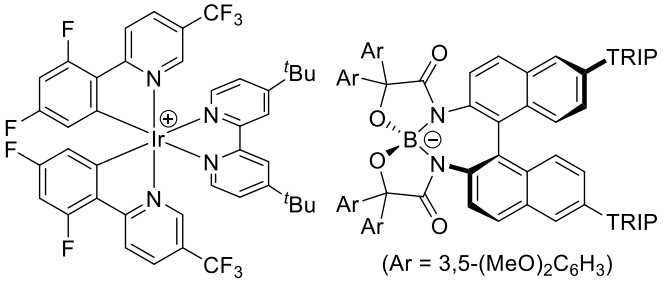


**[*rac*-Ir]·1a (Ar = 3,5-(MeO)$_2$C$_6$H$_3$):** $^1$H NMR (500 MHz, $CDCl_3$) *mixture of diastereomers* $\delta$ 8.46-8.41 (2H, m), 8.36 (2H, s), 8.00 (2H, d, $J$ = 9.0 Hz), 7.94$_2$ (1H, d, $J$ = 6.2 Hz), 7.93$_8$ (1H, d, $J$ = 6.2 Hz), 7.70 (2H, d, $J$ = 8.6 Hz), 7.65 (2H, d, $J$ = 8.6 Hz), 7.63 (1H, dd, $J$ = 6.2, 1.6 Hz), 7.61 (1H, dd, $J$ = 6.2, 1.6 Hz), 7.54 (2H, s), 7.33$_3$ (2H, s), 7.33$_0$ (4H, d, $J$ = 2.2 Hz), 7.13 (2H, d, $J$ = 8.6 Hz), 7.06 (2H, s), 7.03 (2H, s), 6.85 (2H, d, $J$ = 8.6 Hz), 6.65 (2H, t, $J_{H\text{-}F}$ = 10.3 Hz), 6.20 (4H, d, $J$ = 2.2 Hz), 6.19 (2H, t, $J$ = 2.2 Hz), 5.91 (2H, t, $J$ = 2.2 Hz), 5.62 (2H, dd, $J_{H\text{-}F}$ = 8.0 Hz, $J_{H\text{-}H}$ = 2.0 Hz), 3.71 (12H, s), 3.19 (12H, s), 2.94 (2H, sept, $J$ = 6.8 Hz), 2.73 (2H, sept, $J$ = 6.8 Hz), 2.59 (2H, sept, $J$ = 6.8 Hz), 1.39$_1$ (9H, s), 1.38$_7$ (9H, s), 1.31 (12H, d, $J$ = 6.8 Hz), 1.17 (6H, d, $J$ = 6.8 Hz), 1.06 (6H, d, $J$ = 6.8 Hz), 1.03 (6H, d, $J$ = 6.8 Hz), 0.92 (6H, d, $J$ = 6.8 Hz); $^{13}$C NMR (126 MHz, $CDCl_3$) *mixture of diastereomers* $\delta$ 176.9, 168.2 (d, $J_{C\text{-}F}$ = 6.0 Hz), 168.1 (d, $J_{C\text{-}F}$ = 6.0 Hz), 166.7, 165.1 (dd, $J_{C\text{-}F}$ = 263.1, 12.7 Hz), 162.8 (dd, $J_{C\text{-}F}$ = 265.5, 12.7 Hz), 159.8, 159.5, 155.2$_8$, 155.2$_6$, 153.9 (d, $J_{C\text{-}F}$ = 6.0 Hz), 150.7, 150.6, 148.6, 147.9, 147.7, 147.2, 146.7, 144.3 (d, $J_{C\text{-}F}$ = 4.9 Hz), 138.7, 137.5, 137.0, 136.9, 136.4, 132.5, 132.0, 130.3, 128.4, 128.1, 127.7, 127.1, 126.9, 126.3, 126.0 (q, $J_{C\text{-}F}$ = 35.1 Hz), 124.3 (d, $J_{C\text{-}F}$ = 20.5 Hz), 124.2 (d, $J_{C\text{-}F}$ = 20.5 Hz), 121.7 (q, $J_{C\text{-}F}$ = 273.3 Hz), 121.6$_3$, 121.6$_1$, 120.6, 120.5, 114.1 (d, $J_{C\text{-}F}$ = 18.1 Hz), 106.1, 105.8, 100.4 (t, $J_{C\text{-}F}$ = 26.6 Hz), 99.6, 99.5, 85.4, 55.4, 54.9, 36.2, 34.3, 30.3$_4$, 30.2$_8$, 24.6, 24.5, 24.3, 24.2$_4$, 24.1$_8$, 23.9, 50 carbon atoms were not found probably due to overlapping.; $^{19}$F NMR (470 MHz, $CDCl_3$) *mixture of diastereomers* $\delta$ −62.8, −100.5, −104.7, three fluorine atoms were not found probably due to overlapping.; $^{11}$B NMR (160 MHz, $CDCl_3$) *mixture of diastereomers* $\delta$ 11.0 (overlapped); IR (film): 2965, 1660, 1600, 1560, 1455, 1389, 1329, 1295, 1146, 1109, 1057, 903, 841 cm$^{-1}$.

**Synthesis and Characterization of α-Substituted Methyl Acrylates**

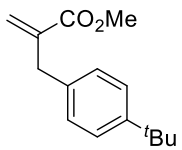


**Methyl 2-(4-(*tert*-butyl)benzyl)acrylate 3e:** The title compound was prepared from diethyl malonate and 4-*tert*-butylbenzyl bromide by following the literature procedure.[14a] $^1$H NMR (500 MHz, $CDCl_3$) $\delta$ 7.31 (2H, d, $J$ = 8.5 Hz), 7.13 (2H, d, $J$ = 8.5 Hz), 6.22 (1H, d, $J$ = 1.4 Hz), 5.47 (1H, q, $J$ = 1.4 Hz), 3.74 (3H, s),

3.60 (2H, brs), 1.30 (9H, s); $^{13}$C NMR (126 MHz, $CDCl_3$) $\delta$ 167.6, 149.3, 140.3, 135.7, 128.8, 126.3, 125.5, 52.0, 37.6, 34.5, 31.5; IR (film): 2960, 2867, 1719, 1631, 1517, 1440, 1193, 1137, 1110, 947, 813 cm$^{-1}$; HRMS (ESI) Calcd for $C_{15}H_{20}O_2Na^+$ ([M+Na]$^+$) 255.1356. Found 255.1355.

**Preparation of methyl 5-((*tert*-butyldimethylsilyl)oxy)-2-methylenepentanoate 3i**

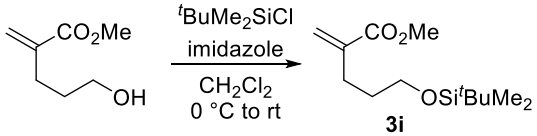


**3i**

To a solution of methyl 5-hydroxy-2-methylenepentanoate (0.14 g, 1.0 mmol)[14c] in $CH_2Cl_2$ (5.0 mL) were added imidazole (0.17 g, 2.5 mmol) and $^t$BuMe$_2$SiCl (0.30 g, 2.0 mmol) at 0 °C. After being stirred for 20 min, the mixture was warmed to ambient temperature and stirred for 21 h. The reaction was quenched by adding water and the aqueous phase was extracted with $CH_2Cl_2$ three times. The combined organic phases were dried over $Na_2SO_4$, filtered, and concentrated. Purification of the residue was performed by column chromatography on silica gel (H/$Et_2O$ = 100:1 to 10:1 as eluent) to afford methyl 5-((*tert*-butyldimethylsilyl)oxy)-2-methylenepentanoate **3i** (0.23 g, 0.89 mmol, 89%) as a colorless oil. **Methyl 5-((*tert*-butyldimethylsilyl)oxy)-2-methylenepentanoate 3i:** $^1$H NMR (500 MHz, $CDCl_3$) $\delta$ 6.15 (1H, dt, *J* = 1.3, 0.5 Hz), 5.55 (1H, q, *J* = 1.3 Hz), 3.75 (3H, s), 3.63 (2H, t, *J* = 6.4 Hz), 2.37 (2H, td, *J* = 7.8, 1.3 Hz), 1.69 (2H, tt, *J* = 7.8, 6.4 Hz), 0.90 (9H, s), 0.05 (6H, s); $^{13}$C NMR (126 MHz, $CDCl_3$) $\delta$ 167.9, 140.4, 125.0, 62.5, 51.9, 31.6, 28.4, 26.1, 18.5, −5.2; IR (film): 2950, 2849, 1724, 1477, 1250, 1149, 1096, 1066, 946, 836 cm$^{-1}$; HRMS (ESI) Calcd for $C_{13}H_{26}O_3SiNa^+$ ([M+Na]$^+$) 281.1543. Found 281.1541.

**Preparation of *tert*-butyl 3-(2-(methoxycarbonyl)allyl)-1*H*-indole-1-carboxylate 3l**

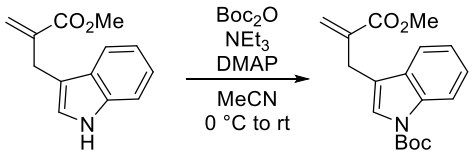


**3l**

To a solution of methyl 2-((1*H*-indol-3-yl)methyl)acrylate (0.68 g, 3.1 mmol)[14d] in MeCN (31.0 mL) were added DMAP (47.6 mg, 0.39 mmol) and $NEt_3$ (0.52 mL, 3.8 mmol) at 0 °C. After $Boc_2O$ (1.73 mL, 7.5 mmol) was added, the mixture was stirred for 1.5 h at 0 °C and then allowed to warm to ambient temperature and stirred for 4 h. The reaction was quenched by adding a saturated aqueous solution of $NH_4Cl$ at 0 °C and the aqueous phase was extracted with $CH_2Cl_2$ three times. The combined organic phases were dried over $Na_2SO_4$, filtered, and concentrated. Purification of the residue was performed by column chromatography on silica gel (H/EA = 50:1 to 5:1 as eluent) to

afford *tert*-butyl 3-(2-(methoxycarbonyl)allyl)-1*H*-indole-1-carboxylate **3l** (0.96 g, 3.0 mmol, 97%) as a colorless sticky oil. ***tert*-butyl 3-(2-(methoxycarbonyl)allyl)-1*H*-indole-1-carboxylate 3l:** $^{1}$H NMR (500 MHz, $CDCl_3$) $\delta$ 8.12 (1H, br), 7.46 (1H, d, $J$ = 7.6 Hz), 7.41 (1H, brs), 7.31 (1H, t, $J$ = 7.6 Hz), 7.22 (1H, t, $J$ = 7.6 Hz), 6.24 (1H, d, $J$ = 1.5 Hz), 5.52 (1H, d, $J$ = 1.5 Hz), 3.78 (3H, s), 3.71 (2H, s), 1.67 (9H, s); $^{13}$C NMR (126 MHz, $CDCl_3$) $\delta$ 167.6, 149.9, 138.4, 135.7, 130.4, 126.4, 124.5, 124.2, 122.6, 119.4, 117.7, 115.4, 83.7, 52.1, 28.4, 27.4 cm$^{-1}$; IR (film): 1720, 1452, 1368, 1256, 1156, 1083, 1017, 938, 840 cm$^{-1}$; HRMS (ESI) Calcd for $C_{18}H_{21}O_4NNa^+$ ([M+Na]$^+$) 338.1363. Found 338.1363.

**Asymmetric [3+2] Photocycloaddition Reaction**

**Representative Procedure for the Asymmetric [3+2] Photocycloaddition Reaction**

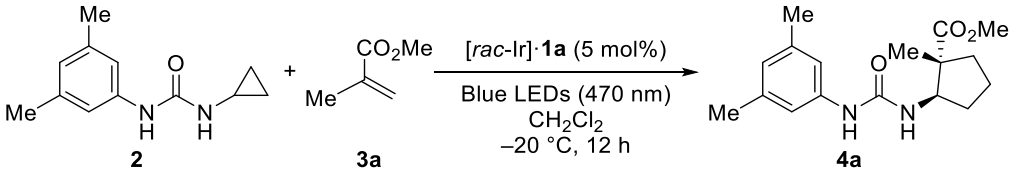


To a mixture of 1-cyclopropyl-3-(3,5-dimethylphenyl)urea (**2**) (20.4 mg, 0.10 mmol) and [*rac*-Ir]·**1a** (13.4 mg, 0.0050 mmol) in $CH_2Cl_2$ (0.5 mL) was added methyl methacrylate (**3a**) (50.1 mg, 0.50 mmol) under Ar atmosphere. The suspension was then subjected to freeze-pump-thaw process (1 cycle) and backfilled with Ar. The reaction mixture was illuminated with blue LEDs (470 nm) at −20 °C for 12 h. After exposing to air, the reaction mixture was concentrated to give the crude residue, which was analyzed by $^{1}$H NMR (500 MHz) to determine the diastereomeric ratio of the product (dr = 15:1). Purification of the residue by column chromatography on silica gel (H/$Et_2O$ = 3:1 to 1:1 as eluent) afforded **4a** (25.3 mg, 0.083 mmol, 83%) as a mixture of diastereomers. Enantiomeric excess of the major diastereomer of **4a** was determined by HPLC analysis on chiral stationary phase. **4a**: HPLC OZ3, H/$^{i}$PrOH = 10:1, flow rate = 1.0 mL/min, rt, λ = 254 nm, 8.3 min (minor diastereomer), 9.7 min (minor diastereomer), 13.7 min (minor enantiomer of major diastereomer), 24.3 min (major enantiomer of major diastereomer); $^{1}$H NMR (500 MHz, $(CD_3)_2CO$) *major diastereomer* $\delta$ 7.67 (1H, br), 7.07 (2H, s), 6.55 (1H, s), 5.71 (1H, brd, $J$ = 8.6 Hz), 4.53 (1H, q, $J$ = 8.6 Hz), 3.63 (3H, s), 2.21 (1H, ddd, $J$ = 13.0, 8.8, 6.8 Hz), 2.20 (6H, s), 2.07 (1H, ddt, $J$ = 16.0, 8.6, 4.4 Hz), 1.74-1.64 (2H, m), 1.59-1.47 (2H, m), 1.13 (3H, s); $^{13}$C NMR (126 MHz, $(CD_3)_2CO$) *major diastereomer* $\delta$ 177.8, 155.5, 141.4, 138.7, 123.9, 116.7, 58.0, 52.1, 51.7, 37.3, 31.8, 21.5, 21.4, 18.1; IR (film): 3324, 2917, 2823, 1727, 1653, 1559, 1437, 1203, 1127, 941, 854 cm$^{-1}$; HRMS (ESI) Calcd for $C_{17}H_{24}O_3N_2Na^+$ ([M+Na]$^+$) 327.1679. Found 327.1672.

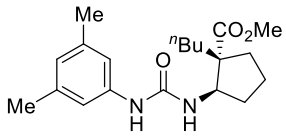

**4b**: HPLC IC3, H/$^{i}$PrOH = 10:1, flow rate = 1.0 mL/min, 30 °C, λ = 254 nm, 16.9 min (minor diastereomer), 19.3 min (minor diastereomer), 30.1 min (major enantiomer of major diastereomer), 35.7 min (minor enantiomer of major diastereomer); $^{1}$H NMR (500 MHz, $(CD_3)_2CO$) major diastereomer $\delta$ 7.73 (1H, br), 7.07 (2H, s), 6.56 (1H, s), 5.82 (1H, brd, $J$ = 9.6 Hz), 4.55 (1H, dt, $J$ = 9.6, 7.0 Hz), 3.63 (3H, s), 2.26 (1H, ddd, $J$ = 12.9, 7.9, 5.1 Hz), 2.20 (6H, s), 1.97 (1H, dddd, $J$ = 12.9, 8.9, 7.0, 5.8 Hz), 1.83 (1H, ddd, $J$ = 12.9, 11.1, 5.1 Hz), 1.72-1.60 (2H, m), 1.60-1.48 (2H, m), 1.44-1.36 (1H, m), 1.32-1.23 (2H, m), 1.23-1.14 (2H, m), 0.86 (3H, t, $J$ = 7.3 Hz); $^{13}$C NMR (126 MHz, $(CD_3)_2CO$) major diastereomer $\delta$ 177.0, 155.6, 141.3, 138.7, 124.0, 116.8, 57.4$_2$, 57.3$_7$, 52.1, 32.8, 32.6, 32.4, 28.3, 24.0, 21.5, 21.4, 14.3; IR (film): 3325, 2942, 2870, 1726, 1637, 1560, 1430, 1270, 1203, 1145, 1128, 838 cm$^{-1}$; HRMS (ESI) Calcd for $C_{20}H_{30}O_3N_2Na^+$ ([M+Na]$^+$) 369.2149. Found 369.2155.

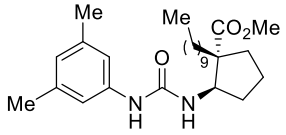

**4c**: HPLC IC3, H/$^{i}$PrOH = 10:1, flow rate = 1.0 mL/min, 30 °C, λ = 254 nm, 12.7 min (minor diastereomer), 14.5 min (minor diastereomer), 21.8 min (major enantiomer of major diastereomer), 24.5 min (minor enantiomer of major diastereomer); $^{1}$H NMR (500 MHz, $(CD_3)_2CO$) major diastereomer $\delta$ 7.67 (1H, br), 7.08 (2H, s), 6.56 (1H, s), 5.76 (1H, brd, $J$ = 9.4 Hz), 4.55 (1H, dt, $J$ = 9.4, 6.7 Hz), 3.64 (3H, s), 2.26 (1H, ddd, $J$ = 12.7, 7.8, 4.8 Hz), 2.20 (6H, s), 1.97 (1H, ddt, $J$ = 13.2, 9.1, 6.7 Hz), 1.86-1.78 (1H, m), 1.72-1.60 (2H, m), 1.60-1.48 (2H, m), 1.45-1.35 (1H, m), 1.31-1.19 (16H, m), 0.86 (3H, t, $J$ = 6.8 Hz); $^{13}$C NMR (126 MHz, $(CD_3)_2CO$) major diastereomer $\delta$ 177.0, 155.4, 141.4, 138.7, 123.9, 116.7, 57.5, 57.3, 52.1, 33.0, 32.9, 32.6, 32.4, 31.0, 30.3, 30.2, 30.1, 26.1, 23.3, 21.5, 21.4, 14.4, one carbon atom was not found probably due to overlapping.; IR (film): 3329, 2925, 2858, 1727, 1636, 1558, 1450, 1237, 1167, 1043, 833 cm$^{-1}$; HRMS (ESI) Calcd for $C_{26}H_{42}O_3N_2Na^+$ ([M+Na]$^+$) 453.3088. Found 453.3109.

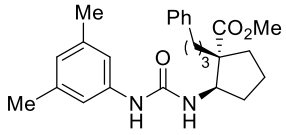

**4d**: HPLC IC3, H/$^{i}$PrOH = 10:1, flow rate = 1.0 mL/min, 30 °C, λ = 254 nm, 21.5 min (minor diastereomer), 25.7 min (minor diastereomer), 35.5 min (major enantiomer of major diastereomer), 44.1 min (minor enantiomer of major diastereomer); $^{1}$H NMR (500 MHz, $(CD_3)_2CO$) major diastereomer $\delta$ 7.72 (1H, br), 7.21 (2H, t, $J$ = 7.1 Hz), 7.15 (2H, d, $J$ = 7.1 Hz), 7.12 (1H, t, $J$ = 7.1 Hz), 7.10 (2H, s), 6.57 (1H, s), 5.84 (1H, br), 4.60 (1H, dt, $J$ = 9.0, 6.6 Hz), 3.63 (3H, s), 2.58 (1H, ddd, 13.8, 8.3, 5.7 Hz), 2.54 (1H, ddd, 13.8, 8.3, 5.7 Hz), 2.25 (1H, ddd, $J$ = 12.7, 7.8, 5.3 Hz), 2.21 (6H, s), 1.98 (1H, ddt, $J$ = 13.0, 8.6, 6.6 Hz), 1.92-1.83 (1H, m), 1.69-1.45 (7H, m); $^{13}$C NMR (126 MHz, $(CD_3)_2CO$) major diastereomer $\delta$ 176.9, 155.6, 143.1, 141.3, 138.8, 129.1, 129.0, 126.4, 124.0, 116.8, 57.6, 57.1, 52.1, 37.1, 33.1, 32.7, 32.4, 28.2, 21.5, 21.4; IR (film): 3301, 2957, 2862, 1725, 1640, 1559, 1448, 1230, 1153, 840 cm$^{-1}$; HRMS (ESI) Calcd for $C_{25}H_{32}O_3N_2Na^+$ ([M+Na]$^+$)

431.2305. Found 431.2322.

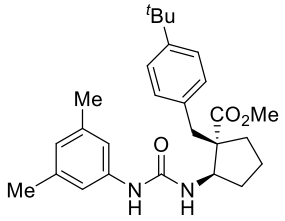

**4e**: The title compound was purified by column chromatography on silica gel topped with 4 cm of CHROMATOREX NH-DM-2035 (H/EA = 6:1 to 2:1 as eluent). HPLC IBN3, H/EtOH = 92:8, flow rate = 1.0 mL/min, rt, λ = 254 nm, 6.8 min (minor diastereomer), 9.2 min (major enantiomer of major diastereomer), 15.0 min (minor diastereomer), 16.8 min (minor enantiomer of major diastereomer); $^1$H NMR (500 MHz, $(CD_3)_2CO$) major diastereomer $\delta$ 7.75 (1H, br), 7.27 (2H, d, $J$ = 8.3 Hz), 7.12 (2H, s), 7.08 (2H, d, $J$ = 8.3 Hz), 6.57 (1H, s), 5.95 (1H, brd, $J$ = 9.1 Hz), 4.58 (1H, dt, $J$ = 9.1, 7.1 Hz), 3.62 (3H, s), 3.33 (1H, d, $J$ = 13.5 Hz), 2.59 (1H, d, $J$ = 13.5 Hz), 2.21 (6H, s), 2.16-2.07 (1H, m), 2.05-1.98 (1H, m), 1.82-1.72 (1H, m), 1.72-1.58 (3H, m), 1.27 (9H, s); $^{13}$C NMR (151 MHz, $(CD_3)_2CO$) major diastereomer $\delta$ 176.2, 155.5, 149.6, 141.4, 138.8, 136.4, 130.3, 125.8, 124.0, 116.8, 58.7, 58.5, 52.0, 37.1, 34.8, 31.7, 31.6, 31.3, 21.5, 20.7; IR (film): 3272, 2965, 1729, 1702, 1634, 1560, 1319, 1244, 1040, 814 cm$^{-1}$; HRMS (ESI) Calcd for $C_{27}H_{36}O_3N_2Na^+$ ([M+Na]$^+$) 459.2618. Found 459.2611.

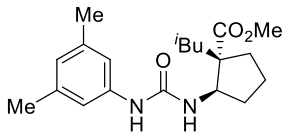

**4f**: HPLC IC3, H/$^i$PrOH = 10:1, flow rate = 1.0 mL/min, 30 °C, λ = 254 nm, 18.1 min (minor diastereomer), 20.9 min (minor diastereomer), 28.3 min (major enantiomer of major diastereomer), 32.5 min (minor enantiomer of major diastereomer); $^1$H NMR (500 MHz, $(CD_3)_2CO$) major diastereomer $\delta$ 7.73 (1H, br), 7.07 (2H, s), 6.56 (1H, s), 5.82 (1H, brd. $J$ = 9.5 Hz), 4.52 (1H, dt, $J$ = 9.5, 6.5 Hz), 3.63 (3H, s), 2.34 (1H, ddd, $J$ = 12.9, 7.6, 5.6 Hz), 2.20 (6H, s), 1.92 (1H, ddt, $J$ = 13.1, 8.9, 6.5 Hz), 1.85 (1H, dd, $J$ = 13.6, 6.6 Hz), 1.71-1.47 (5H, m), 1.40 (1H, dd, $J$ = 13.6, 6.6 Hz), 0.88 (3H, d, $J$ = 6.5 Hz), 0.80 (3H, d, $J$ = 6.5 Hz); $^{13}$C NMR (126 MHz, $(CD_3)_2CO$) major diastereomer $\delta$ 177.3, 155.6, 141.3, 138.8, 124.0, 116.8, 58.2, 57.1, 52.0, 41.3, 32.4, 32.0, 26.3, 24.6, 23.5, 21.5, 21.3; IR (film): 3324, 2958, 1734, 1701, 1644, 1559, 1457, 1244, 1038, 842 cm$^{-1}$; HRMS (ESI) Calcd for $C_{20}H_{30}O_3N_2Na^+$ ([M+Na]$^+$) 369.2149. Found 369.2144.

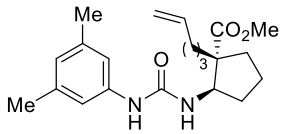

**4g**: HPLC IC3, H/$^i$PrOH = 10:1, flow rate = 1.0 mL/min, 30 °C, λ = 254 nm, 16.7 min (minor diastereomer), 19.4 min (minor diastereomer), 29.5 min (major enantiomer of major diastereomer), 34.0 min (minor enantiomer of major diastereomer); $^1$H NMR (500 MHz, $(CD_3)_2CO$) major diastereomer $\delta$ 7.72 (1H, br), 7.07 (2H, s), 6.56 (1H, s), 5.83 (1H, brd, $J$ = 9.3 Hz), 5.77 (1H, ddt, $J$ = 17.2, 10.3, 6.8 Hz), 4.96 (1H, ddt, $J$ = 17.2, 2.3, 1.3 Hz), 4.88 (1H, ddt, $J$ = 10.3, 2.3, 1.3 Hz), 4.56 (1H, dt, $J$ = 9.3, 7.0 Hz), 3.64 (3H, s), 2.26 (1H, ddd, $J$ = 13.0, 8.3, 5.3 Hz), 2.20 (6H, s), 2.01-1.93 (3H, m), 1.84 (1H, td, $J$ = 12.4, 4.2 Hz), 1.72-1.48 (4H, m), 1.46-1.37 (1H, m), 1.37-1.23 (2H, m); $^{13}$C NMR (126 MHz,

$(CD_3)_2CO$) major diastereomer $\delta$ 176.9, 155.6, 141.3, 139.4, 138.7, 124.0, 116.8, 114.9, 57.4, 52.1, 35.0, 32.9, 32.3, 25.5, 21.5, 21.3, two carbon atoms were not found probably due to overlapping.; IR (film): 3345, 2916, 2847, 1728, 1638, 1560, 1456, 1272, 1236, 1193, 1170, 839 $cm^{-1}$; HRMS (ESI) Calcd for $C_{21}H_{30}O_3N_2Na^+$ ($[M+Na]^+$) 381.2149. Found 381.2142.

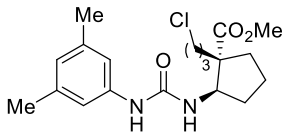


**4h**: HPLC IC3, H/$^i$PrOH = 10:1, flow rate = 1.0 mL/min, 30 °C, λ = 254 nm, 18.5 min (minor diastereomer), 22.2 min (minor diastereomer), 30.4 min (minor enantiomer of major diastereomer), 33.8 min (major enantiomer of major diastereomer); $^1$H NMR (500 MHz, $(CD_3)_2CO$) major diastereomer $\delta$ 7.73 (1H, br), 7.07 (2H, s), 6.56 (1H, s), 5.88 (1H, brd, $J$ = 8.8 Hz), 4.58 (1H, dt, $J$ = 8.8, 6.7 Hz), 3.65 (3H, s), 3.58 (1H, dt, $J$ = 10.7, 6.4 Hz), 3.53 (1H, dt, $J$ = 10.7, 6.4 Hz), 2.26 (1H, ddd, $J$ = 13.1, 8.1, 5.1 Hz), 2.20 (6H, s), 2.00 (1H, ddt, $J$ = 12.9, 8.5, 6.7 Hz), 1.92 (1H, td, $J$ = 12.5, 4.3 Hz), 1.83-1.72 (1H, m), 1.72-1.49 (6H, m); $^{13}$C NMR (126 MHz, $(CD_3)_2CO$) major diastereomer $\delta$ 176.7, 155.6, 141.2, 138.8, 124.0, 116.8, 57.5, 56.9, 52.2, 46.2, 33.0, 32.2, 21.5, 21.4, two carbon atoms were not found probably due to overlapping.; IR (film): 3317, 2952, 2868, 1724, 1641, 1561, 1428, 1276, 1235, 1162, 835 $cm^{-1}$; HRMS (ESI) Calcd for $C_{19}H_{27}O_3N_2{}^{35}ClNa^+$ ($[M+Na]^+$) 389.1602. Found 389.1595.

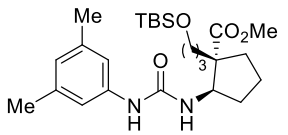


**4i**: HPLC IBN3, H/$^i$PrOH = 10:1, flow rate = 1.0 mL/min, rt, λ = 254 nm, 6.9 min (minor diastereomer), 8.9 min (major enantiomer of major diastereomer), 23.3 min (minor diastereomer), 24.7 min (minor enantiomer of major diastereomer); $^1$H NMR (500 MHz, $(CD_3)_2CO$) major diastereomer $\delta$ 7.71 (1H, br), 7.07 (2H, s), 6.55 (1H, s), 5.83 (1H, br), 4.56 (1H, dt, $J$ = 9.3, 6.6 Hz), 3.64 (3H, s), 3.63-3.52 (2H, m), 2.27 (1H, ddd, $J$ = 13.1, 8.1, 5.4 Hz), 2.20 (6H, s), 1.98 (1H, ddt, $J$ = 13.1, 8.3, 6.6 Hz), 1.84 (1H, td, $J$ = 10.4, 2.7 Hz), 1.73-1.60 (2H, m), 1.60-1.35 (5H, m), 0.86 (9H, s), $0.02_2$ (3H, s), $0.01_5$ (3H, s); $^{13}$C NMR (126 MHz, $(CD_3)_2CO$) major diastereomer $\delta$ 176.9, 155.5, 141.3, 138.7, 123.9, 116.8, 64.0, $57.4_0$, $57.3_5$, 52.1, 32.8, 32.3, 29.7, 29.1, 26.3, 21.5, 21.3, 18.8, $-5.1_0$, $-5.1_2$; IR (film): 3314, 2952, 2857, 1730, 1654, 1560, 1460, 1243, 1194, 1097, 832 $cm^{-1}$; HRMS (ESI) Calcd for $C_{25}H_{43}O_4N_2Si^+$ ($[M+H]^+$) 463.2987. Found 463.3006.

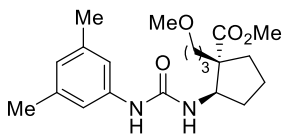


**4j**: The title compound was purified by column chromatography on silica gel topped with 4 cm of CHROMATOREX NH-DM-2035 (H/EA = 6:1 to 2:1 as eluent). HPLC IC3, H/$^i$PrOH = 85:15, flow rate = 1.0 mL/min, 30 °C, λ = 254 nm, 18.1 min (minor diastereomer), 21.1 min (minor diastereomer), 37.3 min (minor enantiomer of major diastereomer), 42.1 min (major enantiomer of major diastereomer); $^1$H NMR (500 MHz, $(CD_3)_2CO$) major diastereomer $\delta$ 7.75 (1H, br), 7.07 (2H,

s), 6.56 (1H, s), 5.84 (1H, brd, *J* = 9.0 Hz), 4.55 (1H, dt, *J* = 9.0, 6.6 Hz), 3.64 (3H, s), 3.30 (1H, dt, *J* = 9.4, 6.3 Hz), 3.27 (1H, dt, *J* = 9.4, 6.3 Hz), 3.21 (3H, s), 2.26 (1H, ddd, *J* = 12.9, 7.9, 5.4 Hz), 2.20 (6H, s), 1.98 (1H, ddt, *J* = 13.0, 8.3, 6.6 Hz), 1.88-1.80 (1H, m), 1.72-1.60 (2H, m), 1.60-1.40 (5H, m); $^{13}$C NMR (126 MHz, $(CD_3)_2CO$) major diastereomer $\delta$ 176.9, 155.6, 141.3, 138.7, 124.0, 116.8, 73.4, 58.3, 57.5, 57.0, 52.1, 32.9, 32.3, 26.3, 21.5, 21.3, one carbon atom was not found probably due to overlapping.; IR (film): 3327, 2944, 2869, 1724, 1641, 1569, 1450, 1278, 1237, 1209, 1117, 839 cm$^{-1}$; HRMS (ESI) Calcd for $C_{20}H_{30}O_4N_2Na^+$ ([M+Na]$^+$) 385.2098. Found 385.2094.

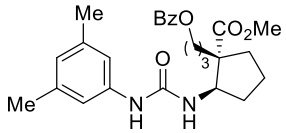


**4k**: HPLC IBN3, H/EtOH = 94:6, flow rate = 1.0 mL/min, rt, λ = 254 nm, 15.4 min (minor diastereomer), 21.6 min (major enantiomer of major diastereomer), 30.6 min (minor enantiomer of major diastereomer), 33.5 min (minor diastereomer); $^1$H NMR (500 MHz, $(CD_3)_2CO$) major diastereomer $\delta$ 7.99 (2H, d, *J* = 7.5 Hz), 7.71 (1H, br), 7.59 (1H, t, *J* = 7.5 Hz), 7.44 (2H, t, *J* = 7.5 Hz), 7.07 (2H, s), 6.55 (1H, s), 5.88 (1H, br), 4.61 (1H, q, *J* = 7.5 Hz), 4.26 (2H, t, *J* = 6.3 Hz), 3.65 (3H, s), 2.32-2.25 (1H, m), 2.19 (6H, s), 2.04-1.97 (2H, m), 1.83-1.73 (1H, m), 1.73-1.50 (6H, m); $^{13}$C NMR (126 MHz, $(CD_3)_2CO$) major diastereomer $\delta$ 176.8, 166.7, 155.6, 141.2, 138.7, 133.7, 131.4, 130.1, 129.3, 124.0, 116.8, 65.8, 57.4, 57.1, 52.2, 33.0, 32.3, 29.1, 25.6, 21.5, 21.4; IR (film): 3292, 2937, 1719, 1653, 1555, 1452, 1264, 1119, 1070, 1026, 835 cm$^{-1}$; HRMS (ESI) Calcd for $C_{26}H_{31}O_5N_2^-$ ([M−H]$^-$) 451.2227. Found 451.2235.

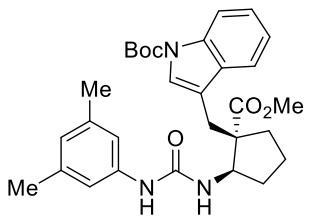


**4l**: HPLC IC3, H/$^i$PrOH = 10:1, flow rate = 1.0 mL/min, rt, λ = 254 nm, 23.0 min (minor diastereomer), 48.1 min (minor enantiomer of major diastereomer), 52.5 min (major enantiomer of major diastereomer), 63.8 min (minor diastereomer); $^1$H NMR (400 MHz, $(CD_3)_2CO$) major diastereomer $\delta$ 8.11 (1H, brd, *J* = 7.6 Hz), 7.72 (1H, br), 7.57 (1H, d, *J* = 7.6 Hz), 7.42 (1H, s), 7.29 (1H, t, *J* = 7.6 Hz), 7.22 (1H, t, *J* = 7.6 Hz), 7.13 (2H, s), 6.58 (1H, s), 6.00 (1H, brd, *J* = 9.1 Hz), 4.66 (1H, dt, *J* = 9.1, 6.8 Hz), 3.60 (3H, s), 3.36 (1H, d, *J* = 14.6 Hz), 2.87 (1H, d, *J* = 14.6 Hz), 2.30-2.20 (1H, m), 2.22 (6H, s), 2.10-2.02 (1H, m), 1.88-1.67 (4H, m), 1.66 (9H, s); $^{13}$C NMR (126 MHz, $(CD_3)_2CO$) major diastereomer $\delta$ 176.5, 155.6, 150.2, 141.3, 138.8, 135.9, 132.3, 125.0, 124.9, 124.1, 123.1, 119.8, 118.0, 116.9, 115.8, 84.1, 58.5, 58.3, 52.1, 32.4, 31.8, 28.2, 26.9, 21.5, 21.1; IR (film): 3320, 2982, 1724, 1642, 1614, 1555, 1452, 1364, 1223, 1150, 1073, 1017, 837 cm$^{-1}$; HRMS (ESI) Calcd for $C_{30}H_{37}O_5N_3Na^+$ ([M+Na]$^+$) 542.2625. Found 542.2620.

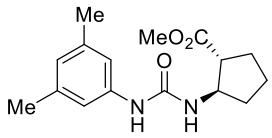

**4m**: HPLC OZ3, H/$^{i}$PrOH = 10:1, flow rate = 1.0 mL/min, 30 °C, λ = 254 nm, 11.1 min (minor diastereomer), 12.4 min (minor diastereomer), 19.0 min (minor enantiomer of major diastereomer), 25.7 min (major enantiomer of major diastereomer); $^{1}$H NMR (500 MHz, $(CD_3)_2CO$) *major diastereomer* $\delta$ 7.68 (1H, br), 7.07 (2H, s), 6.56 (1H, s), 5.88 (1H, brd, *J* = 7.6 Hz), 4.29 (1H, quin, *J* = 7.6 Hz), 3.62 (3H, s), 2.66 (1H, q, *J* = 7.6 Hz), 2.20 (6H, s), 2.06 (1H, dq, *J* = 12.8, 7.6 Hz), 1.98 (1H, dq, *J* = 13.7, 7.6 Hz), 1.82 (1H, dtd, *J* = 13.7, 7.6, 6.7 Hz), 1.76-1.65 (2H, m), 1.54 (1H, dq, *J* = 12.8, 7.6 Hz); $^{13}$C NMR (126 MHz, $(CD_3)_2CO$) *major diastereomer* $\delta$ 175.8, 155.7, 141.3, 138.7, 124.0, 116.8, 56.2, 51.9, 51.3, 33.8, 29.2, 23.7, 21.5; IR (film): 3333, 2943, 2866, 1734, 1647, 1612, 1558, 1423, 1284, 1156, 1035, 835 cm$^{-1}$; HRMS (ESI) Calcd for $C_{16}H_{22}O_3N_2Na^+$ ($[M+Na]^+$) 313.1523. Found 313.1519.

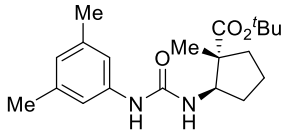

**4n**: HPLC IB3, H/EtOH = 97:3, flow rate = 1.0 mL/min, 30 °C, λ = 254 nm, 10.3 min (minor diastereomer), 11.1 min (major enantiomer of major diastereomer), 16.7 min (minor enantiomer of major diastereomer), 22.2 min (minor diastereomer); $^{1}$H NMR (500 MHz, $(CD_3)_2CO$) *major diastereomer* $\delta$ 7.74 (1H, br), 7.08 (2H, s), 6.55 (1H, s), 5.69 (1H, brd, *J* = 8.3 Hz), 4.56 (1H, q, *J* = 8.3 Hz), 2.19 (6H, s), 2.18 (1H, ddd, *J* = 13.0, 9.0, 6.0 Hz), 2.04 (1H, ddt, *J* = 16.0, 8.3, 4.3 Hz), 1.72-1.58 (2H, m), 1.54-1.45 (2H, m), 1.44 (9H, s), 1.11 (3H, s); $^{13}$C NMR (126 MHz, $(CD_3)_2CO$) *major diastereomer* $\delta$ 176.6, 155.5, 141.4, 138.7, 123.9, 116.8, 80.2, 57.4, 52.6, 37.1, 32.2, 28.1, 21.4$_9$, 21.4$_5$, 18.6; IR (film): 3288, 2969, 2859, 1718, 1696, 1654, 1613, 1539, 1456, 1367, 1247, 1153, 834 cm$^{-1}$; HRMS (ESI) Calcd for $C_{20}H_{30}O_3N_2Na^+$ ($[M+Na]^+$) 369.2149. Found 369.2151.

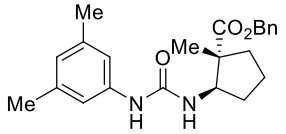

**4o**: HPLC IC3, H/$^{i}$PrOH = 10:1, flow rate = 1.0 mL/min, 30 °C, λ = 254 nm, 20.6 min (minor diastereomer), 24.7 min (minor diastereomer), 32.1 min (minor enantiomer of major diastereomer), 40.7 min (major enantiomer of major diastereomer); $^{1}$H NMR (500 MHz, $(CD_3)_2CO$) *major diastereomer* $\delta$ 7.74 (1H, br), 7.41 (2H, d, *J* = 7.8 Hz), 7.35 (1H, t, *J* = 7.8 Hz), 7.28 (2H, t, *J* = 7.8 Hz), 7.08 (2H, s), 6.56 (1H, s), 5.81 (1H, brd, *J* = 8.5 Hz), 5.11 (1H, d, *J* = 12.5 Hz), 5.09 (1H, d, *J* = 12.5 Hz), 4.62 (1H, q, *J* = 8.5 Hz), 2.25 (1H, ddd, *J* = 12.8, 8.8, 6.5 Hz), 2.20 (6H, s), 2.07 (1H, ddt, *J* = 15.5, 8.5, 4.3 Hz), 1.75-1.62 (2H, m), 1.61-1.48 (2H, m), 1.16 (3H, s); $^{13}$C NMR (126 MHz, $(CD_3)_2CO$) *major diastereomer* $\delta$ 177.2, 155.7, 141.3, 138.7, 137.8, 129.2, 128.7, 128.6, 124.0, 116.9, 66.9, 58.1, 51.8, 37.3, 31.8, 21.5, 21.4, 18.0; IR (film): 3336, 2952, 2858, 1719, 1638, 1616, 1558, 1454, 1231, 1149, 857 cm$^{-1}$; HRMS (ESI) Calcd for $C_{23}H_{28}O_3N_2Na^+$ ($[M+Na]^+$) 403.1992. Found 403.1989.

**Deprotection and Sulfonylation of 4a**

**Removal of Urea to Give *N*-Boc-aminocyclopentane 5**

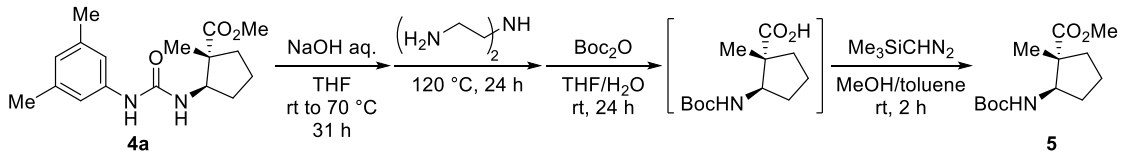

(single diastereomer, 94% ee)

To a solution of diastereomerically-pure urea **4a** (22.8 mg, 0.075 mmol) in THF (0.70 mL) was added a 2 N aqueous solution of NaOH (0.38 mL, 0.75 mmol) at ambient temperature. After being stirred for 12 h in a test tube sealed with a screw cap, the mixture was heated at 70 °C and stirred for another 19 h. The resulting mixture was concentrated in vacuo at 20 °C and then treated with diethylenetriamine (49.0 μL, 0.45 mmol)[13] at 120 °C for 24 h in a test tube sealed with a screw cap. The reaction mixture was cooled to ambient temperature and diluted with THF (0.55 mL) and $H_2O$ (0.35 mL). $Boc_2O$ (0.37 mL, 1.58 mmol) was added to the solution and the resulting mixture was stirred there for 24 h. The reaction was quenched by addition of a 2 N aqueous solution of NaOH (0.75 mL). The aqueous phase was washed with $Et_2O$ (one time) and then acidified to pH = 1 with a 2 N aqueous solution of $KHSO_4$. The resulting aqueous phase was extracted with EA (three times). The combined organic phases were washed with brine, dried over $Na_2SO_4$, and concentrated under reduced pressure. The crude mixture was passed through a silica gel column ($CH_2Cl_2$/MeOH = 100:1 to 20:1 as eluent) and fractions containing the Boc-protected amino acid were concentrated. The obtained material was dissolved in toluene (0.38 mL) and MeOH (0.18 mL). After adding trimethylsilyldiazomethane (*ca*. 0.6 M in hexane, 0.82 mL, 0.49 mmol), the mixture was stirred for 2 h at ambient temperature and concentrated in vacuo. The crude residue was purified by column chromatography on silica gel (H/EA = 10:1 to 3:1 as eluent) to furnish **5** (10.9 mg, 0.042 mmol, 56% from **4a**). Preservation of the enantiomeric excess was confirmed after exchanging *N*-protecting group from Boc to 4-bromophenylsulfonyl (see below). **5:** $^1$H NMR (400 MHz, $CDCl_3$) $\delta$ 4.46 (1H, br), 4.32 (1H, q, $J$ = 7.8 Hz), 3.69 (3H, s), 2.31-2.18 (1H, m), 2.12 (1H, dtd, $J$ = 12.9, 7.8, 5.4 Hz), 1.75-1.64 (2H, m), 1.55 (1H, dt, $J$ = 12.8, 7.4 Hz), 1.47-1.38 (1H, m), 1.43 (9H, s), 1.12 (3H, s); $^{13}$C NMR (101 MHz, $CDCl_3$) $\delta$ 177.5, 155.4, 79.4, 58.1, 52.2, 51.0, 36.3, 31.0, 28.5, 20.6, 17.5; IR (film): 2983, 1723, 1698, 1517, 1458, 1364, 1243, 1164, 1055 cm$^{-1}$; HRMS (ESI) Calcd for $C_{13}H_{23}O_4NNa^+$ ([M+Na]$^+$) 280.1519. Found 280.1517; $[\alpha]_D^{24}$ +14.9 (*c* = 10.9, acetone).

**Sulfonylation of *N*-Boc-aminocyclopentane 5 to Give Sulfonamide 6**

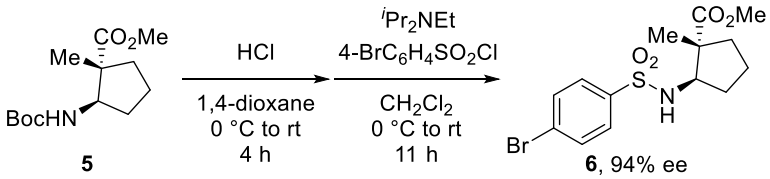

*N*-Boc amino ester **5** (9.9 mg, 0.038 mmol) was dissolved into a solution of hydrochloric acid in 1,4-dioxane (4 M, 0.39 mL) at 0 °C. The solution was allowed to warm to ambient temperature and stirred there for 4 h. After concentration of the reaction mixture, anhydrous $CH_2Cl_2$ (0.40 mL), 4-$BrC_6H_4SO_2Cl$ (15.6 mg, 0.061 mmol), and diisopropylethylamine (0.13 mL, 0.77 mmol) were added to the residue at 0 °C. The reaction mixture was allowed to warm to ambient temperature and stirred there for 11 h. The reaction was quenched by adding 1 N hydrochloric acid at 0 °C and the aqueous phase was extracted with $CH_2Cl_2$ three times. The combined organic phases were dried over $Na_2SO_4$ and filtered. All volatiles were removed under reduced pressure to give the crude residue. Purification of the residue was performed by column chromatography on silica gel (H/EA = 10:1 to 1.5:1 as eluent) to afford **6** (13.2 mg, 0.035 mmol, 91%). Enantiomeric excess of **6** was determined by HPLC analysis on chiral stationary phase. **6**: HPLC IBN3, H/$^i$PrOH = 10:1, flow rate = 1.0 mL/min, rt, λ = 254 nm, 15.0 min (major enantiomer), 17.2 min (minor enantiomer); $^1$H NMR (500 MHz, $CDCl_3$) $\delta$ 7.74 (2H, d, $J$ = 8.5 Hz), 7.65 (2H, d, $J$ = 8.5 Hz), 4.90 (1H, brd, $J$ = 8.1 Hz), 3.86 (1H, dt, $J$ = 9.9, 8.1 Hz), 3.57 (3H, s), 2.03 (1H, ddd, $J$ = 13.8, 10.2, 6.7 Hz), 1.98 (1H, dtd, $J$ = 13.0, 8.1, 4.2 Hz), 1.73-1.63 (1H, m), 1.63-1.54 (2H, m), 1.47 (1H, dtd, $J$ = 13.0, 9.9, 7.9 Hz), 1.16 (3H, s); $^{13}$C NMR (151 MHz, $CDCl_3$) $\delta$ 176.9, 139.5, 132.4, 129.0, 127.7, 60.1, 52.3, 51.2, 36.2, 31.1, 20.2, 17.7; IR (film): 3244, 2951, 1734, 1576, 1436, 1332, 1263, 1158, 1068, 1009, 825 cm$^{-1}$; HRMS (ESI) Calcd for $C_{14}H_{18}O_4N^{79}BrSNa^+$ ([M+Na]$^+$) 398.0032. Found 398.0051; $[\alpha]_D^{23}$ +25.3 (*c* = 13.0, acetone).

**Crystallographic Analysis**

**Recrystallization of 4e:** Recrystallization was performed by using a $H_2O$/DMF solvent system at ambient temperature to afford single crystals of **4e**. The crystallographic data are summarized in Table S1 and the ORTEP diagram is shown in Figure S1.

**Crystallographic Structure Determination of 4e:** The single crystal, which was obtained by the above procedure, was mounted on MicroMesh. Data of X-ray diffraction were collected at 123 K on a RAPID 100x100 IP-Cu diffractometer with fine-focus sealed tube Cu/Kα radiation (λ = 1.54187 Å). An absorption correction was made using Primary Mu Option. The structure was solved by direct methods and Fourier syntheses, and refined by full-matrix least squares on $F^2$ by using SHELXL-2014.[16] All non-hydrogen atoms were refined with anisotropic displacement parameters. Hydrogen atom bonded to the nitrogen atom was located from a difference synthesis, and its coordinates and isotropic thermal parameters were refined. The other hydrogen atoms were placed in calculated positions and their isotropic thermal parameters were refined.

**Table S1.** Crystal data and structure refinement for **4e** (CCDC 2051437).

| | | |
|---|---|---|
| Empirical formula | $C_{27}H_{36}N_2O_3$ | |
| Formula weight | 436.58 | |
| Temperature | 123(2) K | |
| Wavelength | 1.54187 Å | |
| Crystal system | Orthorhombic | |
| Space group | P2(1)2(1)2(1) | |
| Unit cell dimensions | a = 8.29650(10) Å | α = 90°. |
| | b = 8.9484(2) Å | β = 90°. |
| | c = 34.1519(6) Å | γ = 90°. |
| Volume | 2535.45(8) $Å^3$ | |
| Z | 4 | |
| Density (calculated) | 1.144 $Mg/m^3$ | |
| Absorption coefficient | 0.585 $mm^{-1}$ | |
| F(000) | 944 | |
| Crystal size | 1.000000 x 0.300000 x 0.010000 $mm^3$ | |
| Theta range for data collection | 5.110 to 68.196°. | |
| Index ranges | −9<=h<=9, −10<=k<=10, −41<=l<=40 | |
| Reflections collected | 29661 | |
| Independent reflections | 4629 [R(int) = 0.0210] | |
| Completeness to theta = 67.687° | 99.9 % | |
| Absorption correction | Empirical | |
| Max. and min. transmission | 1.0000 and 0.8270 | |
| Refinement method | Full-matrix least-squares on $F^2$ | |
| Data / restraints / parameters | 4629 / 0 / 308 | |
| Goodness-of-fit on $F^2$ | 1.058 | |
| Final R indices [I>2sigma(I)] | $R_1$ = 0.0301, $wR_2$ = 0.0797 | |
| R indices (all data) | $R_1$ = 0.0305, $wR_2$ = 0.0800 | |
| Absolute structure parameter | 0.04(3) | |
| Extinction coefficient | 0 | |
| Largest diff. peak and hole | 0.162 and −0.178 e.$Å^{-3}$ | |

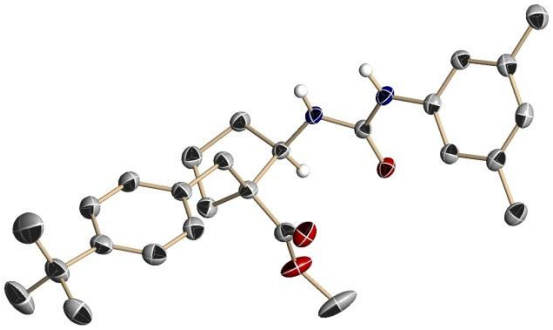

**Figure S1.** Molecular structure of **4e**. The thermal ellipsoids of non-hydrogen atoms are shown at the 50% probability level. Calculated hydrogen atoms except them attached to the stereogenic carbon are omitted for clarity. Blue = nitrogen, red = oxygen, gray = carbon.

## References and Notes


(1) (a) Griffith, O. W. *Ann. Rev. Biochem.* **1986**, *55*, 855. (b) Steer, D. L.; Lew, R. A.; Perlmutter, P.; Smith, A. I.; Aguilar, M.-I. *Curr. Med. Chem.* **2002**, *9*, 811. (c) Lelais, G.; Seebach, D. *Biopolymers* **2004**, *76*, 206. (d) von Nussbaum, F.; Spiteller, P. In *Highlights in Bioorganic Chemistry: Methods and Applications*, eds. Schmuck, C.; Wennemers, H. Wiley-VCH Verlag, Weinheim, 2004, pp 63. (e) Pilsl, L. K. A.; Reiser, O. *Amino Acids* **2011**, *41*, 709.

(2) (a) Cheng, R. P.; Gellman, S. H.; DeGrado, W. F. *Chem. Rev.* **2001**, *101*, 3219. (b) Seebach, D.; Gardiner, J. *Acc. Chem. Res.* **2008**, *41*, 1366. (c) Seebach, D.; Beck, A. K.; Capone, S.; Deniau, G.; Grošelj, U. ; Zass, E. *Synthesis* **2009**, 1. (d) Cabrele, C.; Martinek, T. A.; Reiser, O.; Berlicki, Ł. *J. Med. Chem.* **2014**, *57*, 9718. (e) Wang, P. S. P.; Schepartz, A. *Chem. Commun.* **2016**, *52*, 7420.

(3) (a) Ma, J.-A. *Angew. Chem. Int. Ed.* **2003**, *42*, 4290. (b) *Enantioselective Synthesis of β-Amino Acids*, ed. Juaristi, E.; Soloshnok, V. John Wiley & Sons Inc, Hoboken, 2005. (c) Weiner, B.; Szymański, W.; Janssen, D. B.; Minnaard, A. J.; Feringa, B. L. *Chem. Soc. Rev.* **2010**, *39*, 1656. (d) Noda, H.; Shibasaki, M. *Eur. J. Org. Chem.* **2020**, 2350. (e) Kim, S. M.; Yang, J. W. *Org. Biomol. Chem.* **2013**, *11*, 4737.

(4) (a) Fülöp, F. *Farmaco* **2000**, *55*, 181. (b) Kuhl, A.; Hahn, M. G.; Dumić, M.; Mittendorf, J. *Amino Acids* **2005**, *29*, 89. (c) Fülöp, F.; Martinek, T. A.; Tóth, G. K. *Chem. Soc. Rev.* **2006**, *35*, 323. (d) Kiss, L.; Fülöp, F. *Chem. Rev.* **2014**, *114*, 1116.

(5) (a) Konishi, M.; Nishio, M.; Saitoh, K.; Miyaki, T.; Oki, T.; Kawaguchi, H. *J. Antibiotics* **1989**, *42*, 1749. (b) Iwamoto, T.; Tsujii, E.; Ezaki, M.; Fujie, A.; Hashimoto, S.; Okuhara, M.; Kohsaka, M.; Imanaka, H.; Kawabata, K.; Inamoto, Y.; Sakane, K. *J. Antibiotics* **1990**, *43*, 1. (c) Ohki, H.; Inamoto, Y.; Kawabata, K.; Kamimura, T.; Sakane, K. *J. Antibiotics* **1991**, *44*, 546. (d) Miyata, O.; Muroya, K.; Koide, J.; Naito, T. *Synlett* **1998**, 271. (e) Pou, A.; Moyano, A. *Eur. J. Org. Chem.*, 2013, 3103. (f) Kiss, L.; Kardos, M.; Forró, E.; Fülöp, F. *Eur. J. Org. Chem.* **2015**, 1283. (g) Forro, E.; Fulop, F. *Mini-Rev. Org. Chem.* **2016**, *13*, 219.

(6) Qin, S.; Liu, T.; Luo, Y.; Yan, J.; Kang, H.; Jiang, S.; Yang, G. *Synlett* **2019**, *30*, 593.

(7) (a) Ooi, T.; Miki, T.; Taniguchi, M.; Shiraishi, M.; Takeuchi, M.; Maruoka, K. *Angew. Chem. Int. Ed.* **2003**, *42*, 3796. (b) Verma, K.; Banerjee, P. *Adv. Synth. Catal.* **2016**, *358*, 2053.

(8) (a) Wang, C.; Lu, Z. *Org. Chem. Front.* **2015**, *2*, 179. (b) Meggers, E. *Chem. Commun.* **2015**, *51*, 3290. (c) Brimioulle, R.; Lenhart, D.; Maturi, M. M.; Bach, T. *Angew. Chem. Int. Ed.* **2015**, *54*, 3872. (d) Lu, Q.; Glorius, F. *Angew. Chem. Int. Ed.* **2017**, *56*, 49. (e) Silvi, M.; Melchiorre, P. *Nature* **2018**, *554*, 41. (f) Garrido-Castro, A. F.; Maestro, M. C.; Alemán, J. *Tetrahedron Lett.* **2018**, *59*, 1286. (g) Jiang, C.; Chen, W.; Zheng, W.-H.; Lu, H. *Org. Biomol. Chem.* **2019**, *17*, 8673. (h) Hong, B.-C. *Org. Biomol. Chem.* **2020**, *18*, 4298. (i) Saha, D.

*Chem. - Asian J.* **2020**, *15*, 2129. (j) Rigotti, T.; Alemán, J. *Chem. Commun.* **2020**, *56*, 11169.

(9) (a) Maity, S.; Zhu, M.; Shinabery, R. S.; Zheng, N. *Angew. Chem. Int. Ed.* **2012**, *51*, 222. (b) Cai, Y.; Wang, J.; Zhang, Y.; Li, Z.; Hu, D.; Zheng, N.; Chen, H. *J. Am. Chem. Soc.* **2017**, *139*, 12259. (c) Staveness, D.; Collins III, J. L.; McAtee, R. C.; Stephenson, C. R. J. *Angew. Chem. Int. Ed.* **2019**, *58*, 19000. (d) Muriel, B.; Gagnebin, A.; Waser, J. *Chem. Sci.* **2019**, *10*, 10716. (e) Yin, Y.; Li, Y.; Gonçalves, T. P.; Zhan, Q.; Wang, G.; Zhao, X.; Qiao, B.; Huang, K.-W.; Jiang, Z. *J. Am. Chem. Soc.* **2020**, *142*, 19451.

(10) Uraguchi, D.; Kimura, Y.; Ueoka, F.; Ooi, T. *J. Am. Chem. Soc.* **2020**, *142*, 19462.

(11) A variety of α-substituted acrylates is readily accessible. For actual preparation, see: (a) Stetter, H.; Kuhlmann, H. *Synthesis* **1979**, 29. (b) Fu, M.-C.; Shang, R.; Cheng, W.-M.; Fu, Y. *ACS Catal.* **2016**, *6*, 2501.

(12) Uraguchi, D.; Ueoka, F.; Tanaka, N.; Kizu, T.; Takahashi, W.; Ooi, T. *Angew. Chem. Int. Ed.* **2020**, *59*, 11456.

(13) Noshita, M.; Shimizu, Y.; Morimoto, H.; Ohshima, T. *Org. Lett.* **2016**, *18*, 6062.

(14) (a) Farley, A. J. M.; Sandford, C.; Dixon, D. J. *J. Am. Chem. Soc.* **2015**, *137*, 15992. (b) Shu, C.; Mega, R. S.; Andreassen, B. J.; Noble, A.; Aggarwal, V. K. *Angew. Chem. Int. Ed.* **2018**, *57*, 15430. (c) Shu, C.; Noble, A.; Aggarwal, V. K. *Angew. Chem. Int. Ed.* **2019**, *58*, 3870. (d) Ji, X.; Li, Y.; Xie, L.; Lu, H.; Ding, W.; Zhang, Q. *Angew. Chem. Int. Ed.* **2016**, *55*, 11845.

(15) Rohe, S.; Morris, A. O.; McCallum, T.; Barriault, L. *Angew. Chem. Int. Ed.* **2018**, *57*, 15664.

(16) Sheldrick, G. M. *Acta Cryst.* **2015**, *C71*, 3.

# Appendix

## Molecular Design, Synthesis, and Asymmetric Catalysis of a Hexacoordinated Chiral Phosphate Ion

**Abstract:**

The author describes the design, synthesis, and characterization of a chiral hexacoordinated phosphate ion that features an octahedral P(V) core consisting of two *N*,*N*,*O*-tridentate backbones. The author further demonstrates that the corresponding hydrogen phosphate acts as an effective catalyst for a highly enantioselective Pictet–Spengler-type reaction, wherein the relationship between the structure of the chiral phosphate ion and its ability to dictate the absolute stereochemistry is revealed in conjunction with precise structural elucidation of the phosphate ion.

## A.1. Introduction

Phosphorus is a ubiquitous element that is essential for biological machinery; phosphates are a key component of ATP as well as the backbone of DNA and RNA. In turn, in organic chemistry, phosphorus plays a critical role in forming numerous organophosphorus compounds that are utilized as useful reagents and effective ligands and catalysts, rendering organophosphorus chemistry an active research field of significant importance.[1] This is largely owing to the distinct ability of the phosphorus atom to adopt variable oxidation and coordination numbers, which provides remarkable structural diversity for phosphorus-containing organic molecules.

Among them, compounds that obey the octet rule constitute the majority and generally comprise either tricoordinated P(III) or tetracoordinated P(IV) and P(V) cores. On the other hand, organophosphorus compounds possessing a P(V) center with higher coordinating character, particularly the pentacoordinated phosphorane family, have had a rich history ever since Georg Wittig prepared pentaphenylphosphorane ($Ph_5P$);[2] a wide variety of single- and mixed-atom phosphoranes have been elaborated and characterized.[3,4] In contrast, the chemistry of hexacoordinated phosphorus compounds is far less understood, probably because it has been mainly studied with specific interest in the intermediacy of hexacoordinated phosphate ions in the reactions of pentacoordinated phosphoranes.[5]

The first hexacoordinated phosphate ion was synthesized and isolated by Hellwinkel in 1965 (Figure 1a),[6a] which was assembled from 2,2-biphenylenes and had a unique yet gen-eral structural feature of an octahedral geometry consisting of three 3-center 4-electron (3c-4e) bonds (hyperbonding) between a central phosphorus atom and the ligands. Importantly, this phosphate ion had helical chirality and the helicity was found to be robust enough for separation of the enantiomers.[6b] Although this notion inspired the synthesis of chiral phosphate ions, the practical difficulties associated with this endeavor have hampered the understanding and utilization of chiral hexacoordinated phosphates in a broader context. Under such circumstances, Lacour introduced readily accessible chiral phosphate ions, such as TRISPHAT (Figure 1b), and uncovered their utility as an NMR shift reagent and a stoichiometric stereo-regulator of a pairing organic cation.[7]

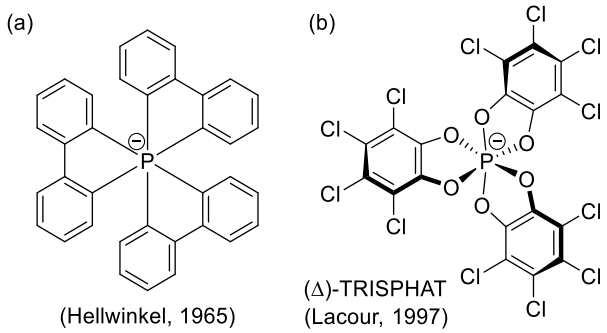


**Figure 1.** Representative Structures of Hexacoordinated Phosphate ions.

However, the available structural variation of chiral hexacoordinated phosphate ions is still very limited; hence, possible functions arising from their individual structures are yet to be fully explored. In particular, their inherent potential as a molecular catalyst remains entirely unknown, despite the obvious advantage of a weakly coordinating chiral anion in controlling a reactive cationic intermediate.[8] This situation primarily stems from the lack of a viable concept that could inform the design of suitable molecular scaffolds. Here, the author discloses the approach to address this problem; namely, the synthesis and structural elucidation of a novel designer chiral hexacoordinated phosphate ion (next section, **1** in Figure 2b) and demonstration of its capability to exert efficient asymmetric catalysis in achieving a highly enantioselective Pictet–Spengler-type reaction.

## A.2. Result and Discussion

The strategy for the molecular design was to employ the *P*-spiro cyclic $PN_4$ core motif as a structural platform, in conjunction with continuous interest of the author in the catalysis of chiral aminophosphonium salts,[9-11] and to introduce an *ortho*-hydroxyaromatic unit into two of four nitrogen atoms (Figure 2a). In view of the extremely high oxophilicity of the phosphorus atom, the author envisaged that facile intramolecular P—O bond formation would afford a hexacoordinated phosphate ion consisting of two *N*,*N*,*O*-tridentate chiral backbones, which feature unsymmetrical charge distribution in the delocalized anion, possibly endowing the anionic sphere with directivity when pairing with a counterion. In addition, the author planned to install an electron-withdrawing group as the remaining nitrogen substituent with the expectation that this would stabilize the hypercoordinated P(V) architecture by enhancing delocalization of the negative charge.

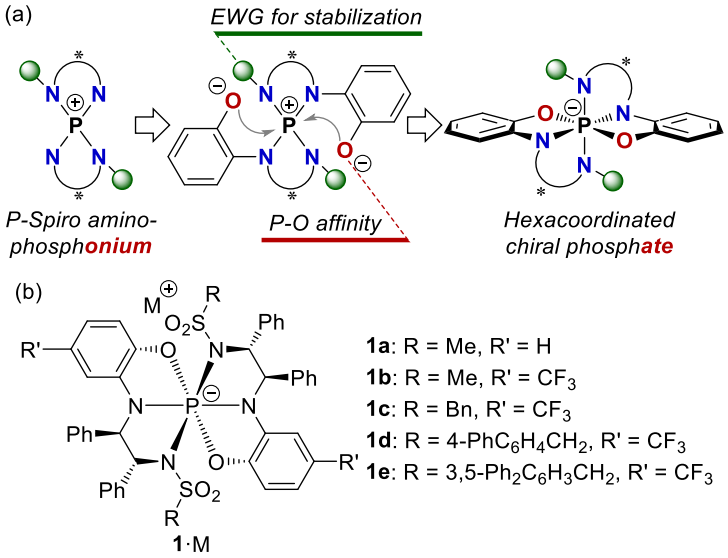


**Figure 2.** (a) Molecular Design of a Novel Hexacoordinated Chiral Phosphate Ion. (b) Structure of Chiral Phosphate Salts **1**·M.

Concrete structure of the novel phosphate salt **1** is shown in Figure 2b. For the assembly of this molecular framework, (*R*,*R*)-1,2-diphenylethylenediamine (DPEN) was selected as a commercially available chiral source. After introduction of methoxymethyl (MOM)-protected *ortho*-hydroxyphenyl group to one of the nitrogen atoms of DPEN by palladium-catalyzed amination,[12] the tetracoordinated *P*-spiro aminophosphonium core was built as a chloride salt **2a**·Cl (*M*,*R*,*R*-form),[13] from which the synthesis of **1a** was implemented, as illustrated in Scheme 1. Initially, an electron-withdrawing methanesulfonyl functionality (Ms) was attached to the free nitrogen atoms of **2** by treatment with MsCl and NaH in MeCN. The resulting **3a** was then

subjected to $BCl_3$ to unmask the internal oxygen nucleophile and generation of the corresponding aminophosphonium salt **4a**·Cl was confirmed by NMR and HRMS analyses. After removal of all the volatiles under reduced pressure, MeOH and an excess amount of triethylamine were added to the crude mixture of **4a**·Cl to actuate hypercoordination on the phosphorous center. The triethylammonium salt of **1a** was isolated by standard silica-gel column chromatography.

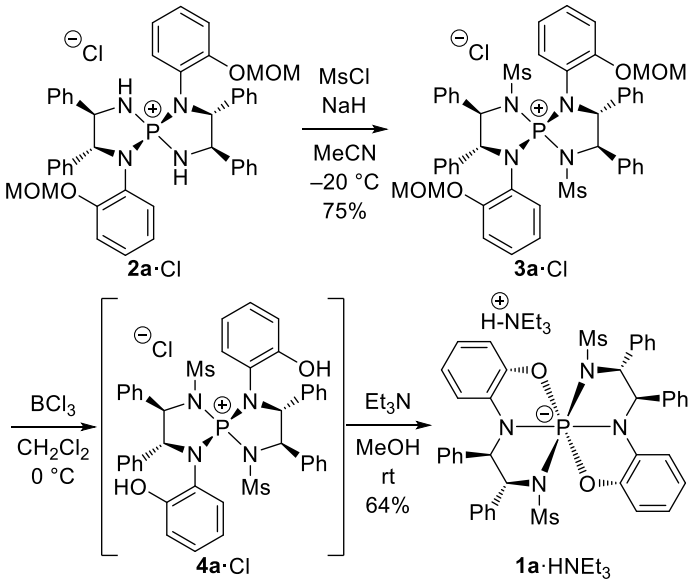


**Scheme 1.** Synthesis of **1a**·$HNEt_3$

The three-dimensional structure of **1a**·$HNEt_3$ was unambiguously determined by single-crystal X-ray diffraction analysis, unveiling the unique structural properties (Figure 3a and 3b). The *N*,*N*,*O*-tridentate backbones construct planes that almost perpendicularly intersect at the central phosphorous atom, forming the (*OC*-6-22'-*A*)-isomer [Δ-(*R*,*R*)-isomer]. The $PN_4O_2$ core adopts slightly distorted octahedral geometry. The P—N bonds of **1a** (1.75~1.82 Å) are 8~11% longer than the average P—N bond length (1.63 Å, Figure S1) of its precursor, the tetraaminophosphonium ion **2**. Bond elongation is also observed by comparison with the P—N bonds of pentacoordinated phosphoranes.[14] Although there are a limited number of phosphoranes having unbiased trigonal-bipyramidal geometry with nitrogen-containing ligands, the bond length between the phosphorus center and the apical nitrogen atom involved in the hyperbonding of such phosphoranes is around 1.69 Å, which is much shorter than the P-N bonds of **1a**. Similarly, the P—O bonds of **1a** (1.76 Å) are 5% longer than those of phosphoranes possessing apical oxygen atoms of aryloxide ligands.[14] It is of interest that the P—O bond length of **1a** is even longer than that of the reported hexacoordinated phosphates, such as TRISPHAT and tris(*o*-phenylenedioxy)phosphate ion (average of 1.71 Å).[7a,15] These observations support that **1a** consists of three 3c-4e bonds, which are known to be longer and weaker than conventional covalent (2c-2e) bonds. An additional important feature

of **1**·$HNEt_3$ is that the two Ms groups are situated on the same side and the N—H proton of the triethylammonium ion interacts with both the sulfonyl oxygens through the formation of weak hydrogen bonds ($Et_3NH\cdots O{=}S$ = 2.2~2.5 Å), placing the cation at a defined position toward the chiral anion. The assistance of these hydrogen-bonding interactions would be beneficial for eliciting the ability of the phosphate ion **1** to transmit its chiral information to the stereochemistry of a bond-forming event on the pairing cation, while maintaining its weakly coordinating character.

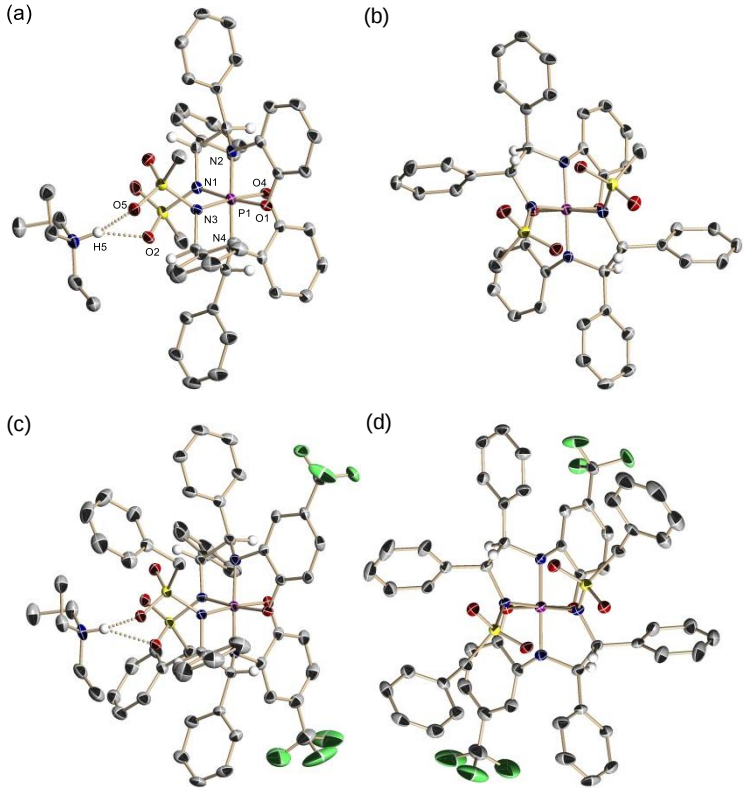


**Figure 3.** ORTEP Diagrams of Triethylammonium Phosphates **1**·$HNEt_3$; (a) side view of **1a**·$HNEt_3$, (b) front view of **1a**, (c) side view of **1c**·$HNEt_3$, (d) front view of **1c** (Ellipsoids displayed at 50% probability. Solvent molecule (a, b), $Et_3NH^+$ (b, d), and calculated hydrogen atoms except for those attached to stereogenic carbons are omitted for clarity. Black: carbon, Red: oxygen, Purple: phosphorus, Blue: nitrogen, Yellow: sulfur, Green: fluorine). Selected bond lengths (Å) and angles (°) for **1a**·$HNEt_3$: P1—O1 1.756(2), P1—O4 1.764(2), P1—N1 1.814(3), P1—N2 1.754(3), P1—N3 1.815(3), P1—N4 1.764(3), O5—H5 2.53(4), O2—H5 2.17(4), N1—P1—N3 95.67(12), O1—P1—O4 88.37(11), N2—P1—N4 178.00(13).

To examine this hypothesis, the author sought to evaluate the potential of the novel hexacoordinated phosphate ion **1** as a molecular catalyst. The two elements crucial for this pursuit were the preparation of a catalytically active phosphate salt and the setting of a suitable reaction platform. Among the possible catalysis manifolds, the author decided to focus on Brønsted acid catalysis with hydrogen phosphate **1**·H, which was prepared as a urea complex through

cation-exchange processes from **1**·HNEt$_3$ (see SI), taking into consideration that the hydrogen salts of weakly coordinating anions are commonly stabilized with the aid of Lewis basic molecules.[16,17]

As an acid-catalyzed bond-forming reaction of synthetic value, the author chose the Pictet–Spengler-type reaction[18] of 2-(1-pyrrolyl)anilines and carbonyl compounds to directly assemble chiral dihydropyrrolo[1,2-*a*]quinoxaline frameworks. Although dihydropyrrolo[1,2-*a*]quinoxalines and their derivatives exhibit various intriguing biological and physiological activities,[19] catalytic methods for the asymmetric synthesis of this class of *N*-heterocycles are underdeveloped, and only two systems are known to be effective for this type of coupling reactions.[20] An initial trial was performed by treatment of 5-methyl-2-(1-pyrrolyl)aniline (**5a**) with 3-phenylpropionaldehyde (**6a**) in the presence of **1a**·H·(urea)$_2$ (2 mol%) in dichloromethane at –90 °C. The reaction reached completion within 10 h to produce the desired product **7aa** in 84% yield and its enantiomeric excess was determined to be 24% (Table 1, entry 1). It is worthy of note that installation of the electron-withdrawing trifluoromethyl group at the 4-position of the aminophenol subunit (**1b**·H·(urea)$_2$) slightly improved stereoselectivity (entry 2). These promising results corroborate the validity of the molecular design concept for imparting catalytic activity and stereocontrolling ability to the chiral phosphate salts.

**Table 1.** Optimization of Catalyst Structure[a]

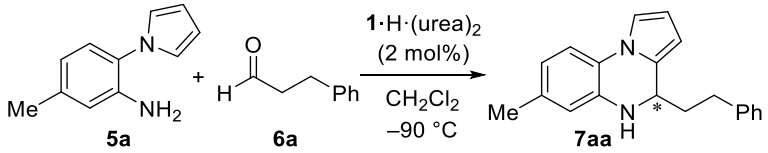


| entry | **1**·H·(urea)$_2$ | time (h) | yield (%)[b] | ee (%)[c] |
|---|---|---|---|---|
| 1 | **1a**·H·(urea)$_2$ | 10 | 84 | –24 |
| 2 | **1b**·H·(urea)$_2$ | 9 | 98 | –38 |
| 3 | **1c**·H·(urea)$_2$ | 14 | 89 | 85 |
| 4 | **1d**·H·(urea)$_2$ | 24 | 97 | 91 |
| 5 | **1e**·H·(urea)$_2$ | 33 | 98 | 96 |

[a] The reactions were performed with 0.1 mmol of **5a** and 0.2 mmol of **6a** with 2 mol% of **1**·H·(urea)$_2$ in 1.0 mL of $CH_2Cl_2$ at –90 °C. [b] Isolated yields are indicated. [c] Enantiomeric excess was determined by chiral stationary phase HPLC (Daicel CHIRALPAK AS-3, hexane/2-propanol = 10:1 as eluent).

At this stage of catalyst optimization for selectivity improvement, the author considered relevant information obtained in the structural analysis of **1**·HNEt$_3$; this led us to expect that the structure of the sulfonyl substituents would have a notable influence on the stereochemical outcome. Thus, the author prepared **1c**·H·(urea)$_2$ bearing phenylmethanesulfonyl groups in a manner similar to that of **1a**·H·(urea)$_2$. Subsequent crystallographic analysis revealed that the two pendant phenyl groups

filled the vacant space and extended the aromatic surface over the triethylammonium cation, creating a significantly different chiral environment (see Figure 3c and 3d). Indeed, the use of **1c**·H·(urea)$_2$ as a catalyst under otherwise identical conditions dramatically altered the selectivity profile, leading to formation of the opposite enantiomer of **7aa** with 85% ee (entry 3). This key finding prompted the author to pursue modification of the benzylic moiety of the sulfonyl substituent. The extension of the aromatic linkage at the *para*-position was beneficial for further enhancement of enantioselectivity (entry 4); eventually, 3,5-diphenylphenylmethanesulfonyl-substituted **1e**·H·(urea)$_2$ was identified as an optimal stereocontroller (entry 5).

Other selected examples in Table 2 demonstrate the effectiveness of the present catalysis of the chiral hydrogen phosphate for the combinations of different aliphatic aldehydes and 2-(1-pyrrolyl)anilines. In general, 2 mol% of **1e**·H·(urea)$_2$ was sufficient for a smooth transformation, and the corresponding dihydropyrrolo[1,2-*a*]quinoxaline derivatives were isolated in high yield with excellent levels of enantioselectivity. Specifically, not only the linear aldehyde **6b**, but also the β-branched aldehyde **6c** were well accommodated (entries 1 and 2). Aldehydes incorporating functional groups such as olefin, ether, or halogen atom also appeared to be good coupling partners (entries 3-6). In addition, variation in the substituents on the aniline component was possible without detrimental effect on the reactivity and selectivity (entries 7 and 8). The absolute configuration of the product **7** was assigned as *S* by X-ray diffraction analysis of a *N*-trifluoroacetylated derivative of **7ca** (**8ca**, Fig. S5).

**Table 2.** Substrate Scope[a]

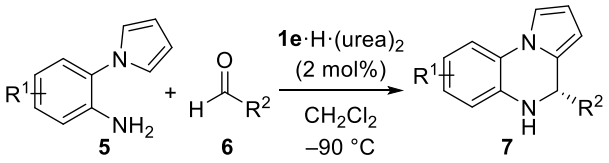


| entry | $R^1$ (**5**) | $R^2$ (**6**) | time (h) | yield (%)[b] | ee (%)[c] | prod. (**7**) |
|---|---|---|---|---|---|---|
| 1 | 5-Me (**5a**) | $Me(CH_2)_4$ (**6b**) | 20 | 96 | 93 | **7ab** |
| 2 | **5a** | $Me_2CHCH_2$ (**6c**) | 11 | 99 | 94 | **7ac** |
| 3 | **5a** | $CH_2=CH(CH_2)_3$ (**6d**) | 23 | 99 | 90 | **7ad** |
| 4 | **5a** | $MeO(CH_2)_3$ (**6e**) | 24 | 97 | 88 | **7ae** |
| 5 | **5a** | $Cl(CH_2)_4$ (**6f**) | 18 | 88 | 87 | **7af** |
| 6 | **5a** | 4-$BrC_6H_4(CH_2)_2$ (**6g**) | 22 | 89 | 95 | **7ag** |
| 7 | 5-MeO (**5b**) | **6a** | 15 | 87 | 94 | **7ba** |
| 8 | 5-Cl (**5c**) | **6a** | 24 | 96 | 96 | **7ca** |

[a] The reactions were performed with 0.1 mmol of **5** and 0.2 mmol of **6** with 2 mol% of **1e**·H·(urea)$_2$ in 1.0 mL of $CH_2Cl_2$ at –90 °C. [b] Isolated yields are indicated. [c] Enantiomeric excess was determined by chiral stationary phase HPLC.

## A.3. Conclusion

In conclusion, the author has introduced a chiral hexacoordinated phosphate ion and uncovered its distinctive structural features that originate from the octahedral P(V) core consisting of two *N*,*N*,*O*-tridentate chiral backbones. Furthermore, the author has clearly demonstrated the ability of the corresponding chiral hydrogen phosphates to act as an effective catalyst for a highly enantioselective Pictet–Spengler-type reaction. Appropriate structural modifications of the chiral phosphate salts should further improve the reactivity and selectivity, emphasizing the unequivocal advantage of the approach for the development of stereoselective chemical transformations that rely on the catalytic control of prochiral cationic intermediates. The author anticipates that this study opens a door to a new avenue for exploring the potential of the asymmetric catalysis of chiral hexacoordinated phosphate ions based on the design of pertinent molecular scaffolds.

## A.4. Experimental Section

**General Information:** Infrared spectra were recorded on a Shimadzu IRAffinity-1 spectrometer. $^{1}$H NMR spectra were recorded on a JEOL JNM-ECS600 (600 MHz) spectrometer, JEOL JNM-ECS500 (500 MHz) spectrometer, and JEOL JNM-ECS400 (400 MHz) spectrometer. Chemical shifts are reported in ppm from the solvent resonance ($CD_3OD$; 3.31 ppm, and DMSO-$d_6$; 2.50 ppm) or tetramethylsilane (0.0 ppm) resonance ($CDCl_3$) as the internal standard. Data are reported as follows: chemical shift, integration, multiplicity (s = singlet, d = doublet, t = triplet, q = quartet, m = multiplet, br = broad) and coupling constants (Hz). $^{13}$C NMR spectra were recorded on a JEOL JNM-ECS600 (151 MHz) spectrometer, JEOL JNM-ECS500 (121 MHz) spectrometer, and JNM-ECS400 (101 MHz) spectrometer with complete proton decoupling. Chemical shifts are reported in ppm from the solvent resonance as the internal standard ($CD_3OD$; 49.0 ppm, $CDCl_3$; 77.16 ppm, and DMSO-$d_6$; 39.52 ppm). $^{31}$P NMR spectra were recorded on a JEOL JNM-ECS500 (202 MHz) spectrometer and JEOL JNM-ECS400 (162 MHz) spectrometer with complete proton decoupling. Chemical shifts are reported in ppm from $H_3PO_4$ resonance (0.0 ppm) as the external standard. $^{19}$F NMR spectra were recorded on a JEOL JNM-ECS500 (471 MHz) spectrometer and JEOL JNM-ECS400 (376 MHz) spectrometer with complete proton decoupling. Chemical shifts are reported in ppm from $CF_3C_6H_5$ resonance (–64.0 ppm) as the external standard. Optical rotations were measured on a HORIBA SEPA-500 polarimeter. High resolution mass spectra were conducted on Thermo Fisher Scientific Exactive (FT-ESI and APCI). Analytical thin layer chromatography (TLC) was performed on Merck precoated TLC plates (silica gel 60 GF254, 0.5 mm). Flash column chromatography was performed on silica gel 60 (spherical, 40−50 μm; Kanto Chemical Co., Inc.), PSQ 60B (spherical, av. 55 μm; Fuji Silysia Chemical ltd.), and CHROMATOREX NH-DM-2035 (spherical, av. 60 μm; Fuji Silysia Chemical ltd.). Enantiomeric excesses were determined by HPLC analysis using chiral columns [□□4.6 mm x 250 mm, DAICEL CHIRALCEL OD-3 (OD3), CHIRALCEL OJ-3 (OJ3), CHIRALCEL OZ-3 (OZ3), and CHIRALPAK AS-3 (AS3)] with hexane (H), 2-propanol (IPA), and ethanol (EtOH) as eluent.

Toluene, dichloromethane ($CH_2Cl_2$), and acetonitrile (MeCN) were supplied from Kanto Chemical Co., Inc. as "Dehydrated" and further purified by passing through neutral alumina under nitrogen atmosphere. Other simple chemicals were purchased and used as such.

**Experimental Section:**

**Preparation and Characterization of Chiral Phosphate Salts**

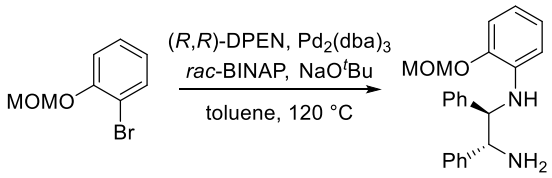


**Procedure for the Synthesis of (1*R*,2*R*)-*N*$^1$-(2-Methoxymethoxyphenyl)-1,2-diphenylethane-1,2-diamine:** To a solution of 1-bromo-2-(methoxymethoxy)benzene (2.17 g, 10.0 mmol) in toluene (33.3 mL) were added (1*R*,2*R*)-(+)-diphenylethylenediamine ((*R*,*R*)-DPEN) (2.55 g, 12.0 mmol), $Pd_2(dba)_3$ (0.183 g, 0.20 mmol), *rac*-BINAP (0.249 g, 0.40 mmol), and NaO$^t$Bu (1.92 g, 20.0 mmol) under argon (Ar) atmosphere. After degassing the whole reaction mixture, stirring was continued for 12 h at 120 °C. The mixture was cooled to ambient temperature and filtered through a pad of Celite overlaid with silica gel with the aid of ethyl acetate (EA). The filtrate was concentrated under vacuum to afford the crude residue. Purification of the residue was performed by column chromatography on silica gel (H/EA = 6:1-1:2 as eluent) and the obtained material was further purified by column chromatography on CHROMATOREX NH-DM-2035 (H/EA = 10:1-1:1 as eluent) to furnish (1*R*,2*R*)-*N*$^1$-(2-methoxymethoxyphenyl)-1,2-diphenylethane-1,2-diamine (2.76 g, 7.9 mmol, 79%) as a yellow solid. **(1*R*,2*R*)-*N*$^1$-(2-Methoxymethoxyphenyl)-1,2-diphenylethane-1,2-diamine:** $^1$H NMR (600 MHz, $CDCl_3$) $\delta$ 7.39 (2H, d, $J$ = 7.8 Hz), 7.33-7.26 (6H, m), 7.24-7.20 (2H, m), 6.93 (1H, dd, $J$ = 7.2, 1.2 Hz), 6.66 (1H, dt, $J$ = 7.2, 1.2 Hz), 6.50 (1H, dt, $J$ = 7.2, 1.2 Hz), 6.21 (1H, dd, $J$ = 7.2, 1.2 Hz), 5.63 (1H, d, $J$ = 3.9 Hz), 5.25 (1H, d, $J$ = 6.9 Hz), 5.18 (1H, d, $J$ = 6.9 Hz), 4.47 (1H, t, $J$ = 3.9 Hz), 4.36 (1H, d, $J$ = 3.9 Hz), 3.50 (3H, s), 1.50 (2H, brs); $^{13}$C NMR (151 MHz, $CDCl_3$) $\delta$ 144.6, 143.1, 141.7, 138.3, 128.7, 128.4, 127.5, 127.3, 127.1$_0$, 127.0$_6$, 122.7, 116.3, 114.1, 111.7, 95.3, 63.6, 61.5, 56.3; IR (film): 3313, 3248, 1602, 1506, 1452, 1219, 1152, 1076, 996, 922 cm$^{-1}$; HRMS (ESI) Calcd for $C_{22}H_{25}N_2O_2^+$ ([M+H]$^+$) 349.1911. Found 349.1907.; $[\alpha]_D^{27}$ +51.3 ($c$ = 10.0, $CHCl_3$).

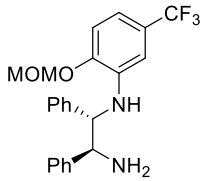


**(1*R*,2*R*)-*N*$^1$-(2-Methoxymethoxyphenyl-5-(trifluoromethyl))-1,2-diphenylethane-1,2-diamine:** $^1$H NMR (400 MHz, $CDCl_3$) $\delta$ 7.40 (2H, d, $J$ = 7.2 Hz), 7.33-7.19 (6H, m), 6.96 (1H, d, $J$ = 8.2 Hz), 6.75 (1H, d, $J$ = 8.2 Hz), 6.35 (1H, s), 5.86 (1H, d, $J$ = 4.6 Hz), 5.30 (1H, d, $J$ = 6.8 Hz), 5.24 (1H, d, $J$ = 6.8 Hz), 4.47 (1H, t, $J$ = 4.6 Hz), 4.39 (1H, d, $J$ = 4.6 Hz), 3.51 (3H, s), 1.50 (2H, s); $^{13}$C NMR (151 MHz, $CDCl_3$) $\delta$ 147.1, 143.3, 141.3, 138.7, 129.2, 128.9, 128.1, 128.0, 127.4, 127.3, 125.0 (q, $J_{C-F}$ = 271.8 Hz), 124.9 (q, $J_{C-F}$ = 31.8 Hz), 113.8, 113.2, 108.0, 95.3, 63.8, 61.7, 56.8; $^{19}$F NMR (376 MHz, $CDCl_3$) $\delta$ –61.8; IR (film): 3392, 3027, 2934, 1603, 1527, 1451, 1354, 1321, 1153, 1111, 1079, 985, 921 cm$^{-1}$; HRMS (ESI) Calcd for $C_{23}H_{24}N_2O_2F_3^+$ ([M+H]$^+$) 417.1784. Found 417.1788.; $[\alpha]_D^{29}$ +44.2 ($c$ = 10.0, $CHCl_3$).

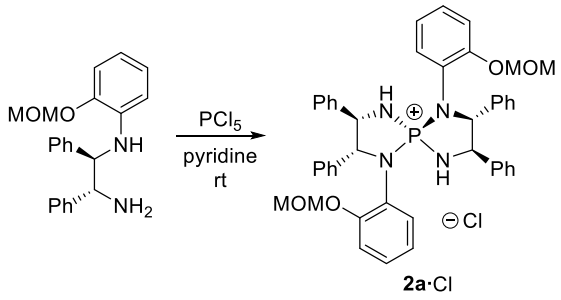


**Procedure for the Synthesis of Chiral Phosphonium Chloride 2a·Cl:** A solution of (1*R*,2*R*)-$N^1$-(2-methoxymethoxyphenyl)-1,2-diphenylethane-1,2-diamine (2.09 g, 6.0 mmol) in pyridine (60 mL) was added to solid $PCl_5$ (0.625 g, 3.0 mmol) at ambient temperature under Ar atmosphere. After being stirred for overnight, all volatiles were removed under reduced pressure. The residual solid was dissolved into $CH_2Cl_2$ and the resulting solution was washed with 1 *N* hydrochloric acid. The organic phase was dried over $Na_2SO_4$, filtered, and concentrated. Purification of the residue by column chromatography on silica gel was performed twice (EA/MeOH = 1:0-10:1 as eluent and $CH_2Cl_2$/MeOH = 1:0-20:1 as eluent) to obtain analytically pure **2a**·Cl (1.56 g, 2.05 mmol, 68%) as a white solid. **2a**·Cl**:** $^1$H NMR (600 MHz, $CDCl_3$) $\delta$ 7.92 (2H, br), 7.27 (6H, br), 7.22-7.02 (16H, m), 6.95 (4H, br), 5.12 (2H, d, $J$ = 7.8 Hz), 4.82 (4H, br), 4.48 (2H, br), 3.18 (6H, brs), NH protons were not found due to broadening.; $^{13}$C NMR (151 MHz, $CDCl_3$) $\delta$ 154.8, 139.1, 136.2, 132.8, 129.0, 128.8, 128.5, $128.4_2$, $128.3_8$, 128.1, 127.3, 124.3, 121.7, 114.5, 95.1, 70.9, 63.6 (d, $J_{C-P}$ = 5.9 Hz), 56.6; $^{31}$P NMR (202 MHz, $CDCl_3$) $\delta$ 38.3; IR (film): 3387, 3076, 3036, 1598, 1501, 1296, 1276, 1243, 1234, 1198, 1154, 1124, 1078, 988, 918 cm$^{-1}$; HRMS (ESI) Calcd for $C_{44}H_{44}N_4O_4P^+$ ([M−Cl]$^+$) 723.3095. Found 723.3081.; $[\alpha]_D^{25}$ +70.8 ($c$ = 11.6, $CHCl_3$).

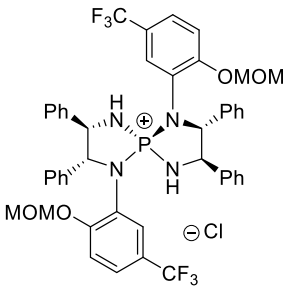


**2b·Cl:** $^1$H NMR (600 MHz, $CDCl_3$) $\delta$ 8.62 (2H, br), 8.40 (2H, br), 7.34 (2H, br), 7.27 (2H, br), 6.99-6.85 (6H, m), 5.13 (2H, br), 4.76 (4H, br), 4.35 (2H, br), 3.11 (6H, br); $^{13}$C NMR (151 MHz, $CDCl_3$) $\delta$ 157.0, 138.1, 135.3, 129.6, 129.3, 128.8, $128.5_4$, $128.4_6$, 128.1, 126.8, 125.8, 125.2, 124.3 (q, $J_{C-F}$ = 31.9 Hz), 123.9 (q, $J_{C-F}$ = 272.3 Hz), 114.5, 95.2, 71.2, 63.7, 56.9; $^{31}$P NMR (202 MHz, $CDCl_3$) $\delta$ 40.5; $^{19}$F NMR (471 MHz, $CDCl_3$) $\delta$ −61.3; IR (film): 3037, 3003, 1428, 1333, 1245, 1201, 1161, 1140, 1116, 1089, 1073, 1002, 963 cm$^{-1}$; HRMS (ESI) Calcd for $C_{46}H_{42}N_4O_4F_6P^+$ ([M−Cl]$^+$) 859.2842. Found 859.2832.; $[\alpha]_D^{26}$ +87.6 ($c$ = 11.2, $CHCl_3$).

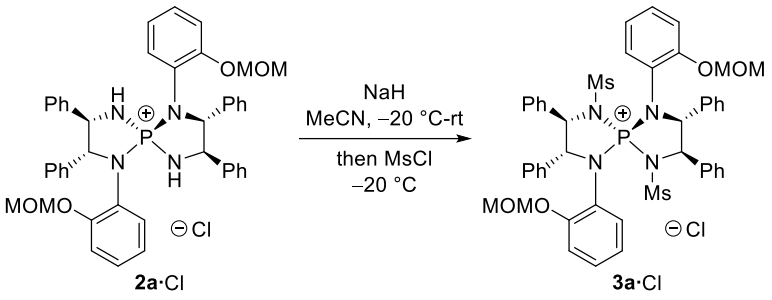


**Procedure for Sulfonylation of Chiral Phosphonium Chloride 2a·Cl to Prepare 3a·Cl:** A solution of **2a**·Cl (75.9 mg, 0.10 mmol) in MeCN (1.0 mL) was added to sodium hydride (60%, dispersion in oil) (20.0 mg, 0.5 mmol) at –20 °C under Ar atmosphere. The mixture was allowed to warm to room temperature and stirred for 12 h. After being cooled to –20 °C, a solution of methanesulfonyl chloride (MsCl) (54.2 μL, 0.70 mmol) in MeCN (1.0 mL) was added to the mixture and stirring was continued for 12 h. The resulting mixture was then quenched by the addition of $H_2O$. The aqueous phase was extracted with EA twice and the organic phases were washed with brine. The combined organic phases were dried over $Na_2SO_4$, filtered, and concentrated. Purification of the residue was performed by column chromatography on silica gel ($CH_2Cl_2$/MeOH = 1:0-6:1 as eluent) to afford **3a**·Cl (68.4 mg, 0.075 mmol, 75%) as a white solid. **3a**·Cl**:** $^1$H NMR (500 MHz, $CD_3OD$) $\delta$ 7.83 (2H, d, $J$ = 7.5 Hz), 7.66 (4H, br), 7.52 (2H, t, $J$ = 7.5 Hz), 7.41 (2H, t, $J$ = 7.5 Hz), 7.25 (2H, t, $J$ = 7.5 Hz), 7.21-7.07 (16H, m), 5.65 (2H, d, $J$ = 10.0 Hz), 5.35 (2H, d, $J$ = 10.0 Hz), 5.03 (2H, dd, $J_{H–P}$ = 7.0 Hz, $J_{H–H}$ = 1.5 Hz), 4.54 (2H, dd, $J_{H–P}$ = 7.0 Hz, $J_{H–H}$ = 1.5 Hz), 3.33 (6H, s), 3.20 (6H, s); $^{13}$C NMR (121 MHz, $CDCl_3$) $\delta$ 156.6 ($J_{C–P}$ = 4.7 Hz), 134.9 (d, $J_{C–P}$ = 6.9 Hz), 134.5 (d, $J_{C–P}$ = 6.9 Hz), 133.1, 132.8, 132.7, 131.5, 131.4, 130.8, 130.6, 123.8, 122.8 (d, $J_{C–P}$ = 3.3 Hz), 117.7, 97.4, 71.7 (d, $J_{C–P}$ = 8.1 Hz), 70.9 (d, $J_{C–P}$ = 12.7 Hz), 58.7, 43.9, one carbon atom was not found probably due to overlapping.; $^{31}$P NMR (202 MHz, $CDCl_3$) $\delta$ 20.8; IR (film): 3407, 2925, 1628, 1597, 1498, 1458, 1352, 1283, 1177, 1162, 1081, 1041, 989, 954 cm$^{-1}$; HRMS (ESI) Calcd for $C_{46}H_{48}N_4O_8S_2P^+$ ([M−Cl]$^+$) 879.2646. Found 879.2626.; $[\alpha]_D^{29}$ +61.3 ($c$ = 23.9, $CHCl_3$).

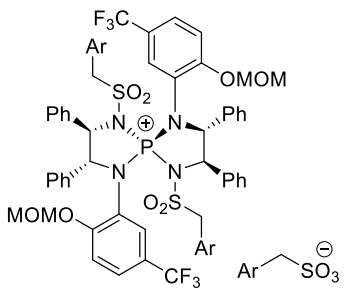


**3e·$SO_3CH_2$(3,5-$Ph_2C_6H_3$) (Ar = 3,5-$Ph_2C_6H_3$):** $^1$H NMR (500 MHz, $CD_3OD$) $\delta$ 8.15 (2H, s), 7.76 (2H, d, $J$ = 8.5 Hz), 7.73 (2H, s), 7.61 (2H, s), 7.59 (1H, s), 7.60-7.52 (8H, m), 7.44 (8H, d, $J$ = 7.5 Hz), 7.38 (4H, s), 7.32-7.20 (26H, m), 7.14-7.12 (2H, m), 7.08 (4H, t, $J$ = 7.5 Hz), 6.99 (4H, t, $J$ = 7.5 Hz), 5.68 (2H, d, $J$ = 10.0 Hz), 5.57 (2H, d, $J$ = 10.0 Hz), 5.08 (2H, d, $J$ = 6.0 Hz), 4.79 (2H, d, $J$ = 13.5 Hz), 4.75 (2H, d, $J$ = 6.0 Hz), 4.38 (2H, d, $J$ = 13.5 Hz), 4.14 (2H, s), 3.22 (6H, s); $^{13}$C NMR (151 MHz, $CD_3OD$) $\delta$ 159.1, 145.0, 143.6, 143.0, 141.7, 136.6, 133.9 (d, $J_{C–P}$ = 8.1 Hz), 133.8 (d, $J_{C–P}$ = 8.1 Hz), 133.4, 132.1, 131.7, 131.0, 130.8, 130.7, 130.2,

130.0, 129.4, 129.3, 129.2, 129.0, 127.5, 126.4, 126.0 (q, $J_{C-F}$ = 261.4 Hz), 125.7 (q, $J_{C-F}$ = 32.5 Hz), 123.1 (d, $J_{C-P}$ = 4.6 Hz), 118.6, 98.4, 71.7 (d, $J_{C-P}$ = 6.9 Hz), 71.1 (d, $J_{C-P}$ = 11.6 Hz), 64.1, 59.3, seven carbon atoms were not found probably due to overlapping.; $^{31}$P NMR (162 MHz, $CD_3OD$) $\delta$ 21.5; $^{19}$F NMR (376 MHz, $CD_3OD$) $\delta$ −62.3; IR (film): 3425, 1597, 1434, 1370, 1332, 1223, 1173, 1143, 1079, 1075, 1034, 960, 927 cm$^{-1}$; HRMS (ESI) Calcd for $C_{84}H_{70}N_4O_8F_6S_2P^+$ ($[M-C_{19}H_{15}O_3S]^+$) 1471.4271. Found 1471.4255.; $[\alpha]_D^{25}$ +28.3 (*c* = 4.6, $CHCl_3$).

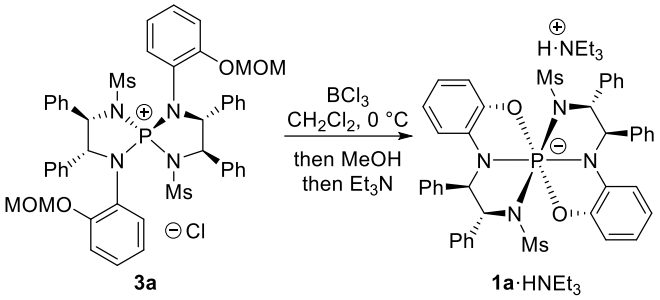


**Procedure for the Synthesis of Hexacoordinated Chiral Triethylammonium Phosphate 1a·HNEt$_3$:** To a solution of **3a**·Cl (68.4 mg, 0.075 mmol) in $CH_2Cl_2$ (1.49 mL) was added a 1.0 M solution of $BCl_3$ in $CH_2Cl_2$ (1.49 mL) at 0 °C. After being stirred for 15 min, MeOH was added dropwise to the mixture until the completion of bubbling, and then the volatiles were removed under vacuum. The residual white solid was dissolved into $Et_3N$ and MeOH, and the resulting solution was concentrated. Purification of the residue by column chromatography on silica gel (EA/MeOH = 1:0-10:1 containing 5 v/v% of $Et_3N$ as eluent, silica gel was washed with 1 *N* hydrochloric acid and MeOH prior to use) gave **1a**·HNEt$_3$ (42.9 mg, 0.048 mmol, 64%) as a white solid. **1a·HNEt$_3$:** $^1$H NMR (600 MHz, $CDCl_3$) $\delta$ 8.40 (2H, brs), 7.78 (1H, brs), 7.40 (2H, brs), 7.28 (2H, t, *J* = 7.5 Hz), 7.22-7.08 (12H, m), 6.78 (2H, d, *J* = 7.8 Hz), 6.69 (2H, brs), 6.65 (2H, t, *J* = 7.8 Hz), 6.31 (2H, t, *J* = 7.8 Hz), 5.77 (2H, d, *J* = 7.8 Hz), 5.11 (2H, dd, $J_{H-H}$ = 9.0 Hz, $J_{H-P}$ = 3.0 Hz), 4.88 (2H, d, *J* = 9.0 Hz), 3.26 (6H, q, *J* = 7.2 Hz), 2.50 (6H, s), 1.32 (9H, t, *J* = 7.2 Hz); $^{13}$C NMR (151 MHz, $CDCl_3$) $\delta$ 147.6, 143.9 (d, $J_{C-P}$ = 17.3 Hz), 142.3, 138.3 (d, $J_{C-P}$ = 15.9 Hz), 130.6, 128.7, 128.5, 127.6, 127.3, 127.0, 120.1, 118.0, 112.8 (d, $J_{C-P}$ = 18.7 Hz), 110.1 (d, $J_{C-P}$ = 11.6 Hz), 69.4 (d, $J_{C-P}$ = 2.9 Hz), 68.3 (d, $J_{C-P}$ = 8.6 Hz), 46.4, 44.4, 8.5; $^{31}$P NMR (202 MHz, $CDCl_3$) $\delta$ −107.8; IR (film): 3060, 3028, 2886, 1587, 1487, 1355, 1302, 1254, 1140, 1028, 972 cm$^{-1}$; HRMS (ESI) Calcd for $C_{42}H_{38}N_4O_6S_2P^-$ ($[M-HNEt_3]^-$) 789.1965. Found 789.1974.; $[\alpha]_D^{26}$ −97.6 (*c* = 10.4, $CHCl_3$).

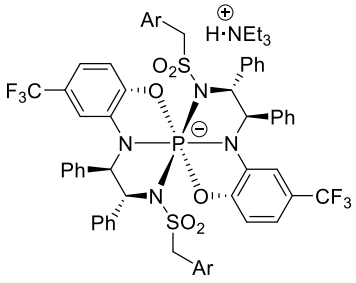

**1e·HNEt$_3$ (Ar = 3,5-Ph$_2$C$_6$H$_3$):** $^1$H NMR (400 MHz $CDCl_3$) $\delta$ 8.57 (2H, brs), 7.67 (2H, s), 7.53-7.48 (10H, m), 7.46-7.40 (10H, m), 7.39-7.33 (6H, m), 7.23 (4H, t, $J$ = 7.4 Hz), 7.10 (4H, d, $J$ = 1.2 Hz), 7.01 (4H, d, $J$ = 8.2 Hz), 6.92 (4H, d, $J$ = 8.2 Hz), 6.03 (2H, s), 5.28 (2H, dd, $J_{H-H}$ = 9.8 Hz, $J_{H-P}$ = 3.6 Hz), 5.09 (2H, d, $J$ = 9.8 Hz), 4.15 (2H, d, $J$ = 13.8 Hz), 3.24 (2H, d, $J$ = 13.8 Hz), 2.86-2.69 (6H, br), 0.86 (9H, t, $J$ = 7.0 Hz); $^{13}$C NMR (121 MHz, $CDCl_3$) $\delta$ 150.2, 142.6 (d, $J_{C-P}$ = 15.1 Hz), 141.5, 141.2, 140.6, 138.1 (d, $J_{C-P}$ = 16.3 Hz), 132.1, 130.8, 129.0, 128.5, 127.9, 127.7, 127.5, 127.2, 125.0, 125.0 ($J_{C-P}$ = 261.3 Hz), 120.3 ($J_{C-P}$ = 30.3 Hz), 118.1, 109.7, 109.5, 109.4, 69.1 ($J_{C-P}$ = 3.5 Hz), 68.2 ($J_{C-P}$ = 8.1 Hz), 62.3, 46.1, 8.0, two carbon atoms were not found probably due to overlapping.; $^{31}$P NMR (162 MHz, $CDCl_3$) $\delta$ −106.3; $^{19}$F NMR (376 MHz, $CDCl_3$) $\delta$ −61.1; IR (film): 3061, 3031, 1597, 1502, 1444, 1364, 1315, 1274, 1153, 1130, 1108, 1025, 969, 874, 814 cm$^{-1}$; HRMS (ESI) Calcd for $C_{80}H_{60}N_4O_6F_6S_2P^-$ ([M−H·NEt$_3$]$^-$) 1381.3591. Found 1381.3569.; $[\alpha]_D^{29}$ +42.5 ($c$ = 10.6, $CHCl_3$).

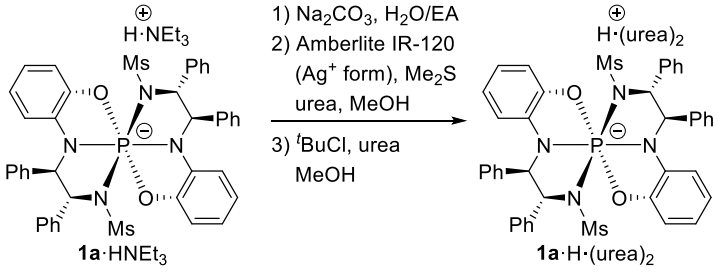


**Procedure for the Preparation of Hexacoordinated Chiral Hydrogen Phosphate 1a·H·(urea)$_2$:** A solution of **1a**·HNEt$_3$ (31.6 mg, 0.035 mmol) in EA was washed with an aqueous solution of $Na_2CO_3$ (0.1 M, 3 x 15 mL). After drying the combined organic phases over $Na_2SO_4$, all volatiles were removed under reduced pressure. A methanolic solution of the resulting solid was passed through a column of Amberlite IR120 resin ($Ag^+$ form) with MeOH/$Me_2S$ = 20:1 as eluent. To the eluate thus obtained was added a methanolic solution of urea (0.01 M, 3.5 mL). The whole solvent was evaporated and the resulting white solid was dissolved into MeOH containing urea (2.1 mg, 0.035 mmol). To the mixture was added 2-chloro-2-methylpropane (190.0 μL, 1.75 mmol) at 0 °C and the resulting suspension was stirred there for 10 min. The mixture was allowed to warm to room temperature and stirred for additional 20 min. The resulting mixture was concentrated at 0 °C and the residue was filtered through a syringe filter to remove precipitated AgCl by the aid of MeOH. The filtrate was concentrated under vacuum at 0 °C to afford **1a**·H·(urea)$_2$ (31.6 mg, 0.035 mmol) as a white solid, which was used as a catalyst for the asymmetric Pictet-Spengler reaction without further purification. **1a·H·(urea)$_2$:** $^1$H NMR (600 MHz, $CD_3OD$) $\delta$ 8.55 (2H, brs), 7.43 (2H, brs), 7.28 (2H, t, $J$ = 7.0 Hz), 7.17-7.05 (12H, m), 6.68 (2H, d, $J$ = 7.0 Hz), 6.61 (2H, d, $J$ = 6.5 Hz), 5.70

(2H, d, $J$ = 5.5 Hz), 5.23 (2H, d, $J$ = 8.5 Hz), 4.74 (2H, d, $J$ = 8.5 Hz), 2.40 (6H, s); $^{13}$C NMR (121 MHz, $CDCl_3$) $\delta$ 162.2, 147.5, 143.6 (d, $J_{C-P}$ = 16.2 Hz), 142.7, 138.3 (d, $J_{C-P}$ = 14.0 Hz), 130.1, 128.9, 128.6, 127.0, 126.9, 126.4, 119.4, 117.4, 112.5 (d, $J_{C-P}$ = 17.4 Hz), 109.0 (d, $J_{C-P}$ = 10.4 Hz), 69.9, 67.8 (d, $J_{C-P}$ = 8.1 Hz), 43.2; $^{31}$P NMR (202 MHz, $CDCl_3$) $\delta$ −108.3; IR (film): 3371, 2437, 1599, 1588, 1294, 1255, 1133, 1114, 1093, 975 cm$^{-1}$; HRMS (ESI) Calcd for $C_{42}H_{38}N_4O_6S_2P^-$ ([M−H·(urea)$_2$]$^-$) 789.1965. Found 789.1965.; $[\alpha]_D^{27}$ −46.1 ($c$ = 1.0, MeOH).

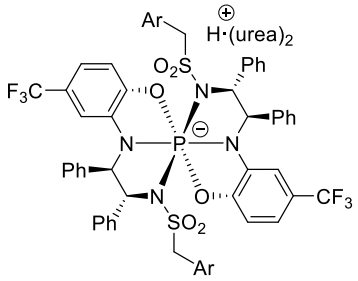


**1e·H·(urea)$_2$ (Ar = 3,5-Ph$_2$C$_6$H$_3$):** $^1$H NMR (400 MHz, $CD_3OD$) $\delta$ 8.71 (2H, brs), 8.27 (1H, s), 7.65 (2H, t, $J$ = 2.0 Hz), 7.51 (10H, d, $J$ = 7.2 Hz), 7.41 (10H, t, $J$ = 7.2 Hz), 7.34 (6H, t, $J$ = 7.2 Hz), 7.22 (4H, t, $J$ = 7.2 Hz), 7.08 (4H, t, $J$ = 7.2 Hz), 7.03 (4H, d, $J$ = 1.2 Hz), 6.99 (4H, d, $J$ = 7.2 Hz), 6.90 (4H, d, $J$ = 7.2 Hz), 6.77 (4H, br), 6.09 (2H, s), 5.40 (2H, dd, $J_{H-H}$ = 9.4 Hz, $J_{H-P}$ = 3.6 Hz), 5.04 (2H, d, $J$ = 9.4 Hz), 4.11 (2H, d, $J$ = 14.0 Hz), 3.26 (2H, d, $J$ = 14.0 Hz); $^{13}$C NMR (101 MHz, $CD_3OD$) $\delta$ 163.6, 151.9, 143.8 (d, $J_{C-P}$ = 16.4 Hz), 142.9, 142.8, 141.9, 139.9 (d, $J_{C-P}$ = 15.6 Hz), 134.1, 133.1, 131.6, 130.3, 129.8, 129.3, 128.8, 128.5, 128.4, 128.2, 126.4 (q, $J_{C-F}$ = 271.9 Hz), 125.9, 121.1 (q, $J_{C-F}$ = 31.9 Hz), 118.7, 110.4 (d, $J_{C-P}$ = 19.4 Hz), 110.1 (d, $J_{C-P}$ = 10.7 Hz), 71.0 (d, $J_{C-P}$ = 3.8 Hz), 69.2 (d, $J_{C-P}$ = 7.8 Hz), 63.3, one carbon atom was not found probably due to overlapping.; $^{31}$P NMR (162 MHz, $CDCl_3$) $\delta$ −106.3; $^{19}$F NMR (376 MHz, $CDCl_3$) $\delta$ −62.5; IR (film): 3369, 3211, 1663, 1598, 1502, 1444, 1321, 1275, 1153, 1111, 1025, 971 cm$^{-1}$; HRMS (ESI) Calcd for $C_{80}H_{60}N_4O_6F_6S_2P^-$ ([M−H·(urea)$_2$]$^-$) 1381.3591. Found 1381.3555.; $[\alpha]_D^{27}$ +60.2 ($c$ = 10.1, MeOH).

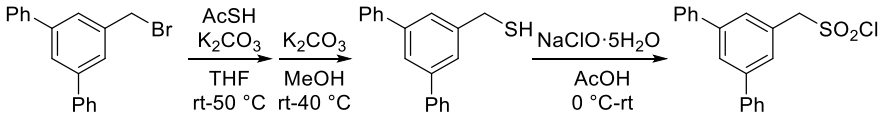


**Procedure for the Synthesis of 3,5-Diphenylphenylmethanethiol:** To a solution of 3,5-diphenylphenylmethyl bromide (0.163 g, 0.50 mmol) in THF (1.7 mL) were added thioacetic acid (44.1 μL, 0.63 mmol) and $K_2CO_3$ (0.153 g, 1.1 mmol) at ambient temperature under Ar atmosphere. After being stirred for 30 min, the mixture was warmed to 50 °C and stirred there for 10 h. The reaction was quenched by adding $H_2O$ and the aqueous phase was extracted with EA twice. The combined organic phases were washed with brine and dried over $Na_2SO_4$. Subsequent filtration followed by concentration of the filtrate gave crude 3,5-diphenylphenylmethyl thioacetate. The resulting thioacetate ester was treated with $K_2CO_3$ in MeOH (0.3 M) for 1 h at ambient temperature and for additional 5 h at 40 °C. After being cooled to 0 °C, the reaction mixture was acidified to pH 5~6 by the addition of 1 $N$ hydrochloric acid. The aqueous phase was extracted with $CHCl_3$ and the organic phase was dried over $Na_2SO_4$, filtrated, and concentrated. Purification

of the residue by column chromatography on silica gel (H/EA = 50:1-10:1) afforded 3,5-diphenylphenylmethanethiol (92.7 mg, 0.34 mmol, 67%) as a white solid. **3,5-Diphenylphenylmethanethiol:** $^1$H NMR (600 MHz, $CDCl_3$) $\delta$ 7.69 (1H, t, $J$ = 3.6 Hz), 7.65 (4H, d, $J$ = 7.8 Hz), 7.54 (2H, s), 7.46 (4H, t, $J$ = 7.8 Hz), 7.38 (2H, td, $J$ = 7.8, 1.2 Hz), 3.88 (2H, d, $J$ = 7.2 Hz), 1.86 (1H, t, $J$ = 7.2 Hz); $^{13}$C NMR (151 MHz, $CDCl_3$) $\delta$ 142.6, 142.5, 141.2, 129.2, 127.9, 127.6, 126.2, 125.3, 29.5; IR (film): 3058, 3052, 1596, 1577, 1498, 1456, 1435, 1410, 1246, 1076, 1029, 877 cm$^{-1}$; HRMS (ESI) Calcd for $C_{19}H_{15}S^-$ ([M−H]$^-$) 275.0889. Found 275.0901.

**Procedure for the Preparation of 3,5-Diphenylphenylmethanesulfonyl Chloride:** To a solution of 3,5-diphenylphenylmethanethiol (0.751 g, 2.7 mmol) in acetic acid (27.0 mL) was added a solid of $NaClO{\cdot}5H_2O$ (0.715 g, 4.4 mmol) at 0 °C and the resulting mixture was stirred for 5 min at ambient temperature. Then, an additional amount of $NaClO{\cdot}5H_2O$ (0.715 g, 4.35 mmol) was added and the whole reaction mixture was stirred for 1 h. The reaction was quenched by the addition of $H_2O$ (10 mL) and the aqueous phase was extracted with EA. The organic phase was washed with brine, dried over $Na_2SO_4$, and concentrated. Purification of the residue by column chromatography on silica gel (H/EA = 50:1-5:1) gave 3,5-diphenylphenylmethanesulfonyl chloride (76.9 mg, 2.24 mmol, 83 %) as a white solid. **3,5-Diphenylphenylmethanesulfonyl chloride:** $^1$H NMR (600 MHz, $CDCl_3$) $\delta$ 7.87 (1H, s), 7.63 (2H, s), 7.62 (4H, d, $J$ = 8.4 Hz), 7.46 (4H, t, $J$ = 8.4 Hz), 7.39 (2H, t, $J$ = 8.4 Hz), 4.94 (2H, s); $^{13}$C NMR (151 MHz, $CDCl_3$) $\delta$ 143.0, 140.0, 129.1, 129.0, 128.1$_4$, 128.0$_5$, 127.4, 127.3, 71.0; IR (film): 3059, 3035, 2983, 2918, 1597, 1578, 1499, 1458, 1436, 1368, 1250, 1164, 1077, 1029, 908, 884 cm$^{-1}$; HRMS (APCI) Calcd for $C_{19}H_{14}O_2ClS^-$ ([M−H]$^-$) 341.0398. Found 341.0407.

**Representative Procedure for the Asymmetric Pictet-Spengler Reaction of 2-(1-Pyrrolyl)anilines and Aldehydes:**

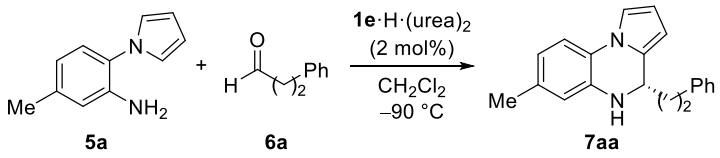


A solution of **5a** (17.2 mg, 0.10 mmol) and **6a** (26.3 μL, 0.20 mmol) in $CH_2Cl_2$ (1.0 mL) was stirred for 1 h at −90 °C under Ar atmosphere. To the solution was added **1e**·H·(urea)$_2$ (3.01 mg, 0.002 mmol) and stirring was continued for 33 h. The reaction mixture was directly charged on a silica gel column and eluted with H/EA = 20:1-10:1 to afford **7aa** (28.3 mg, 98%). **7aa:** $^1$H NMR (600 MHz, $CDCl_3$) $\delta$ 7.30 (2H, t, $J$ = 7.8 Hz), 7.21 (1H, d, $J$ = 7.8 Hz), 7.21 (2H, t, $J$ = 7.8 Hz), 7.16 (1H, d, $J$ = 7.8 Hz), 7.12 (1H, dd, $J$ = 3.0, 1.2 Hz), 6.60 (1H, d, $J$ = 7.8 Hz), 6.47 (1H, brs), 6.29 (1H, t, $J$ = 3.0 Hz), 6.01 (1H, d, $J$ = 3.0 Hz), 4.49 (1H, d, $J$ = 7.8, 6.0 Hz), 3.85 (1H, s), 2.81 (1H, t, $J$ =

7.8 Hz), 2.78 (1H, t, *J* = 7.8 Hz), 2.26 (3H, s), 2.19 (1H, dtd, *J* = 13.2, 7.8, 6.0 Hz), 2.09 (1H, dq, *J* = 13.2, 7.8 Hz); $^{13}$C NMR (151 MHz, $CDCl_3$) $\delta$ 141.6, 135.6, 134.5, 129.2, 128.7, 128.5, 126.2, 123.4, 119.9, 116.1, 114.6, 114.2, 109.8, 103.9, 51.0, 37.0, 32.1, 21.2; IR (film) 3369, 3025, 2917, 2851, 1618, 1602, 1529, 1489, 1343, 1295, 1179, 1093, 1030 cm$^{-1}$; HRMS (ESI) Calcd for $C_{20}H_{21}N_2^+$ ([M+H]$^+$) 289.1699. Found 289.1694.; $[\alpha]_D^{24}$ +11.6 (*c* = 14.0, $CHCl_3$) for 96% ee; HPLC AS3, H/IPA = 10:1, flow rate = 1.0 mL/min, λ = 254 nm, 6.6 min (major enantiomer), 7.4 min (minor enantiomer).

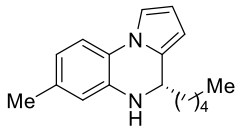

**7ab:** $^1$H NMR (600 MHz, $CDCl_3$) $\delta$ 7.15 (1H, d, *J* = 8.4 Hz), 7.10 (1H, dd, *J* = 3.0, 1.8 Hz), 6.60 (1H, d, *J* = 8.4 Hz), 6.55 (1H, brs), 6.27 (1H, t, *J* = 3.0 Hz), 5.96 (1H, d, *J* = 3.0 Hz), 4.39 (1H, dd, *J* = 7.2, 5.4 Hz), 3.91 (1H, brs), 2.26 (3H, s), 1.85 (1H, ddt, *J* = 13.8, 10.8, 5.4 Hz), 1.74 (1H, dddd, *J* = 13.8, 10.8, 7.2, 5.4 Hz), 1.52-1.37 (2H, m), 1.36-1.30 (4H, m), 0.90 (3H, t, *J* = 6.9 Hz); $^{13}$C NMR (151 MHz, $CDCl_3$) $\delta$ 135.9, 134.4, 129.8, 123.5, 119.8, 116.1, 114.6, 114.1, 109.7, 103.6, 51.2, 35.3, 31.9, 25.4, 22.7, 21.2, 14.2; IR (film): 3369, 2928, 2853, 1615, 1603, 1529, 1487, 1341, 1294, 1176, 1129, 1088 cm$^{-1}$; HRMS (ESI) Calcd for $C_{17}H_{23}N_2^+$ ([M+H]$^+$) 255.1856. Found 255.1848.; $[\alpha]_D^{28}$ +12.6 (*c* = 9.7, $CHCl_3$) for 93% ee; HPLC OD3, H/IPA = 10:1, flow rate = 1.0 mL/min, λ = 254 nm, 8.1 min (minor enantiomer), 13.8 min (major enantiomer).

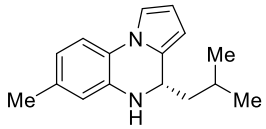

**7ac:** $^1$H NMR (600 MHz, $CDCl_3$) $\delta$ 7.16 (1H, d, *J* = 8.1 Hz), 7.10 (1H, dd, *J* = 3.0, 1.2 Hz), 6.61 (1H, d, *J* = 8.1 Hz), 6.56 (1H, brs), 6.27 (1H, t, *J* = 3.0 Hz), 5.96 (1H, d, *J* = 3.0 Hz), 4.46 (1H, dd, *J* = 8.1, 6.6 Hz), 3.90 (1H, brs), 2.26 (3H, s), 1.78 (1H, d-octet, *J* = 8.1, 6.6 Hz), 1.70 (1H, ddd, *J* = 12.9, 8.1, 6.6 Hz), 1.65 (1H, ddd, *J* = 12.9, 8.1, 6.6 Hz), 1.00 (3H, d, *J* = 6.0 Hz), 0.95 (3H, d, *J* = 6.6 Hz); $^{13}$C NMR (151 MHz, $CDCl_3$) $\delta$ 135.8, 134.4, 130.0, 123.7, 119.9, 116.2, 114.6, 114.2, 109.7, 103.5, 49.1, 44.3, 24.7, 23.5, 22.1, 21.2; IR (film): 3357, 2956, 2916, 2868, 1620, 1604, 1530, 1487, 1468, 1427, 1340, 1295, 1175, 1134, 1121, 1088 cm$^{-1}$; HRMS (ESI) Calcd for $C_{16}H_{21}N_2^+$ ([M+H]$^+$) 241.1699. Found 241.1698.; $[\alpha]_D^{27}$ +13.1 (*c* = 12.1, $CHCl_3$) for 94% ee; HPLC OJ3, H/IPA = 10:1, flow rate = 1.0 mL/min, λ = 254 nm, 11.0 min (minor enantiomer), 12.1 min (major enantiomer).

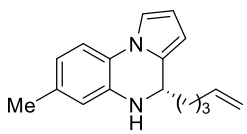

**7ad:** $^1$H NMR (600 MHz, $CDCl_3$) $\delta$ 7.15 (1H, d, *J* = 8.1 Hz), 7.11 (1H, dd, *J* = 3.0, 1.2 Hz), 6.60 (1H, d, *J* = 8.1 Hz), 6.55 (1H, brs), 6.27 (1H, t, *J* = 3.0 Hz), 5.96 (1H, d, *J* = 3.0 Hz), 5.81 (1H, ddt, *J* = 17.2, 10.2, 6.6 Hz), 5.02 (1H, dd, *J* = 17.2, 1.5 Hz), 4.97 (1H, d, *J* = 10.2 Hz), 4.42 (1H, dd, *J* = 7.8, 5.4 Hz), 3.89 (1H, brs), 2.26 (3H, s), 2.11 (2H, q, *J* = 6.6 Hz), 1.86 (1H, ddt, *J* = 13.2, 10.2, 5.4 Hz), 1.76 (1H, dddd, *J* = 13.2, 10.2, 7.8, 5.4 Hz), 1.62-1.48 (2H, m); $^{13}$C NMR (151 MHz, $CDCl_3$) $\delta$ 138.5, 135.8, 134.5, 129.5,

123.4, 119.8, 116.1, 115.1, 114.6, 114.1, 109.7, 103.8, 51.1, 34.9, 33.7, 24.9, 21.2; IR (film): 3353, 2922, 2853, 1619, 1530, 1487, 1343, 1293, 1177, 1125, 910 $cm^{-1}$; HRMS (ESI) Calcd for $C_{17}H_{21}N_2^+$ ($[M+H]^+$) 253.1699. Found 253.1696.; $[\alpha]_D^{26}$ +15.9 (*c* = 21.2, $CHCl_3$) for 90% ee; HPLC OD3, H/IPA = 10:1, flow rate = 1.0 mL/min, λ = 254 nm, 9.0 min (minor enantiomer), 17.3 min (major enantiomer).

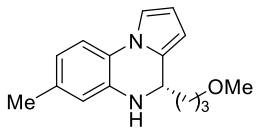


**7ae:** $^1$H NMR (600 MHz, $CDCl_3$) $\delta$ 7.15 (1H, d, *J* = 7.8 Hz), 7.10 (1H, dd, *J* = 3.0, 1.2 Hz), 6.59 (1H, d, *J* = 7.8 Hz), 6.53 (1H, brs), 6.27 (1H, t, *J* = 3.0 Hz), 5.97 (1H, d, *J* = 3.0 Hz), 4.45 (1H, dd, *J* = 6.6, 5.4 Hz), 4.16 (1H, brs), 3.42 (2H, t, *J* = 6.6 Hz), 3.34 (3H, s), 2.26 (3H, s), 1.93 (1H, dtd, *J* = 13.8, 6.6, 5.4 Hz), 1.81 (1H, dq, *J* = 13.8, 6.6 Hz), 1.73 (1H, quintet, *J* = 6.6 Hz); $^{13}$C NMR (151 MHz, $CDCl_3$) $\delta$ 135.8, 134.4, 129.5, 123.4, 119.6, 116.1, 114.5, 114.1, 109.7, 103.8, 72.7, 58.8, 51.0, 32.6, 25.9, 21.2; IR (film): 3351, 2923, 2860, 1619, 1603, 1530, 1489, 1343, 1293, 1178, 1117, 1093, 1028 $cm^{-1}$; HRMS (ESI) Calcd for $C_{16}H_{21}N_2O^+$ ($[M+H]^+$) 257.1648. Found 257.1644.; $[\alpha]_D^{27}$ +7.4 (*c* = 23.6, $CHCl_3$) for 88% ee; HPLC OD3, H/IPA = 10:1, flow rate = 1.0 mL/min, λ = 254 nm, 10.8 min (minor enantiomer), 15.3 min (major enantiomer).

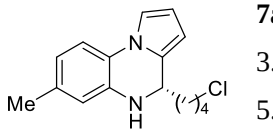


**7af:** $^1$H NMR (600 MHz, $CDCl_3$) $\delta$ 7.16 (1H, d, *J* = 8.1 Hz), 7.14 (1H, dd, *J* = 3.0, 1.2 Hz), 6.61 (1H, d, *J* = 8.1 Hz), 6.56 (1H, brs), 6.28 (1H, t, *J* = 3.0 Hz), 5.97 (1H, d, *J* = 3.0 Hz), 4.44 (1H, t, *J* = 6.3 Hz), 3.91 (1H, brs), 3.55 (2H, t, *J* = 6.6 Hz), 2.26 (3H, s), 1.89-1.74 (4H, m), 1.67-1.55 (2H, m); $^{13}$C NMR (151 MHz, $CDCl_3$) $\delta$ 135.6, 134.5, 129.2, 123.4, 119.9, 116.1, 114.6, 114.2, 109.8, 103.8, 51.1, 45.0, 34.8, 32.6, 23.0, 21.2; IR (film): 3360, 2934, 2865, 1617, 1602, 1529, 1488, 1343, 1291, 1177, 1124, 1093, 1029 $cm^{-1}$; HRMS (ESI) Calcd for $C_{16}H_{20}N_2{}^{35}Cl^+$ ($[M+H]^+$) 275.1310. Found 275.1305.; $[\alpha]_D^{27}$ +6.3 (*c* = 13.2, $CHCl_3$) for 87% ee; HPLC OD3, H/IPA = 10:1, flow rate = 1.0 mL/min, λ = 254 nm, 13.2 min (minor enantiomer), 25.2 min (major enantiomer).

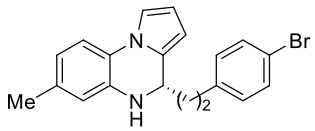


**7ag:** $^1$H NMR (600 MHz, $CDCl_3$) $\delta$ 7.40 (2H, d, *J* = 8.1 Hz), 7.16 (1H, d, *J* = 8.1 Hz), 7.12 (1H, dd, *J* = 3.0, 1.2 Hz), 7.06 (2H, d, *J* = 8.1 Hz), 6.61 (1H, d, *J* = 8.1 Hz), 6.48 (1H, brs), 6.29 (1H, t, *J* = 3.0 Hz), 5.99 (1H, d, *J* = 3.0 Hz), 4.49 (1H, dd, *J* = 7.8, 6.0 Hz), 3.83 (1H, brs), 2.73 (1H, t, *J* = 7.8 Hz), 2.71 (1H, t, *J* = 7.8 Hz), 2.26 (3H, s), 2.12 (1H, dtd, *J* = 14.4, 7.8, 6.0 Hz), 2.04 (1H, dq, *J* = 14.4, 7.8 Hz); $^{13}$C NMR (151 MHz, $CDCl_3$) $\delta$ 140.7, 135.4, 134.6, 131.7, 130.2, 128.8, 123.3, 119.9$_4$, 119.8$_8$, 116.1, 114.6, 114.3, 109.8, 104.0, 50.9, 37.0, 31.4, 21.2; IR (film): 3360, 2934, 2865, 1617, 1602, 1488, 1529, 1488, 1343, 1291, 1177, 1124, 1093 $cm^{-1}$; HRMS (ESI) Calcd for $C_{20}H_{20}N_2{}^{79}Br^+$ ($[M+H]^+$) 367.0804. Found 367.0795.; $[\alpha]_D^{27}$ +11.7 (*c* = 25.8, $CHCl_3$) for 95% ee; HPLC OD3, H/IPA = 10:1, flow rate = 1.0 mL/min, λ = 254 nm, 15.4 min (minor enantiomer), 25.1 min (major enantiomer).

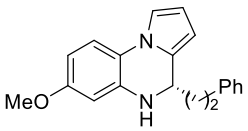

**7ba:** $^{1}$H NMR (600 MHz, $CDCl_3$) $\delta$ 7.30 (2H, t, $J$ = 7.8 Hz), 7.21 (2H, d, $J$ = 7.8 Hz), 7.21 (1H, t, $J$ = 7.8 Hz), 7.18 (1H, d, $J$ = 9.0 Hz), 7.09-7.08 (1H, m), 6.35 (1H, dd, $J$ = 9.0, 3.0 Hz), 6.28 (1H, t, $J$ = 3.0 Hz), 6.20 (1H, d, $J$ = 3.0 Hz), 6.00 (1H, d, $J$ = 3.0 Hz), 4.50 (1H, dd, $J$ = 7.2, 5.4 Hz), 3.90 (1H, brs), 3.76 (3H, s), 2.79 (2H, t, $J$ = 8.1 Hz), 2.18 (1H, dtd, $J$ = 14.4, 7.2, 5.4 Hz), 2.09 (1H, dq, $J$ = 14.4, 7.2 Hz); $^{13}$C NMR (151 MHz, $CDCl_3$) $\delta$ 157.2, 141.6, 136.9, 128.8, 128.7, 128.5, 126.2, 119.8, 115.4, 114.0, 109.6, 104.0, 103.7, 101.4, 55.5, 51.1, 37.0, 32.1; IR (film): 3364, 2931, 2835, 1617, 1603, 1524, 1490, 1288, 1272, 1202, 1166, 1125, 1113, 1094, 1040, 828 cm$^{-1}$; HRMS (ESI) Calcd for $C_{20}H_{21}N_2O^+$ ($[M+H]^+$) 305.1648. Found 305.1638.; $[\alpha]_D^{29}$ +11.4 ($c$ = 23.3, $CHCl_3$) for 94% ee; HPLC OD3, H/IPA = 10:1, flow rate = 1.0 mL/min, λ = 254 nm, 29.7 min (minor enantiomer), 36.4 min (major enantiomer).

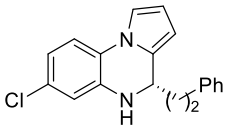

**7ca:** $^{1}$H NMR (600 MHz, $CDCl_3$) $\delta$ 7.31 (2H, t, $J$ = 7.8 Hz), 7.22 (1H, t, $J$ = 7.8 Hz), 7.21 (2H, d, $J$ = 7.8 Hz), 7.17 (1H, d, $J$ = 8.4 Hz), 7.10 (1H, dd, $J$ = 3.0, 1.5 Hz), 6.74 (1H, dd, $J$ = 8.4, 1.8 Hz), 6.59 (1H, d, $J$ = 1.8 Hz), 6.31 (1H, d, $J$ = 3.0 Hz), 6.03 (1H, d, $J$ = 3.0 Hz), 4.52 (1H, t, $J$ = 6.3 Hz), 3.94 (1H, brs), 2.83-2.74 (2H, m), 2.18 (1H, dddd, $J$ = 13.8, 9.0, 6.3, 5.4 Hz), 2.09 (1H, ddt, $J$ = 13.8, 9.0, 6.3 Hz); $^{13}$C NMR (151 MHz, $CDCl_3$) $\delta$ 141.4, 136.7, 129.7, 128.9, 128.8, 128.5, 126.4, 124.1, 118.8, 115.6, 115.2, 114.4, 110.5, 104.5, 51.0, 37.2, 32.1; IR (film): 3378, 2929, 1611, 1512, 1468, 1342, 1289, 1179, 1119, 1101, 894, 846 cm$^{-1}$; HRMS (ESI) Calcd for $C_{19}H_{18}N_2Cl^+$ ($[M+H]^+$) 309.1153. Found 309.1148.; $[\alpha]_D^{26}$ +11.3 ($c$ = 24.3, $CHCl_3$) for 96% ee; HPLC OD3, H/IPA = 10:1, flow rate = 1.0 mL/min, λ = 254 nm, 15.6 min (*R*-enantiomer), 19.0 min (*S*-enantiomer).

**Procedure for Trifluoroacetylation of 7ca:**

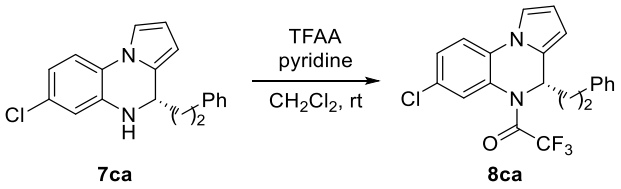


**7ca** **8ca**

To a solution of **7ca** (25.0 mg, 0.099 mmol) in $CH_2Cl_2$ (1.0 mL) were added trifluoroacetic anhydride (16.8 μL, 0.12 mmol) and pyridine (16.5 μL, 0.20 mmol). After being stirred for 2 h at room temperature, the mixture was directly charged on a silica gel column and eluted with H/$CH_2Cl_2$ = 6:1-1:1 to afford **8ca** in 36% yield (14.4 mg, 0.036 mmol). **8ca:** $^{1}$H NMR (500 MHz, DMSO-$d_6$, 100 °C) $\delta$ 7.79-7.73 (1H, m), 7.62-7.56 (1H, m), 7.54-7.46 (2H, m), 7.28-7.21 (2H, m), 7.20-7.13 (1H, m), 7.13-7.07 (2H, m), 6.34-6.29 (1H, m), 6.27-6.22 (1H, m), 5.62-5.56 (1H, m), 2.68-2.61 (2H, m), 1.91-1.76 (2H, m); $^{13}$C NMR (121 MHz, DMSO-$d_6$, 100 °C) $\delta$ 154.5 (q, $J_{C-F}$ = 34.8 Hz), 139.9, 129.1, 127.8, 127.7, 127.6, 127.5, 127.1, 125.7, 125.4, 124.4, 117.3, 115.7, 115.7 (q, $J_{C-F}$ = 278.8 Hz), 110.2, 106.1, 52.6, 34.2, 30.7; $^{19}$F NMR (471 MHz, $CDCl_3$) $\delta$ −65.7 (minor rotamer), −68.5

(major rotamer); IR (film): 3028, 2918, 1696, 1605, 1507, 1437, 1412, 1341, 1209, 1182, 1149, 1092, 816 $cm^{-1}$; HRMS (ESI) Calcd for $C_{21}H_{16}N_2OF_3ClNa^+$ ($[M+Na]^+$) 427.0795. Found 427.0797.; $[\alpha]_D^{22}$ +107.5 (*c* = 2.4, $CHCl_3$) for >99.9% ee (*S*); HPLC OZ3, H/IPA = 99:1, flow rate = 0.5 mL/min, λ = 254 nm, 11.0 min (*S*-enantiomer), 12.7 min (*R*-enantiomer).

**Crystallographic Structure Determination of Phosphonium Nitrate 2a·$NO_3$:** The single crystal, which was obtained by the procedure described below, was mounted on MicroMesh. Data of X-ray diffraction were collected at 123 K on a Rigaku VariMax with Pilatus diffractometer with fine-focus sealed tube Mo/Kα radiation (λ = 0.71075 Å). An absorption correction was made using Crystal Clear. The structure was solved by direct methods and Fourier syntheses, and refined by full-matrix least squares on $F^2$ by using SHELXL-2014.[21] All non-hydrogen atoms were refined with anisotropic displacement parameters. Hydrogen atoms bonded to nitrogen atoms were located from a difference synthesis and their coordinates and isotropic thermal parameters refined. The other hydrogen atoms were placed in calculated positions and isotropic thermal parameters refined.

**Recrystallization of 2a·$NO_3$:** Recrystallization was performed by using a H/EA/toluene solvent system at room temperature to afford single crystals of **2a**·$NO_3$. The crystallographic data are summarized in Table S1 and the ORTEP diagram is shown in Fig. S1.

**Crystallographic Structure Determination of Triehylammonium Phosphate 1a·$HNEt_3$:** The single crystal, which was obtained by the procedure described below, was mounted on MicroMesh. Data of X-ray diffraction were collected at 113 K on a Rigaku VariMax with Saturn diffractometer with fine-focus sealed tube Mo/Kα radiation (λ = 0.71075 Å). An absorption correction was made using Crystal Clear. The structure was solved by direct methods and Fourier syntheses, and refined by full-matrix least squares on $F^2$ by using SHELXL-2014.[21] All non-hydrogen atoms were refined with anisotropic displacement parameters. Hydrogen atom bonded to the nitrogen atom of triethylamine was located from a difference synthesis and their coordinates and isotropic thermal parameters refined. The other hydrogen atoms were placed in calculated positions and isotropic thermal parameters refined.

**Recrystallization of 1a·$HNEt_3$:** Recrystallization was performed by using a H/EA solvent system at room temperature to afford single crystals of **1a**·$HNEt_3$. The crystallographic data are summarized in Table S2 and the ORTEP diagram is shown in Fig. S2.

**Crystallographic Structure Determination of Triethylammonium Phosphate 1b·$HNEt_3$:** The single crystal, which was obtained by the procedure described below, was mounted on MicroMesh. Data of X-ray diffraction were collected at 123 K on a Rigaku VariMax with Pilatus diffractometer with fine-focus sealed tube Mo/Kα radiation (λ = 0.71075 Å). An absorption correction was made

using Crystal Clear. The structure was solved by direct methods and Fourier syntheses, and refined by full-matrix least squares on $F^2$ by using SHELXL-2014.[21] All non-hydrogen atoms were refined with anisotropic displacement parameters. Hydrogen atom bonded to the nitrogen atom of triethylamine was located from a difference synthesis and their coordinates and isotropic thermal parameters refined. The other hydrogen atoms were placed in calculated positions and isotropic thermal parameters refined.

**Recrystallization of 1b·HNEt$_3$:** Recrystallization was performed by using a H/EA solvent system at room temperature to afford single crystals of **1b**·HNEt$_3$. The crystallographic data are summarized in Table S3 and the ORTEP diagram is shown in Fig. S3.

**Crystallographic Structure Determination of Triethylammonium Phosphate 1c·HNEt$_3$:** The single crystal, which was obtained by the procedure described below, was mounted on MicroMesh. Data of X-ray diffraction were collected at 123 K on a Rigaku VariMax with Pilatus diffractometer with fine-focus sealed tube Mo/Kα radiation (λ = 0.71075 Å). An absorption correction was made using Crystal Clear. The structure was solved by direct methods and Fourier syntheses, and refined by full-matrix least squares on $F^2$ by using SHELXL-2014.[21] All non-hydrogen atoms were refined with anisotropic displacement parameters. Hydrogen atom bonded to the nitrogen atom of triethylamine was located from a difference synthesis and their coordinates and isotropic thermal parameters refined. The other hydrogen atoms were placed in calculated positions and isotropic thermal parameters refined.

**Recrystallization of 1c·HNEt$_3$:** Recrystallization was performed by using a cyclohexane/$CHCl_3$ solvent system at room temperature to afford single crystals of **1c**·HNEt$_3$. The crystallographic data are summarized in Table S4 and the ORTEP diagram is shown in Fig. S4.

**Crystallographic Structure Determination of 8ca:** The single crystal, which was obtained by the procedure described below, was mounted on MicroMesh. Data of X-ray diffraction were collected at 123 K on a Rigaku VariMax with Pilatus diffractometer with fine-focus sealed tube Mo/Kα radiation (λ = 0.71075 Å). An absorption correction was made using Crystal Clear. The structure was solved by direct methods and Fourier syntheses, and refined by full-matrix least squares on $F^2$ by using SHELXL-2014.[21] All non-hydrogen atoms were refined with anisotropic displacement parameters. Hydrogen atoms were placed in calculated positions and isotropic thermal parameters refined.

**Recrystallization of 8ca:** Recrystallization was performed by using cyclohexane as a solvent at room temperature to afford single crystals of **8ca**. The crystallographic data are summarized in Table S5 and the ORTEP diagram is shown in Fig. S5.

**Table S1.** Crystal data and structure refinement for **2a**·$NO_3$ (CCDC 1817498).

| | | |
|---|---|---|
| Empirical formula | $C_{44}H_{44}N_5O_7P$ | |
| Formula weight | 785.81 | |
| Temperature | 123(2) K | |
| Wavelength | 0.71075 Å | |
| Crystal system | Monoclinic | |
| Space group | P2(1) | |
| Unit cell dimensions | a = 12.4253(11) Å | α = 90°. |
| | b = 12.5926(10) Å | β = 97.359(2)°. |
| | c = 12.9927(11) Å | γ = 90°. |
| Volume | 2016.2(3) $Å^3$ | |
| Z | 2 | |
| Density (calculated) | 1.294 $Mg/m^3$ | |
| Absorption coefficient | 0.126 $mm^{-1}$ | |
| F(000) | 828 | |
| Crystal size | 0.180 x 0.030 x 0.010 $mm^3$ | |
| Theta range for data collection | 3.162 to 25.492°. | |
| Index ranges | −15<=h<=15, −14<=k<=15, −15<=l<=15 | |
| Reflections collected | 31061 | |
| Independent reflections | 7449 [R(int) = 0.0548] | |
| Completeness to theta = 25.242° | 99.8 % | |
| Absorption correction | Semi-empirical from equivalents | |
| Max. and min. transmission | 1.000 and 0.796 | |
| Refinement method | Full-matrix least-squares on $F^2$ | |
| Data / restraints / parameters | 7449 / 1 / 524 | |
| Goodness-of-fit on $F^2$ | 1.145 | |
| Final R indices [I>2sigma(I)] | $R_1$ = 0.0385, $wR_2$ = 0.0856 | |
| R indices (all data) | $R_1$ = 0.0481, $wR_2$ = 0.0923 | |
| Absolute structure parameter | 0.07(4) | |
| Extinction coefficient | 0 | |
| Largest diff. peak and hole | 0.184 and −0.266 $e.Å^{-3}$ | |

(a) Front view ($NO_3$ is omitted) (b) Side view ($NO_3$ is omitted)

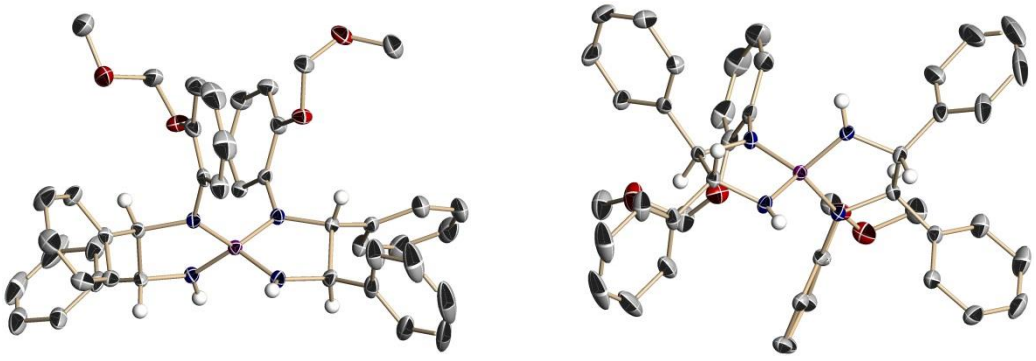

**Fig. S1.** Molecular structure of **2a**·$NO_3$. The thermal ellipsoids of non-hydrogen atoms are shown at the 50% probability level. Calculated hydrogen atoms except them attached to stereogenic carbon atoms are omitted for clarity. Blue = nitrogen, red = oxygen, gray = carbon, purple = phosphorus.

**Table S2.** Crystal data and structure refinement for **1a**·$HNEt_3$ (CCDC 1581651).

| | | |
|---|---|---|
| Empirical formula | $C_{48}H_{54}N_5O_6PS_2$ | |
| Formula weight | 892.05 | |
| Temperature | 113(2) K | |
| Wavelength | 0.71075 Å | |
| Crystal system | Orthorhombic | |
| Space group | P2(1)2(1)2(1) | |
| Unit cell dimensions | a = 10.174(3) Å | α = 90°. |
| | b = 19.220(5) Å | β = 90°. |
| | c = 22.736(6) Å | γ = 90°. |
| Volume | 4445.9(19) $Å^3$ | |
| Z | 4 | |
| Density (calculated) | 1.333 $Mg/m^3$ | |
| Absorption coefficient | 0.212 $mm^{-1}$ | |
| F(000) | 1888 | |
| Crystal size | 0.300 x 0.150 x 0.020 $mm^3$ | |
| Theta range for data collection | 3.050 to 25.495°. | |
| Index ranges | −11<=h<=12, −21<=k<=23, −27<=l<=27 | |
| Reflections collected | 31357 | |
| Independent reflections | 8262 [R(int) = 0.0396] | |
| Completeness to theta = 25.242° | 99.7 % | |
| Absorption correction | Multi-scan | |
| Max. and min. transmission | 1.0000 and 0.9029 | |
| Refinement method | Full-matrix least-squares on $F^2$ | |
| Data / restraints / parameters | 8262 / 0 / 568 | |
| Goodness-of-fit on $F^2$ | 1.118 | |
| Final R indices [I>2sigma(I)] | $R_1$ = 0.0390, $wR_2$ = 0.0848 | |
| R indices (all data) | $R_1$ = 0.0429, $wR_2$ = 0.0878 | |
| Absolute structure parameter | 0.02(2) | |
| Extinction coefficient | 0 | |
| Largest diff. peak and hole | 0.213 and −0.280 e.$Å^{-3}$ | |

(a) Front view ($HNEt_3$ is omitted) (b) Side view

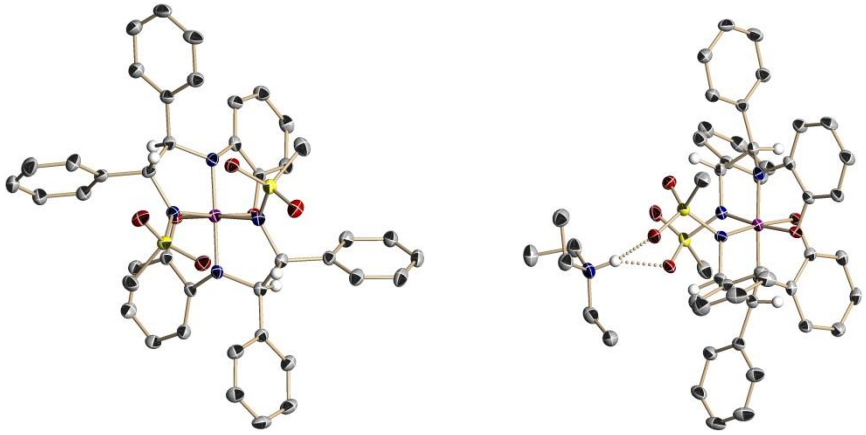

**Fig. S2.** Molecular structure of **1a**·$HNEt_3$. The thermal ellipsoids of non-hydrogen atoms are shown at the 50% probability level. Calculated hydrogen atoms except them attached to stereogenic carbon atoms are omitted for clarity. Blue = nitrogen, red = oxygen, gray = carbon, purple = phosphorus, yellow = sulfur.

**Table S3.** Crystal data and structure refinement for **1b**·$HNEt_3$ (CCDC 1581654).

| | | |
|---|---|---|
| Empirical formula | $C_{50}H_{52}F_6N_5O_6PS_2 \cdot C_6H_{14}$ | |
| Formula weight | 1114.22 | |
| Temperature | 123(2) K | |
| Wavelength | 0.71075 Å | |
| Crystal system | Orthorhombic | |
| Space group | P2(1)2(1)2(1) | |
| Unit cell dimensions | a = 10.3061(5) Å | α = 90°. |
| | b = 20.5931(13) Å | β = 90°. |
| | c = 26.0626(17) Å | γ = 90°. |
| Volume | 5531.4(6) $Å^3$ | |
| Z | 4 | |
| Density (calculated) | 1.338 $Mg/m^3$ | |
| Absorption coefficient | 0.200 $mm^{-1}$ | |
| F(000) | 2344 | |
| Crystal size | 0.200 x 0.050 x 0.050 $mm^3$ | |
| Theta range for data collection | 3.067 to 27.489°. | |
| Index ranges | −11<=h<=13, −26<=k<=26, −33<=l<=33 | |
| Reflections collected | 41940 | |
| Independent reflections | 12244 [R(int) = 0.0180] | |
| Completeness to theta = 25.242° | 99.0 % | |
| Absorption correction | Multi-scan | |
| Max. and min. transmission | 1.000 and 0.926 | |
| Refinement method | Full-matrix least-squares on $F^2$ | |
| Data / restraints / parameters | 12244 / 2 / 724 | |
| Goodness-of-fit on $F^2$ | 1.024 | |
| Final R indices [I>2sigma(I)] | $R_1$ = 0.0337, $wR_2$ = 0.0938 | |
| R indices (all data) | $R_1$ = 0.0355, $wR_2$ = 0.0957 | |
| Absolute structure parameter | −0.009(7) | |
| Extinction coefficient | 0 | |
| Largest diff. peak and hole | 0.736 and −0.349 e.$Å^{-3}$ | |

(a) Front view ($HNEt_3$ is omitted) (b) Side view

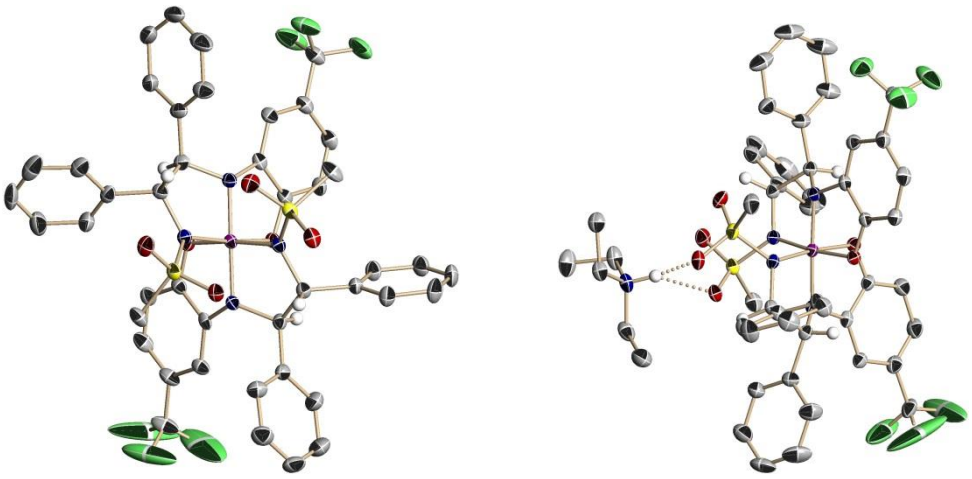

**Fig. S3.** Molecular structure of **1b**·$HNEt_3$. The thermal ellipsoids of non-hydrogen atoms are shown at the 50% probability level. Solvent molecule ($^n$hexane) and calculated hydrogen atoms except them attached to stereogenic carbon atoms are omitted for clarity. Blue = nitrogen, red = oxygen, gray = carbon, light green = fluorine, purple = phosphorus, yellow = sulfur.

**Table S4.** Crystal data and structure refinement for **1c**·$HNEt_3$ (CCDC 1581655).

| | | |
|---|---|---|
| Empirical formula | $C_{62}H_{60}F_6N_5O_6PS_2$ | |
| Formula weight | 1180.24 | |
| Temperature | 123(2) K | |
| Wavelength | 0.71075 Å | |
| Crystal system | Orthorhombic | |
| Space group | P2(1)2(1)2(1) | |
| Unit cell dimensions | a = 10.407(3) Å | α = 90°. |
| | b = 22.291(5) Å | β = 90°. |
| | c = 25.239(6) Å | γ = 90°. |
| Volume | 5855(3) $Å^3$ | |
| Z | 4 | |
| Density (calculated) | 1.339 $Mg/m^3$ | |
| Absorption coefficient | 0.193 $mm^{-1}$ | |
| F(000) | 2464 | |
| Crystal size | 0.300 x 0.010 x 0.010 $mm^3$ | |
| Theta range for data collection | 3.034 to 25.499°. | |
| Index ranges | −12<=h<=12, −26<=k<=26, −30<=l<=26 | |
| Reflections collected | 40217 | |
| Independent reflections | 10834 [R(int) = 0.0619] | |
| Completeness to theta = 25.242° | 99.6 % | |
| Absorption correction | Multi-scan | |
| Max. and min. transmission | 1.000 and 0.710 | |
| Refinement method | Full-matrix least-squares on $F^2$ | |
| Data / restraints / parameters | 10834 / 0 / 746 | |
| Goodness-of-fit on $F^2$ | 1.007 | |
| Final R indices [I>2sigma(I)] | $R_1$ = 0.0429, $wR_2$ = 0.0842 | |
| R indices (all data) | $R_1$ = 0.0683, $wR_2$ = 0.0927 | |
| Absolute structure parameter | 0.04(3) | |
| Extinction coefficient | 0 | |
| Largest diff. peak and hole | 0.582 and −0.307 e.$Å^{-3}$ | |

(a) Front view ($HNEt_3$ is omitted) (b) Side view

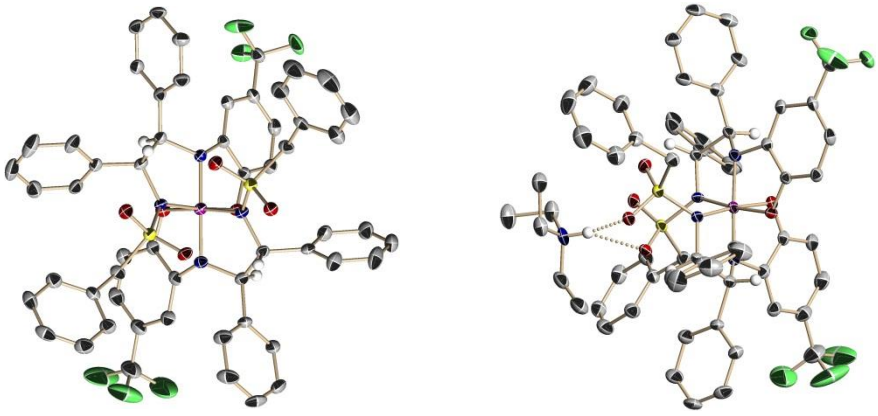

**Fig. S4.** Molecular structure of **1c**·$HNEt_3$. The thermal ellipsoids of non-hydrogen atoms are shown at the 50% probability level. Calculated hydrogen atoms except them attached to stereogenic carbon atoms are omitted for clarity. Blue = nitrogen, red = oxygen, gray = carbon, light green = fluorine, purple = phosphorus, yellow = sulfur.

**Table S5.** Crystal data and structure refinement for **8ca** (CCDC 1585518).

| | | |
|---|---|---|
| Empirical formula | $C_{21}H_{16}ClF_3N_2O$ | |
| Formula weight | 404.81 | |
| Temperature | 293(2) K | |
| Wavelength | 0.71075 Å | |
| Crystal system | Orthorhombic | |
| Space group | P2(1)2(1)2(1) | |
| Unit cell dimensions | a = 7.2745(15) Å | α = 90°. |
| | b = 10.702(2) Å | β = 90°. |
| | c = 23.579(5) Å | γ = 90°. |
| Volume | 1835.7(6) $Å^3$ | |
| Z | 4 | |
| Density (calculated) | 1.465 $Mg/m^3$ | |
| Absorption coefficient | 0.252 $mm^{-1}$ | |
| F(000) | 832 | |
| Crystal size | 0.20 x 0.05 x 0.02 $mm^3$ | |
| Theta range for data collection | 3.216 to 25.480°. | |
| Index ranges | −8<=h<=8, −10<=k<=12, −27<=l<=28 | |
| Reflections collected | 12634 | |
| Independent reflections | 3397 [R(int) = 0.0484] | |
| Completeness to theta = 25.242° | 99.6 % | |
| Absorption correction | Semi-empirical from equivalents | |
| Max. and min. transmission | 1.000 and 0.739 | |
| Refinement method | Full-matrix least-squares on $F^2$ | |
| Data / restraints / parameters | 3397 / 0 / 253 | |
| Goodness-of-fit on $F^2$ | 0.968 | |
| Final R indices [I>2sigma(I)] | $R_1$ = 0.0343, $wR_2$ = 0.0772 | |
| R indices (all data) | $R_1$ = 0.0425, $wR_2$ = 0.0797 | |
| Absolute structure parameter | −0.04(3) | |
| Extinction coefficient | 0 | |
| Largest diff. peak and hole | 0.238 and −0.299 e.$Å^{-3}$ | |

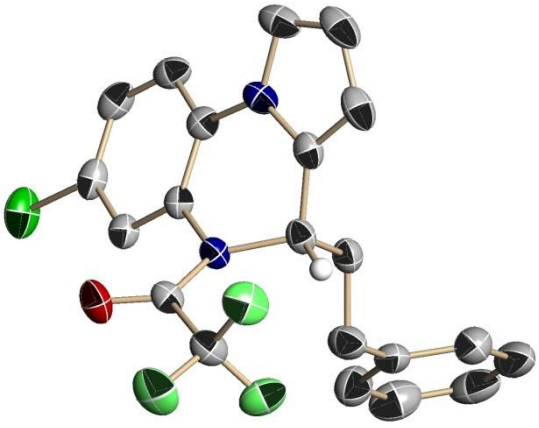

**Fig. S5.** Molecular structure of **8ca**. The thermal ellipsoids of non-hydrogen atoms are shown at the 50% probability level. Calculated hydrogen atoms except them attached to stereogenic carbon atom are omitted for clarity. Blue = nitrogen, red = oxygen, gray = carbon, light green = fluorine, green = chlorine.

## References and Notes


(1) (a) Kosolapoff, G. M. In *Organophosphorus Compounds*, John Wiley & Sons: New York, 1950. (b) *A Guide to Organophosphorus Chemistry*; Quin, L. D., Ed.; John Wiley & Sons: New York, 2000.

(2) Wittig, G.; Rieber, M. *Justus Liebigs Ann. Chem.* **1949**, *562*, 187.

(3) (a) Allen, D. W.; Tebby, J. C.; Hall, C. D. *Organophosphorus Chem.* **2003**, *33*, 68. (b) Pajkert, R.; Röeschenthaler, G.-V. *Organophosphorus Chem.* **2017**, *46*, 323. (c) Holmes, R. R. *Chem. Rev.* **1996**, *96*, 927. (d) Kumara Swamy, K. C.; Satish Kumar, N. *Acc. Chem. Res.* **2006**, *39*, 324.

(4) *Chemistry of Hypervalent Compounds*; Akiba, K.-y, Ed.; Wiley-VCH, Weinheim, 1998.

(5) For reviews on chiral hexacoordinated phosphates, see: (a) Lacour, J.; Hebbe-Viton, V. *Chem. Soc. Rev.* **2003**, *32*, 373. (b) Lacour, J.; Moraleda, D. *Chem. Commun.* **2009**, 7073. (c) Lacour, J. *C. R. Chim.* **2010**, *13*, 985.

(6) (a) Hellwinkel, D. *Chem. Ber.* **1965**, *98*, 576. (b) Hellwinkel, D. *Chem. Ber.* **1966**, *99*, 3642.

(7) (a) Lacour, J.; Ginglinger, C.; Grivet, C.; Bernardinelli, G. *Angew. Chem. Int. Ed. Engl.* **1997**, *36*, 608. (b) Lacour, J.; Londez, A.; Goujon-Ginglinger, C.; Buss, V.; Bernardinelli, G. *Org. Lett.* **2000**, *2*, 4185.

(8) (a) Strauss, S. H. *Chem. Rev.* **1993**, *93*, 927. (b) Krossing, I.; Raabe, I. *Angew. Chem. Int. Ed.* **2004**, *43*, 2066.

(9) For reviews on phosphonium salt catalyses, see: (a) Werner, T. *Adv. Synth. Catal.* **2009**, *351*, 1469. (b) Uraguchi, D.; Ooi, T. *J. Synth. Org. Chem. Jpn.* **2010**, *68*, 1185. (c) Enders, D.; Nguyen, T. V. *Org. Biomol. Chem.* **2012**, *10*, 5327.

(10) (a) Uraguchi, D.; Yamada, K.; Ooi, T. *Angew. Chem. Int. Ed.* **2015**, *54*, 9954. (b) Uraguchi, D.; Kinoshita, N.; Kizu, T.; Ooi, T. *J. Am. Chem. Soc.* **2015**, *137*, 13768. (c) Uraguchi, D.; Yoshioka, K.; Ooi, T. *Nat. Commun.* **2017**, *8*, 14793. (d) Uraguchi, D.; Ito, T.; Kimura, Y.; Nobori, Y.; Sato, M.; Ooi, T. *Bull. Chem. Soc. Jpn.* **2017**, *90*, 546. (e) Yoshioka, K.; Yamada, K.; Uraguchi, D.; Ooi, T. *Chem. Commun.* **2017**, *53*, 5495. (f) Tanaka, N.; Tsutsumi, R.; Uraguchi, D.; Ooi, T. *Chem. Commun.* **2017**, *53*, 6999.

(11) Krawczyk, H.; Dzięgielewski, M.; Deredas, D.; Albrecht, A.; Albrecht, Ł. *Chem. – Eur. J.* **2015**, *21*, 10268.

(12) Maiti, D.; Fors, B. P.; Henderson, J. L.; Nakamura, Y.; Buchwald, S. L. *Chem. Sci.* **2011**, *2*, 57.

(13) Uraguchi, D.; Asai, Y.; Ooi, T. *Angew. Chem. Int. Ed.* **2009**, *48*, 733.

(14) (a) Kommana, P.; Kumaraswamy, S.; Vittal, J. J.; Swamy, K. C. K. *Inorg. Chem.* **2002**, *41*, 2356. (b) Timosheva, N. V.; Chandrasekaran, A.; Holmes, R. R. *Z. Anorg. Allg. Chem.* **2005**,

*631*, 2683. (c) Timosheva, N. V.; Chandrasekaran, A.; Holmes, R. R. *Inorg. Chem.* **2006**, *45*, 10836.

(15) Allcock, H. R.; Bissell, E. C. *J. Chem. Soc., Chem. Commun.* **1972**, 676.

(16) (a) Siu, P. W.; Gates, D. P. *Organometallics* **2009**, *28*, 4491. (b) Siu, P. W.; Hazin, K.; Gates, D. P. *Chem. – Eur. J.* **2013**, *19*, 9005.

(17) Judging from the $^{31}$P NMR signal of hydrogen phosphate **1a**·H·$(urea)_2$ (−108.3 ppm in $CDCl_3$) in comparison with that of **1a**·$HNEt_3$ (−107.8 ppm in $CDCl_3$), hexacoordination at the phosphorus center isretained (cf. the related pentacoordinated phosphorus compounds having six heteroatoms on the phosphorus center generally show a signal in the range of −20 ~ −70 ppm).[3d, 16b]

(18) (a) Cox, E. D.; Cook, J. M. *Chem. Rev.* **1995**, *95*, 1797. (b) Stöckigt, J.; Antonchick, A. P.; Wu, F.; Waldmann, H. *Angew. Chem. Int. Ed.* **2011**, *50*, 8538.

(19) Snyder, D. S.; Tradtrantip, L.; Yao, C.; Kurth, M. J.; Verkman, A. S. *J. Med. Chem.* **2011**, *54*, 5468.

(20) (a) Li, Y.; Su, Y.-H.; Dong, D.-J.; Wu, Z.; Tian, S.-K. *RSC Adv.* **2013**, *3*, 18275. (b) Fan, Y.-S.; Jiang, Y.-J.; An, D.; Sha, D.; Antilla, J. C.; Zhang, S. *Org. Lett.* **2014**, *16*, 6112.

(21) Sheldrick, G. M. *Acta Cryst.* **2015**, *C71*, 3.

# List of Publications

## Publications Related to the Thesis

### Chapter 2.

Urea as a Redox-Active Directing Group under Asymmetric Photocatalysis of Iridium-Chiral Borate Ion Pairs

Uraguchi, D.; Kimura, Y.; Ueoka, F.; Ooi, T. *J. Am. Chem. Soc.* **2020**, *142*, 19462.

### Chapter 3.

Catalytic Asymmetric Synthesis of 5-Membered Alicyclic α-Quaternary β-Amino Acids via [3 + 2]-Photocycloaddition of α-Substituted Acrylates

Kimura, Y.; Uraguchi, D.; Ooi, T. *Org. Biomol. Chem.* **2021**, *19*, 1744.

## Other Publications

(1) [5.5]-*P*-Spirocyclic Chiral Triaminoiminophosphorane-Catalyzed Asymmetric Hydrophosphonylation of Aldehydes and Ynones
Uraguchi, D.; Ito, T.; Kimura, Y.; Nobori, Y.; Sato, M.; Ooi, T.
*Bull. Chem. Soc. Jpn.* **2017**, *90*, 546.

(2) Molecular Design, Synthesis, and Asymmetric Catalysis of a Hexacoordinated Chiral Phosphate Ion
Uraguchi, D.; Sasaki, H.; Kimura, Y.; Ito, T.; Ooi, T. *J. Am. Chem. Soc.* **2018**, *140*, 2765.

# Acknowledgement

The studies in this thesis have been accomplished under the direction of Professor Takashi Ooi at Nagoya University. The author would like to express his sincere gratitude to his supervisor, Professor Takashi Ooi for providing him this precious study opportunity as a Ph.D student in the laboratory.

The author especially would like to express his deepest appreciation to his supervisor, Professor Daisuke Uraguchi for his attentive coaching, serious discussion and substantial encouragement that leaded to his great achievement.

The author wishes to express his appreciations to Professor Kohsuke Ohmatsu, Professor Yoshitaka Aramaki and Professor Ken Yamanomoto for their gracious advice and encouragement.

The author would like to express his special thanks to Professor Kazuaki Ishihara and Professor Susumu Saito for their helpful suggestions and discussion on his dissertation committee. It is his great honor to have had thesis reviewed by two of the foremost experts in the area of synthetic organic chemistry.

The author wishes to express great appreciations to Professor Richmond Sarpong for accepting him as a visiting student at University of California, Berkeley,

The author wishes to thank Dr. Yuto Tsuchiya and Dr. Tsubasa Nakashima for his kind encouragement and discussion.

The author thanks all other members of Ooi group ther kind considerations.

| | | |
|---|---|---|
| Dr. Tomohito Kizu | Dr. Naomichi Imagawa | Dr. Yoshiyuki Hara |
| Dr. Yuichiro Ando | Dr. Ken Yoshioka | Dr. Masahiro Torii |
| Dr. Hitoshi Sasaki | Dr. Naoya Tanaka | Dr.Yukino Furukawa |
| Dr. Kohei Yamada | Dr. Tsuyoshi Ohtani | Dr. Yuya Nagato |
| Mr. Masaki Nishimura | Mr. Kohsuke kato | Mr. Yusuke Morita |
| Mr. Ryo Shibazaki | Ms. Wakana Takahashi | Mr. Misaki Ito |
| Ms. Seina Nakao | Mr. Yuma Uezono | Mr. Yasutaka Kawai |
| Ms. Yumiko Nobori | Mr. Naoki Imaizumi | Mr. Nozomi Kato |
| Mr. Shota Tanigchi | Mr. Ryo Magofuku | Mr. Daiki Ishikawa |
| Mr. Yaoki Kansaku | Mr. Kohdai Minami | Mr. Fumito Ueoka |
| Mr. Ryuhei Suzuki | Mr. Ryo Ishikawa | Ms. Mao Hotta |
| Mr. Ryota Onai | Mr. Kazuho Kurata | Mr. Yuto Shirai |
| Mr. Akihiro Nagata | Ms. Naho Matsuyama | Mr. Yuki Uchida |
| Mr. Masato Ohta | Mr. Sei Kakusho | Mr. Hiroki Fujita |
| Mr. Shohei Morita | Mr. Trinh Tuan Anh | Mr. Takuya Kojima |
| Mr. Yuya Taura | Mr. Takuya Kojima | Mr. Kohsuke Nomura |
| Ms. Haruka Fujimori | Mr. Ryuki Maekawa | Dr. Makoto Sato |
| Dr. Takaki Ito | Ms. Rie Yamaguchi | Ms. Mari Teraoka |
| Dr. Kailong Zhu | Ms. Kayo Sato | |

The author would like to express gratitude to the Program for Leading Graduate Schools “Integrate Graduate Education and Research in Green Natural Sciences” and “Graduate Program of Transformative Chem-Bio Research” for his financial support.

Finally, the author expresses his deep appreciation to his family, Mr. Shinobu Kimura and Mrs. Yukari Kimura for their constant assistance and encouragement.